

## Evaluating the Impact of Dysregulated Complement Activation on Monocytes in alpha-1 anti-trypsin Deficiency

AUTHOR(S)

Ciara Gough

CITATION

Gough, Ciara (2022): Evaluating the Impact of Dysregulated Complement Activation on Monocytes in alpha-1 anti-trypsin Deficiency. Royal College of Surgeons in Ireland. Thesis.  
<https://doi.org/10.25419/rcsi.14866458.v1>

DOI

[10.25419/rcsi.14866458.v1](https://doi.org/10.25419/rcsi.14866458.v1)

LICENCE

CC BY-NC-SA 4.0

This work is made available under the above open licence by RCSI and has been printed from <https://repository.rcsi.com>. For more information please contact [repository@rcsi.com](mailto:repository@rcsi.com)

URL

[https://repository.rcsi.com/articles/thesis/Evaluating\\_the\\_Impact\\_of\\_Dysregulated\\_Complement\\_Activation\\_on\\_Monocytes\\_in\\_alpha-1\\_anti-trypsin\\_Deficiency/14866458/1](https://repository.rcsi.com/articles/thesis/Evaluating_the_Impact_of_Dysregulated_Complement_Activation_on_Monocytes_in_alpha-1_anti-trypsin_Deficiency/14866458/1)



**Evaluating the impact of dysregulated complement  
activation on monocytes in alpha-1 anti-trypsin  
deficiency**

Dr Ciara Gough MB BCh BAO MRCPI

Respiratory Research Division

Department of Medicine

Royal College of Surgeons in Ireland

A thesis submitted to the School of Postgraduate Studies, Faculty of Medicine and  
Health Sciences, Royal College of Surgeons in Ireland in fulfilment of the degree of

Doctor of Medicine

Supervisors: Professor Noel Gerry McElvaney & Dr Emer Reeves PhD

April 2021

## **Candidate Thesis Declaration**

I declare that this thesis, which I submit to RCSI for examination in consideration of the award of a higher degree is my own personal effort. Where any of the content presented is the result of input or data from a related collaborative research programme this is duly acknowledged in the text such that it is possible to ascertain how much of the work is my own. I have not already obtained a degree in RCSI or elsewhere on the basis of this work. Furthermore, I took reasonable care to ensure that the work is original, and, to the best of my knowledge, does not breach copyright law, and has not been taken from other sources except where such work has been cited and acknowledged within the text

Signed: Ciara Gough

Student Number: 18195083

Date: 30/04/2021

## Table of Contents

Candidate Thesis Declaration.....	2
IP Declaration .....	<b>Error! Bookmark not defined.</b>
Glossary of Abbreviations.....	14
List of Figures .....	20
List of Tables .....	24
Posters and presentations .....	25
Abstract .....	26
Acknowledgments.....	27
Dedication.....	29
Chapter 1: Introduction.....	30
1.1 Alpha One Anti-Trypsin Deficiency .....	31
1.1.1 Background.....	31
1.1.2 Alpha One anti-trypsin protein.....	33
1.1.3 Glycosylation of AAT .....	36
1.1.4 Genetics of AAT deficiency .....	39
1.1.5 Diagnosis of AATD .....	40
1.1.6 Rationale for diagnostic testing .....	41
1.1.7 Anti-protease effects of AAT .....	42
1.1.8 Anti-inflammatory effects of AAT .....	44
1.1.9 Pro-inflammatory milieu of AATD .....	46

1.1.10 AATD lung disease .....	47
1.1.11 AATD liver disease.....	52
1.1.12 AATD skin disease.....	56
1.1.13 AATD vasculitis .....	57
1.1.14 Treatment of AATD .....	58
1.2 Monocyte Physiology in AATD.....	60
1.2.1 Introduction .....	60
1.2.2 The monocyte .....	61
1.2.3 Monocyte structure.....	62
1.2.4 Monocyte subsets .....	63
1.2.5 Monocyte life cycle.....	67
1.2.6 Monocyte differentiation to pulmonary macrophages.....	71
1.2.7 Monocytes and lung disease.....	74
1.2.8 Monocytes in AATD .....	75
1.2.9 Expression of CD14 by monocytes .....	79
1.2.10 Expression of CD14 by monocytes in AATD .....	80
1.2.11 Expression of CD16 by monocytes .....	80
1.2.12 Complement receptors on monocytes.....	81
1.2.13 Cytokine production by monocytes .....	84
1.2.14 Protease production by monocytes .....	87
1.2.15 Matrix metalloproteinases (MMPs) .....	89

1.2.16 MMP production by monocytes .....	92
1.2.17 Monocytes and MMP-9 .....	92
1.3 The Complement System .....	95
1.3.1 Background .....	95
1.3.2 The complement system .....	96
1.3.3 Complement activation and lung disease .....	101
1.3.4 Complement fragment C3d .....	102
1.3.5 C3d in AATD .....	105
1.3.6 Complement receptor CR2 .....	106
1.3.7 Soluble CR2 (sCR2) .....	110
1.3.8 Complement targeted therapeutics .....	110
1.4 Summary .....	113
1.5 Study Aims .....	115
Chapter 2: Materials and Methods .....	117
2.1 Equipment .....	118
2.1.1 Chemicals and Reagents .....	118
2.1.2 Antibodies .....	118
2.2 Sampling .....	123
2.2.1 Cell line work .....	123
2.2.2. Patient sampling .....	123
2.2.3 Isolation of plasma from whole blood .....	124

2.2.4 Bronchoalveolar lavage (BAL) sample collection .....	124
2.2.5 Ethical Approval .....	126
2.3 Laboratory Techniques .....	127
2.3.1 U937 cell culturing.....	127
2.3.2 Raji B cell culturing.....	127
2.3.3 U-937 cell treatment.....	128
2.3.4 Trypan blue testing for cell viability .....	128
2.3.5 Monocyte isolation .....	128
2.3.6 Treatment of purified peripheral circulating monocytes .....	130
2.3.7. BAL processing of supernatants .....	130
2.3.8 Processing of BAL pellet for cell counting and viability .....	131
2.3.9 Determining cell differential of BAL samples .....	131
2.3.10 Quantification of urea in BAL samples .....	132
2.3.11 Protease array membranes.....	132
2.3.12 RNA extraction with Trizol reagent.....	135
2.3.13 RNA extraction with Nucleospin RNA columns .....	135
2.3.13 Complementary deoxyribonucleic acid (cDNA) synthesis .....	138
2.3.14 Confirmation of qRT PCR product by agarose gel .....	138
2.3.15 RT-PCR.....	139
2.3.16 FACS analysis for surface expression of CR2 on U937 cells and purified monocytes.....	139

2.3.17 Flow cytometry analysis of CR2 on lymphocyte subsets obtained from BAL .....	142
2.3.18 Gating strategy used to identify myeloid cells in BAL .....	143
2.3.19 MTS assay for cell viability .....	144
2.3.20 Preparation of whole cell lysates .....	145
2.3.21 Bicinchonic acid (BCA) protein determination .....	145
2.3.22 Sodium Dodecyl Sulphate Polyamide Gel Electrophoresis (SDS PAGE) .....	146
2.3.23 Western Blot Analysis .....	149
2.3.24 Enzyme linked immunosorbent assay (ELISA) .....	149
2.3.25 Confocal microscopy .....	153
2.4 Statistical Analyses .....	154
Chapter Three: Establishing a signalling axis for C3d on monocytes in the circulation and airways .....	155
3.1 Introduction .....	156
3.1.1 Chapter Aims .....	159
3.2. Investigating expression of CR2 on a monocyte-like cell line .....	161
3.2.1 Rationale for cell line work .....	161
3.2.2 Design of early U937 experiments .....	161
3.2.3 Summary of initial U937 results .....	164
3.2.4 Conclusion .....	166
3.3 Further evaluation of CR2 on the surface of U937 cells by FACS analysis ..	168

3.3.1 Rationale for further U937 work .....	168
3.3.2 Amendments to U937 treatment protocol.....	168
3.3.3 Summary of results using extended panel of pro-inflammatory stimuli ..	170
3.3.4 Conclusion of U937 cell line work .....	172
3.4. Evaluating CR2 gene expression in circulating monocytes by RT-PCR .....	174
3.4.1 Background .....	174
3.4.2 Rationale for RTPCR selection .....	174
3.4.3 Methods and technical challenges .....	175
3.4.4 Overview of Results .....	178
3.4.5 Conclusions from RTPCR .....	180
3.5 Confirmation of MM and ZZ monocyte expression of CR2 protein by Western blotting .....	182
3.5.1 Rationale for Western Blotting.....	182
3.5.2 Methods and technical considerations .....	182
3.5.3 Results .....	183
3.5.4 Conclusion of whole cell lysates experiments .....	186
3.6 Evaluation of CR2 on the membrane of circulating MM monocytes by FACS analysis.....	188
3.6.1 Background and rationale .....	188
3.6.2 Methods and technical considerations .....	189
3.6.3 Results of FACS analysis of circulating MM monocytes .....	189
3.6.4 Conclusion of Flow Cytometric Analyses .....	191

3.7 Elucidation of CR2 on the membrane of MM and ZZ monocytes by Confocal Microscopy .....	192
3.7.1 Background .....	192
3.7.2 Methods .....	192
3.7.3 Results of Confocal Microscopy .....	193
3.7.4 Conclusion of confocal microscopy results .....	196
3.8 Identifying CR2 on the surface of a population of airway cells using multi colour flow cytometry.....	197
3.8.1 Background .....	197
3.8.2 Methods and technical considerations .....	198
3.8.3 Results of multi colour FACS analysis of BAL samples .....	206
3.8.4 Conclusion .....	215
3.9 Discussion of overall results .....	218
Chapter Four: Evaluating the effects of C3d on MM and ZZ monocytes .....	223
4.1 Introduction .....	224
4.1.1 Chapter Aims .....	227
4.2 Assessing production of the pro-inflammatory cytokine IL-8 by U937 cells in response to treatment with C3d .....	229
4.2.1 Background and rationale .....	229
4.2.2 U937 treatment with C3d and choice of control.....	230
4.2.3 Overview of results.....	230
4.2.4 Discussion of Results.....	232

4.3 Assessing the viability of peripheral circulating monocytes in response to C3d by MTS Assay .....	234
4.3.1 Background .....	234
4.3.3 Results of MTS Assay .....	235
4.3.4 Discussion of impact of C3d on monocyte viability .....	238
4.4 Investigating production of IL-8 by circulating MM monocytes in response to C3d .....	240
4.4.1 Background .....	240
4.4.2 Monocyte treatment with C3d and recovery of supernatants .....	241
4.4.3 Summary of Results .....	242
4.4.4 Discussion of the effect of C3d on IL-8 production by MM monocytes ...	244
4.5 Profiling the cytokine response of monocytes to C3d using cytokine array membranes .....	245
4.5.1 Background .....	245
4.5.2 Methods .....	246
4.5.3 Summary of Cytokine Array Results .....	246
4.5.4 Discussion of cytokine array results .....	249
4.6 Measurement of CD14 production by MM compared to ZZ monocytes in response to C3d .....	253
4.6.1 Background .....	253
4.6.2 Methods: ELISA for CD14 .....	254
4.6.3 Summary of CD14 ELISA results .....	254

4.6.4 Overview of effect of C3d on sCD14 production by ZZ and MM monocytes .....	257
4.7 ELISA for MMP-9 in the supernatants of monocytes treated with C3d .....	259
4.7.1 Background .....	259
4.7.2 Methods: Measuring MMP-9 in monocyte supernatants .....	260
4.7.3 Summary of MMP-9 ELISA results.....	260
4.7.4 Implications of results.....	263
4.8 Profiling the protease response of MM and ZZ monocytes to C3d using protease array membranes.....	265
4.8.1 Background .....	265
4.8.2 Principles of protease arrays and methods .....	266
4.8.3 Results .....	267
4.8.4 Discussion.....	270
4.9 ELISA for MMP-12 in supernatants of MM and ZZ monocytes treated with C3d .....	273
4.9.1 Background .....	273
4.9.2 Quantifying MMP-12 in monocyte supernatants: Methods .....	274
4.9.3 Results .....	274
4.9.4 Discussion.....	277
4.10 Measurement of MMP12 in plasma by ELISA .....	278
4.10.1 Background .....	278
4.10.2 Methods .....	279

4.10.3 Results .....	280
4.10.4 Discussion .....	282
4.11 ELISA for MMP-1 in monocyte supernatants .....	284
4.11.1 Background .....	284
4.11.2 Methods .....	285
4.11.3 Results .....	286
4.11.4 Conclusion .....	288
4.12 ELISA for PR3 in the extracellular supernatants of MM and ZZ monocytes treated with C3d.....	290
4.12.1 Introduction .....	290
4.12.2 Methods: Quantifying PR3 in C3d treated monocyte supernatants.....	291
4.12.3 Results .....	292
4.12.4 Discussion.....	294
4.13 General Discussion.....	296
Chapter 5: Discussion and Future Directions .....	303
5.1 Summary .....	304
5.2 Establishing a signalling axis for C3d .....	308
5.2.1 Observations from cell line work .....	308
5.2.2 Confirming CR2 expression by circulating MM and ZZ monocytes .....	309
5.2.3 Identification of CR2 on lymphocyte subsets in the airways.....	312
5.3.0 Establishing the effect of C3d on monocyte function.....	315
5.4 Challenges and criticisms .....	320

5.5 Future Directions .....	327
References .....	330

## **Glossary of Abbreviations**

AAT	alpha one anti-trypsin deficiency
AATD	alpha one anti trypsin deficiency
AM	Alveolar macrophage
ANCA	anti- neutrophil cytoplasmic antibody
APC	antigen presenting cells
ARDS	Acute respiratory distress syndrome
ATCC	American Type Culture Collection
ATS	American Thoracic Society
BAL	Bronchoalveolar lavage
BCA	Bicinchonic acid
BM	Bone Marrow
BPI	Bacteriacidal permeability increasing protein
BSA	Bovine Serum Albumin
C3d	Complement fragment C3d
C3aR	Receptor for complement fragment 5a
CAD	Coronary artery disease
Cath G	Cathepsin G
CD 14	Cluster of differentiation 14
CD21	Cluster of differentiation 21 a.k.a CR2
CD 169	a.k.a Siglec F

CF	Cystic Fibrosis
COPD	Chronic Obstructive Pulmonary Disease
CR2	Complement Receptor 2 a.k.a. CD21
CR4	Complement receptor 4
CRP	C reactive protein
CSF	Colony stimulating factor
CT	Computed Tomography
Ct	Cycle threshold
CXR	Chest X-ray
DC	Dendritic cells
DepC	diethyl pyrocarbonate
DFP	Diisopropylfluorophosphate
DTT	Dithiothreitol
EBV	Ebstein Barr virus
ECM	Extra cellular matrix
EDTA	Ethylene diamine tetra acetic acid
EGPA	Eosinophilic granulomatosis with polyangiitis
EGTA	Ethylene glycol tetracetic acid
ELF	Epithelial Lining Fluid
ELISA	Enzyme linked immunosorbent assay
ER	Endoplasmic reticulum

ERAD	Endoplasmic reticulum associated degradation
ERS	European respiratory society
FACS	Flouroscein activated cell sorting
FcRs	Fc Receptors
FcR1	Fc Receptor one a.k.a. CD64
FCS	Foetal calf serum
FDC	Follicular dendritic cells
FCS	Forward Scatter
FMO	Florescence minus one
G-CSF	Granulocyte colony stimulating factor
GM-CSF	Granulocyte Macrophage colony stimulating factor
GMP	Granulocyte macrophage progenitors
GN	Glomerulonephritis
GOLD	Global initiative for obstructive lung disease
GPA	Granulomatous polyangitis
HC	Healthy Control
HCl	Hydrochloric acid
HEPES	4-(2-hydroxyethy)piperazine-1-ethanesulfonic acid
HSC	Haematopoietic stem cells
ICAM-1	Intracellular adhesion molecule 1
IEF	Isoelectric focusing

IL-F	Á	Interleukin one beta
IL-8		Interleukin 8
IM		Interstitial macrophage
IV		Intravenous
LBP		Lipopolysaccharide binding protein
LPS		Lipopolysaccharide
MAB		monoclonal antibody
MAP		mean arterial pressure
mCD14		Membrane bound CD14
MDP		Macrophage dendritic progenitors
MFI		Median fluorescent intensity
MHC		Membrane Histocompatibility complex
MMP		Matrix Metalloproteases
MoAM		Monocyte derived alveolar macrophage
MPO		Myeloperoxidase
MPS		Mononuclear phagocyte system
NE		Neutrophil Elastase
NCFB		Non CF Bronchiectasis
NHLBI		National Heart Lung and blood institute
NS		Normal Saline
PAMPs		Pathogen Associated Molecular Patterns

PAS	Periodic Acid Schiff
PBS	Phosphate buffered saline
PERK	Protein kinase RNA like ER kinase
PBGB	Pulmonary blood gas barrier
PFA	Paraformaldehyde
PMA	Phorbol 12-myristate 13-acetate
PMN	Polymorphonucleocytes
PR3	Proteinase 3
qRT PCR	qualitative real time polymerase chain reaction
RA	Rheumatoid arthritis
RCL	Reactive central loop
ROS	Reactive Oxygen species
SB	Sample Buffer
SCR	Short consensus repeats
sCD14	Soluble CD14
SDS	Sodium Dodecyl Sulphate
SDS PAGE	Sodium Dodecyl Sulphate Polyamide Gel Electrophoresis
sCR2	Soluble CR2 aka soluble CD21
SLE	Systemic lupus erythematosus
SPEP	Serum protein electrophoresis
SSC	Side scatter (in flow cytometric analysis)

V Ö Ø	Transforming Growth Factor Beta
TLR	Toll like receptor
V Þ Ø	Tumour necrosis factor alpha
TRAMs	Tissue resident alveolar macrophages
UPR	Unfolded protein response
WHO	World health organisation

## List of Figures

Figure 1.1: AAT Structure with asparagine residues and attached glycans

Figure 1.2 AAT phenotypes assessed by Isoelectric focusing (IEF)

Figure 1.3 Coronal CT of the thorax in a patient with ZZ AATD

Figure 1. 4 Liver biopsy slide showing PAS positive inclusion bodies from an individual with ZZ AATD

Figure 1. 5 Liver biopsy slide showing PAS positive inclusion bodies from an individual with ZZ AATD

Figure 1.6 Monocyte Lifecycle

Figure 1.7 Heterogeneity of lung macrophage populations

Figure 1.8 Key differences between ZZ and MM monocytes

Figure 1.8: Production and regulation of MMPs by monocytes

Figure 1.10 Overview of the Complement System

Figure 1.11 Mechanism of C3d production

Figure 1.12: Structure of the C3d:Complement Receptor 2 Complex

Figure 2.1: Workflow for RNA isolation using the Nucleospin RNA extraction kit (ThermoFisher)

Figure 2.2: Workflow for PR3 and sCD14 ELISAs using the SimpleStep ELISA kit (Abcam)

Figure 3.1: Measurement of CR2 on the surface of U937 cells in the presence and absence of protease inhibitors and following exposure to pro-inflammatory stimuli for 10mins

Figure 3.2: Assessment of CR2 on the surface of U937 cells by FACS demonstrates increased expression following 10min treatment with PMA

Figure 3.3: Expression of CR2 on MM and ZZ monocytes by qRT-PCR with confirmation of PCR product on agarose gel

Figure 3.4: Whole cell lysates of MM monocytes and Raji B cell control run in the presence of DTT generates a smaller than expected 50kDa immunoband suggestive of protein fragmentation

Figure 3.5: Whole cell lysates of monocytes and Raji B cells run on a 10% (w/w) gel without DTT shows >175kDa immunoband across all samples investigated

Figure 3.6: Confirmation of CR2 on the membrane of circulating MM monocytes with no increase in expression following 10 min treatment with pro-inflammatory stimuli

Figure 3.7 Confirmation of CR2 on the surface of MM and ZZ monocytes by confocal microscopy

Figure 3.8 Monocytes stained with DAPI without CR2 anti body visualised by confocal microscopy with inclusion of CR2 anti-body and DAPI stained Raji B cells as a positive control

Figure 3.9: Speedy Diff staining of BAL sample with labelling of visible lymphocyte subsets

Figure 3.10 Identification of macrophages in BAL samples using multi-colour flow cytometry

Figure 3.11 Multi colour flow cytometry identifying expression of CR2 on alveolar macrophages

Figure 3.12 Multi colour flow cytometry identifying 3 subsets of monocytes in BAL samples

Figure 3.13 Multi-colour flow cytometry identifying CR2 on the surface of 3 monocyte subsets obtained from BAL samples

Figure 3.14 Relative expression of CR2 on monocyte subsets and alveolar macrophages in BAL using multi colour flow cytometry

Figure 4.1 Measurement of IL-8 production by U937 cells in response to C3d as determined by ELISA

Figure 4.2: Cell viability as measured by MTS assay does not decrease significantly following 24h treatment with C3d

Figure 4.3 Measurement of IL-8 production by healthy control monocytes in response to treatment with C3d by ELISA

Figure 4.4 Cytokine expression by MM monocytes in response to C3d assessed by cytokine array membranes and densitometry

Figure 4.5: ELISA for sCD14 in the supernatants of monocytes treated with C3d

Figure 4.6: ELISA for MMP-9 in the supernatants of monocytes treated with C3d

Figure 4.7 Protease array membranes and densitometry from MM and ZZ monocytes treated with C3d

Figure 4.8: Measurement of MMP-12 production by ELISA following C3d treatment of MM monocytes compared to ZZ cells

Figure 4.9 Levels of MMP-12 were measured in plasma by ELISA

Figure 4.10: Measurement of MMP-1 production by ELISA in MM versus ZZ

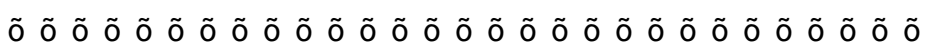
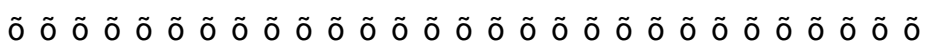
monocytes  È 89

Figure 4.11: Measurement of PR3 production by ELISA in MM versus ZZ

monocytes  È 5J

## List of Tables

Table 1.1: Overview of monocyte subset surface markers, proportional representation, cytokine profiles and function in the circulation

Table 1.2: Summary of the physiologic activities of complement

Table 2.1: Primary anti-bodies

Table 2.2: Secondary Anti-bodies

Table 2.3: Anti bodies used in flow cytometric analysis of BAL samples

Table 2.4: List of proteases identifiable by the R&D Human Protease Array Kit

Table 2.5: Protease inhibitors

Table 2.6: Running gel components

Table 2.7: Stacking gel components

Table 3.1: Pro-inflammatory stimuli used in early U937 experiments and rationale for selection

Table 3.2: Choice and rationale for additional pro-inflammatory agents used in U937 flow cytometry experiments

Table 3.3: Demographics of patients involved in multi colour flow cytometric analysis of lymphocyte subsets from BAL

## **Posters and presentations**

Establishing the impact of dysregulated complement activation on monocytes in alpha-1 anti-trypsin deficiency. Gough C., Fee L., Dunlea D., Reeves E, McElvaney NG. Beaumont Hospital Translational Research Awards; Beaumont Hospital, Dublin. September 2019. Poster Presentation.

Role of monocytes in Alpha-1 Antitrypsin Deficiency (AATD). Hussein I., Gough C., Reeves E., McElvaney NG. Beaumont Hospital Translational Research Awards; Beaumont Hospital, Dublin. September 2019. Poster Presentation.

Establishing the impact of dysregulated complement activation on monocytes in alpha-1 anti-trypsin deficiency. Gough C., Fee L., Dunlea D., Reeves E, McElvaney NG. RCSI research day, March 2019, Poster presentation

## **Abstract**

The term alpha one anti-trypsin deficiency (AATD) refers to any qualitative or quantitative deficiency of alpha one anti-trypsin (AAT) protein. AATD represents a major cause of early onset emphysema and liver failure and is frequently under-diagnosed. AAT acts as a binding partner of complement protein C3. Cleavage of C3 by proteases represents the final common step of all 3 described pathways of complement activation.

High levels of the complement fragment C3d has been previously identified in the plasma and airways of those with ZZ AATD suggesting dysregulated activation of the complement cascade in AATD. The aim of this study was to explore what kind of effect C3d was likely to have on monocytes in ZZ AATD and healthy MM controls.

The receptor for C3d, CR2 was identified on the surface of ZZ and MM monocytes. Findings were confirmed using a combination of reverse transcription polymerase chain reaction (RT PCR), Flow cytometry, western blotting (WB) and confocal microscopy (CM). Multi colour flow cytometry was used to identify CR2 on the surface of leucocyte subsets in the airways. Treatment of MM and ZZ monocytes resulted in significant increases in the levels of matrix metalloproteinase 9 (MMP-9), proteinase 3 (PR3) and soluble CD14 (sCD14) detectable in monocyte supernatants. This raises questions about the role C3d signalling through monocytes and monocyte-derived macrophages plays in the pathogenesis of AATD lung disease.

In conclusion, this study confirms the presence of the C3d receptor CR2 on the surface of monocytes. Results presented facilitate the generation of hypotheses that expand our understanding of the role monocytes play in the pathogenesis of ZZ AATD

## Acknowledgments

The experience of undertaking and completing this MD project has revealed to me, in a very tangible way, the meaning of the phrase: it takes a village.

To Prof. McElvaney, you gave me an important opportunity for which I am grateful. Thank you.

To Dr. Emer Reeves, you pushed me to stretch my thinking and challenge myself. You navigated the way for me and gave me so much of your time. Thank you.

To Mark Murphy, Karen McQuilian, Danielle Dunlea and Laura Fee- you showed me patience and kindness in sharing your expertise. This project would not have been possible without your guidance. Thank you.

To Tomás, Geraldine and Ann in the alpha one foundation. We had some laughs (they were needed!). Thank you.

To my family- Mum, Dad, siblings numbered 3-11 inclusive. Q • } q c Á ã c Á \* ! ^ æ c Á @[ , ^ q ç ^ Á & [ { ^ Á c [ \* ^ c @ ^ ! Ñ Á Ÿ [ ~ Á æ ! Thank you Á [ } | ^ Á c ^ æ { Á ,

To Kelly, mo leathchúpla, for reminding me I can do hard things. Thank you.

To Orla, Jen, Sarah, Emily you ensured something close to sanity was maintained during the writing process. Thank you.

To the doctors, nurses, HCAs, clinical engineers and everyone working in Beaumont Hospital who welcomed me back into the fold in March 2020. May we never see the like again. Thank you.

To the patients I have met over the past 2 years- your generosity is needed to move any scientific endeavour forward. Without you, there is no progress. Thank you.

To Tom, Ø! æ} \ Á U q P æ! æÁ [ } & ^ Á , ! [ c ^ K Á Q} Á c ã { ^ • Á [ ~ Á & ! ã  
again whom we love. For your perseverance, thank you.

Funding for this project was provided by the Alpha-1 Foundation, Ireland.

## Dedication

This thesis is dedicated to my uncle Niall Hughes.  $\mathbb{C}^2 \times \mathbb{C}^2 \rightarrow \mathbb{C}^2 \times \mathbb{C}^2$  @æq Á à [ ! } Á c [ [ Á •  
the rewards of all we learned since 1963.

## **Chapter 1: Introduction**



considerable heterogeneity in epidemiological study methodology. Scandinavian studies from the 1970s employed prospective screening of neonates, while others have directed their efforts towards targeted screening of at risk populations(7). A 2002 meta-analysis reported the highest prevalence of the most severe Pi\*Z variant in northern and western European countries (mean gene frequency 0.0140)(4). A 2004 update estimated global prevalence of MZ and MS heterozygotes at 116 million and the prevalence of ZZ, SS and SZ at 3.4 million(8).

Whilst the rate of detection of clinically significant genotypes may be low, the evidence suggests that severe AATD is overrepresented in certain populations. Targeted detection has been used to determine the prevalence of AATD in symptomatic cohorts and is estimated to be present in as many as 2% of patients with chronic obstructive pulmonary disease (COPD)(9). As Ireland has amongst the highest prevalence, mortality and hospital admission for COPD in the organisation for economic co-operation and development (OECD) ascertaining the contribution of AATD to this has been a topic of great interest in recent years(10). In addition to its high prevalence in COPD cohorts, AATD has also been linked to the development of auto immune diseases including rheumatoid arthritis (RA) and systemic lupus erythematosus (SLE)(11).

Irish data on the epidemiology of AATD in Ireland was published for the first time in 2011(12). Carroll and colleagues took samples from 3000 Irish patients with COPD, refractory asthma, cryptogenic liver disease and first-degree relatives of known AATD patients. In addition, they tested 1100 samples from the Trinity College Dublin

biobank. This cohort was randomly selected from the electoral register and was thought to be more representative of the general population. A prevalence of 0.054 for the S allele and 0.024 for the Z allele was determined, which is amongst the highest previously reported. From this data we can extrapolate that 9.8% of the population carry the S allele and 4.6% will have a Z variant. It is probable that 1 in 2,104 Irish people are ZZ (approximately 2200 individuals), though only a fraction of these have been identified.

### 1.1.2 Alpha One anti-trypsin protein

Alpha one anti-trypsin (AAT) is a 52 kDa plasma glycoprotein encoded by the SERPINA1 gene on chromosome 14q32.1-32.2(13). Ninety percent of AAT protein is synthesised by hepatocytes (Koj et al 1978) with smaller contributions made by monocytes (14), macrophages (15), neutrophils (16), pulmonary alveolar cells and intestinal epithelial cells (17).

Mature AAT is a polypeptide chain composed of 394 amino acids. The secondary

structure of AAT is a  $\beta$ -sheet structure that supports a mobile reactive central loop (RCL) at the C terminal region (18). The action of AAT is often likened to that of a mouse trap. The exposed central loop presents a methionine residue (met 358) to a target protease. Cleavage of the Met 358 residue by the protease results in linkage of the serpin (AAT) carboxyl group and the serine hydroxyl of the protease.

This binding event results in a structural rearrangement of the AAT protein (19). The

rearrangement of the AAT protein occurs(20). This distorts the protease binding site and resulting in its inactivation. Oxidation of the Met 358 and Met 351 residues results in loss of the anti-protease activity of AAT -an effect that is exaggerated by cigarette smoking (21).

The structure of mature AAT protein is depicted in Figure 1.1. Post translational modification of AAT includes the addition of glycan residues which will be discussed further in section 1.1.3.

Newly synthesised AAT protein is transported to the endoplasmic reticulum (ER) where it is folded and assembled for function. The most commonly described mutations in SERPINA1 result in misfolding of AAT, formation of polymer aggregates and sequestration within hepatocytes(22) The most common variants include the Z (Glu342Lys) and S (Glu264Val) mutations (23), which will be described in greater detail in section 1.1.4.

AAT is found in abundance in plasma. Normal concentration is between 0.9-1.75 g/L (13). As AAT is an acute phase reactant, levels rise during any period of intercurrent illness. Thus, care must be taken, and consideration given to the clinical context

, @^ } Á ã } c ^ | ] | ^ c ã } \* Á æÁ ± } [ | { æ| q Á ] | æ• { æÁ ŒŒEV Á | ^ ç ^

with moderate to severe deficiency (PiMZ, PiSS, PiSZ) may demonstrate levels suggestive of normal AAT status if tested during an acute inflammatory illness (9).

The level of C-reactive protein (CRP) is commonly used in clinical practice to follow levels of inflammation. AAT levels greater than 1g/L are seen in as many as 80% of patients with moderate AAT deficiency in the setting of a mild increase in CRP (>8mg/L) (24). Conversely, levels of >1.1g/L in the setting of normal CRP all but rule out a deficient genotype (25).

Once released into the peripheral circulation AAT protein has a half-life of 4-5 days. 80% of circulating AAT diffuses into tissues with between 0.5 and 10% eventually reaching pulmonary alveolar fluid(4).

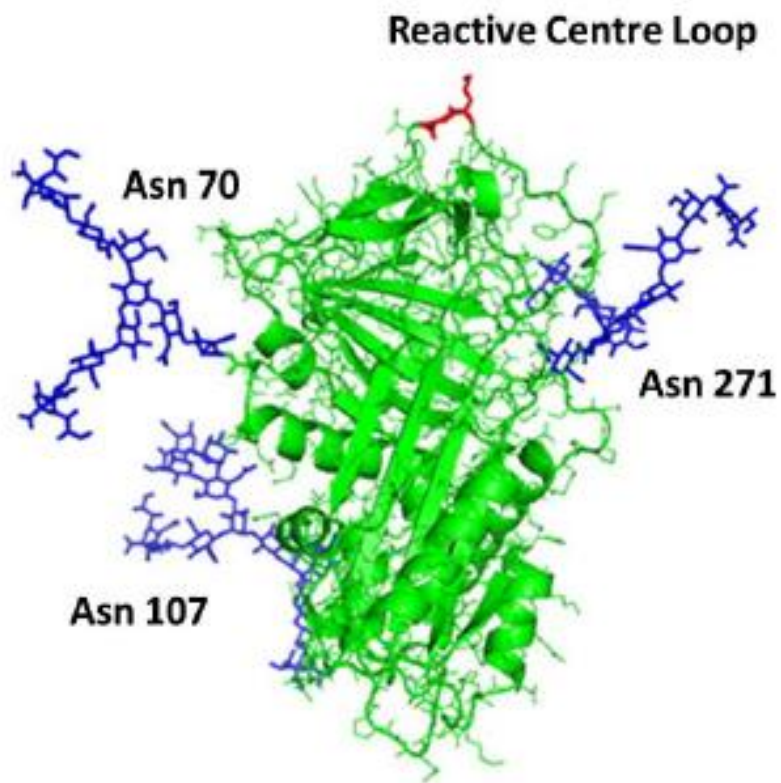


**Figure 1.1: AAT Structure with asparagine residues and attached glycans**

The main structure of the AAT protein is represented in green. The reactive centre loop with the Methionine at residue 358 (Met 358) is depicted in red. Attached glycan side chains are shown in blue.

Adapted from McCarthy C et al, The role and importance of glycosylation of acute phase proteins with focus on alpha-1 antitrypsin in acute and chronic inflammatory conditions. *J Proteome Res.* 2014;13(7):3131-43.

### 1.1.3 Glycosylation of AAT

Under normal conditions, AAT undergoes post translation modification by glycosylation within the ER. Aberrant glycosylation has been previously linked to the development of inflammatory disorders and malignancy (26).

Addition of glycan residues to AAT serves to protect the protein from proteolysis thereby extending its half-life and preventing protein aggregation within the ER and resultant down-stream ER stress. Within the ER, AAT is modified by the addition of 3 *N*-glycosidically linked oligosaccharides at asparagine sites 70, 107 and 271 (Figure 1.1). Each *N*-glycosylation site feature biantennary structures in addition to diantennary and traces of tetraantennary *N*-glycans(27). Variations in glycan residues result in differing protein charges. Owing to this, 7 different glycoforms of AAT designated as M0-M8 are identifiable on isoelectric focusing gels (IEF) (28) (Example provided in Figure 1.2). The technique of IEF is discussed further in section 1.1.5. Briefly, IEF uses electrophoresis to separate analytes based on their isoelectric point (29). Mutation-causing base pair substitutions such as Glu342Lys and Glu264Val that encode for Z and S AAT respectively alter the net charge of the protein. Movement through the IEF polyacramide gel occurs at different rates resulting in the generation of distinctive patterns that allow distinction between phenotypes(9).

Factors including age, gender, smoking status, and levels of the pro-inflammatory cytokine IL-6 have been previously shown to influence the degree to which AAT undergoes glycosylation (30). Within our laboratory, studies of subjects with resolving community acquired pneumonia (CAP) demonstrate that AAT protein becomes more heavily endowed with negatively charged glycans during the resolution phase of CAP (31). This heavily sialylated AAT complexes with greater

affinity to the pro inflammatory cytokine interleukin 8 (IL-8) when compared to normal AAT produced during the acute phase. Under normal conditions IL-8 signals through the neutrophil surface receptor CXCR1 mediating neutrophil chemotaxis. Binding of AAT to circulating IL-8 allows for enhanced inhibition of CXCR mediated neutrophil chemotaxis and more rapid resolution of the inflammatory response (32).

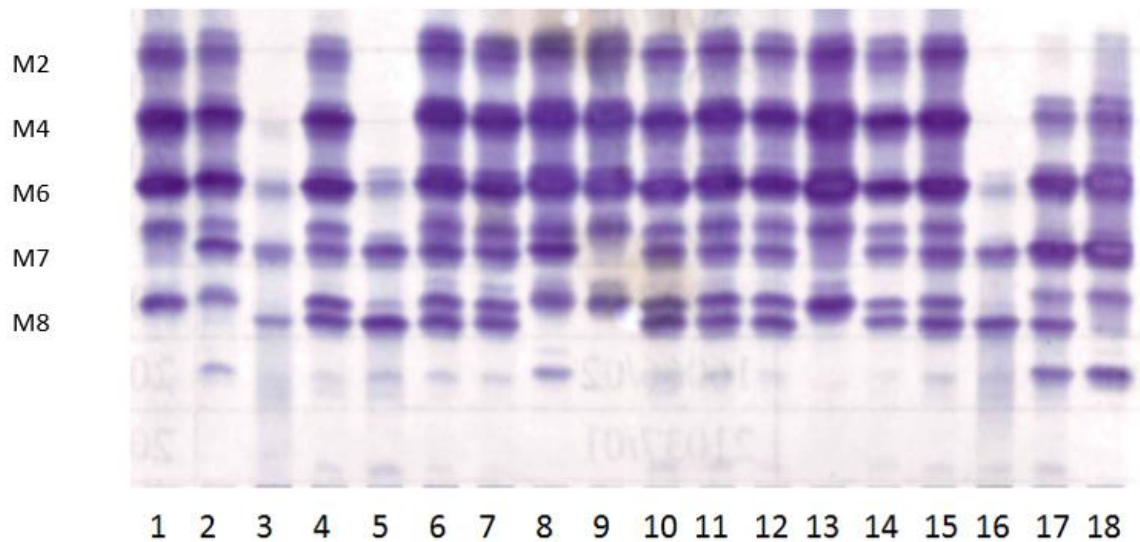


**Figure 1.2 AAT phenotypes assessed by Isoelectric focusing (IEF)**

Phenotyping for AATD is performed using IEF on a polyacramide pH-gradient gel. PiMM (lane 1), PiMS (lane 2) and PiZZ (lane 3) controls are included for reference.

The major bands (M2,4, 6, 7 and 8) that correspond to the main glycoforms of M AAT are labelled.

Here, PiMS (lane 8), PiMZ (lanes 4,6-7,10-12,14-15), PiSS (lane 18), PiSZ (lane 17) and PiZZ (lanes 5, 16) are detected.

### 1.1.4 Genetics of AAT deficiency

As alluded to previously, AATD occurs due to autosomal co-dominant inheritance of mutations in the SERPINA1 gene on chromosome 14 (locus 14q32.1) (33). The most common and severe form of AAT deficiency occurs as a result of the Z mutation. The Z mutation is a single point mutation caused by substitution of a lysine for a glutamic acid residue at position 342 (Glu342Lys). This mutation occurs at the hinge-point of AAT and results in a conformational change in the shape of the AAT molecules forming dimers or polymers (22). Mis-folding of AAT protein leads to its retention and sequestration within the ER of hepatocytes. This has two major downstream effects- activation of an ER stress response within hepatocytes and reduced secretion of AAT into the circulation. The former is associated with the development of cirrhosis (34) whilst the later reduces the anti-protease capacity of AAT in biologic fluids and reduces neutrophil elastase (NE) inhibition (19-21).

Other commonly encountered genotypes include Pi\*MZ, Pi\*ZZ, Pi\*SZ and Pi\*MS. As well as Pi\*ZZ individuals, compound heterozygotes such as Pi\*SZ and Pi\*MZ are also at increased risk of emphysema (35, 36). The S mutation is a point-mutation with substitution of a valine for a glutamic acid at position 264 (Glu264Val) (37).

± P ~ | | q Á ç æ! ã æ} c • Á æ! ^ Á Ù Ò Û Ú Q P Œ F Á p r e m a t u r e s t a p } • Á c @ æ c Á codon(38). Homozygotes for these variants have undetectable AAT levels and a particularly high risk of emphysema(39). Interestingly, these cohorts do not go on to develop AATD-related liver disease. Liver disease in AATD is attributable to a toxic ± \* æ ã } Á [ ~ Á ~ s e e n i n h e p a t o c y t e s w h e r e a b n o r m a l A A T p r o t e i n i n sequestered in the ER(40). This triggers a series of stress reactions collectively referred to as the unfolded protein response (UPR) (discussed further in section

1.1.10). As those with null variants fail to produce any AAT protein this effect is not observed in these cohorts.

### 1.1.5 Diagnosis of AATD

Though several laboratory techniques can be used to diagnose AATD, most physicians will initially opt for a quantitative measurement of serum AAT levels commonly carried out by nephelometry or turbidimetry (41). Quantification of plasma levels of AAT is useful for screening populations for whom the index of suspicion of AATD is low. The hallmark of AATD is the presence of low circulating levels of AAT ] ! [ c ^ ã } Á ã } Á à | [ [ â È Á Á Š ^ ç ^ | • Á ^ ¢ & ^ ^ â ã } \* Á F ® € I \* Đ Š Á negative predictive value for the presence of the PiZZ genotype (42). This holds true even amongst those patients with symptoms of AATD related disease.

As previously mentioned AAT levels >1g/L are observed in as many as 80% of patients with moderate AATD in the setting of a CRP greater than 8mg/L (43).

Combined measurement of CRP and AAT levels can be used to screen for milder variants of AATD. Levels >1.1g/L together with a normal CRP have been shown to reliably out-rule the PiMZ genotype (24, 44). If low circulating levels are detected, samples should be sent for further analysis including phenotyping and genotyping.

Phenotyping using isoelectric focusing (IEF) enables visual identification of specific AAT isomers in circulating plasma(45). In this manner it can be regarded as an imperfect surrogate for genetic testing. Each allele is allocated a letter code based on the pattern observed when the protein is separated out in pH gradient gel. IEF is performed by loading the samples of interest on to the gel alongside three known control phenotypes. The distinct migration patterns of the AAT proteins in each

sample are compared to the controls and allow determination of the biochemical phenotype. IEF allows for the detection of multiple AAT variants in one assay but interpreting the result requires a degree of expertise and is best performed in specialist centres(9). An example of an AAT phenotyping by IEF is shown in Figure 1.2.

Genotyping provides definitive identification of the AAT allelic combinations that give rise to misfolded AAT protein in the circulation. DNA is collected and probed for mutations in the SERPINA1 gene using polymerase chain reaction (PCR). PCR multiplies PiZ-mutation containing regions of the gene. Amplicons generate

When results of PCR are compared to those obtained with IEF it has

gene sequencing are less open to interpretation than those obtained with IEF it has some limitations. PCR amplifies only those genes which are deliberately sought. This means that rare mutations can be falsely reported as normal. In cases where there is discordance between the IEF and genetic analysis, consideration should be given as to whether a rare mutation is responsible for the findings on IEF.

### 1.1.6 Rationale for diagnostic testing

Current European and North American guidelines recommend testing for AATD in those with COPD, bronchiectasis, cryptogenic liver disease, panniculitis or vasculitis (44, 47). The World Health Organisation (WHO) advocate phenotyping for first degree relatives of index AATD cases (48).

Work by Thelin and colleagues in 1996 confirmed that individuals who are aware of their AATD status are less likely to smoke in adulthood(49). Sixtyone patients previously identified through neonatal screening and their parents were followed up

at 5-7 and 18-20 years. Whilst smoking rates amongst parents were unchanged between the AATD group and matched controls, smoking rates amongst 18-20 AATD patients were significantly reduced ( $p < 0.05$ ). This presents a powerful argument in favour of screening.

Diagnosis of AATD can be achieved by any one of three means: screening in high risk cohorts, selected population screening, or as was the case leading to its discovery, by serendipitous detection (50). In recent years cases have also been identified as a result of commercially available genetic testing kits (51).

#### **1.1.7 Anti-protease effects of AAT**

AAT was originally named for its ability to inhibit pancreatic derived trypsin(52) and its action as an inhibitor of proteases is described at length in the literature(13, 18). Proteases can be categorised based on their catalytic residues. The 4 major groups of proteases described to date are the serine proteases, cysteine proteases, metalloproteases (MMPs) and aspartic acid proteases. AAT is considered to be the archetype of the serine protease inhibitor (SERPIN) superfamily and preferentially inhibits the actions of serine proteases such as NE (53), Cathepsin G and Proteinase 3 (PR3) (54). The mature forms of each have been previously identified as being stored in the azurophilic granules of neutrophils(55). Serine proteases can act both intra and extra cellularly. Within cells, they play a role in degrading microbial proteins within phagosomes. Extracellularly, they act to degrade an array of proteins that collectively form the extracellular matrix (ECM) (56).

Of all the serine proteases, AAT has the greatest specificity for NE to which it binds in an equimolar ratio (57). The RCL at Met 358 residue has been previously shown

to determine protease specificity (58). As previously alluded to, SERPINs inhibit

the exposed RCL presents a Met358 for

cleavage by the target protease. Cleavage results in irreversible linkage of the serpin

(AAT) carboxyl group and the serine hydroxyl of the protease ultimately causing

structural rearrangement and inactivation of the AAT protein (14). This binding event

exposes a binding site on the AAT-protease complex that is recognised by serpin-

enzyme receptors on hepatocytes facilitating removal from the circulation (32).

Increased recognition of AAT-protease complexes by hepatocytes sets up a positive

feedback loop that increases AAT gene expression thereby maintaining circulating

levels of AAT during times of high demand (33). Published data has shown activity of

AAT across a variety of proteases including mast cell derived tryptase and chymase

(59), lymphocyte derived granzyme B(60) and matrilysin localised to the membrane

of epithelial cells (61). More recent evidence suggests that AAT is capable of

inhibiting other classes of proteases including the MMP ADAM-17 (62) and aspartic

cysteine proteases (63).

Mutations in the SERPINA1 result in the production of abnormal variants of AAT

protein which do not display the same affinity for proteases as MM-AAT protein. Z-

AAT has previously been reported as being 5-fold less efficient at inhibiting NE than

M protein (34). Lung disease in AATD is in part attributable to an imbalance between

proteases and anti-proteases. Without the inhibitory influence of AAT, lung tissue is

left vulnerable to the unopposed proteolytic effects of proteases. Hubbard and

colleagues have previously described increased numbers of neutrophils and high

chemotactic indices of neutrophils in the airway of those who are hetero or

homozygous for the Z mutation compared to healthy controls (64). Without the

protective effect of AAT, the unopposed action of NE has also been shown to

stimulate release of leukotriene B4 from airway macrophages which serves to recruit more neutrophils to the airways exacerbating tissue loss through proteolysis (65). Within the lungs, degradation of the ECM manifests as emphysema in addition to thickening of the small airways attributable to ongoing inflammation.

### 1.1.8 Anti-inflammatory effects of AAT

Early theories of disease pathogenesis in AATD centred around the protease-anti protease hypothesis (13). This theory dictated that disease in AATD, particularly development of early onset emphysema was attributable to an imbalance between levels of proteases such as NE and endogenous inhibitors. Since the original description of AATD in 1963, our understanding of the pathogenesis of disease within and outside of the lungs has evolved considerably (54). More recent studies have suggested a dysregulated inflammatory response in AATD in addition to elucidating some of the anti-inflammatory properties of AAT protein.

AAT has been previously shown to inhibit neutrophil chemotaxis through a number of distinct, mechanisms working in parallel. Bergin et al have shown that glycosylated AAT protein binds with greater affinity to the pro inflammatory cytokine IL-8 than non-glycosylated protein (32). Binding of AAT to IL-8 prevents engagement of IL-8 with its target receptor chemokine C-X-C motif receptor 1 (CXCR1) mitigating resultant CXCR1 mediated neutrophil chemotaxis. Furthermore, they showed that AAT also inhibits soluble immune complex induced neutrophil chemotaxis by inhibiting the action of the MMP, ADAM metalloproteinase domain 17 (ADAM-17). Inhibition of ADAM-17 prevents cleavage of the cell membrane and resultant chemotaxis. Data from in vivo work examining individuals with ZZ AATD receiving intra venous (IV) AAT augmentation therapy showed

increased serum levels of AAT bound IL-8. and normal levels of membrane expression of CD16 on neutrophils, with normalized neutrophil chemotactic responses(62, 66).

The anti-inflammatory properties of AAT are further demonstrated by the interaction between AAT and leukotriene B<sub>4</sub> (LTB<sub>4</sub>). High levels of NE, as seen in the airways of those with AATD can stimulate release of LTB<sub>4</sub> by neutrophils and macrophages(67). LTB<sub>4</sub> has been previously shown to play a role in neutrophil chemotaxis(68), adhesion(69) and degranulation. The presence of a central hydrophobic pocket on the surface of LTB<sub>4</sub> facilitates binding of AAT and competitively blocks receptor engagement by alternative ligands mitigating the downstream effects of LTB<sub>4</sub> (70).

The anti-inflammatory properties of AATD are further demonstrated by its effects on the pro- $\alpha_1$   $\sim$  |  $\alpha$  { {  $\alpha$  c [ | ^ Á & ^ c [ \ \tilde{a} } ^ Á \vee \text{P} \emptyset \quad \text{È Á Ó ^ | \* \tilde{a} } Á ^ c Á \alpha | / \tilde{a} } \& | ^ \alpha \bullet ^ \grave{a} Á | ^ \text{ç} ^ | \bullet Á [ \sim Á \vee \text{P} \emptyset \quad Á [ \} Á c @^ Á \bullet \sim | \sim \alpha \& ^ Á [ \sim Á \} of individuals with ZZ AATD (66). They showed à \tilde{a} } \grave{a} \tilde{a} } \* Á [ \sim Á \text{ŒŒEV} Á c [ Á c @^ Á \vee receptor with resultant decrease in release of tertiary and secondary granule proteases.

Ù c ~ \grave{a} \tilde{a} ^ \bullet Á ~ \bullet \tilde{a} } \* Á { [ ~ \bullet ^ Á { [ \grave{a} ^ | \bullet Á & [ \} \sim \tilde{a} ! { Á c @\alpha c Á \text{ŒŒEV} Á caspases 3, 6 and 7 which mediate apoptosis (71). In human studies, Hurley and colleagues have previously demonstrated the rate of neutrophil apoptosis is 2-fold higher in individuals who are homozygous for the Z mutation compared to healthy MM controls (72). They attributed this effect to sequestration of misfolded AAT within the ER and resultant ER stress response that includes increased expression of pro- $\alpha_1$  [ ] c [ c \tilde{a} \& Á \bullet \tilde{a} \* } \alpha | \bullet Á \tilde{a} } \& | ~ \grave{a} \tilde{a} } \* Á \vee \text{P} \emptyset \quad \text{È Á \vee @\tilde{a} \bullet Á ^ \sim \sim ^ \& therapy which was shown to decrease ADAM-17 activity and apoptosis in vivo.

Bucurenci and colleagues showed that AAT can down-regulate the inflammatory response by inhibiting the neutrophil respiratory burst (73). They demonstrated reduced superoxide production by neutrophils treated with AAT following exposure to a variety of pro-inflammatory stimuli.

Though much of the early research base has focused on the role of the neutrophil in AATD, increasing light is being shed on the role monocytes play in driving inflammation in AATD. Monocytes in AATD have been shown to be primed for generating an excessive cytokine response following exposure to a pro inflammatory stimulus. Janciauskiene and colleagues have shown that in vitro, AAT inhibits

enhanced the production of the anti-inflammatory cytokine IL-10 an effect thought to be mediated by increase cAMP and activation of cAMP dependent protein kinase A (74).

### 1.1.9 Pro-inflammatory milieu of AATD

Considering the expansive evidence base exploring the anti-inflammatory properties of AAT, it is perhaps unsurprising that AATD is considered to be pro-inflammatory state. Carroll and colleagues have previously shown that ZZ monocytes are intrinsically abnormal in their cytokine responses. They demonstrated increased production of IL-6 and IL-8 in addition to lower levels of IL-10 production by ZZ monocytes compared to MM controls exposed to lipopolysaccharide (LPS)(13). The authors attribute this to activation of an ER stress response triggered by sequestration of misfolded protein in the ER of individuals with ZZ AATD. Evidence for this is provided by the observation that genes involved in the ER UPR are upregulated in AATD.

Furthermore, it is well established that polymers of ZZ protein are themselves intrinsically pro-inflammatory. Polymers of ZZ protein have previously been detected in bronchoalveolar lavage (BAL) fluid(75) and parenchymal samples of the lungs of individuals with ZZ AATD (76). ZZ polymers influence neutrophil chemotaxis and drive inflammation with levels of activity comparable to that of IL-8 and the anaphylatoxin, complement fragment C5a (77).

They identified increased levels of the complement fragment C3d in the plasma and airway samples of the those with ZZ AATD. C3d is a reliable marker of overall complement activation (79) and its increased presence in AATD suggests ongoing activation of the complement cascade and dysregulated inflammation. They found a correlation between levels of C3d and severity of emphysema suggesting a role for C3d as biomarker for lung disease in AATD (78).

#### 1.1.10 AATD lung disease

The first trials linking AATD to lung disease are attributed to Laurell and Eriksson who in 1963 described the electrophoretic pattern of alpha one globulin on an agarose gel(80). Further studies of relatives of patients with AATD established a definitive connection between AATD and emphysema (50). Emphysema refers to pathological, permanent dilatation of the terminal airspaces. Though historically explained by the protease anti protease hypothesis, factors contributing to the development of emphysema include an increase in neutrophil and macrophage burden within the airways, increased alveolar cell death, chronic inflammation and increased oxidative stress (81). Emphysema can be diagnosed using CT imaging of the lungs. Though biopsy findings of emphysema are distinctive, in practice biopsy is

not used to identify emphysema owing to the widespread availability of effective, non-invasive tests such as CT scanning and pulmonary function testing. Findings suggestive of emphysema on PFTs include a reduction in the diffusion capacity of carbon monoxide usually accompanied by obstruction to expiratory airflow. An increased total lung capacity (TLC) and residual volume (RV) attributable to hyperinflation of emphysematous lungs may be evident in later stages of disease. Emphysema is best considered as a component of chronic obstructive pulmonary disease (COPD) and usually co-exists with inflammatory changes in the small airways. The global initiative for obstructive diseases (GOLD) defines COPD as an  $\% \tilde{a} \} \sim | \text{æ} \{ \{ \text{æ} c [ | ^ \acute{A} \text{å} \tilde{a} \bullet [ | \text{å} ^ | \acute{A} [$  indicating damaged lung tissue  $\acute{A} \text{æ} \} \text{å} \acute{A} | \text{´}$  and progressive obstruction to expiratory airflow. COPD is a common and largely preventable disease affecting approximately 440,000 people in Ireland. It is estimated that approximately half of those with COPD have been formally diagnosed. Individuals with AATD, particularly those who smoke develop an accelerated form of COPD. AATD is currently the only readily identifiable hereditary cause of COPD.

A finding of emphysema on radiological imaging of the thorax is ubiquitous in Pi\*ZZ patients who smoke (82). Emphysema in this group occurs earlier than MM matched smokers often appearing in the 4<sup>th</sup> and 5<sup>th</sup> decade of life (80). Furthermore, the pattern of distribution of emphysema in AATD is notable for its basal predominance and pan acinar distribution (83). Under normal conditions, smoking in healthy MM individuals induces a low grade, repetitive inhalational injury to lung tissue. As the upper zones are preferentially ventilated (relative to their perfusion), emphysema in MM smokers affects the upper lobes predominantly with basal involvement indicative of very advanced disease (84). Smoke is conducted through the small airways to the

respiratory bronchioles and eventually the alveoli giving the classical centrilobular appearance to emphysema on a CT scan. The functional unit of gas exchange within the lung includes the terminal respiratory bronchiole and all attached alveoli- collectively referred to as the acinus(84). Emphysema in AATD involves the acinus in its entirety -| ^ • ~ | c ã } \* Á ã } Á-æ@ã Á æ| æÁ-æã & ææÁ æ} æ Á [ } Á Ô V Á •

example of the classical appearance of basal predominant emphysema on the CT of an individual with ZZ AATD is shown in Figure 1.3.

Lung disease in AATD is heavily influenced by smoking exposure which remains the most important risk factor for development (85). Registry based studies of AATD confirm accelerated loss of FEV1 in active smokers with AATD compared to non-smoking controls (86, 87). An analysis of a Danish registry showed that median life expectancy in ZZ AATD was reduced by 20 years compared to non-smokers (86). Non-smokers with ZZ AATD have previously been shown to have a similar life expectancy to life long non-smokers (88). A recent meta-analysis examining the risk of lung disease in AATD highlighted that passive smoking and environmental exposure to smoke can also accelerate the loss of lung function and development of symptoms in those with more moderate and severe AATD variants (85).

Other lung diseases including bronchiectasis and asthma are seen with increased prevalence in AATD cohorts (42). Bronchiectasis is a disease of the airways. Repetitive cycles of inflammation and infection within the airways leads to structural changes in the airways seen as enlargement and dilatation on CT imaging. The bronchial wall is typically thickened by an inflammatory infiltrate of lymphocytes and macrophages which form lymphoid follicles (89). Classically, bronchiectasis presents with a chronic productive cough. This symptoms profile has been described in 40% of those with AATD (90). Clinically significant bronchiectasis that is evident

on CT imaging and causing symptoms has been reported in up to 27% of patients with Pi\*ZZ AATD (91).

Asthma is a heterogeneous disease of the small airways characterised by inflammation and bronchial hyperresponsiveness that is fully or partially reversible by bronchodilators. Asthma is one of the most common respiratory diseases encountered in clinical practice. Published data suggests a prevalence of physician diagnosed asthma in Ireland of 7-9.4% amongst adult populations (92). Rates in paediatric populations are higher again with an estimated prevalence of 21.5%. Lorenzo et al have previously reported a high prevalence of AATD in individuals with allergic type asthma. In a cross-sectional study of 643 patients with a diagnosis of asthma they identified an S or Z allele in 22.4%(93). No correlation between phenotype and asthma severity was identified.

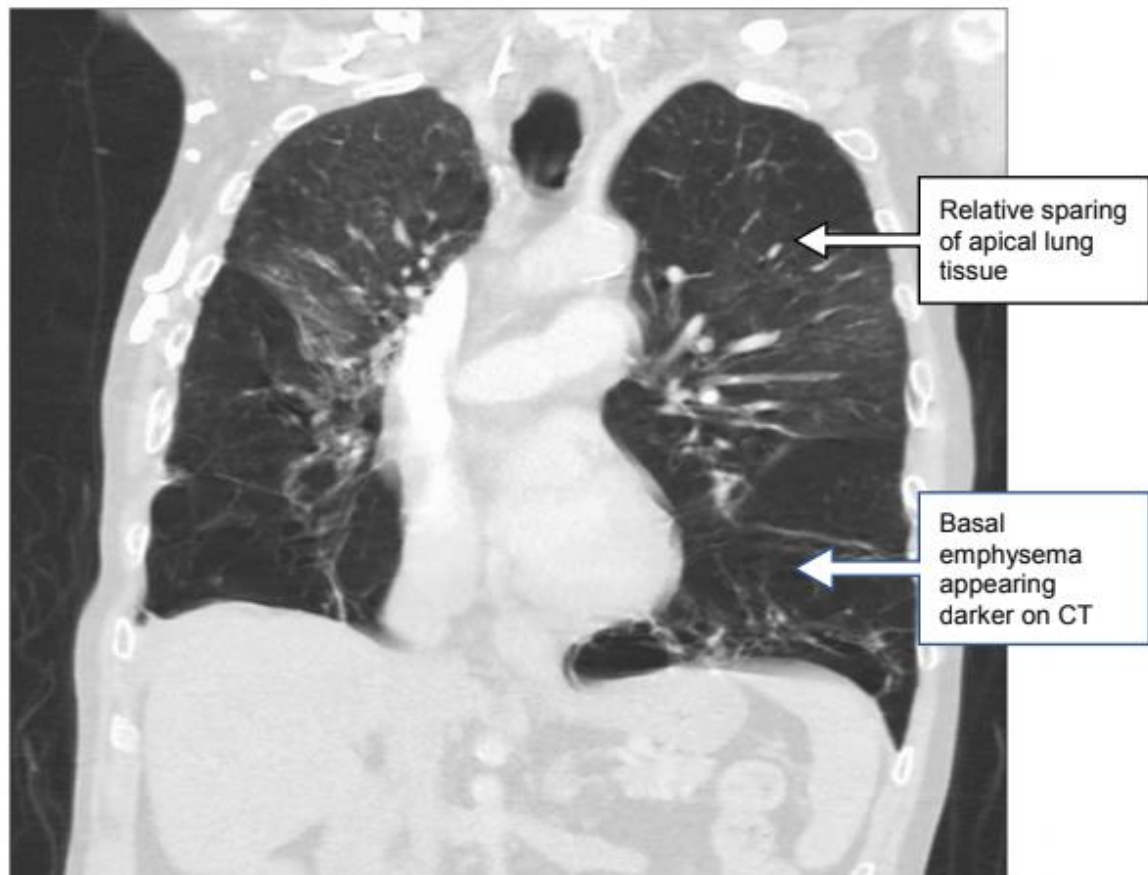


**Figure 1.3 Coronal CT of the thorax in a patient with ZZ AATD.**

CT imaging demonstrates extensive emphysematous disease with a basal predominance suggestive of severe AATD.

### 1.1.11 AATD liver disease

The pathogenesis of liver disease in AATD differs substantially from that of lung

and is a multi-step process. It begins with the production of a mutant AAT protein that is prone to misfold and aggregate in the endoplasmic reticulum (ER). This leads to the retention of the protein in the ER, which triggers an ER stress response. The ER stress response is a protective mechanism that results in translation attenuation of protein synthesis, transcriptional induction of ER resident chaperones and ER associated protein degradation (ERAD).

reaction triggered by aberrant retention of misfolded protein in the ER of hepatocytes

(13). A schematic delineating the differences between the pathophysiology of lung

and liver disease in AATD is provided in Figure 1.4.

Within the liver, retained Z AAT protein forms polymer aggregates that stain positive for periodic acid Schiff (PAS)(94) and are readily identifiable on liver biopsy (Figure 1.5). Retention of misfolded AAT protein in the ER triggers an ER stress responsive referred to as the UPR (13). The UPR is a protective mechanism that results in translation attenuation of protein synthesis, transcriptional induction of ER resident chaperones and ER associated protein degradation (ERAD).

Available evidence suggests a bimodal peak for liver disease in AATD- early life (0-5 years) and a later peak at 60-65 years(95). Individuals with alleles that tend towards polymerisation in the ER can develop a spectrum of liver disease ranging from acute hepatitis to cirrhosis with or without the attendant complication of hepatocellular carcinoma (95). A 2018 systematic review of 47 studies examining AATD related liver disease found that 10% of those with polymerogenic phenotypes developed clinically meaningful liver disease i.e. cirrhosis with 14.7% requiring liver transplantation (95).

As most of those with polymerogenic phenotypes do not go on to develop liver

disease, the 2 hit hypothesis is supported. The 2 hit hypothesis proposes that environmental and

epigenetic changes during the course of a lifetime may induce pathology in an

ã } å ã ç ã å ~ æ | Á , @[ Á ã • Á ± æ c Á ! ã • \ q Á [ , ã } \* Á c [ Á c @ ^ ã ! Á \*

recurrent elevation in the liver enzymes aspartate aminotransferase (AST) and gamma glutamyl transferase have been previously identified as predictors of future liver disease (7). Predictors in adults include excessive alcohol consumption, high BMI and co-existence of non alcoholic steatohepatitis (NASH) (96). Male gender correlates with a need for transplant and mouse models provide some interesting insights into the role testosterone may play in disease pathogenesis. In this regard, Rudnick and colleagues (2004) injected testosterone into female mice and found an increase in the number of polymers containing hepatocytes in liver sections of treated mice (97).

The only currently available, effective treatment for liver failure arising from AATD is liver transplantation. In the USA 1.5% of liver transplants performed annually are for a primary diagnosis of AATD (98). Outcomes following liver transplant are favourable with a 72% 10-year survival rate for those with AATD (99). This is compared to a 50% 5-year survival seen in those who undergo lung transplant (100).

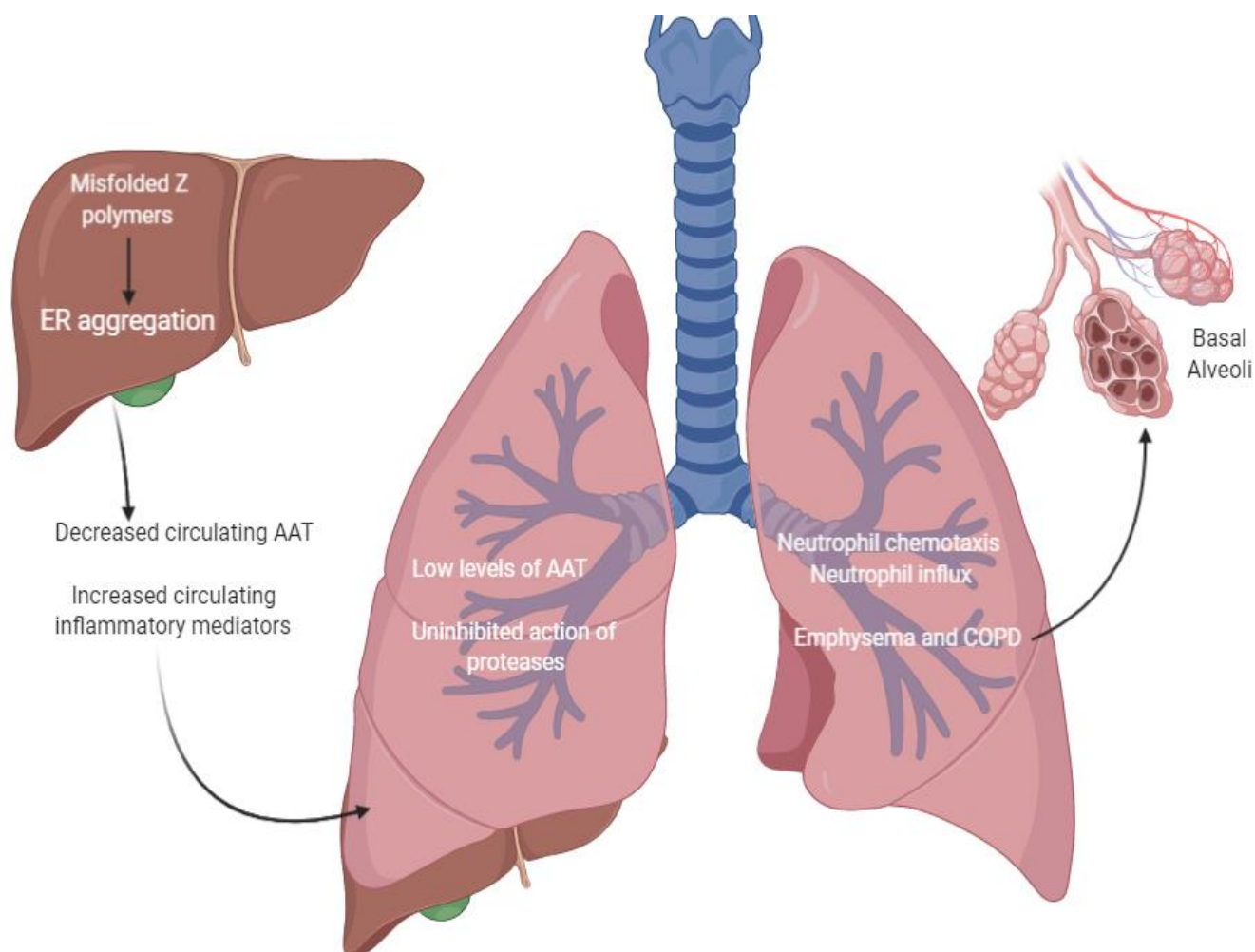


**Figure 1.4 Pathophysiology of lung and liver disease in AATD**

Cirrhosis of the liver arises from retention of misfolded Z-AAT polymers within

and the unopposed actions of neutrophil derived proteases cause emphysema and COPD (loss of function).

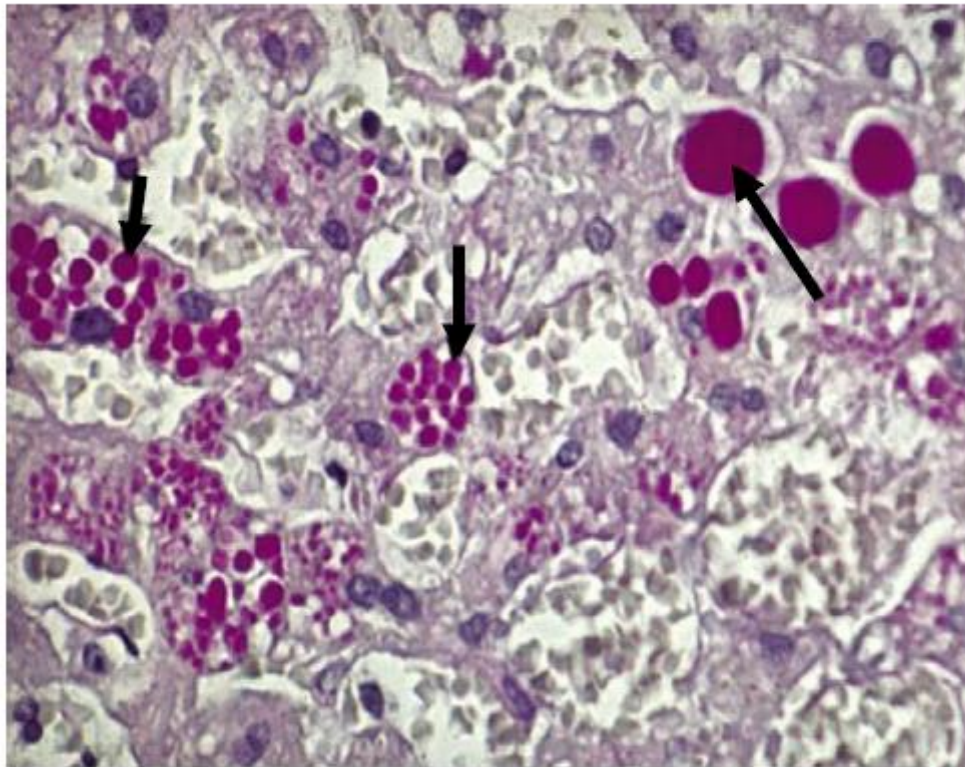


**Figure 1.5 Liver biopsy slide showing PAS positive inclusion bodies from an individual with ZZ AATD**

Arrows indicate PAS positive inclusion bodies formed by retention of ZZ polymers within hepatocytes. Adapted from Janciauskiene et al, 2011(1)

### **1.1.12 AATD skin disease**

Panniculitis refers to inflammation of the subcutaneous adipose tissue and likely reflects the unopposed action of proteases in the skin. To date, just over 100 cases of panniculitis have been described in the literature (101). Prevalence as a complication of AATD is estimated to be 0.1% (54). Clinically, panniculitis can present as a widely disseminated, relapsing, painful inflammation of the skin. Though encountered infrequently, identification of panniculitis is clinically important as skin changes are sensitive to treatment in the form of intravenous (IV) AAT augmentation (102).

Several pathogenetic mechanisms for the development of panniculitis have been proposed. Smith et al implicate a lack of membrane bound serine proteases, and enhanced elastin degradation (103). Excessive complement activation (78), neutrophil accumulation and release of serine proteases, and oxidation of the active site of AAT by myeloperoxidase (MPO) have also been implicated in the development of skin disease (103). Gross et al have shown deposition of ZZ polymers in skin lesions associated with panniculitis (104).

Administration of IV AAT has been shown previously to ameliorate symptoms and reduce the frequency of disease flares (104). In the majority of cases, no identifiable trigger for the development of panniculitis is identified. If left untreated, it can progress to a chronic phase characterised by focal lesions with proliferation of fat filled histiocytes (105).

### **1.1.13 AATD vasculitis**

Several studies have highlighted the over representation of certain AATD phenotypes in cohorts with anti-neutrophil anti cytoplasmic (ANCA) associated vasculitides (AAVs)(106). ANCAs are autoantibodies that are specific for neutrophil granule proteases such as PR3 or MPO. AAVs are systemic diseases characterised by inflammation in blood vessels. Small, medium and large vessels may be involved, and single or multiple organs involved simultaneously or sequentially. Measurement of specific ANCA anti bodies such as ant-PR3, anti-MPO, or anti BPI are routinely used as part of the diagnostic work up of patients with suspected vasculitis(107). ANCAs have been described in cases of necrotising vasculitis such as eosinophilic granulomatous with polyangiitis (EGPA) and granulomatosis with polyangiitis (GPA)(107).

The role of the PiZ phenotype in the development of AAVs has been highlighted repeatedly and is a known risk factor for the development of AAV(108). The American Thoracic Society recommends measurement of AAT levels in all cases of anti-PR3 vasculitis(44). Bergin and colleagues showed that excessive neutrophil degranulation in AATD contributes to the development of ANCAs against other granule contents such as lactoferrin(66). ANCAs cause further activation of neutrophils by targeting surface bound antigens. Signalling of ANCAs triggers a number of down-stream effects including ROS production and protease release that perpetuate tissue damage (109).

The mechanisms underlying the development of auto anti-bodies to PR3 in AATD is unclear. Some authors have hypothesised that it may be a function of increased levels of unbound PR3 stimulating auto anti body production. AAT protein has been shown to inhibit anti-PR3 IgG from binding to its target antigen reducing the oxidative

burst in primed neutrophils(110). In a similar series of experiments, Bergin and colleagues showed that administration of exogenous AAT attenuated neutrophil degranulation and auto antibody formation. Owing to this, administration of plasma purified AAT has been used as rescue therapy for those with drug resistant vasculitis causing end organ failure(111).

#### **1.1.14 Treatment of AATD**

Treatment of AATD requires correction of the underlying deficiency in addition to supportive therapies such as inhaled bronchodilators commonly used in the management of COPD. Administration of IV AAT protein, referred to as augmentation therapy, has been shown to correct both serum and lung epithelial protein deficiencies (112-114).

Studies from the 1980s established that weekly IV augmentation with pooled human AAT increased serum levels to above 1g/L(113). Furthermore, day seven nadir values confirmed levels remained above a protective threshold of 0.5g/L(115).

Following the success of early trials, augmentation therapy was introduced in the 1980s as a way of correcting the biochemical deficiency without reference to clinical effects. Multiple attempts were made to clarify the magnitude of clinical benefit in the latter part of the 1980s and on to the 1990s. Designing trials that were sufficiently powered to detect a difference was challenge in view of the perceived rarity of AATD at the time.

The largest prospective cohort study was undertaken by the National Heart, Lung and Blood institute (NHLBI) in 1988. Hubbard and colleagues published their results in 1998 having shown a slower rate of decline in FEV1 in the subgroup of patients

with advanced emphysema receiving therapy(112). The hazard ratio for death was reduced at 0.64 ( $p=0.02$ ) in the augmentation group. This finding appeared to be supported by a Danish study from 1997. Seersholm and colleagues compared rates of decline in FEV1 amongst former smokers with AATD to an age-matched German cohort receiving augmentation therapy (116). They reported a modest but statistically significant decrease in the rate of decline in FEV1 in the treatment group ( -53ml/year versus -75ml/year,  $p=0.02$ ).

Though results of early clinical trials using FEV1 as a primary outcome measure were encouraging, they were by no means conclusive. The EXACTLE trial eschewed the use of FEV1 in favour of a novel primary end point- changes in lung density scores as measured by CT scanning(117). 77 patients were randomised to receive either augmentation or placebo over a 2-and-a-half-year period. Results showed an attenuated loss of lung density over time and a reduction in the severity of exacerbations. In view of the small number of patients included in the study, questions were raised about the trial was sufficiently powered to detect a clinically meaningful difference. This shortcoming was addressed by the RAPID trial.

RAPID recruited 180 PI\*ZZ patients and randomised them to either weekly intravenous infusion of 60mg/kg purified AAT or placebo(118). At the end of a 2-year trial period results showed a significant attenuation of the decline in lung density in the intervention group (-1.45 g/L/yr vs. -0.74 g/L/yr,  $p=0.03$ ). A subsequent open label extension of this trial, RAPID-OLE, confirmed that this benefit was maintained over a further two years(119). Furthermore, subjects who crossed over to active treatment had significant reduction in disease progression.

## **1.2 Monocyte Physiology in AATD**

### **1.2.1 Introduction**

This project is focused on exploring an interaction between monocytes and the complement fragment C3d which has been shown to be increased in the plasma and airways of individuals with ZZ AATD (78). Our interest in monocytes was prompted largely by observations from Carroll and colleagues who showed that ZZ monocytes are intrinsically programmed to generate an excessive cytokine response following exposure to a pro-inflammatory stimulus (12). Van Wout et al (2015) subsequently found contrasting results and showed no significant differences in the cytokine levels produced by MM and ZZ monocytes (120). Van Wout went a step further and used granulocyte macrophage colony stimulating factor (GM-CSF) and macrophage CSF (M-CSF) to induce differentiation to a pro and anti-inflammatory monocyte derived macrophage phenotype. Again, they identified no significant difference in cytokine levels produced by MM and ZZ cells. Interpreted collectively, these results suggest that there is some ambiguity over whether the cytokine response of monocytes is altered in ZZ AATD that warrants further exploration.

Monocytes represent a heterogenous cell population and our understanding of monocyte ontogeny has evolved considerably over the past decade. In consideration of this, we will now review what is known about the monocytes and their derivative cells and highlight gaps in the current knowledge base.

### 1.2.2 The monocyte

Monocytes, also referred to as mononuclear phagocytes, are a type of leucocyte and form part of the mononuclear phagocyte system (MPS). The MPS is comprised of 3 cell lines; monocytes, macrophages and follicular dendritic cells (FDC) in addition to their bone marrow (BM) progenitors(121).

Monocytes contribute to immunity via three main functions: phagocytosis, antigen presentation and the production of cytokines. Monocytes use several different mechanisms to carry out phagocytosis including the utilisation of intermediary

complement & present on the surface of the pathogen(121). In addition, monocytes are capable of binding directly to a microbe directly using receptors on its own surface that recognise those on the invading pathogen. In some cases, monocytes may kill a host cell via anti-body dependant cell mediated toxicity.

To date, three separate monocyte subsets have been identified in human circulation- classical (CM), intermediate (IM) and non-classical monocytes (NCM)(122).

Collectively, monocytes represent a highly plastic cell population with context dependent functions that vary between subsets. The function of different monocyte subsets has been studied extensively in mice and human models. Though murine studies provide a useful basis for the study of monocytes several key differences exist between species. Most notably, mice have only 2 phenotypically and functionally distinct monocyte populations in blood- classical (Ly6C<sup>hi</sup>) and non-classical (Ly6C<sup>low</sup>) whilst humans have a third intermediate subset(123). In mice and humans CMs are known to circulate in the blood and are recruited to sites of inflammation where they are capable of differentiation into macrophages and dendritic cells (DCs). NCM monocytes of both species demonstrate a crawling

behaviour along the luminal surface of blood vessels and represent of the first lines of defence against invading pathogens(124).

### 1.2.3 Monocyte structure

Monocytes are the largest of circulating leucocytes measuring between 15-20µm in diameter(125). Considerable heterogeneity in size is attributable to differences in maturity and activation of circulating cells. In addition to their size, monocytes can be distinguished from other leucocyte populations by the presence of a large ellipsoidal

[ ! Á ± \ ã å } ^ ^ Á à ^ æ } q Á • @æ ] ^ å Á } ~ & | ^ ~ • È Á V @ ^ Á } ~ & | ^ æ ! distinguishing the monocyte from other polymorphonuclearcytes (PMNs). The nucleus is surrounded by a relatively scant amount of cytoplasm that has a

& @æ ! æ & c ^ ! ã • c ã & Á ± \* ! [ ~ } å Á \* | æ • (126) Á æ ] ] ^ æ ! æ } & ^ Á [ } Á

The surface of monocytes possesses microvilli on an undulating cell membrane.

Embedded within this membrane are cell surface receptors. Relative expression of different receptors allows distinction between mature and immature cells to be made in addition to providing information on the state of activation and the function of the monocyte(127). Monocyte surface receptors are characterised by their ability to bind to specific antibodies. Receptors expressed constitutively on the membrane of { [ } [ & ^ c ^ • Á ã } & | ~ å ^ Á Ô Ö F F à È Á Ô Ö F F & Á Ç æ } Á Á ã } c ^ \* ! ã receptor 4 (CR4), CD14 in humans, CD16 (an Fc receptor) and CD11b (128).

In addition, monocytes possess receptors for other peptides and small molecules such as toll like receptors (TLRs) and complement receptors.

Fc receptors (FcRs) for IgG are expressed on the surface of all mononuclear cells and can be divided into three subclasses: FcR1, 2 and 3. FcR1 (also known as

CD64) binds monomeric IgG through the Fc portion of the molecule and is ubiquitously expressed in monocytes. Expression is upregulated when monocytes are activated by an LPS trigger. Binding of an IgG-antigen complex to FcR1/CD64 triggers endocytosis and facilitates antigen presentation to T cells(129). It also triggers cytokine release and the generation of reactive oxygen species.

FcR2 (or CD32) is capable of binding complexed IgG as opposed to the FcR1 mediated binding of monomeric IgG (130). FcR3 (or CD16) is expressed by monocytes, macrophages, natural killer cells and neutrophils(121). CD16 binds complexed Ig and Ig bound to the surface of cells and is the FcR implicated in antibody dependent cell toxicity. As alluded to previously, the level of expression of CD16 relative to expression of CD14 has been used to identify three distinct subsets of monocytes in the circulation(107).

#### **1.2.4 Human monocyte subsets**

To date, 3 subclasses of monocytes have been described; classical, non-classical and intermediate with each subtype distinguishable by their relative expression of the cell surface markers CD14 (an LPS receptor) and CD16 (an Fc receptor involved in signal transduction)(121). In humans, these subsets exist in a state of dynamic equilibrium. The classical monocyte is identifiable by high levels of the CD14 receptor on the cell membrane(131). The non-classical monocyte displays low levels of surface CD14 expression but high surface expression of the receptor CD16. The intermediate monocyte expresses high levels of CD14 and low levels of CD16(128).

Classical monocytes account for 85% of the circulating monocyte population and function primarily as drivers of the inflammatory response via the production of

& ^ c [ \ ã } ^ • Á • ~ & @Á æ• Á c ~ { [ ~ ! Á } ^ & ! [ • ã • Á ~ æ& c [ ! Á æ| ]

IL-8(131). In contrast to the pro-inflammatory role of the classical monocyte, non-classical subsets display a patrolling behaviour and are responsible for ensuring the integrity of the vascular endothelium is not breached by invading pathogens.

Stimulation of this subset with microbial products leads to the production of large amounts of pro inflammatory cytokines such as tumour necrosis factor (TNF) and interleukin-12 (IL-12)(131). A study by Bianchini et al. showed that non-classical monocytes show a predilection for expression of the programmed death ligand one (PDL-1)(132). PDL-1 staining can be used to identify and study this subset in isolation. Targeting of PDL-1 has been a topic of much interest in recent years specifically for its use as a therapeutic target in the treatment of lung, colorectal , cervical cancer and metastatic malignant melanoma(133).

The origins of different monocyte subsets have been debated heavily in published literature(131). Several studies of monocytes under steady state conditions using murine models suggest monocyte subsets represent different stages of a single developmental sequence(134). CD14++ murine classical monocytes develop a non-classical profile of altering CD14/CD16 expression over time(135). Others have proposed that rather than being a developmental step in monocyte differentiation, intermediate monocytes are best considered as a separate and unique subpopulation of monocytes(136). This theory is supported by the observation of high levels of expression of receptors such as vascular endothelial growth factor receptor 1 and 2 (VEGF-1 and 2), CXCR4 and Tie-2(137). This pattern of surface marker expression suggests that intermediate monocytes are functionally distinct

from other subsets and have been identified as playing a role in reparative processes such as wound healing and angiogenesis(137).

Whilst murine models are useful for studying the classical and non-classical subsets, rodents lack an intermediate subset equivalent and significant gaps exist in our understanding of the development and function of intermediate monocytes. Though much has yet to be clarified about the life cycle of monocyte subsets in the circulation, what is clear is that alterations in the pattern of relative expression of surface markers and proportional representation of different monocyte subsets, has important clinical implications.

An increase in the proportion of circulating intermediate monocytes has been observed in those with rheumatoid arthritis (RA). Radwan et al demonstrated an increase in number of intermediate CD14<sup>++</sup> CD16<sup>+</sup> subset in RA(138). This correlated with increased levels of the cytokine IL-17 which may serve as an attractive target for future therapies. Other studies showed a similar increase in the number of IMs in circulation in the 48 hours following an ischemic stroke(139). In the same study, Urra and colleagues identified high levels of circulating classical monocytes as being predictive of poor outcome following stroke. Circulating monocytes from patients with the chronic, granulomatous inflammatory condition sarcoidosis express higher levels of Fc receptors including CD16 and complement receptors, priming them for enhanced phagocytic activity(140).

Factors known to alter the expression CD14 and CD16 include AAT, LPS, Lipid A, *E coli* and components of gram-positive bacterial cell walls(141-143). A summary of monocyte subsets is provided in Table 1.1.

**Table 1.1: Overview of monocyte subset surface markers, proportional representation, cytokine profiles and function in the circulation.**

CD14/CD16 levels	% Total	Cytokine Profile	Subset	Life span	Function
CD14++ CD16-	85%(127)	IL-6, IL-8, CCL2, CCL3, and CCL5	Classical	24 hours	Phagocytosis, adhesion(124), migration, anti-microbial responses
CD14++ CD16+	7.5%(127)	TNF- $\alpha$ , IL-1, IL-6, CCL3, IL-10	Intermediate	4.3-5 days	Antigen presentation, regulation of apoptosis(137), transendothelial migration(144)
CD14- CD16++	7.5%(127)	V $\beta$ $\delta$ $\epsilon$ , IL-1, IL-6 (lo)	Non-Classical	7 days	Complement and Fc mediated phagocytosis(145, 146), (147)transendothelial migration, adhesion(124), anti-viral responses

### 1.2.5 Monocyte life cycle

Understanding the life cycle of the monocyte is key to understanding how they contribute to disease pathogenesis, particularly within the lungs. Up until the early 20th century the origin of monocytes was debated. The eminent 19th century pathologist Virchow postulated that monocytes arose from mesenchymal cells(148). Development of radioautography and chromosome marker techniques in the 1960s shifted popular theory away from the mesenchymal origin story and confirmed that monocytes began their life cycle as a rapidly proliferating pool of precursor cells in the bone marrow (BM)(125). Development of monocytes within the BM commences during early embryogenesis and continues throughout adulthood with production increasing in response to inflammatory stimuli (74).

The life cycle of monocytes is depicted in Figure 1.6 Monocytes are derived from haematopoietic stem cells (HSC). When activated towards the myeloid lineage they form common myeloid progenitors. Further differentiation results in the formation of granulocyte macrophage progenitors (GMPs) followed in turn by macrophage dendritic progenitors (MDP). It from these MDPs that mature circulating monocytes arise. Differentiation into myeloid dendritic cells results in the formation of monocyte derived antigen presenting cells (APCs)(149). APCs are responsible for presenting antigens to T cells. Phagocytosed microbial fragments are incorporated into membrane histocompatibility complex (MHC) molecules and trafficked to the cell surface where they are identified by T cells. This interaction leads to the activation of a specific immune response against the antigen(149).

Monocytes account for only 1-2% of the total population of nucleated cells within the BM. Release from the BM is dependent on the expression of CCR2, the expression of which is confined to the classical subset(150). Patel and colleagues used a non-

toxic stable isotope (deuterium) approach and cell sorting to characterise human subset kinetics under steady state and inflammatory conditions(122). They noted an absence of deuterium labelled monocytes for the first 24 hours (h) following injection. They hypothesised that under steady state conditions monocyte BM precursors undergo a post mitotic maturation phase within the BM. Furthermore, they noted early integration of deuterium in classical subsets which peaked at day 3. In contrast, labelling was not apparent in non-classical subsets until day 7. Taken together this suggests that in a pattern similar to that seen in mice, classical monocytes may convert to a non-classical subset over time(122).

CMs in circulation have a relatively short half-life (24 hours) in the circulation after which they migrate to tissues where further differentiation to macrophages may occur. Alternatively, they convert from a classical to an intermediate phenotype with increased expression of the Fc receptor CD16(151) This subset has a longer half-life of between 4.3-5 days. These in turn transition to a non-classical phenotype which has the longest half-life of each subset at 7 days.

P ã • c [ ! ã & æ | | ^ Á c @^ Á c ^ ! { Á ± ! ^ c ã & ~ | [ ^ } å [ c @^ | ã æ | Á • resident macrophages. Exposure of monocytes to local tissue derived growth factors, microbial products, or chemokines triggers recruitment of monocytes and differentiation to macrophages or dendritic cells(152). This pattern of migration occurs both as part of normal homeostasis and as a result of inflammation (75). It is important to note that though some tissue resident macrophages arise from differentiated monocyte subsets it is increasingly recognised that the many resident macrophage populations are seeded before birth. This population of tissue macrophages is self-sustaining, replenishing themselves via self-proliferation with minimal monocyte input under steady state conditions (76-79). Individuals who

harbour mutations in the gene encoding GATA2, a haematopoietic and myeloid transcription factor, demonstrate an absence of peripheral circulating monocytes with preserved alveolar and dermal macrophage populations (74). This suggests an alternative source of macrophage development that is independent of monocyte precursors.

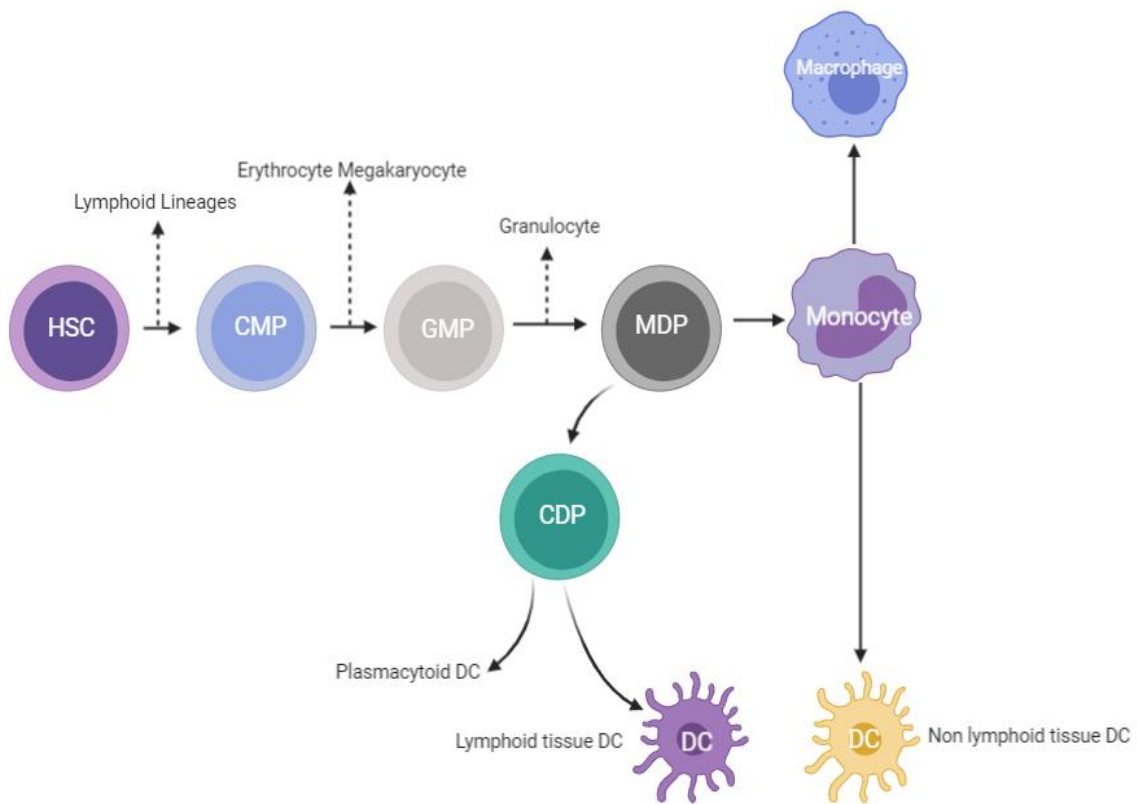


**Figure 1.6 Monocyte Lifecycle**

Monocytes are derived from haematopoietic stem cells (HSC) within the bone marrow. When activated towards myeloid lineage, sequential differentiation into common myeloid progenitors (CMPs), granulocyte macrophage progenitors (GMPs) and macrophage dendritic progenitors (MDP). It is from MDPs that mature monocytes arise. Further differentiation into tissue macrophages or dendritic cells (DCs) may be triggered by changes in microenvironmental signals.

### **1.2.6 Monocyte differentiation to pulmonary macrophages**

Broadly speaking, lung macrophages can be categorised by their origin or the location in which they are found in the lung. When categorised by location two populations emerge- alveolar macrophages (AMs) that populate the alveolar space and interstitial macrophages (IMs) that local to the interstitium. AMs and IMs can be distinguished from one another by differential expression of the surface markers CD11b, CD11c and colony stimulating factor receptor (CSFR) subtypes(153). AMs preferentially express CSFR2 whilst CSFR1 expression characterises all IM subtypes.

Sub populations of both AMs and IMs are further distinguishable based on their cell of origin . monocytes recruited from circulation or tissue resident embryonic precursors. 75% of the lung macrophage pool comprises tissue resident AMs (TRAMs)(154). Under steady state conditions TRAMs are long living cells derived from the yolk sac during embryonic development(155). This low turnover population seed the lungs shortly following birth and replenish themselves independent of circulating monocytes.

Following diverse mechanisms of lung injury (i.e aging, the development of pneumonia, exposure to radiation, exposure to pneumotoxins such as bleomycin etc.) tissue resident alveolar and interstitial macrophages are replaced by the recruitment of circulating monocytes capable of differentiation into an AM or IM phenotype(155). Recruitment occurs via the CCL2/CCR2 axis(154). Recruited populations demonstrate different functional and metabolic profiles from resident counterparts. Recruited monocyte derived macrophages are primed for inflammation and are enriched for immune (129) signalling (16). They rely on glycolysis and

arginine metabolism. This is in contrast to resident macrophage populations which are involved in proliferative processes and characterised by TCA, fatty and amino acid metabolic pathways. Recruited monocyte -derived pulmonary macrophages have been implicated in a number of disease processes. A 2013 study by Osterholzer and colleagues used a mouse model of repetitive injury to type 2 alveolar epithelial cells to conclusively demonstrate that Ly6C+ monocyte derived macrophages are drivers of aberrant fibrosis in the recovery phase(156). It is worth noting that this Ly6C+ cell population in mice is analogous to the CD14+/CD16- classical monocyte. A schematic highlighting the diversity of lung macrophage populations over the course of a lifetime is presented in Figure 1.7.

In advance of discussing the clinical implications of monocyte recruitment to the lungs it is worth revisiting older models of macrophage function. For many years, the function of pulmonary macrophages was seldom considered without reference to the behaviour in response to stimulation with interferon gamma and/or IL-4 and represents 2 extremes of polarisation(157). M1 refers to a macrophage that is functionally active in the response to pathogens and contributes to tissue destruction during lung injury. M2 macrophages are implicated less in pathogen response being less toxic to microbes. They elaborate an anti-inflammatory cytokine response and have been implicated in the development of fibrosis and aberrant reparative processes. Though conceptually useful it should be borne in mind that in vivo, macrophages are highly plastic and exist in various states of transient activation rendering the M1/M2 model less useful than once thought(158). The terminal phenotype of a macrophage will be heavily influenced by signals from its microenvironment and as discussed, the origin of the cell.

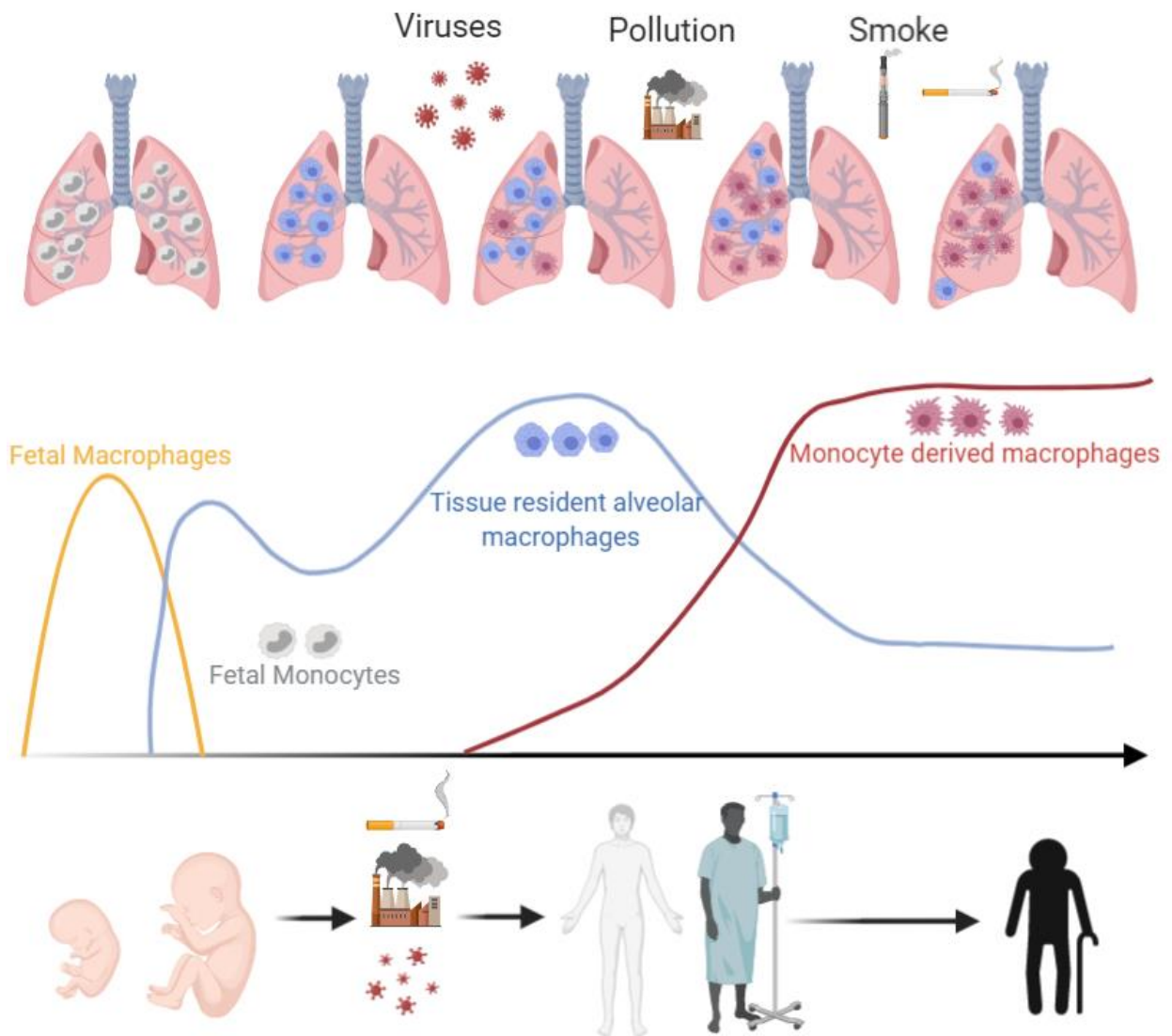


**Figure 1.7 Heterogeneity of lung macrophage populations**

Foetal monocytes populate the lung during early embryogenesis differentiate into macrophages are long-lived and capable of self-renewal in homeostatic conditions (blue line). Environmental exposures including viruses, environmental pollution and smoke over the lifespan may induce the recruitment of monocytes that differentiate into alveolar macrophages in response to cues provided by the local tissue microenvironment in the lung (red line).

### **1.2.7 Monocytes and lung disease**

In a 2020 paper published in Nature Immunology Aegerter and colleagues showed that infection with the influenza virus alters the composition of lung macrophage (AM) populations due to the emergence of a monocyte derived population of AMs(155). This study builds on the work of Halsted and colleagues who had demonstrated that infection with influenza virus led to a rapid decline in AM numbers and replacement by monocyte derived or recruited AMs(159). Aegerter et al note that whilst monocyte derived macrophages have a similar surface phenotype to RAMs, they have a unique functional, transcriptional and epigenetic profiles. Using an animal model, they showed that monocyte derived AMs produce increased IL-6 when compared to resident AMs. This increased IL-6 was shown to protect against subsequent bacterial superinfection with streptococcus pneumoniae in mice recently infected with the influenza virus. The authors confirmed that recruitment of monocytes to the airways was CCR2 dependant thus, AMs are derived from classical monocytes to which CCR2 expression is largely restricted(160). This raises particularly interesting questions as at the time of writing, the novel respiratory pathogen SARSCoV2 continues its global march. The anti-IL-6 therapy tocilizumab is currently licenced for use in those with COVID19 respiratory failure and high circulating levels of IL-6(161).

The characteristics and behaviour of monocyte derived pulmonary macrophages has been a topic of much interest in recent years. Recruited populations have been conclusively linked to diseases such as idiopathic pulmonary fibrosis, radiation and drug induced fibrosis(162, 163). Results of early studies on CCR2 knockout mice were initially encouraging. In 2001 Moore and colleagues demonstrated that CCR2

depletion was associated with more rapid recovery from bleomycin induced lung injury(162). The work of Gurczynski in 2016 however confirmed that though CCR2 inhibition is appealing in its simplicity, the reality is much more nuanced. Gurczynski showed that loss of CCR2 exacerbated HSV induced pneumonitis and fibrosis following bone marrow transplantation(154). This suggests that recruited populations may serve different functions depending on the mechanism of lung injury- sterile vs pathogen instigated tissue damage.

Studies of blood monocytes in severe COPD have shown an increase in total monocyte number and over representation of the non-activated subset in advanced disease(164). Higher absolute monocyte counts have also been shown to be predictive of shortened survival in fibrotic lung diseases including systemic sclerosis and myelofibrosis(165). Multi colour flow cytometry has been used to characterise the phenotypic profile of individuals subsets in COPD. Cornell et al have shown that monocytes in COPD are characterised by increased surface expression of the chemoattractant receptor CCR5(164). The authors hypothesise that this represents a population that can be recruited more rapidly to the lungs during times of illness.

### 1.2.8 Monocytes in AATD

Monocytes in ZZ AATD differ in several aspects from MM controls. Carroll and colleagues showed that ZZ monocytes are intrinsically abnormal in their cytokine responses(13). Following 24-hour treatment with LPS at a concentration of 20µg/ml they measured increased levels of the cytokines IL-6, 8 and 10 in supernatants recovered from ZZ monocytes. ZZ monocytes were also shown to produce 4-fold

| ^ • • Á ŒœV Á ] ! [ c ^ ã } Á c @æ} Á T T Á & [ } c ! [ | • È Á ŒZ à • ^ ~ ~ ^ }

monocyte derived macrophages to examine whether a similar cytokine effect could be observed(120). ZZ and MM monocytes were cultured in for 6 days and stimulated with granulocyte-macrophage (GM) or macrophage colony stimulating factor (M-CSF) to induce an M1 or M2 phenotype respectively. No differences in the cytokine profiles generated by MM and ZZ macrophages in response to an LPS trigger were detected.

Expression of the subset-defining surface marker CD14 has been shown to be altered by AAT. Nlta and colleagues isolated peripheral circulating monocytes and cultured them with 10ng/ml of pseudomonas LPS in the presence and absence of AAT protein(166). Cells treated with AAT, with or without LPS induced rapid release of sCD14 whilst LPS alone had no significant effect. Western blot performed at 2 hours, showed that AAT also increased the expression of mCD14 and blocked the ability of LPS to decrease its expression. Whilst the authors do not measure proportions of CD14+ and CD16+ monocytes, this study that the phenotype of monocytes and the attendant cytokine response may be altered in AATD.

Flow cytometry has been used to examine monocyte subsets in AATD. Stolk and colleagues studied monocyte profiles in patients with ZZ AATD and compared them to MM controls with known COPD(142). Baseline characteristics differed across with two groups with the MM cohort having a higher diffusion capacity of carbon monoxide (DLCO) and a greater smoking history. Interestingly despite a moderate reduction in FEV1% in both groups (mean (SD) for MM 47.3% (11.8), ZZ 35% (9)) no subject had had an exacerbation in the 6/12 preceding the trial. This is notable as the importance of COPD phenotypes i.e. exacerbators and non-exacerbators is increasingly being recognised by physicians. In this non-exacerbator cohort, the intermediate subset of monocytes had the lowest expression in the ZZ group. Non

classical monocytes were almost totally absent in ZZ patients. This raises the possibility that AATD patients have a breach in the first line of defence against invading pathogens.

AATD has historically been thought of as a neutrophil driven disease. Reflecting this, there is a relative paucity of research examining monocyte behaviour in AATD. What is known of key differences between MM and ZZ monocytes from published data is summarised in Figure 1.8. With increasing recognition of the immunomodulatory role of AAT and emerging insights into monocyte and monocyte derived macrophage functions within the lungs, there is reason to hope that the imbalance between what is known about neutrophil versus monocyte function in AATD will be addressed.

Much of the published data on monocyte function in AATD has focused on the expression of the surface receptors CD14 and CD16. We will now proceed to examine this in further detail.

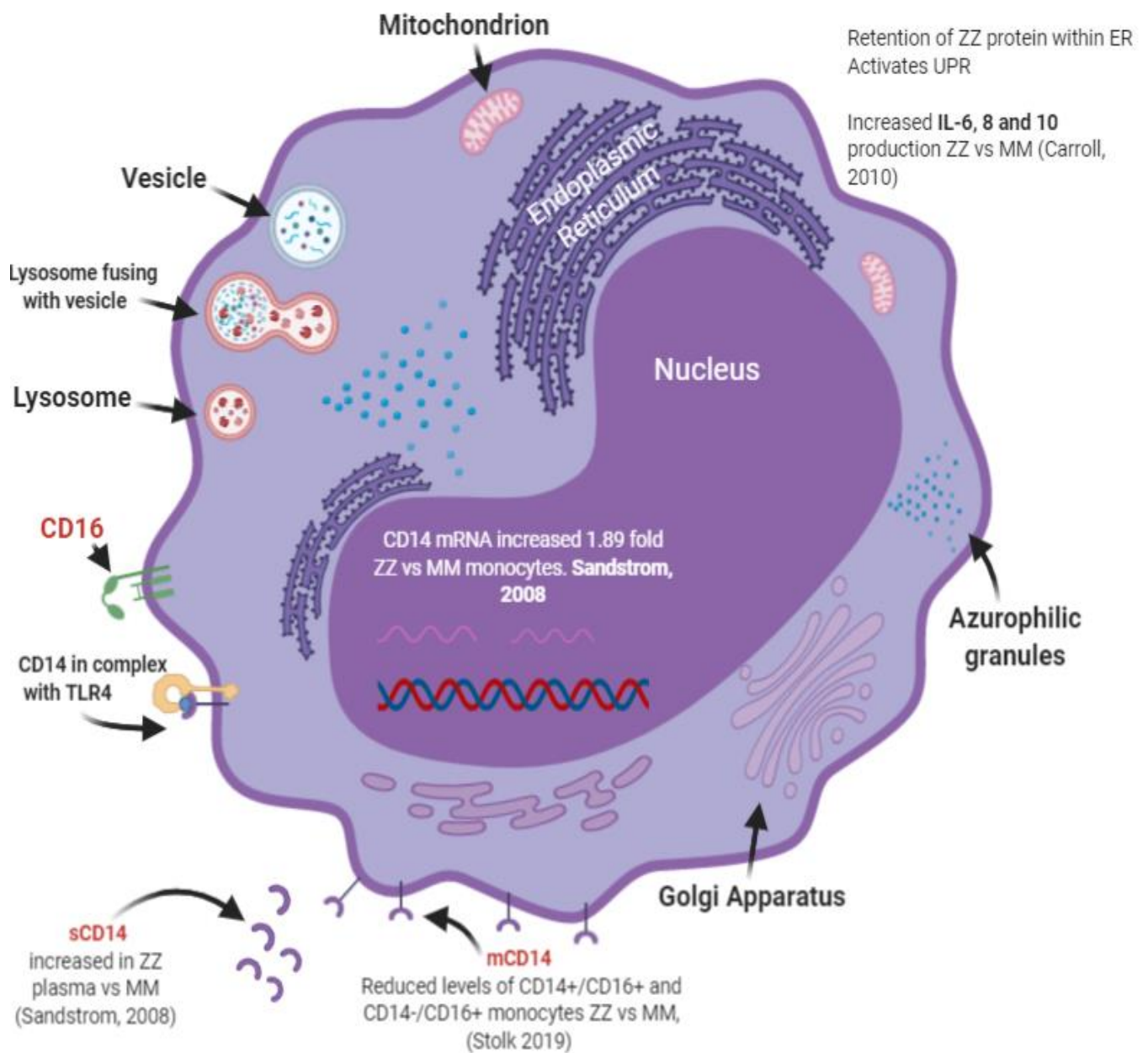


**Figure 1.8 Key differences between ZZ and MM monocytes**

Several key differences between ZZ and MM monocytes have been previously described in published literature. Expression of mCD14 is upregulated in ZZ AATD(167). CD14+/CD16- CMs predominate in ZZ AATD(142). ZZ monocytes are also known to produce increased levels of cytokines in response to an LPS trigger compared to MM controls(13).

### 1.2.9 Expression of CD14 by monocytes

Cluster of differentiation 14 (CD14) is a glycolipid anchored glycoprotein found on the surface of cells of myelomonocyte lineage including monocytes, macrophages and select populations of granulocytes(168). CD14 exists in two forms- soluble (sCD14) or membrane bound (mCD14) and is synthesised primarily by hepatocytes. Studies using confocal microscopy have identified large intracellular stores of CD14 in human monocytes(169). CD14 lacks both a transmembrane and intracellular domain(170). As a result, it relies on forming a complex between lipopolysaccharide binding protein (LBP) and Toll-like receptor 4 (TLR4) to initiate cell signalling. LBP targets LPS aggregates and presents LPS monomers to CD14. One complexed to TLR4 a number of intracellular signalling events are triggered including activation of the NF- $\kappa$ B.

Multiple stimuli have previously been shown to alter monocyte expression of CD14.

Landamann et al showed that expression of mCD14 and sCD14 by human monocytes increased in response to stimulation with LPS(141). Maximal upregulation of both membrane and soluble forms were observed at 48 hours. A similar effect was observed in monocytes treated with Lipid A, heat inactivated *E. coli* and components of the cell wall of the gram-positive coccus *Staphylococcus aureus*. In a separate study, the same group also showed that sCD14 is capable of activating monocytes and monocyte like cell lines independent of LPS exposure(172). They showed that monocytes and monocyte like cells (THP-1 cells) exposed to sCD14, observed to disappear following pre-treatment of recombinant sCD14 with 50% plasma or sCD14 depleted serum.

### **1.2.10 Expression of CD14 by monocytes in AATD**

Published data confirms that AAT protein influences the expression of mCD14 by monocytes in vitro(173). Stolk et al have previously suggested that altered CD14 expression in AATD contributes to a shift in the profile of monocyte subsets in the circulation of those with ZZ AATD(142). Using multi colour flow cytometry they showed lower levels of intermediate and non-classical monocytes in circulation and relative expansion of the classical subset which typically express high levels of mCD14. Sandstrom et al have also shown increased levels of both sCD14 and mCD14 in the plasma and on the surface of monocytes obtained from individuals who are hetero or homozygous for the PiZ mutation(167). Unfortunately, the study was not designed to test whether increased levels of both forms of CD14 correlated with specific pathophysiological changes between groups examined. It is notable however that monocyte expression of mCD14 has also been found to be elevated in individuals with ANCA associated vasculitis (AAV)(174). Tarzi et al found a correlation between CD14, PR3 and MPO expression on classical monocytes in those with active vasculitis and those with PR3-ANCA vasculitis in remission. The authors hypothesised that this correlation may reflect monocyte activation and a shift towards a pro-inflammatory monocyte phenotype. Of note, a high incidence of ZZ AATD has been previously reported in those with AAVs associated with anti-bodies against proteinase-3 (PR3)(175).

### **1.2.11 Expression of CD16 by monocytes**

Increased levels of CD16 by monocytes has been previously documented in patients recovering following cardiac surgery(176). This effect was noted to be restricted to monocytes and was not observed in natural killer cells or neutrophils isolated from

the same subjects. Randolph et al demonstrated that monocytes that highly express CD16 are preferentially selected out to differentiate into dendritic cells in response to signals in the micro-environment(177). Furthermore, they showed that expression of CD16 and the migratory characteristics of CD16+ monocytes could be induced in CD16- cells by pre-ā } & ~ à æc ā [ } Á , ā c @Á V Õ Ø F

### 1.2.12 Complement receptors on monocytes

Despite an abundance of complement receptors being identified on the surface of monocytes to date, the receptor for our complement fragment of interest C3d, remains elusive. A study by Inada et al, (1983) suggested that a receptor for C3d may be present on the surface of monocytes. They demonstrated a time dependent increase in rosette formation between monocytes and red blood cells coated with C3d and cultured on a glass slide. This suggests that CR2 may be present on the monocyte surface and capable of binding C3d without providing definitive proof. In consideration of this, identifying CR2 on the monocyte surface was identified as a key aim of this project.

As monocytes and monocyte derived macrophages represent one of the first lines of defence against pathogen invasion, it is advantageous from an evolutionary perspective that they possess multiple receptors for complement proteins on their surface. Broadly speaking, the complement system is an extensive network of proteins, protein fragments and their receptors that form an integral part of the innate immune response. The importance of the complement system as an executor of immune response is underscored by the observation that genes encoding the complement protein C3 and the regulatory co-Factor B are identifiable in the genome of primitive protosomes (179). This suggests that the complement system first emerged over 1 billion years ago(145).

Complement fragments and other ligands that are capable of binding to the surface of monocytes via their respective cell surface receptors. Whilst three separate pathways of complement activation have been described, formation of the complement protein C3 represents a final common step in complement activation(180). As formation and subsequent cleavage of C3 represents the point of

convergence of all 3 complement activation pathways, it is unsurprising that C3 signalling in monocytes and other cell types has been reported extensively in the literature(145, 180).

Within monocytes and macrophages expression of the C3 receptor (CR3) is known to be critical for facilitating phagocytosis(147). CR3 is comprised of the integrin CD11b and CD18(181). To date 4 separate receptors that bind fragments of C3 have previously been described on the surface of monocytes. CR1 (a.k.a. CD35) binds complement fragment C3bi and CR3 (a.k.a. CD11b) binds C3b. Blocking of CR3 in monocytes has previously been shown to reduce intracellular viral antigen expression of dengue virus suggesting CR3 may serve as an entry port for opportunistic viruses. Blockade of CR3 is also known to abrogate expression of TNF

(182).

Marinhno et al., (2014) have described CR3 and CR4 on the surface of human monocytes, They demonstrated down regulation of both CR3 and CR4 on the surface of monocytes infected with dengue virus(183). Other studies have demonstrated an increase in CR3 expression in monocytes obtained from those with active rheumatoid arthritis (RA). Whilst both CR3 and complement receptor 1 (CR1) have been shown to be elevated on monocytes of those with RA and the autoimmune disease systemic lupus erythematosus (SLE)(184). Studies of patients with pneumonia and respiratory failure because of infection with the SARs-CoV2 virus have also shown increased levels of CR3 when compared to controls without respiratory failure (185). Gupta et al emphasise that CR3 functions as a fibrinogen receptor in monocytes and is a key effector of the exaggerated thrombotic effects seen in COVID19 pneumonia(185).

Other receptors for complement proteins and fragments described on the monocyte surface include Cc1qR and the C5a receptor CD88. cC1qR is formed by a complex of calreticulin and CD91. Ligands for include C1q and mannose binding lectin (MBL)(186). C1q acts as a regulatory protein and is necessary for activation of the classical complement pathway. C5a is an anaphylatoxin that has a chemotactic effect on monocytes, macrophages and granulocytes(187). Furebring et al have previously showed surface expression of the C5a receptor CD88 by monocytes is down regulated in severe sepsis(146).

When we considered collectively the early observations of Inada et al (1983) and the above referenced studies highlighting several complement on the surface of monocytes and macrophages, we had reasonable hope that peripheral circulating monocytes may express a receptor for C3d. Identifying CD21/CR2 was key to the success of this project as its identification would confirm a signalling axis for C3d in monocytes. The potential impact of this signalling event was unclear at the outset of the study but unpublished data from our lab suggested that C3d may induce a cytokine response(188).

### **1.2.13 Cytokine production by monocytes**

Fee et al, (2019) have previously shown that neutrophil like HL-60 cells exposed to the complement fragment C3d produced increased levels of the chemoattractant IL-8(188). As Carroll et al (2011) had demonstrated that ZZ monocytes secrete increased levels of IL-8 compared to MM controls(12), this prompted a degree of interest in establishing whether C3d might induce a similar effect on monocyte production of IL-8 and other pro-inflammatory cytokines. We hypothesised that an

interaction between monocytes and C3d may contribute to disease pathogenesis in AATD via the production of cytokines.

The cytokine producing capacity of various monocyte subsets has been well studied.

In a study examining the ontogeny of the innate immune system, Yerkowich et al

studied the ability of monocytes at various stages of life to produce IL-6, 10, 12, 18

æ} å Á G H Ê Á V Þ Ø Á Á ã } Á ! ^ • ] [ } • ^ Á c [ Á • (189).{U\$irþgæc ã [ } Á , ã c

samples from cord blood through to adulthood they found that all cytokines

examined followed a similar developmental pattern. Though slow up-regulation from

the neonatal stage of life to adulthood was observed for most cytokines, levels of IL-

6, IL-F € Ê Á V Þ Ø Á æ} å Á Q Ø Þ Á å ^ { [ } • c ! æc ^ å Á • ã { ã | æ! Á ã } &

blood to adult samples. This effect was lost at 2 months and thought to be

attributable to variations in TLR4 expression which was found to highest on neonatal

monocytes post LPS stimulation. Brichard et al have previously shown that immature

and early cord blood monocytes also have less capacity to generate the pro-

inflammatory cytokine IL-F (190) which is produced prodigiously by intermediate and

classical monocytes treated with LPS(191). The profile of cytokines and propensity

for chemotaxis and phagocytosis changes with age. Ginaldi et al have previously

identified depressed antigen processing and presentation as a feature of monocytes

obtained from older adults(192). Furthermore, they note that from a biochemical

paradox, aging represents something of a paradox. Though antigen presentation and

processing by monocytes is depressed in older age, monocyte activation and

production of cytokines IL-1, IL-Î Á æ} å Á V Þ Ø Á ã } & ! ^ æ• ^ È

Schutte et al have previously examined the pro and anti -inflammatory cytokine

profiles elaborated by monocytes and macrophages at various stages of

differentiation and culture(193). A monocyte like cell line, THP-1 cells were seeded

onto various biomaterials and left untreated, exposed to PMA or LPS. Levels of TNF- $\alpha$ , MCP-1, IL-6, IL-1 $\beta$ , IL-1ra, and IL-10 were measured in supernatants at 24 and 48 h. The highest levels of cytokines were observed in those treated with PMA for 48 h. The authors also noted phenotypic changes in PMA treated cells that were not apparent in untreated and LPS treated cells. Using phase contrast microscopy, they observed that PMA treated cells were larger, with extended filopodia and less clustering apparent in their growth pattern. Flow cytometry also showed increased surface expression of the integrin CD11b. Collectively these findings suggest that THP-1 monocyte like cells were differentiating towards a macrophage phenotype in response to prolonged exposure to PMA. Stimulated monocytes can produce large concentrations of reactive oxygen species, complement factors, prostaglandins; nitric oxide (NO) and cytokines such as TNF- $\alpha$ , MCP-1, IL-6, IL-1 $\beta$ , IL-1ra, and IL-10; vascular endothelial growth factor; and proteolytic enzymes such as metalloproteinases (144, 194, 195).

Published data suggests that monocytes are primed towards a more inflammatory profile in certain disease states. Patel et al identified higher levels of pro inflammatory cytokine production by intermediate and non-classical monocyte subsets from individuals with dyslipidemia (196). They identified higher levels of TNF- $\alpha$ , MCP-1, IL-6, IL-1 $\beta$ , IL-1ra, and IL-10; vascular endothelial growth factor; and proteolytic enzymes such as metalloproteinases (144, 194, 195) compared to classical subsets. This finding overrides the usual functional distinction between subsets and implicates all monocyte subsets in the development of coronary artery disease in this cohort.

In AATD the cytokine response generated by stimulated monocytes has also been shown to be altered. Carroll and colleagues demonstrated that ZZ monocytes exhibit enhanced cytokine production and activation of the NF- $\kappa$ B pathway when compared

with MM monocytes(13)- a finding that likely contributes to the inflammatory phenotype observed in AATD.

#### 1.2.14 Protease production by monocytes

In addition to their capacity to generate cytokines, monocytes and macrophages are known to produce a number of different proteases. Broadly speaking, proteases cleave proteins into polypeptides or amino acids. Sub types of proteases are identifiable by the expression of different catalytic residues. The 4 groups or proteases, metalloproteases and aspartic acid proteases(197).

Under homeostatic conditions proteases are necessary to regulate tissue regeneration and repair. Diseases such as AATD or Cystic Fibrosis (CF) reflect an imbalance between protease and anti-protease activity. The former is characterised by low circulating levels of the serpin inhibitor AAT permitted unfettered action of proteases such as NE that degrade the extra cellular matrix. In CF thick, tenacious mucus within the airways perpetuates cycles of infection and inflammation.

Production of cytokines such as the neutrophil chemoattractant IL-8 facilitates neutrophil recruitment to the lung(198). The cell population within epithelial lining fluid (ELF) becomes dominated by neutrophils (70% vs 1% in HC lungs(199)). Once activated, neutrophils produce proteases at a rate that exceeds the anti-protease capacity of available anti-proteases propagating tissue damage. AAT acts to preferentially inhibit the action of serine proteases, in particular neutrophil elastase which its binds in an equimolar ratio.

Like their neutrophil cousins, monocytes are also capable of producing serine proteases. The serine protease activity of monocytes was highlighted by Chateau et al who showed degradation of the enzyme HIV-1 Reverse Transcriptase when incubated with cell extracts from human monocytes(200). Protease activity was similar across all monocyte subsets and was also shown to be present in monocyte precursors. Degradation of HIV-1RT was inhibited by the addition of PMSF and aprotinin. PMSF and aprotinin are both protease inhibitors which preferentially inhibit the serine proteases. This implicates this sub-group of proteases in the degradation of HIV-1RT.

Multiple studies have since clarified the relationship between monocytes and serine proteases. Schuldhaus et al showed inducible expression of granzyme B in monocytes exposed to LPS(201). They identified LPS/TLR4 signalling as being central to the upregulation of granzyme B production by monocytes. Studies of individuals with CF which is characterised by repeated cycles of infection within the lungs, show up regulation of the serine protease PR3 mRNA in monocytes of people experiencing an exacerbation(202). Interestingly, this effect was abrogated by treatment with anti-IL-1. They identified preferential surface expression of PR3 and monocytes in AAVs. They identified preferential surface expression of PR3 by the intermediate subset of monocytes in individuals with known vasculitis(203).

In addition to playing a role in the production of proteases, monocytes possess surface receptors that enable them to respond to stimulation by proteases.

Johannson et al have previously identified the protease receptor protease-activated receptor 2 (PAR-2) on the surface of monocytes(204). Surface bound PAR-2 must be cleaved to its active form by trypsin and other serine proteases. Surface expression can be up regulated by mobilisation of internal stores to the cell surface.

When activated by the PAR-2 ligand 2-furoyl-LIGKV-OH, monocytes are stimulated to produce the pro inflammatory cytokines IL-6, IL-8 and IL-1

Our understanding of how monocytes contribute to the pathogenesis of disease, in particular lung disease has evolved considerably over the past 10 years. New insights have highlighted the important role that matrix metalloprotease (MMP) production by monocytes contributes to disease. In view of this, the role MMPs play in disease will now be discussed in greater depth.

### **1.2.15 Matrix metalloproteinases (MMPs)**

MMPs are a family of zinc dependant endopeptidases that have been implicated in both normal physiological and pathophysiological tissue remodelling. MMPs all share a zinc-based catalytic mechanism and can degrade the majority of proteins that comprise the extra cellular matrix (ECM) and basement membrane(205). To date, 25 MMPs have been described 22 of which are detectable in humans(206). Individual MMPs can be classified by variations in their structure, function, and substrate preferences. For simplicity, MMPs are grouped according to function: the interstitial collagenases (i.e. MMP-1, 8, 13 and 18), gelatinases which are implicated in the degradation of type 4 collagen ( i.e. MMP-2, 9) and the stromelysins (i.e. MMP-3, 10, 11) that are specific for laminin. Cells of the MPS secrete a diverse range of metalloproteases (MMPs) in large quantities. In addition to their dominant role in protein degradation MMPs influence cell migration and the processing and activation of soluble factors(207). MMPs play a role in many vital physiological processes including angiogenesis, bone formation and elongation, antigen processing and presentation and embryonic implantation(205). It is therefore

perhaps surprising that most MMPs are not constitutively expressed and require some form of cell activation to initiate transcription.

Production of MMPs is tightly regulated across many levels including transcription, post translational modification and by exogenous inhibitors. Imbalances between the production of MMPs and endogenous tissue inhibitors of MMPs (TIMPs) can result in dysregulation of many normal physiological processes(207, 208). A relative excess of MMPs versus TIMPs has been implicated in the development of cardiovascular disease- in particular the formation of unstable coronary artery plaques and reperfusion injury following an ischaemic injury to the myocardium(208). The role MMPs play in the development of chronic inflammatory lung disease has yet to be elucidated. It has been demonstrated that activation and inactivation of MMPs modulates the activity and effects of chemokines and cytokines(205). In this manner they may contribute to driving inflammation in chronic lung disease.

MMPs are secreted as inactive pre cursors (zymogens) that require cleavage of a pro-peptide domain to activate enzymatic activity(31). Activation of MMPs is mediated by a range of proteinases including other MMPs and in many cases this occurs extracellularly following secretion. This pattern of intracellular storage and subsequent release varies between different MMPs. The gelatinase MMP-9 is synthesised and stored in intracellular granule as is the interstitial collagenase MMP-8(209, 210). In contrast pro MMP-1 requires cleavage to its active form by MMP 3, 7 and 10(211). Figure 1.8 provides a schematic overview of the regulation of MMP production by monocytes.

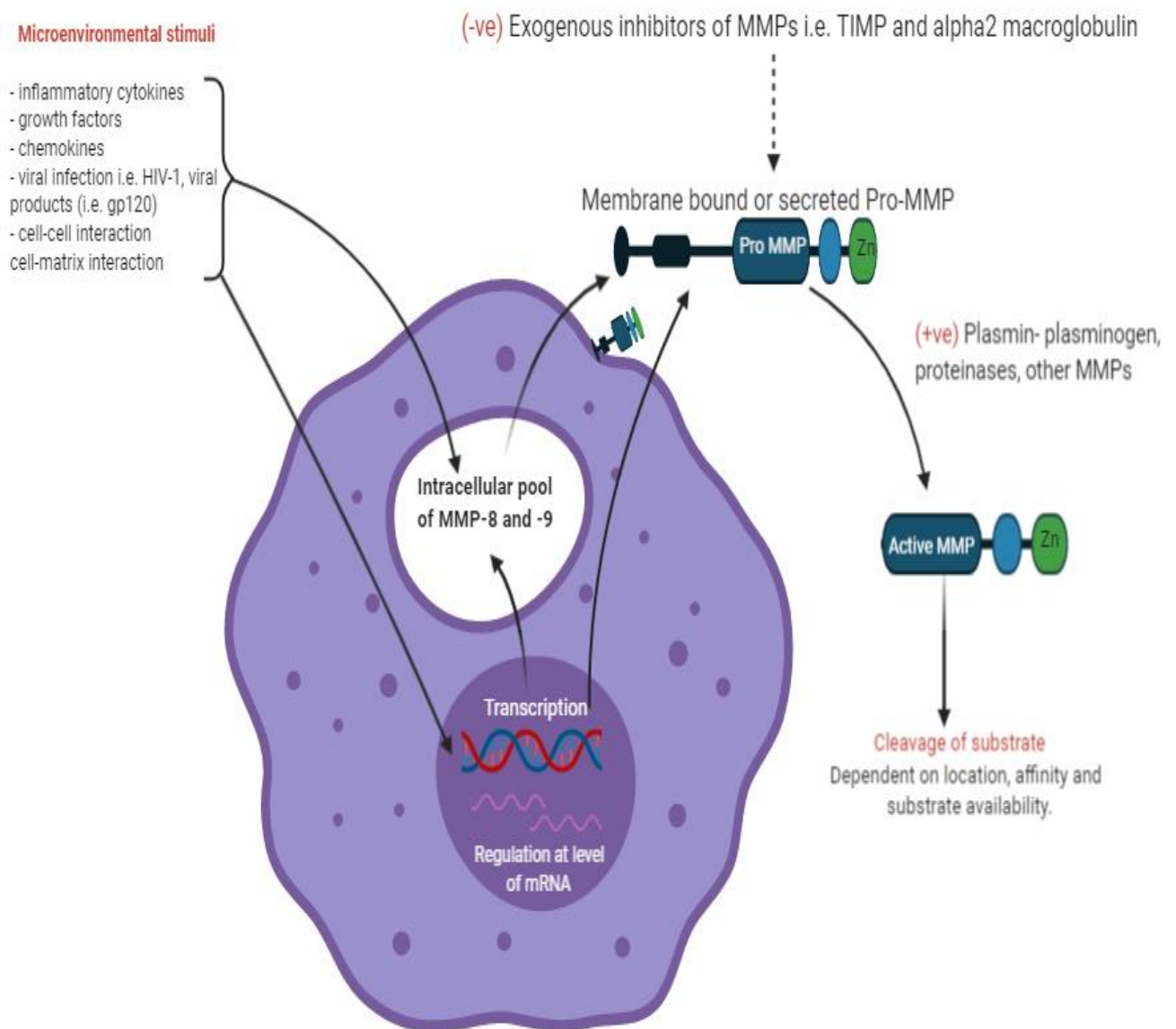


**Figure 1.9: Production and regulation of MMPs by monocytes**

Stimulation of monocytes by signals from their microenvironment results in signal transduction, transcription, expression of MMP on the cell membrane and release to the extracellular environment. Pro MMPs are converted to their active form by proteinases and other MMPs.

### **1.2.16 MMP production by monocytes**

The specific type of MMPs secreted by monocytes and macrophages depends on the degree of differentiation and the state of activation. Members of the MPS including dendritic cells have been found to express the majority of the 23 human MMPs at gene level. Classical monocytes which express high levels of the cell surface receptor CD14 preferentially express MMP1, 3, 9, 10, 14, 19 and 25(212, 213). MMP2 and 17 are also found though at lower levels. A study of the role monocytes production of MMPs play in driving inflammation in the neurodegenerative disease multiple sclerosis (MS) showed that production of MMP-9 was downregulated when cells were exposed to IFN and LPS (100ng/ml) for 8 hours(214). By contrast MMP-3 production was upregulated. Of the all the MMPs produced by monocytes, MMP-9 has been amongst the most extensively studied in the context of its effect on the development and progression of lung disease(215).

### **1.2.17 Monocytes and MMP-9**

MMP-9 production by monocytes was first described in 1984(216). Differences in experimental methods have meant that data quantifying basal levels of MMP-9 production is conflicting. Adherence of monocytes to a glass surface in vitro increases MMP-9 secretion. Following production, MMP-9 is produced either free or in complex with TIMP (205). Lu and Wahl have previously demonstrated that activation of monocytes following exposure to LPS stimulates production of MMP-9 via activation of the NF-KB pathway (217). Other pro inflammatory stimuli such as TNF alpha also enhances MMP-9 production via the prostaglandin E2 pathway(218). The structure of MMP-9 comprises a fibronectin-like domain, which consists of three repeats of fibronectin type II made up of 58 amino acids(50). This fibronectin like

domain is glycosylated and contains an elongated linker between 2 further catalytic and hemopexin-like domains(219). The presence of the fibronectin-like domain enables binding to a substrate of either denatured collagen or gelatin. In the biologically inactive preform of MMP-9 (pro-MMP-9) the hemopexin-like domain forms a complex with the endogenous MMP inhibitors TIMP-1 and TIMP-3 within the Golgi apparatus of the cell(220). TIMP-1 binds pro-MMP-9 via the COOH-terminal domain on the enzyme, leaving the NH2 terminus capable of inhibiting other MMPs(221).

MMP-9 is detectable in healthy normal lungs and is found in increased abundance in the chronic lung diseases IPF, asthma and COPD (222). Some debate exists as to whether MMP-9 is a causal factor in lung remodelling or part of the inflammatory and reparative processes. It is likely that the multiple cell types producing MMP-9 and the different locations where it can be in the lungs (interstitium, airways etc.) reflects a propensity to adapt its function in response to different micro environmental signals (222)

Omachi and colleagues have previously examined the role of MMP-9 as a predictor of outcomes in AATD (223). They examined data from patients with the PiZ and null AAT mutations who were not on augmentation therapy. They found higher levels of plasma MMP-9 correlated with more severe airflow obstruction and impairment of gas exchange as measured by DLCO. In longitudinal analyses they found that increases in MMP-9 predicted further declines in DLCO underscoring its usefulness as a biomarker of lung disease.

MMP-9 is of particular interest to this study as it has been shown to propagate inflammation within the lungs through degradation of the extra cellular matrix, neutrophil chemotaxis and augmentation of the inflammatory response(224). Each of

these features taken individually are key components of an AECOPD. Wells and colleagues have previously shown that elevated plasma levels of MMP-9 are independently associated with the risk of exacerbation in COPD (225).

## 1.3 The Complement System

### 1.3.1 Background

U q Á Ó! ã ^ } Á æ} â Á & [ | | ^ æ\* ~ ^ • Á @æç ^ Á ] ! ^ ç ã [ ~ • | ^ Á â ^ • &

complement fragment C3d in the plasma and BAL samples of individuals with ZZ AATD. Furthermore, they identified a positive correlation between increased levels of C3d and radiographic evidence of emphysema. In vivo, treatment with AAT augmentation therapy significantly reduced plasma levels of C3d. C3d is a reliable marker of overall complement activation. The elevated levels seen in ZZ AATD suggest dysregulated activation of the complement system.

Unpublished work from the McElvaney lab also showed that neutrophils exposed to C3d had increased levels of secondary and tertiary granule proteases detected in cell supernatants. This suggests that C3d may have a direct effect on neutrophil activation and represents a novel mechanism of disease pathogenesis in AATD. These observations prompted us to wonder whether C3d could also influence the behaviour of monocytes in AATD. As discussed previously, monocytes have a massive capacity for cytokine and protease production in response to inflammatory signals in their microenvironment. As C3d represents an end product of complement activation we were keen to assess what effects if any C3d has on monocytes.

To understand why C3d may be elevated in AATD, it is first necessary to review the complement cascade and how complement proteins, receptors and fragments such as C3d contribute to inflammation and the development of disease.

### 1.3.2 The complement system

The complement system or cascade is a vast network of proteins primarily synthesised by hepatocytes in the liver. It comprises more than 30 proteins, regulatory factors, fragments and receptors. Complement proteins in plasma measures approximately 3g/L and accounts for 15% of the total globulin fraction. The main physiological activities of complement are summarised in Table 1.2. Broadly speaking, complement activation plays a role in host defence against infection, linking innate and adaptive immunity and facilitating the disposal of waste products of inflammation

V @^ Á & [ { ] | ^ { ^ } c Á ± & æ • & æ å ^ q Á & æ } Á à ^ Á c ! ã \* \* ^ ! ^ å Á ç ã  
pathways of complement activation have been described- the classical, alternative and lectin pathways (Figure 1.10). Regardless of the inciting trigger and pathway of activation, all 3 pathways share the final common step of cleavage of the complement protein C3.

The classical complement pathway is activated following the formation of antibody antigen complexes. IgM or IgG bind to pathogens or foreign antigens triggering the classical complement response. Antibodies then bind to the complement protein complex C1. C1 is formed by the serine protease C1s and complement fragments C1q and C1r. C1r activates C1s enabling sequential activation of complement proteins C2 and C4 and cleavage into their component fragments (C4a, C4b, C2a and C2b). Fragments of C2 and C4 associate to form C3 convertases which cleave C3. Cleavage of C3 represents the point of convergence of all 3 complement pathways.

Activation of the alternative pathway can occur by several means. Detection of bacterial endotoxin, repeating polysaccharide patterns, formation of IgA antibody

complexes or immunoglobulin light chains are all recognised triggers of the alternative complement pathway(226, 227). Unlike the classical and lectin pathways, activation of the alternative pathway can occur spontaneously via hydrolysis of C3(228).

The lectin pathway is activated following recognition of carbohydrate moieties on the surface of pathogens by mannose binding lectin (MBLs) or ficolin. MBL is complexed with MBL associated serine proteases (MASPs 1-3). In a manner similar to the antibody binding of the classical pathway, binding of MBL to the surface of pathogens activates MASPs facilitating cleavage of C2 and C4 and subsequent formation of C3 convertase.

The majority of complement proteins are synthesised within the liver and secreted as  $\alpha_2$  macroglobulin (229). In addition to this hepatic reservoir, lung tissue represents a further source of complement production. Since the 1980s it has been recognised that in addition to secreting surfactant, type 2 pneumocytes produce a number of complement proteins including C3 and C5 (230). Pulmonary macrophages secrete C2, C3 and Factor B and epithelial cells of the respiratory bronchioles produce C3(231). Macrophage derived serine proteases cleave C5 to form C5a in in-vitro studies(232). C5a acts a potent pro inflammatory peptide. Formation of C5a drives formation of the membrane attack complex and release of histamine further propagating the inflammatory response. Riedemann and colleagues demonstrated that stimulation of alveolar epithelial cells with LPS, IL-6 or TNF alpha increased the affinity of C5a for its receptor C5aR(233, 234). Furthermore, binding of C5a to its ligand was associated with increased mRNA expression for C5aR(234).

Regulatory proteins such as decay acceleration factor (DAF, CD55), C4 binding protein (C4BP) and Factor H are responsible for the guiding the progression of the

complement cascade through both their inhibitory and stimulatory roles. Given the complexity of the interactions involved in the complement cascade it is perhaps

~ } • ~ | ] | ã • ã } \* Á c @æc Á } [ Á ± ] ^ | ~ ^ & c q Á c ^ • c Á ^ ø ã • c • Á c

this, it is widely accepted that levels of complement fragment C3d are a reliable surrogate marker of overall complement activity(235). Unlike the formation of C3a and C3b, C3d is not produced spontaneously by hydrolysis in plasma making it a more consistent indicator of complement activation(235).

**Table 1.2: Summary of the physiologic activities of complement**

Adapted from Mark J. Walport, PhD, FRCP, Complement, New England Journal of Medicine 2001

<b>Activity</b>	<b>Mechanism</b>	<b>Complement proteins involved</b>
Defence against infection	Opsonisation  Chemotaxis and leucocyte activation  Lysis of bacteria and cells	Covalently bound fragments of C3 and C4  Anaphylatoxins C3a, C4a, C5a  Membrane attack complex C5b-C9
Linking innate and adaptive immunity	Augments anti-body response  Immunologic memory	C3b and C4b  C3 receptors on B cells, antigen presenting cells and FDCs
Disposal of waste products of inflammation	Clearance of immune complexes  Clearance of apoptotic cells	C1q  Fragments of C3 and C4

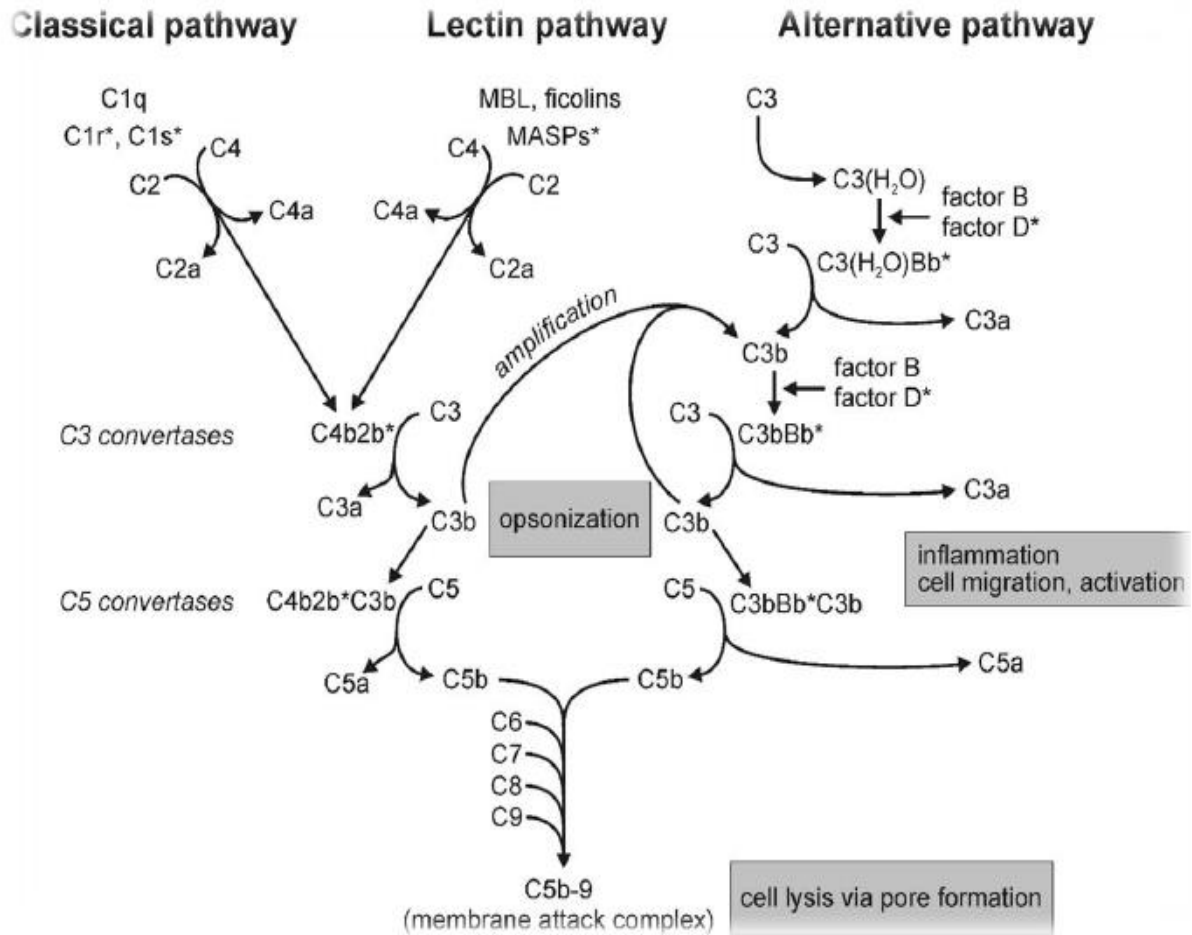


**Figure 1.10 Overview of the Complement System**

The complement system consists of a network of over 30 proteins which play an important role in host defence and inflammation. Complement activation occurs through three different pathways: alternate, classical and lectin. (Adapted from Mihály Józsi., 2011).

(MBL; Mannose binding lectin, MASPs; Mannan-binding lectin serine proteases)

### 1.3.3 Complement activation and lung disease

Activation of the complement system has been described in a number of lung conditions including the acute respiratory distress syndrome (ARDS) (236). First described by military physicians in the 1960s ARDS is a rapidly progressive, and frequently fatal cause of hypoxemic respiratory failure. Lung injury triggers the release of pro inflammatory cytokines such as TNF alpha, IL-8 and IL-6(237). Zilow and colleagues examined plasma levels of complement factors in trauma patients who developed ARDS. They found an increase in the ratio of C3a to C3, suggesting increased cleavage of C3 and overall complement activity levels and an absence of C5a(238). The absence of C5a in plasma contradicted the work of Hammerschmidt and colleagues who in 1980 had measured plasma levels in a separate ARDS cohort and found them to be elevated(239). The conflicting results may be accounted for by differences in the baseline characteristics of both study groups. ARDS represents the final common pathway of a litany of clinical insults including pneumonia, developed ARDS post trauma, Hammerschmidts were a more heterogenous population and included patients with sepsis.

Activation of the complement system has also described in patients with COPD. Marc et al obtained sputum samples from patients with COPD or asthma and compared them to healthy non-smokers. Levels of C5a were significantly elevated in the COPD group (p=0.007) when compared with controls(240). Furthermore, the increase in C5a correlated negatively with the diffusion capacity of carbon monoxide on lung function testing which suggests that complement activity may play a role in the disease pathogenesis.

Kew and colleagues hypothesised that cigarette smoke was causing complement activation in smokers and increasing neutrophil influx into the airways by acting as a chemoattractant(240). In a series of in-vitro experiments they demonstrated that treatment of purified human C3 with smoke modified the molecule such that when it was added to serum (pre-blocked with Mg/ethylene glycol tetra acetic acid (EGTA) to prevent activation of the classical pathway) it resulted in activation of the alternative pathway. Treatment of purified human C3 with whole smoke solution modifies the molecule such that its subsequent addition to serum results in complement activation via alternative pathway. C3 that was treated with cigarette smoke was also shown to be less responsive to the action of the complement regulatory proteins Factor H and I(240).

### 1.3.4 Complement fragment C3d

Given the complexity of the interactions involved in the complement cascade it is

]

Despite this, it is widely accepted that levels of complement fragment C3d are a reliable surrogate marker of overall complement activity (241). Unlike the formation of C3a and C3b, C3d is not produced spontaneously by hydrolysis in plasma making it a more consistent indicator of complement activation (235) (Figure 4).

The major product of C3 cleavage, C3b is covalently bound to the surface of pathogens during activation of the classical and alternative pathways(180). On many cell surfaces C3b is precariously bound leaving it susceptible to further cleavage by factor I. This results in the formation of the inactive form iC3b. This haemolytically inactive form remains attached to the surface of the activating cell or organism. In the presence of a co-factor, Factor H C3b undergoes further cleavage eventually

resulting in the retention in the membrane of a fragment of C3, C3dg. It is cleavage of this C3dg by trypsin, elastase or plasmin results in the generation of membrane bound C3d(235).

Increased activity of C3d has been identified in a number of disease processes.

Doherty and colleagues (1988) examined C3d levels in the synovial fluid of 288 patients with rheumatoid arthritis (RA), osteoarthritis (OA) and crystal arthropathies (242). Raised levels of C3d were found in active RA joints when compared to inactive joints (mean (range) 51 (15-105) and 6 (0-15) units/ml respectively).

Villacorta and colleagues identified C3d positive staining of renal biopsy samples as a novel predictor of progression to end stage renal disease (79). C3d-positivity on biopsy correlated with the severity of renal impairment and with a lower rate of treatment response ( $P=.003$  and  $P=.04$ , respectively). When adjusted for baseline renal function and other lower histologic parameters, C3d staining remained as an independent predictor for renal survival (hazard ratio, 2.5; 95% confidence interval, 1.1-5.7;  $P=.03$ ).

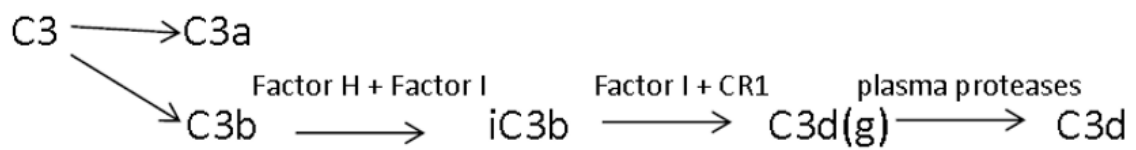


### Figure 1.11 Mechanism of C3d production

C3b, a cleavage product of C3 is cleaved to C3d during complement activation.

Factor H and Factor I are critical for the production of C3d with factor H acting as a cofactor for factor I mediated cleavage of C3b into iC3b and C3dg and finally C3d by nonspecific proteases (79).

### 1.3.5 C3d in AATD

Complement dysregulation in AATD has been a subject of interest since the observation by Taylor and colleagues in 1977 that C3 can be cleaved by neutrophil derived proteases such as NE to activate the complement cascade (243). Given the pro-inflammatory properties of C3 activation, including the production of pro-inflammatory mediators C3a and C5a and opsonin C3b, it is likely AAT may interact with C3 in an anti-inflammatory capacity with binding of AAT to C3 serving to prevent dysregulated proteolysis of C3 and complement activation.

Levels of C3d and overall complement activation were examined by Littleton et al (1991) who investigated children with liver disease attributable to AATD (244). They identified low levels of the C3d parent protein C3 in addition to C4 in children with advanced liver disease. This likely reflected impaired hepatic protein synthesis. To account for this, they used the ratio of C3d:C3 to assess complement activation. This approach corrects for the reduction in the availability of the parent protein C3. Using this strategy, they identified increased levels of complement activation in the ZZ group compared to MM controls. They also noted increased C3d:C3 ratio correlated with disease severity and was highest in those with severe liver disease.

Published data from the McElvaney lab confirms that C3d levels are significantly increased in plasma samples from ZZ AATD patients when compared to healthy MM controls ( $p=0.002$ ) (78). Furthermore, C3d levels were also not significantly elevated in clinically stable, FEV1 matched AAT sufficient COPD controls ( $p=0.001$ ). This suggests that the excessive complement activation seen in ZZ AATD reflects a lack

[ ~ Á ŒŒEV Á † æc @^ † Á c @æ} Á à ^ ã } \* Á æÁ & [ } • ^ ~ ~ ^ } & ^ Á [ ~ Á æÁ

and colleagues also found a positive correlation between increased levels of C3d and worsening of radiographic evidence of emphysema in those with ZZAATD(245).

Trypsin-like enzymes such as NE whose activity, under normal conditions is regulated by AAT has been demonstrated to activate both the classical and alternate complement pathways (246). It is thought that binding of AAT to C3 may prevent dysregulated cleavage of C3 and subsequent complement activation. It is therefore conceivable that a deficiency of AAT may lead to complement activation without the inhibitory influence of AAT.

### 1.3.6 Complement receptor CR2

The receptor for C3d has previously been identified as CR2. CR2 also known as CD21 is a 145kDa glycoprotein first identified on the surface of B cells and follicular dendritic cells (247). CR2 has been described as having 4 classes of ligands including the C3 fragments iC3b, C3dg and C3d(248). CR2 in complex with C3d is shown in Figure 1.12.

CR2 is perhaps best known for its ability to bind the gp350/220 viral coat protein of the Epstein-Barr virus(247). EBV is one of nine human herpes viruses. EBV infection is associated with several benign, pre-malignant and malignant pathologies. Chief amongst these conditions is the commonly encountered infectious mononucleosis  
 æ} å Á c @^ Á | ^ { ] @[ ] † [ | ã ~ ^ † æc ã ç ^ Á å ã • ^ æ• ^ Á Ó ˇ † \ ã c c q  
 immunoregulatory protein CD23(249), and interferon-alpha (IFN- (250).

Though ubiquitously expressed on mature circulating and BM resident B cells, CR2 has not been identified on B cell precursors. CR2 has also been identified on subsets of thymocytes (251), T cells (252), basophils (253) and follicular dendritic

cells (FDCs). FDCs are found in lymphoid follicles and are distinct from DCs. DCs are derived from haematopoietic stem cells within the bone marrow whereas FDCs are of mesenchymal origin. Though monocytes express several complement receptors they have not been conclusively shown to express CR2 (254). A study from 1983 however suggest that this merits further exploration. Inada et al showed a time dependant increase in rosette formation when C3d coated red cells was incubated with monocytes suggesting that monocytes are capable of binding C3d (255).

Structurally CR2 comprises a large extracellular domain a 24 amino acid transmembrane domain and a short 34 amino acid intra cellular tail (256). The extracellular portion of CR2 consists of a series of 15-16 structurally similar complement control proteins (CCPs). Each CCP consists of a 60 amino acid sequence. The two terminal CCPs contain the shared C3d and EBV binding site. Complexed N-linked oligosaccharides contribute approximately 35kDa to a 100kDa peptide backbone but are not necessary for C3d binding.

To date 2 isoforms of CR2 have been identified(257). Short and long isoforms have been found on the surface of, and within the cytoplasm of B cells and FDCs. Studies of the gene products of CR2 demonstrate variable expression of two products of transcription. Alternative splicing of exon 11 (60 aa sequence) results in the generation of a shorter CR2 product absent this CCP that retains capacity to bind C3d and EBV(257). This shorter variant is the predominant form produced by most B cell lines. This is in contrast to FDCs which preferentially express the long form of CR2(258).

CR2 functions to provide a link between innate and adaptive immunity (259). When an antigen becomes opsonised by C3d, the antigen moiety binds to the B cell-

antigen receptor complex. CR2 binds to CD23 and associates with CD19, CD81 and Leu13 to form a large signal-transduction complex. Meanwhile the C3d moiety binds to a complex formed by CR2, CD19 and CD81. This simultaneous co-ligation of receptor complexes lowers the threshold of antigen exposure required by the B cell to activate by up to 10,000 fold (260).

An intact C3d/CR2 signalling axis is crucial for generating a high affinity anti-body response (261). Chen and colleagues have previously demonstrated that CR2 knockout mice demonstrate defective B cell memory and antibody generation (262). CR2 is also known to play a role in the development of autoimmunity, specifically the multi system disease SLE. Patients with SLE have been shown to express very low levels of the complement receptors CR1 and CR2 which promotes the development of anti-DNA antibodies(250). CR2 is capable of binding bacterial, viral and fungal DNA suggesting it may play a role in the recognition of foreign DNA during host immune responses(263).

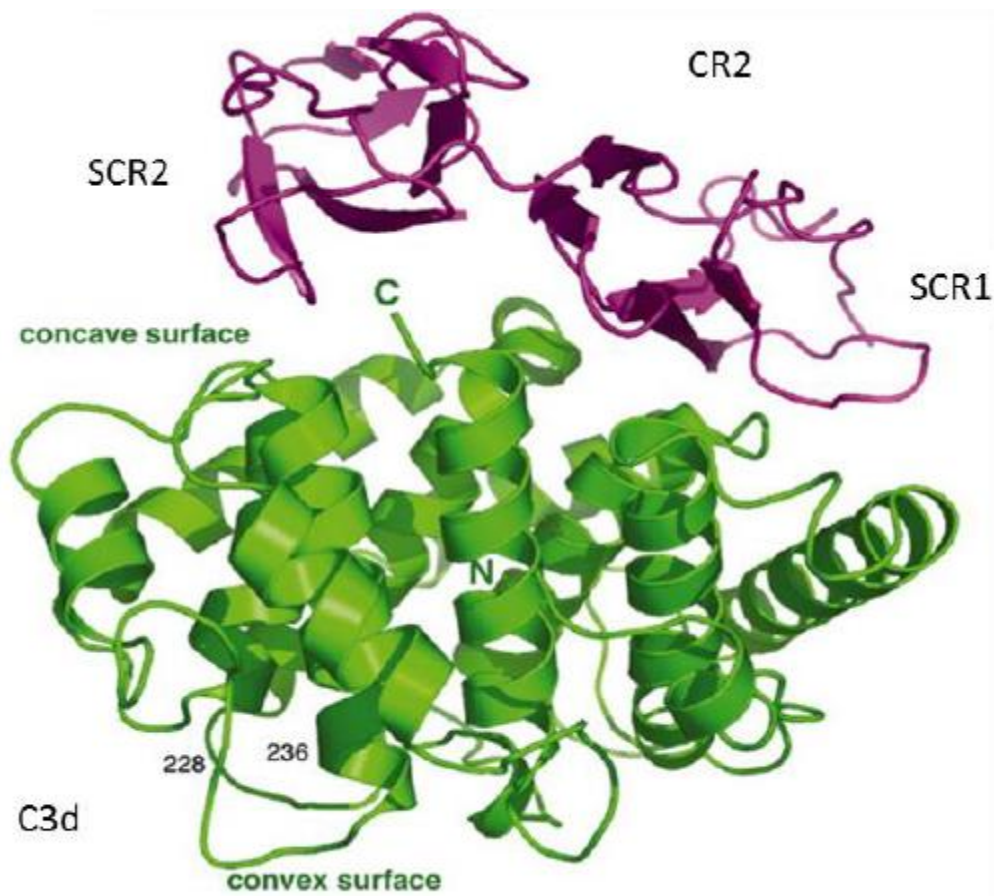


**Figure 1.12: Structure of the C3d:Complement Receptor 2 Complex**

Ribbon diagram of the complement receptor 2 (CR2): C3d complex. C3d molecule is green and CR2 (short consensus repeats (SCRs)) is magenta. Image adapted from (321).

### **1.3.7 Soluble CR2 (sCR2)**

Long and short isoforms of CR2 have previously been identified on the cell surface and also within the cytoplasm of FDCs and B cells. Ling et al., (1998) used confocal microscopy to characterise the cellular distribution of CR2 in the former(264). They demonstrated high levels of CR2 detectable in the supranuclear region of FDCs. A similar clustered distribution has been observed in astrocytes. Gasque et al (1996) demonstrated that the amount of CR2 extracted from whole cell lysates was 5-10 fold greater than surface CR2(265). Furthermore, mirroring the observations made by Ling using FDCs, this study showed that CR2 localised to discrete areas within the cell body and at the end of astrocyte processes.

The soluble form of CR2 is readily detectable in human plasma(264). Levels increase markedly in those with chronic lymphocytic leukemia of B cell origin. Interestingly, the origin of this sCR2 is unlikely to be B cells as levels remain unchanged in those with X linked agammaglobulinemia a condition characterised by defective B cell development and function(266).

### **1.3.8 Complement targeted therapeutics**

The role complement plays in systemic and organ specific disease has been recognised for more than 50 years. Research into therapies targeting complement has been stymied by a reticence to block a crucial arm of innate immunity. In 1966 Rosse and Dacie identified the membrane attack complex as an effector of haemolysis in the ultra-rare, and ultimately fatal disease paroxysmal nocturnal haemoglobinuria (PNH)(267). Rosse and Dacie's discovery allowed development of a drug that could block a specific point in the complement network without sacrificing the utility of the complement network as a whole. Eculizumab (trade name Soliris) is

a monoclonal antibody that blocks C5 mediated activation of the complement cascade and formation of the MAC complex(268). Though prohibitively expensive in certain healthcare systems, eculizumab has been transformative for patients with PHN. Those on treatment can be expected to have a near normal life span in contrast to average of 10 years given to sufferers in the 1970s(269).

A similar C5a receptor inhibitor has also been used successfully as a steroid sparing agent in individuals with ANCA vasculitis and nephropathy(270). In a randomised placebo control trial, Jayne et al showed that the C5a receptor inhibitor Avacopan could be used effectively to slow disease progression and facilitate reduced steroid dosing. Adverse events did not differ significantly between all treatment groups.

Results of phase 2 trials of the complement inhibitor OMS721 (Omeros) which targets the MBL pathway via MASP2 are encouraging. Data from patients recruited with an underlying diagnosis of common glomerulopathy IgA nephropathy showed statistically significant improvements in urine albumin creatinine ratios (ACR). Lower urine ACRs are known to correlate with survival in chronic kidney disease(271).

Results of phase 3 trials are awaited. It is notable that many agents targeting components of the complement pathway have failed in phase 3 studies when phase 2 data suggested cautious optimism.

Lampalizumab, an antibody fragment was developed to treat age related macular degeneration a leading cause of blindness worldwide. Lampalizumab blocks the interaction between Factor D and C3b-bound Factor B thereby preventing activation

of the alternative pathway. Though results of phase 2 trials were promising no significant difference in primary or secondary outcomes were observed in phase 3

trials(272). U c @^ | Á & [ { ] | ^ { ^ } c Á å | ~ \* • Á & ~ | | ^ } c | ^ Á æ ] ] | [ ç  
| ^ ] | æ & ^ { ^ } c Á c @^ | æ ] ã ^ • È Á Ü ^ ] | æ & ^ { ^ } c Á [ ~ Á Ô F ã } @Á  
, @^ | ^ Á Ô F ã } @Á å ^ å ã & ã ^ } & | Á & æ [ } Á { Á Á c @^ Á & [ { ] | ^ { ^ }  
@æ • Á ] | [ ç ^ } Á c [ Á à ^ Á & | ã } ã & æ | | ^ Á ^ ~ Ç G Ë È Ì Í Î Ï Ñ Ò Ó Ô Õ Ö × Ø Ù Ú Û Ü Ý Þ ß à á â ã

## 1.4 Summary

The term AATD refers to any qualitative or quantitative deficiency in AAT protein (9). Historically, disease in AATD was thought to be explainable by the protease anti-protease hypothesis (50). High levels of neutrophil derived serine proteases overwhelm available AAT protein. Within the lungs, proteases such as NE, PR3 and Cathepsins work to degrade the ECM. Clinically, loss of ECM by protease degradation results in the development of emphysema of the alveolar air spaces.

Since the original description of the protease-anti protease hypothesis, our understanding of disease pathogenesis in AATD has evolved considerably. The wide-reaching immunomodulatory effects of AAT have previously described at length (54). In addition to its anti-protease properties, AAT is an acute phase reactant. In vitro and in vivo studies have shown that in addition to its ability to block neutrophil degranulation and chemotaxis (66), AAT abrogates the production of cytokines that are known to drive inflammation (32), normalizes apoptosis (71) and modulates the resolution of local and systemic inflammatory responses(31). Considered collectively, these observations suggest that deficiency of AAT represents a pro-inflammatory state.

Though neutrophil behaviour in AATD have been reported in some detail (110), the phenotype and function of monocytes has yet to be fully elucidated. Carroll et al., (2009) showed an enhanced pro-inflammatory cytokine response in ZZ compared to MM monocytes demonstrating a potential role for monocytes in contributing to the pro-inflammatory milieu observed in AATD (13). Other studies have demonstrated a direct effect of AAT on monocyte phenotype and function. AAT is known to regulate the expression of the surface marker CD14 (142), expression of which can be used to identify various monocyte subsets with differing inflammatory profiles. AAT has

also been shown to increase intracellular cAMP and suppress NF- $\kappa$ B from the nucleus (13, 274).

The concept of AATD representing a model of sustained, inappropriate inflammation

identified AAT as a binding partner of the complement protein C3. Furthermore, they showed higher levels of the C3 fragment C3d in the plasma and airways of individuals with ZZ AATD. This suggests inappropriate or dysregulated complement activation in AATD. The presence of an extensive number of receptors for complement proteins, fragments and co-factors in the surface of monocytes suggest they are programmed to respond to complement activation (139, 182). This prompted us to wonder whether C3d could be having a direct effect on monocytes that could be contributing to the disease profile seen in AATD.

## 1.5 Study Aims

U q Á Ó! ã ^ } Á ^ c Á æ| È Ê Á Ç G € F J D Á ã complement fragment C3d in & ! ^ æ • ^ å  
the plasma of those with ZZ AATD (78). Plasma levels of C3d correlated significantly with radiographic evidence of pulmonary emphysema ( $p=0.001$ ). Furthermore, administration of IV AAT augmentation therapy was shown to decrease C3d levels in parallel with increasing AAT plasma levels.

Unpublished data from the McElvaney lab established that treatment of neutrophils with C3d resulted in increased secretion of primary (BPI) ( $p=0.013$ ), secondary (hCAP-18), ( $p=0.004$ ), and tertiary (MMP9) ( $p=0.018$ ) granule products suggesting that C3d may be a key driver of inflammation in AATD.

We hypothesised that dysregulated C3 cleavage and complement activation may be contributing to the pulmonary disease phenotype seen in AATD via an uncharacterised interaction with monocytes.

The aim of this study was to explore the effect of C3d on the function of circulating monocytes.

To fulfil this aim the following objectives have been set:

1. To explore whether monocytes in the circulation possess a C3d signalling axis. The receptor for C3d has previously been identified as CR2. We used a variety of methods to examine whether MM and ZZ monocytes express CR2 at the gene and protein level.
2. To assess whether monocytes and macrophages within the airways express a receptor for C3d and to determine whether expression of CR2 varies between monocyte subsets in the airways.

3. To establish the downstream effects of C3d signalling in monocytes by examining the cytokine and protease profile expressed by monocytes in response to C3d.

## **Chapter 2: Materials and Methods**

## **2.1 Equipment**

### **2.1.1 Chemicals and Reagents**

All chemicals and reagents used during this study were of the highest purity available and purchased from Sigma Aldrich unless specified differently.

### **2.1.2 Antibodies**

Primary and secondary antibodies used throughout this study are listed in Tables 2.1, 2.2 and 2.3. Concentrations used were in keeping with supplier recommendation as detailed on the product datasheets.

ELISAs for MMP-1, MMP-12, PR3 and sCD14 were performed using precoated ELISA plates kits from Abcam and R&D systems. Details of secondary antibodies used for these experiments are provided in Table 2.2. The detectable range and details of ELISA kits used is included in Table 2.3.

Anti- bodies used to identify lymphocyte subsets in BAL by multi colour flow cytometric analysis are listed in Table 2.4. This panel was adapted from the American Thoracic Society (ATS) protocol for the identification of myeloid cells in BAL samples. Flourophores used were selected using an online multi-colour panel builder (Thermo Fisher) to minimise overlap between excitation and emission spectra of each anti body.

**Table 2.1: Primary antibodies**

<b>Primary antibody</b>	<b>Source</b>	<b>Manufacturer</b>	<b>Catalogue Number</b>	<b>Working concentration</b>	<b>Application</b>
Human CD 21	Mouse	R&D Systems	MAB 4909	2.5µg/ 200µl	Western Blot (WB), FACS
Normal Mouse IgG1 FITC	Mouse	Santa Cruz	SC-2855	200µg/ml	FACS
Normal Mouse IgG2b FITC 2587	Mouse	BD Bioscience	555742	2µl/ml	Confocal microscopy
Anti CD21 Alexa Flour 647	Rabbit	Abcam	Ab202693	5µg/ml	Confocal Microscopy
Anti CD21	Rabbit	Novus	NBP2-38895	2.5µg/ml	FACS
C3d	Mouse	Santa Cruz	AC-58928	0.5µg/ml	FACS
IL-8		R&D Systems	MAB 208	10µg/ml	ELISA
MMP-9	Mouse	R&D Systems	DY911	F * Ø {	ELISA
MMP-1	Goat	R&D Systems	AF901	0.4µg/ml	ELISA

**Table 2.2: Secondary Antibodies**

<b>Secondary Antibody</b>	<b>Source</b>	<b>Manufacturer</b>	<b>Catalogue Number</b>	<b>Working concentration</b>	<b>Application</b>
Goat anti mouse IgG FITC	Goat	Santa Cruz	SC-2010	1µg/200µl	FACS
Human IL-8/CXCL8	Goat	R&D Systems	BAF 208	0.4 µg/ml	ELISA
Anti-rabbit IgG, HRP-linked	Goat	Cell Signalling	70704S	1 µg/ml	Western Blot
FACS Goat mAb to Rb IgG	Goat	Abcam	Ab6717	10µg/ml	FACS
MMP-9	Goat	R&D Systems	DY911	0.5µg/ml	ELISA
MMP-1	Goat	R&D Systems	BAF901	5ng/ml	ELISA

**Table 2.3: ELISA kits used with detection range of assay**

<b>Analyte</b>	<b>Manufacturer</b>	<b>PC</b>	<b>Detection Range</b>
MMP-1	R&D Systems	DY901B	62.5- 4000 pg/ml
MMP-9	R&D Systems	DY911-05	31.3-2000 pg/ml
MMP-12	Abcam	Ab213811	62.5pg/ml-4000 pg/ml
sCD14	Abcam	Ab208983	31.3-2000 pg/ml
PR3	Abcam	Ab226902	1.2 ng/ml - 150 ng/m
IL-8	Lab SOP	N/A	17.5-2000 ng/ml

**Table 2.4: Antibodies used in flow cytometric analysis of BAL samples**

Laser/ Excitation filter (nm)	Emission Filter	Antigen	Dye	Anti body clone	Concentration	Supplier	Product Code
405	450/45	CD16	BV 421	3G8	10µg/ml	BD	562878
405	525/40	Live/Dead stain	N/A	N/A	1 µl/ml	Thermo	L34965
405	660/10	CD24	BV 650	ML5	5µg/ml	BD	563720
488	525/40	CD14	AF 488	M5E2	5µg/ml	Novus	Nb100- 7778af488
561	585/42	CD21	PE	N/A	0.5µg/ml	R&D	FAB4909P
561	690/50	CD45	PE- Cy5	HI30	5µg/ml	Abcam	Ab167004
638	712/25	CD206	AF 700	19.2	5µg/ml	Thermo	56-2069- 42
638	780/60	CD169	APC- vio770	7-239	10µg/ml	Miltenyi	130-101- 278

## 2.2 Sampling

### 2.2.1 Cell line work

Preliminary experiments were carried out on a U937 cell line. U937 cells were bought from American Type Culture Collection (ATCC) and were originally obtained from sampling of a pleural effusion of a 37 year old male with histiocytic lymphoma. U937 are commonly used in studies as a model for monocyte and macrophage function(275). Differentiation of this cell line into macrophages can be achieved with prolonged treatment (72 h) with PMA. Morphologically U937s more closely resemble developing monoblasts than mature peripheral circulating monocytes. Expression of surface markers that are expressed strongly in mature monocytes such as CD14 and HLA DR are notable for their low levels of surface expression in U937 cells (276).

A second cell line . Raji B cells- were utilised as a positive control for the C3d receptor CR2 (also known as CD21). Raji B cells are a human cell line of haematopoietic origin and are commonly used in studies as a model for B cells and as a transfection host (277). Raji cells were first obtained from an 11 year old line. Raji B cells demonstrate ubiquitous surface expression of CR2 and were used as a positive control in Western blots, confocal microscopy and FACS assessment of C3d binding to the surface of cells.

### 2.2.2. Patient sampling

Healthy control (HC) individuals were defined as having an MM AAT phenotype by isoelectric focusing with plasma AAT levels within the normal range (1.1-1.8g/L). All HCs were non-smokers with no clinical or radiographic evidence of lung disease. All AATD patients were recruited from the National AATD clinic in Beaumont Hospital.

All ZZ patients were confirmed as having a ZZ phenotype by isoelectric focusing. ZZ individuals were stable with no exacerbations at the time of recruitment. COPD patients were recruited from the respiratory ward in Beaumont Hospital and confirmed as having an MM phenotype by isoelectric focusing with plasma AAT levels within the normal range.

Peripheral circulating monocytes from healthy MM controls, individuals with MM COPD and ZZ AATD with COPD were isolated using a CD14 negative selection kit without CD16 depletion(278) (StemCell). Isolation of monocytes from whole blood is described in further detail in section 2.3.5.

### **2.2.3 Isolation of plasma from whole blood**

Whole blood was collected in Sarstedt-Monovette® tubes coated with lithium heparin. Samples were centrifuged at 350 xg for 5 min at room temperature. Plasma was aliquoted for immediate use or labelled and stored at -80°C for use in future experiments.

### **2.2.4 Bronchoalveolar lavage (BAL) sample collection**

All patients included within this study were undergoing fiberoptic bronchoscopy for clinical reasons determined by their treating physician. Informed consent was obtained in advance of the procedure. All data was anonymised and stored in accordance with European data protection guidelines. CT scans were reviewed in advance of bronchoscopy to help determine which lobe or segment was likely to give an adequate return.

Matched blood samples for plasma isolation were obtained on the morning of bronchoscopy to allow for comparison of urea concentrations between plasma and BAL samples. Following sedation, a full airway inspection was performed to identify which lobe was most likely to offer adequate return of an alveolar sample.

Preference was given to the right middle lobe (RML) followed by the lingula when patients were in the supine position as anatomically this favours greater sample yield. If anatomic or technical difficulties were encountered, the bronchoscope was repositioned in the superior or anterior segments of either lower lobe. The scope was advanced distally, and gentle suction applied to assess for distal airway collapse confirming an adequate seal between the scope and airway wall.

Two aliquots of 50ml 0.9% normal saline were instilled through the scope and aspirated immediately via the same syringe. Suction was applied by aspirating the syringe. The pressure of the suction was determined by looking directly for airway collapse throughout the procedure. If airway collapse was noted, suction was reduced. Total volume in and out was recorded and a yield of 50% return deemed adequate. Sample collected in the syringe was kept for analysis and any further sample used by the treating team for microbiological culture. Samples were placed directly into pre chilled 50ml Falcon tubes and immediately transported on ice to the lab for analysis.

The volume instilled and collected, cell count and viability assessment with trypan blue staining, plasma and BAL urea gradient and direct visualisation of cell populations using a Wright Giemsa were subsequently used to determine if the sample was of adequate quality

### **2.2.5 Ethical Approval**

Ethical approval was obtained from Beaumont Hospital Ethics Committee and written informed consent was obtained from all patients (REC: 13/92).

## 2.3 Laboratory Techniques

### 2.3.1 U937 cell culturing

U937 (ATCC) cells were stored in liquid nitrogen prior to thawing. Cells were thawed by gentle agitation in a 37°C degree water bath for a period of 2 minutes. Under aseptic conditions, cells were transferred to a centrifuge tube with 9ml complete culture medium. Culture medium consisted of RPMI-1640 with fetal bovine serum (FCS) added to a final concentration of 10% (w/v). Penicillin-streptomycin (1% v/v) was added to limit bacterial growth during culture.

Vials contained U937 cells and complete culture medium were centrifuged at 125 xg for 6 mins. Following aspiration of the supernatant, cells were re suspended in 10ml culture medium and transferred to a culture flask. Cells were incubated horizontally at 37°C in a 5% CO<sub>2</sub> atmosphere. Cells were counted on a weekly basis and density maintained between 1 x10<sup>5</sup> and 2 x 10<sup>6</sup>. Fresh culture medium was added every 2 days.

### 2.3.2 Raji B cell culturing

Raji B cells (ATCC number CCR-86) were cultured in RPMI medium 1640 with 10% (v/v) fetal calf serum (FCS), 2mM L-glutamine 100 units/ml penicillin and 100 microgram/ml streptomycin to a final concentration of 1% (v/v).

Following removal from liquid nitrogen, cells were thawed by immersion in a 37°C waterbath. Under septic conditions cells were suspended in 5ml of complete growth medium prior to centrifugation at 100 xg for 3min. The supernatant was then

discarded, and cells were re-suspended in 15ml of growth media in a 75 sq. cm tissue culture flask. Culture flasks were placed in an incubator at 37°C in a 5% CO<sub>2</sub> atmosphere. Media was changed every 2 days and cell density maintained at 2-3x10<sup>6</sup> / ml of media.

### 2.3.3 U-937 cell treatment

Following culturing as described above, monocytes were washed and re-suspended in RPMI with no FCS (serum free), 1% FCS (v/v) or 10% FCS (v/v). Cells were counted and 2.5x10<sup>6</sup> added to a 12-well 3.8cm<sup>2</sup> round culture dish for treatment.

A dose response treatment was carried out with increasing concentrations of C3d protein (Merck Chemicals) (0-F € Á \* Đ { | D Á µg/ml) @ÁŠÁŠ à Á Q10€ control. Following 6h and 24h cells were centrifuged at 500xg for 5 min.

Supernatants were collected and stored immediately at -80°C and TRI Reagent® was added to the pellet and stored at -80°C.

### 2.3.4 Trypan blue testing for cell viability

Cells (10al) were added to an eppendorf & [ } c æã } ã } \* Á J € | Á c ! ^ ] æ} Á à | ~ agitated gently and F € loµÁd onto a haemocytometer (Olympus BX40) at 20X magnification. Cells were enumerated, with cell viability consistently at 99%.

### 2.3.5 Monocyte isolation

Peripheral circulating monocytes were isolating using the EasySep human CD14 selection kit. Whole blood was collected from patients in lithium-heparin plasma tubes (7.5ml per tube). Blood was immediately transferred to a 50ml Falcon tube and

mixed with an equal volume of 0.9% (w/v) normal saline (NS) preheated to 37°C. This solution was carefully layered (free poured) over an equal volume of lymphoprep maintaining a 1:1:1 ratio of volume whole blood: NS: Lymphoprep. This mixture was centrifuged at 800xg for 10mins with the brake off to facilitate recovery of a tight mononuclear cell band. Following centrifugation, a Pasteur pipette was used to remove the mononuclear cell layer (buffy coat). HBSS (10ml) was then added to the recovered cells and centrifuged at 500 xg for 5 min with the brake on. The supernatant was removed, and cells were re-suspended in 1ml of Easy Sep recommended medium (1mM EDTA, 2% (v/v) FCS in PBS-Dulbecco). Cells were then counted. Monocyte number was approximated as 10% of the total cell population.

T [ } [ } ~ & | ^ æ! Á & ^ | | Á • ~ • ] ^ } • ã [ } Á , æ• Á c @^ } Á ] ! ^ ] æ! ^

in EasySep recommended medium and transferred to a 5ml polystyrene round bottomed tube (BD). EasySep negative selection cocktail was added at 100µl/ml and mixed gently. Samples were left at room temperature for 15min. Easy Sep magnetic nanoparticles were then added at 50µl/ml, mixed and left at room temperature for a further 10 min. Cell suspension was brought to a total volume of 2.5ml with recommended medium and pipetted gently to ensure a homogenous mixture. The polystyrene tube was then fitted snugly into the EasySep magnet for 5min. Following incubation, the magnet containing the 5ml tube was inverted in one swift, continuous motion for 2-3 sec to pour off the supernatant fraction. The tube was then removed from the magnet and 2.5ml of recommended medium added and pipetted gently before being returned to the magnet. This washing process was repeated x3 before re-suspended cells in PBS and treated as detailed in section 2.3.6. .

### **2.3.6 Treatment of purified peripheral circulating monocytes**

Following isolation as described above, monocytes from individuals with ZZ AATD, MM COPD and MM healthy controls were washed x3 in PBS. Cells were then seeded in growth media (RPMI, 1% (v/v) heat inactivated FCS, 1% (w/v) penicillin-streptomycin) at a concentration of  $1 \times 10^5$  cells per ml to 12 well plates. Cells were left untreated or challenged with increasing concentrations of C3d. Concentrations of C3d used were 10, 20 or 40µg/ml. Concentration of C3d was based on published data that confirms levels of 10-40µg/ml C3d in plasma and in the airways of those with AATD(78).

LPS was included as a positive control at a concentration of 50-100ng/ml. Previously published data confirms that monocyte viability will start to decline at ultra-high doses (5000 ng/ml) (279). Doses in the range of 500ng/ml promote monocyte differentiation to macrophages which was not required. Separate studies have shown that stimulation of monocytes for 4 h with *E. coli* LPS at a concentration of 100ng/ml increased the production of TNF alpha markedly without affecting viability(280). Being mindful of our more prolonged treatment protocol and the need for a positive control signal, a lower concentration of 50-100ng/ml was employed. MTS assay was performed at 20 h to check cell viability as described in section 2.3.19.

### **2.3.7. BAL processing of supernatants**

BAL samples were centrifuged at 500 xg for 10 min at 4°C. The supernatant was aspirated and transferred into cold 15ml tubes for a second spin at 1200 xg for 10min. The cell pellet was resuspended in 1% (w/v) BSA, 5mM EDTA, 10mM

HEPES in cold PBS pH7.4 and retained for further isolation of alveolar macrophages.

Half of the recovered supernatant was then aliquoted into 1.5ml eppendorfs on ice.

The remaining volume was mixed gently with a protease inhibitor tablet (Roche) until complete solubilisation and homogenisation was noted. This sample was then aliquoted and stored at -80°C along with samples not containing protease inhibitors.

### **2.3.8 Processing of BAL pellet for cell counting and viability**

Following centrifugation and aspiration of the supernatant (described in section 2.3.7), the cell pellet was re-suspended in 1ml of 1% (w/v) BSA, 5mM EDTA, 10mM HEPES in cold PBS. A small volume of the sample (10µl) was transferred to 90µl trypan blue for counting as described in section 2.3.4. The cell count and viability by trypan blue were recorded.

### **2.3.9 Determining cell differential of BAL samples**

BAL samples (100µl) were transferred to a 1.5ml eppendorph containing 900µl PBS for a 1:10 sample dilution. Two 500µl aliquots of diluted sample were then loaded onto a cytospin slide and centrifuged for 5min at 500 xg. The slide was then recovered from the cytospin holder and allowed to air dry. Cells were then fixed and stained with Giemsa stain and can be used for Romanowsky type staining of blood smears and tissue specimens(281). The slide was left to air dry and cells were then observed by use of a light microscope using a x25 or x40 objective. The predominant cell population was then recorded, the slide labelled and

photographed for future reference. Samples that showed a dominant macrophage population with scattered lymphocytes and mononuclear cells and minimal or no red blood cells (RBCs) apparent were included in flow cytometry experiments.

### **2.3.10 Quantification of urea in BAL samples**

Quantification of urea in BAL samples compared to plasma samples was used to determine what proportion of recovered fluid was likely to represent epithelial lining fluid (and dilution factor). In keeping with the current evidence base, results of urea assays were not the primary or sole determinant of sample adequacy and results were always interpreted in the context of other variables including: volume of fluid instilled during the procedure (volume returned as a percentage of volume instilled >50%), cell counting by TB ( $> 2 \times 10^6$ ) and differential (>10 macrophages visible per high powered field).

Urea concentration of each sample was measured using the Quantichrom Urea Assay kit (BioAssay Systems) and compared to the urea concentration in corresponding plasma samples. The Quantichrom kit is highly sensitive and is capable of detecting levels of urea between 0.08mg/dL - 100mg/dL. The most dilute sample was chosen as the reference concentration. Subsequent samples were diluted to normalise them to the reference samples and allow comparison between individuals.

### **2.3.11 Protease array membranes**

ZZ AATD and healthy MM healthy control monocytes were cultured in the presence of 10µg/ml of C3d. Extracellular supernatants were recovered and applied to a protease array membrane (Proteome Profiler, Human protease array kit, R&D systems). The protease array kit can be used for the parallel determination of relative levels of a variety of human proteases. Each nitrocellulose membrane is

impregnated with capture antibodies to capture each protease analyte in duplicate. Proteases captured by the R&D array are shown in Table 2.4.

Membranes were transferred individually to separate wells of a 4 well multi dish. Blocking buffer (2ml) was added to each well and membranes were blocked for 1h at room temperature on a rocking platform. Samples were brought to a total volume of 1.5ml using array buffer (provided as part of the kit). Protease detection anti-body cocktail (15a1) was added to each prepared sample and left to incubate at room temperature for 1h.

Array buffer was aspirated from each well containing a membrane and the pre-prepared sample-antibody mixture was then added. Membranes and samples were incubated overnight at 4°C on a rocking platform. Membranes were removed from the multi-well dish and transferred to individual containers with 20ml of 1X wash buffer. Membranes were washed for 10 min x3 before being returned to the multi well dish. Streptavidin (2ml) was added to each well and incubated with the membranes in the dark for 30 min at room temperature. Washing was repeated a further three times and the nitrocellulose was transferred onto a plastic sheet. Chemi reagent mix (1ml) was applied evenly to each membrane. A second plastic sheet was then overlaid and excess chemi reagent blotted away with paper towels.

Membranes were imaged using a Chemi Doc MP System (Fannin, Co. Dublin, Ireland). Densitometry was carried out using Image Lab software (Fannin, Co. Dublin, Ireland).

**Table 2.5: List of proteases identifiable by the R&D Human Protease Array Kit**

ADAM8	Cathepsin X/Z/P	MMP-3
ADAM9	DPPIV/CD26	MMP-7
ADAMTS1	Kallikrein 3/PSA	MMP-8
ADAMTS13	Kallikrein 5	MMP-9
Cathepsin A	Kallikrein 6	MMP-12
Cathepsin B	Kallikrein 7	MMP-13
Cathepsin C/DPPI	Kallikrein 10	Neprilysin/CD10
Cathepsin D	Kallikrein 11	Presenilin-1
Cathepsin E	Kallikrein 13	Proprotein Convertase 9
Cathepsin L	MMP-1	Proteinase 3
Cathepsin S	MMP-2	uPA/Urokinase

### 2.3.12 RNA extraction with Trizol reagent

RNase AWAY® was used throughout this method. Total RNA was extracted from cells using the TRI reagent method. Lysed cells were left to thaw for 5 min at room temperature. Chloroform (100µl) was then added, and the samples were shaken vigorously for 15 sec and allowed to stand for 5 min at room temperature. The resulting mixture was then centrifuged at 12,000xg for 15 min at 4°C separating the mixture into three phases. The upper aqueous phase (RNA) was transferred to a fresh tube, 250µl of 2-propanol added and the samples were left to stand for 5 min at room temperature. The samples were then centrifuged at 12000xg for 10 min at 4°C. The supernatant was discarded, and the RNA pellet washed with 500µl of 75% (v/v) ethanol, vortexed and centrifuged at 7500xg for 5 min at 4°C. The supernatant was again discarded, and the RNA pellet was briefly air dried for 5 min. The RNA pellet was then resuspended in 20µl of diethyl pyrocarbonate water and placed in -80°C for 30 min or longer-term storage.

### 2.3.13 RNA extraction with Nucleospin RNA columns

RNase AWAY® was used throughout this method. RNA extraction was performed using the Nucleospin RNA extraction kit (ThermoFisher PC 12373368). Following culture (U937 cells and Raji B cells) or immediately following isolation (peripheral circulating monocytes) cells were washed twice in 5ml of PBS. Cells were counted and  $1 \times 10^6$  transferred to a 1ml eppendorf and a third wash in PBS performed. The PBS was aspirated from cells and the pellet lysed by adding 350 µl of Lysis Buffer RA1 supplied with the extraction kit. 3.5µl of 2-mercaptoethanol was added and the samples were vortexed vigorously for 2 minutes. The lysate was then applied to a

þ ~ & | ^ [ ù ] ã } ï Á Ø ã | c ^ ! Á æ } å Á & ^ } c ! ã ~ ˇ \* ^ å Á ~ [ ! Á F { ã } Á

filter was removed leaving the filtrate remaining in an RNAase free collection tube. Ethanol (70% v/v, 350 µl) was added to the filtrate and pipetted gently x5 to mix. An RNA column was placed into a fresh RNAase free collection tube and the filtrate/ethanol solution (700µl total) was then transferred to the column. The sample was then centrifuged for 30seconds at 11,000G.

The RNA column was transferred to a fresh collection tube. Membrane desalting buffer (350µl) was applied to the RNA column and centrifuged at 11000 xg for 1 min. Filtrate was then discarded. To ensure removal of genomic DNA contaminants, 95µl of DNAase reaction mixture was added to the membrane and the sample was left to stand for 15 min at room temperature.

The membrane within the RNA extraction column was then washed and dried 3 times using the wash buffer supplied with the Nucleospin kit. Wash buffer (200µL) was added to the column and centrifuged for 30s at 11,000xg. The filtrate was discarded and 600µl of wash buffer added to the membrane. The sample was centrifuged for 30s at 11,000xg and the filtrate discarded. Wash buffer (250aL) was added to the membrane and centrifuged for 2mins at 11,000G. The column was then transferred to a fresh 1ml RNAase free epindorph and 60µl of RNAase free water was added to the membrane.

The sample was centrifuged for 1 min at 11,000 xg. RNA was then quantified using the Nanodrop 8000 Spectrophotometer (Fisher Scientific). The instrument was blanked and 2µl of sample added to each well. RNA purity and quality was then recorded using the ND8000 programme (Fisher Scientific). An A260/280 ratio of 1.8-2.0, indicating high RNA purity was considered a prerequisite for inclusion in experiments. Samples were converted to complementary DNA. Work-flow for RNA extraction is shown in Figure 2.1.

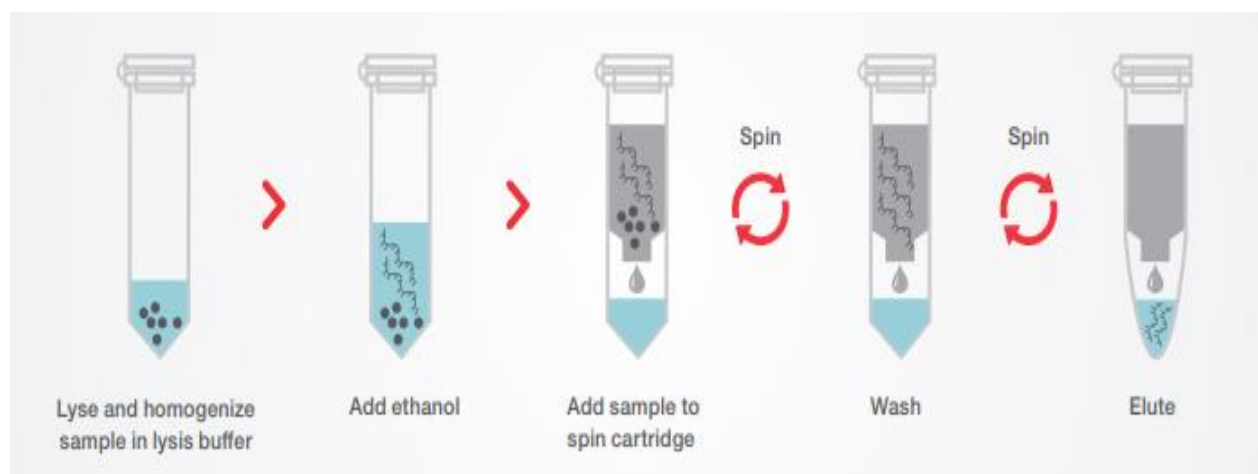


**Figure 2.1: Workflow for RNA isolation using the Nucleospin RNA extraction kit (ThermoFisher)**

### 2.3.13 Complementary deoxyribonucleic acid (cDNA) synthesis

RNA (1µg) was reverse transcribed to cDNA using QuantiTect Reverse Transcription Kit (Qiagen Limited, UK). In reaction 1, contaminating genomic DNA was removed from the RNA samples (1µg RNA in 12 µl RNA free H<sub>2</sub>O) using genomic DNA by cooling to 4°C in a PTC-200 Thermal Cycler (MJ Research, US). A mastermix for reaction 2 was created and samples placed back into the PTC-200 Thermal Cycler and heated to 42°C for 30 min, followed by 95°C for 3 min and finally cooled for 4°C. The cDNA was then stored at -20°C for future use.

### 2.3.14 Confirmation of qRT PCR product by agarose gel

A 1% (w/v) agarose gel was cast by adding 0.4g of agarose powder (EEO <0.19) to 40ml of 1X Bionic Buffer. This mixture was heated on high power in a microwave for 30s and mixed intermittently until dissolved and clear solution formed. 2µl of DNA stain (SyBr Stain) was then added to a final concentration of 0.5µg/ml as per the protocol. The mixture was poured into the Central Chamber of an agarose gel rig and a comb was inserted. The gel was left to set for 30min in a cold room at 4°C. The rig was then filled with 1X bionic buffer and the comb removed. DNA base pair ladder (7µl) was added to the first lane of the gel. 5ul of PCR product was transferred to a piece of parafilm and mixed with 2µl of DNA loading dye. This was repeated sequentially for each sample. The 7µl sample/DNA dye mix was then added to each individual well. Raji B cell PCR product was included as a positive control. GAPDH was included as an internal control.

### 2.3.15 RT-PCR

Primers were designed using Primer-BLAST and purchased from MWG Eurofins (United States). PCR was performed using the following protocol: preincubation (95°C for 3 min), amplification (50 cycles consisting of denaturation, annealing, elongation (95°C for 10 sec; 55°C for 10 sec for both CR2 and GAPDH; and 72°C for 10 sec)); melting curve analysis (95°C for 5 sec, 65°C for 1 min, and 97°C for five continuous acquisitions), and a final cooling step to 4°C. All PCRs were carried out in 96-well plates in 20µl reaction volumes, and a negative control without complementary DNA was included in every run. Amplification was performed using the LightCycler 480 PCR system (Roche) with the expression of target genes relative

c [ Á Õ Œ Ú Ö P Á å ^ c ^ | { ã } ^ å Á , ã c @ Á c @ ^ Á G Ô V Á { ^ c @[ å È

### 2.3.16 FACS analysis for surface expression of CR2 on U937 cells and purified monocytes

Unpublished work by Fee and colleagues identified the presence of the C3d receptor CR2 on the cell surface of circulating neutrophils (188). Following their protocol, we endeavoured to confirm the presence of the CR2 receptor on U-937 cells and subsequently on peripheral circulating monocytes.

Experiments were performed in the presence and absence of protease inhibitors (Table 2.6). In the case of U937 cells, TNF alpha and LPS were added to 2 separate samples to determine whether CR2 expression was influenced by an inflammatory stimulus. Peripheral circulating monocytes were treated with a combination of PMA, LPS, TNF and IL-F for a period of 10mins.

Following activation, cells ( $2 \times 10^6$ ) were fixed using 4% (w/v) paraformaldehyde for 10 min. Cells were then washed with PBS and blocked with 1% (w/v) BSA for 30

min to prevent non-specific antibody binding. Samples were then incubated with primary antibody for 1 h, washed and incubated with a secondary FITC-labelled antibody for 30 min. Control samples were incubated with relevant non-specific isotype control antibodies. All antibodies used for FACs analysis are outlined in Table 2.1 and 2.2. Cells were then washed and fluorescence counted by a BD FACsCalibur (Becton Dickinson) equipped with 2 lasers (Blue at 488nm, Red at 635nm). Ten thousand events per reaction were quantified.

Analysis of fluorescence was carried out using FlowJo software and data represented as Median Fluorescent Intensity (MFI). Statistical analysis was performed using Graph pad prism software.

**Table 2.6: Protease inhibitors**

<b>Protease inhibitor</b>	<b>Concentration</b>	<b>Target Protease</b>
Leupeptin	10µg/ml	Serine and cysteine proteases
TLCK	10µg/ml	Trypsin and trypsin like serine proteases
PMSF	1 mM	Serine, acetylcholinesterases and thiol proteases
Pep A	10µg/ml	Aspartic proteases
PeFabloc	1mM	Serine proteases
EDTA	5mM	Metalloproteases
NaF	10mM	Phosphoseryl and phosphothreonyl phosphatases (PSPs)
NaVO <sub>4</sub>	0.2mM	Phosphotyrosyl phosphatases

### **2.3.17 Flow cytometry analysis of CR2 on lymphocyte subsets obtained from BAL**

This experiment protocol comprised 11 reactions- the control unstained cell population, those with live/dead stain only, a sample with all 8 anti-bodies included and 8 fluorescence minus one (FMO) controls. FMOs are a type of control commonly used in multi-colour flow cytometric experiments. FMOs contain all fluorophores in a panel except for the one being measured. FMOs ensure that any spread of signal from the fluorophores between channels was properly identified and eliminated prior to analysis.

To correct for any residual spectral overlap a compensation matrix was generated using the CytExpert software and flow cytometry beads (BD) tagged with the fluorophores listed in Table 2.3. Compensation is a mathematical process commonly used in multi-colour flow cytometry that corrects for spectral overlap between fluorophores that may otherwise result in inaccurate data collection and analysis.

Following centrifugation of whole BAL samples or isolation from whole blood, the cell pellet was resuspended in 1% (w/v) BSA, 5mM EDTA, 10mM HEPES in cold PBS on ice. Cells were washed once in PBS (300 xg, x 7 min at 4°C) and resuspended at a concentration of  $1 \times 10^6$ /ml. Depending on the overall cell yield, between  $10^3$  and  $10^4$  cells were counted and left in PBS to serve as an unstained population. Live/dead discrimination dye was added at 1µl/ml/  $1 \times 10^6$  as per the manufacturer's instructions. To the remainder of cells, a Live/dead discrimination dye was added at 1µl/ml/  $1 \times 10^6$ . Cells were incubated in the dark at 4°C for 30 mins with the live/dead stain. Samples were then centrifuged at 300 xg for 7 min at 4°C and the supernatant removed.

Cells were then resuspended in 500µl PBS and 500µl of 4% (w/v) paraformaldehyde (PFA) was added to fix the cells. Samples were incubated for 10min at 4°C. Cells were washed twice and the supernatant removed. Cells were resuspended in blocking solution (10% (v/v) human serum, 3% (v/v) FCS, 1% (w/v) BSA in PBS) and incubated for 30 min at room temperature. Cells were then split to their respective tubes prior to staining. Each sample was analysed in its entirety to permit comparison of median fluorescence intensity (MFI) and generation of statistics between relatively scarce populations.

Samples were analysed on a Cytoflex S cytometer from BD. The cytoflex S is equipped with 4 lasers (blue, violet, yellow and red) to allow for more accurate analysis of a spread of surface markers tagged with different flourophores. Lasers, excitation and emission spectra, anti-bodies, conjugated flourophores d are listed in Table 2.3 (Materials section). The final antibody panel was designed using the Thermo Fisher online panel builder to ensure minimal overlap between emission spectra.

### **2.3.18 Gating strategy used to identify myeloid cells in BAL**

The gating strategy described by Yen and colleagues (2015) was adapted for use as part of the study protocol(282). Following counting and staining for differential, cells were examined by forward scatter (FSC) and side scatter (SSC) with gating on single cells to eliminate doublets and debris. This population was then examined for CD45 and gating performed on the CD45+ population. This was taken to represent total leucocytes. A live/dead stain was used to eliminate dead cells from the analysis. Live cells from the CD45+ population were then interrogated for CD206 and CD14. CD206, the macrophage mannose receptor was used to identify total macrophages.

Its use as a macrophage marker is well established in the literature (283). The total macrophage population was then examined for expression of CD14 and CD169. Alveolar macrophages (AMs) were designated as CD14 low and CD169+ve as previously established by cell sorting and Diff Quik staining by Yen and colleagues (282). This AM population was then examined for expression of the C3d receptor CR2.

Further gating was performed on the CD206 negative population which were examined by SSC versus CD14. SSC reflects how granular or complex a cell is. Cells with very granular cytoplasm such as neutrophils generate high levels of SSC by FACs (284). Monocytes were thought to be contained within the SSC low and CD14 positive population and were refined based on relative expression of CD24 and CD14. Monocytes were identified as CD24<sup>-</sup> and CD14<sup>+</sup> cells. Further gating divided monocytes into three previously described distinct populations- classical, non-classical and intermediate based on their relative expression of CD14 and CD16 (131). Each of these sub populations was then examined for the presence of CR2/CD21.

### **2.3.19 MTS assay for cell viability**

Following treatment with increasing concentrations of C3d (1, 3, 5, 10µl/ml and LPS 20µg/ml) cell viability was checked at 18 hours using the CellTiter 96® AQueous One Solution Cell Proliferation Assay (Promega).

Ø [ | | [ , ã } \* Á c @ ^ Á { æ } ~ ~ æ & c ~ ! ^ ! q • Á ã } • c ! ~ & c ã [ } • Ê Á G  
treated samples and transferred to a 96 well plate. Samples were then made up to a final volume of 100µl by the addition of 50µl of their respective media (serum free,

1% (v/v) FCS or 10% FCS). 20µl of cell titer reagent was added to each well to give a final concentration of 317µg/ml of MTS. The plate was covered with tinfoil to protect from light and incubated at 37°C for 4 h in a 5% CO<sub>2</sub> atmosphere. 25µl of 10% (v/v) SDS was added at 4 hours to prevent any further reaction. The plate was stored at room temperature, protected from light before absorbance at 490nm was determined by spectrophotometry.

### 2.3.20 Preparation of whole cell lysates

For protein preparation of whole cell lysates  $1 \times 10^7$  cells were centrifuged at 4°C at 500xg for 5 min. The pellet was resuspended in 100µl of lysis buffer (150mM NaCl, 50mM TrisHCL, 1% (v/v) Triton X-100, 0.2mM NaVO<sub>4</sub>, 10mM NaF, 1mM EDTA and protease inhibitors) was then added and pellet resuspended. The suspension was spun at 4°C at 500xg for 5 min in order to remove insoluble cell debris and the supernatant collected. 10X Sample Buffer (SB) (2% (w/v) SDS, 1% (w/v) sucrose, 0.004% (w/v) bromophenol blue, 5mM ethylenediaminetetraacetic acid (EDTA), 60mM Tris HCl (pH 6.7)) was added to give a final concentration of 1X. Samples were boiled at 99°C for 3 min and stored at -20°C for subsequent western blot analysis.

### 2.3.21 Bicinchonic acid (BCA) protein determination

Prior to SDS-Page and Western blot analysis, protein content of the samples of interest was determined by BCA assay. BSA standard was prepared (2mg/ml) and

serial dilutions performed with lysis buffer to generate a standard curve. The BCA kit used as part of these experiments was the Pierce<sup>TM</sup> BCA Protein Assay kit. This kit generates a strong purple coloured reaction product in the presence of protein. Absorbance is known to be nearly linear with increasing protein concentrations and the kit works over a broad concentration range (20-2000 µg/ml).

Standards and samples were added in triplicate to a 96 well microtiter plate at 5µl per well . BCA protein assay reagents were combined in a 50:1 ratio (A:B) in a 15ml conical tube. 200µl of this working reagent was then added to each well using a multichannel pipette. The plate was incubated in the dark for 30min at 37°C. Absorbance was read at 550nm using the microplate reader (Spectra Max M3, Molecular Devices, Berkshire, UK).

### **2.3.22 Sodium Dodecyl Sulphate Polyamide Gel Electrophoresis (SDS PAGE)**

CR2 is a transmembrane protein comprising a long extracellular component and short intracytoplasmic tail. Though traditionally described as being 110-145kDa protein, shorter forms have been identified on follicular dendritic cells (50kDa) and neutrophils (100kDa)(258, 285). In consideration of the spread of sizes in CR2 reported in different cell types, we elected to run our samples on a 10% (w/v) gel to allow for optimal visualisation of proteins.

Running and stacking gel mixtures were prepared (Tables 2.5 and 2.6). Running gel was poured between 2 ethanol washed plates of the AE-6450 Dual Mini Slab Kit (Atto, Japan). The running gel was overlayed with 1ml isopropanol and allowed to polymerise for 35min. Agents for the stacking gel (Table 2.6) were then combined. Isopropanol was poured off, the gel was washed with H<sub>2</sub>O, and excess removed with

blotting paper. Stacking gel mix was then applied using a Pasteur pipette on top of the gradient gel and a loading comb positioned. The gel was then left to polymerise for a further 15min.

Cast gels were then placed in a tank containing 1X Running Buffer (6g Tris, 2.88g glycine and 2g SDS). 10 $\mu$ l of samples in 10X sample buffer (SB) were loaded and ran at 90V for 10 min then increased to 130V for a further 90 mins. For band size determination, 3 $\mu$ l of protein marker SeeBlue Plus2 Pre-Stained Standard (Invitrogen, Bio Sciences Ltd, Ireland) was included alongside samples in the innermost lane.

**Table 2.7: Running gel components**

<b>10% (w/v) Resolving Gel</b>	
<b>Reagent</b>	<b>Quantity</b>
1.5 M Tris pH 8.9	3ml
30% (w/v) Protogel (National Diagnostics, Atlanta, USA	4ml
10% (w/v) SDS	120µl
Deionised Water	4.8ml
10% (w/v) ammonium persulfate (APS)	75µl
Tetramethylethylenediamine (TEMED)	3µl

**Table 2.8: Stacking gel components**

<b>Reagent</b>	<b>Quantity</b>
0.5M Tris pH 6.8	315µl
30% (w/v) Acrylamide, bisacrylamide solution (protogel)	415µl
10% (w/v) SDS	25µl
Deionised water	1.7 ml
10% w/v) APS	25µl
TEMED	2.5µL

### **2.3.23 Western Blot Analysis**

Following removal from the electrophoresis tank, gels were submerged in transfer buffer. Plates were separated and blotting paper applied directly to the surface of the gel. Gels were sandwiched between PVDF membrane preactivated by methanol submersion (1min), blotting paper and sponges. Transfer was carried out at 100V for 60mins.

PVDF membranes were recovered and placed in blocking buffer (5% (w/v) dried skimmed milk (Marvel, Chivers Ireland Ltd, Ireland), PBS solution containing 0.1% (v/v) Tween® 20 (PBST)) for 1h at room temperature. Following washing, membranes were rolled into 50ml tubes containing 5ml blocking buffer and their relevant antibodies. Tubes were placed on a roller and left at 4° overnight.

Blots were subsequently washed in PBS-Tween® x3 for 10min each and probed with HRP-linked secondary antibodies against the specific primary antibody for 1h at room temperature. Blots were then washed again in PBS-Tween® 3 times for 10min each. Immuno-reactive protein bands were detected by incubating the membrane in Immobilon Western Chemiluminescent HRP substrate solution (Merek Millipore, Co Cork, Ireland) using a Chemi Doc MP System (Fannin, Co. Dublin, Ireland). Densitometry was carried out using Image Lab (Fannin, Co. Dublin, Ireland).

### **2.3.24 Enzyme linked immunosorbent assay (ELISA)**

A quantitative sandwich ELISA technique was used to measure IL-8 (Cambridge Bioscience), MMP-9, MMP-12 and MMP-1 (R&D systems), sCD14 and PR3 (Abcam) production by U937 cells and/or peripheral circulating monocytes following stimulation with C3d.

sCD14 and PR3 ELISAs involved the use of SimpleStep ELISA kits (Abcam). These pre-coated ELISA plates use an affinity-tag labelled capture anti-body and a reporter detector antibody to bind the analyte of interest in solution. This analyte/anti body complex is immobilised via affinity of the tag-labelled capture antibody for an anti-tag anti body coating the plate. This effectively combines a 2-step process into one and distinguishes these ELISAs from other ELISA kits used as part of this study

Workflow for these single step, pre-coated ELISAs is shown in Figure 2.2.

Standards for all ELISAs were made using either serial dilution of a known concentration or by using standards supplied with each ELISA kit. A standard curve was generated using Graph Pad Prism v6.0 software.

In the case of U937 cells, samples were thawed on ice before adding to a 96 well plate in duplicate. In the case of peripheral circulating monocytes, supernatants from treated cells were thawed on ice and diluted (1/100) prior to being applied in duplicate to the 96 well plate.

The day before the ELISA, a 96 well plate was coated with the relevant primary anti-body. Plates were kept at 4°C overnight. The following day plates were washed with PBS containing 0.1% (v/v) Tween 20 (PBS Tween). Non-specific binding was prevented by adding 200µl 1% (w/v) bovine serum albumin (BSA) in PBS Tween to each well and incubating at room temperature for 1h using the orbital shaker. Washing was then repeated x3 with PBS-Tween. Duplicate wells for standards containing 100µl reagent diluent (1% BSA (w/v) in PBS) per well were prepared and control blank wells included in each plate.

Cell supernatants were added at 100µl per well in duplicate. The plate was incubated at room temperature for a further two hours with orbital shaking before 3 further

washes as described. 100µl of secondary anti-body diluted in PBS-Tween were then added to each well and incubated for 2 hat room temperature.

Following repeat washing, 100µl streptavidin (1:40 dilution, 250µl in 10ml PBS Tween) was added to each well for 30 min and kept protected from light. Washes (x3) were repeated. 100µl of tetramethylbenzidine (TMB) solution (R&D Systems) was added to each well and protected from light. Plates were kept covered from light for 15 min and 50µl of 2M Sulfuric acid stop solution was added to each well to prevent any further reaction. Plates were then read for absorbance at 450nm on a Spectra Max M3 (Molecular Devices, Berkshire, UK). Linear regression was used to convert absorbance to concentration using Graphpad Prism software. The blank controls were subtracted from recorded values and the final concentration of each sample determined by interpolation with the standard curve.

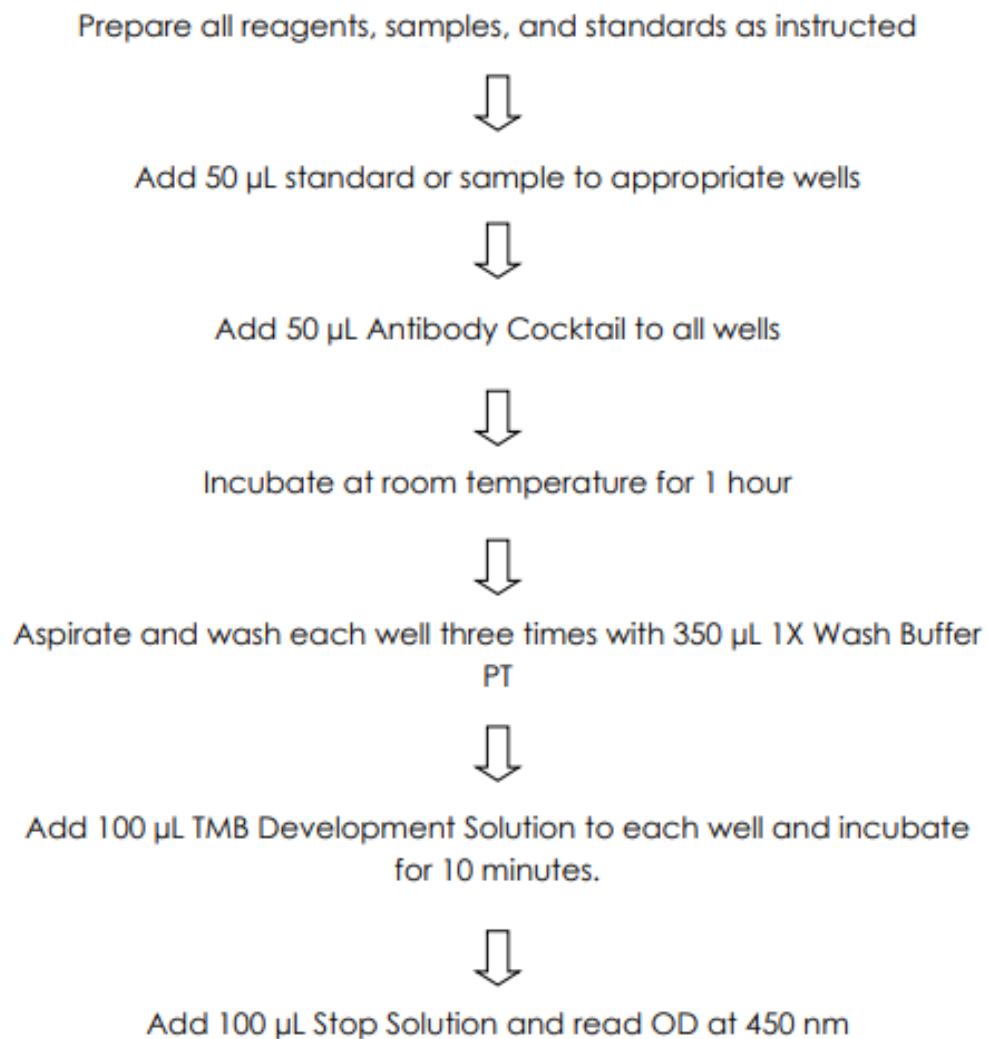


**Figure 2.2: Workflow for PR3 and sCD14 ELISAs** (SimpleStep ELISA kit, Abcam)

### **2.3.25 Confocal microscopy**

Included in all confocal experiments were MM monocytes from healthy individuals with an MM phenotype by isoelectric focusing, ZZ monocytes and Raji B cells, known for their ubiquitous CR2 expression were included as a positive control. Monocytes were isolated as previously described using the Easy Sep negative selection CD14+ kit without CD16 depletion.

Following isolation (or counting of cultured Raji B cells), cells were transferred at a concentration of  $1/10^6$  per ml of media to a culture plate. Plates were coated with poly-d-lysine to allow for rapid adherence of cells to the surface. Cells were left in 1ml of media for 30min to ensure adherence. Cells were fixed with 4% (w/v) PFA for 10 min. Cells were then washed x3 in PBS. PBS was aspirated completely and 1ml of 1% (w/v) BSA, 10% (w/v) normal goat serum and 0.1% (v/v) Tween added to block non-specific binding. After 1h, 5 $\mu$ g/ml of anti-CR2 antibody (Alexa Flour 647, Abcam) was added to all CR2 samples. IgG FITC antibody (2 $\mu$ l/ml) was then added to all isotype samples. Cells were left at 4°C overnight in tinfoil.

Blocking reagent was aspirated completely and 50 $\mu$ l of 4',6-diamidino-2-phenylindole (DAPI) added to the slide for nuclear staining. A coverslip was placed over the cells and sealed with nail polish. Slides were analysed using an LSM confocal microscope.

## **2.4 Statistical Analyses**

Results are expressed as mean  $\pm$  SEM of biological replicates or independent experiments as indicated in figure legends. A Students t test was used where distribution was normal and when comparison was being made between two groups. The Mann Whitney U test was employed where data was not normally distributed. A two-way ANOVA was used to compare groups with two or more variables. Statistical significance was determined with a p-value  $<0.05$ . All data was analysed using Graphpad Prism software.

## **Chapter Three: Establishing a signalling axis for C3d on monocytes in the circulation and airways**

### 3.1 Introduction

As outlined in Chapter One, both monocytes and the complement system play complimentary roles in regulating the innate and adaptive immune response. Monocytes exert their effect via antigen presentation, phagocytosis and cytokine production(286). Complement defends against pathogen invasion, bridges innate and adaptive responses and degrades immune complexes and other products of inflammation(180).

Complement activation in the context of AATD has been a subject of interest since the observation by Taylor and colleagues in 1977 that C3 can be cleaved by neutrophil derived proteases such as NE to activate the complement cascade(287). Cleavage of the complement protein C3 represents a shared final common step between all 3 activation pathways(288). It is perhaps unsurprising then that levels of the C3 cleavage products C3a and C3b are not uncommonly used as a surrogate marker for overall complement activation(289). Reliance on C3a and C3b as a marker of complement activation is limited however as both are known to increase when C3 undergoes spontaneous hydrolysis in plasma. Levels of the complement fragment C3d are not increased during spontaneous hydrolysis of C3 and it is for this reason it is a more consistent marker of overall complement activation(290).

U q Ó! ã ^ } Á æ} å Á & [ | | ^ æ\* ~ ^ • Á å ^ { [ ] • c ! æcandãÁ å ã ! ^ & c Á à vitro(78). Given the pro-inflammatory properties of C3 activation, including the production of pro-inflammatory mediators C3a and C5a and opsonin C3b, the authors hypothesised that AAT may interact with C3 in an anti-inflammatory capacity with binding of AAT to C3 serving to prevent dysregulated proteolysis of C3 and subsequent complement activation. In addition to showing C3 and AAT binding, they determined that when compared with healthy controls, plasma levels of C3d were

increased in AATD (0.04 µg/mL vs 1.96 µg/mL,  $p=0.0002$ ). In vivo, AAT augmentation therapy was found to significantly reduce plasma levels of C3d (0.15 µg/mL without augmentation vs 2.18 µg/mL with augmentation,  $p=0.001$ ).

Furthermore, increased levels of C3d correlated with the severity of emphysema seen on CT imaging of the lungs in those with AATD. Taken together, these observations suggest that C3d may play a role in the pathogenesis of AATD but the mechanisms underlying this effect have yet to be fully elucidated.

Neutrophil behaviour in AATD has been investigated extensively whilst comparatively little is known about the role monocytes play in driving disease pathogenesis. Until relatively recently the paradigm for the development of lung disease in AATD was based on the protease-anti-protease hypothesis(291). Interest in this model stemmed from observations of neutrophil behaviour in AATD.

Neutrophils store proteolytic enzymes and serine proteases within their densely packed cytoplasmic granules. This enables rapid degranulation in response to cellular activation (55) and justifies their study in protease mediated disease.

Previous studies have shown an increase in the number and chemotactic index of neutrophils obtained from BAL of those with ZZ AATD(64, 292). Furthermore, studies of Z homozygotes and heterozygotes have shown increased influx of neutrophils into the airways(293). AAT acts primarily as an inhibitor of serine proteases but has also been shown to inhibit a range of other proteases derived from degranulating neutrophils. These include but are not limited to neutrophil elastase, cathepsin G, PR3(294), mast cell derived tryptase, lymphocyte derived granzyme B(295), matrilysin (61) and the matrix metalloprotease ADAM17(292).

In contrast, monocytes are known to lack the primary, secondary and tertiary granules that characterise neutrophils. Despite a relative paucity of cytoplasmic

protease storage granules, they are undoubtedly prolific producers of cytokines. Monocytes and monocyte derived macrophages are known to produce a wide variety of cytokines including but not limited to TNF- $\alpha$  (296), MCP-1(297), MIP-1 $\alpha$  (298), IL-6(299), IL-8 (300), and IL-10(193). With increasing recognition of the immunomodulatory effects of AAT the paradigm for pathogenesis of AATD lung disease is expanding to include an exaggerated inflammatory milieu(54). The function of monocytes in AATD is of particular interest as Carroll and colleagues (2010) have previously shown that ZZ monocytes exhibit an exaggerated cytokine response in response to a pro-inflammatory stimulus (LPS)(299). They showed that ZZ monocytes produce 1.5 times as much IL-6 and IL-8 in response to LPS than MM monocytes ( $p = 0.0015$  and  $p = 0.0003$ , respectively). This suggests that ZZ monocytes have a greater propensity to elaborate an excessive inflammatory response and contribute to disease pathogenesis.

As more insights are gained into how monocytes and monocyte derived macrophages contribute to lung disease, the question of how dysregulated complement activation interacts with monocytes becomes more compelling. Unpublished data from the McElvaney lab suggests that exposure to C3d correlates with neutrophil degranulation in AATD- an effect which may contribute to disease pathogenesis and clinical trajectory. As part of a PhD thesis, Fee (2019) established that treatment of neutrophils with C3d resulted in increased secretion of primary (BPI;  $p=0.013$ ), secondary (hCAP-18;  $p=0.004$ ), and tertiary (MMP9; $p=0.018$ ) granule components suggesting that C3d may be a key driver of inflammation in AATD. Furthermore, treatment of a neutrophil like cells line (HL60 cells) with C3d increased production of the pro inflammatory cytokine IL-8. Considering the critical

role monocytes play in generating the innate immune response, establishing whether C3d can exert a similar effect is clinically valuable.

### **3.1.1 Chapter Aims**

Increased levels of C3d can be considered a reliable indicator of overall complement activation and ongoing inflammation(300). Published work from the McElvaney lab identified complement fragment C3d as a novel blood biomarker of airways disease in AATD. Higher levels of C3d were identified in the airways and plasma of those with ZZ AATD and correlated with radiographic emphysema(78). As discussed previously, unpublished data from our lab suggests that exposure to C3d results in increased neutrophil degranulation (188). This led us to question of the possible effect of C3d on other cells types found in the circulation and airways. Before endeavouring to ascertain what effect C3d was having on monocytes we first needed to establish the existence of a signalling axis for C3d in this type of cell.

We hypothesised that dysregulated complement activation in AATD contributes to the inflammatory phenotype observed, via an unspecified reaction with monocytes. The receptor for C3d, CD21/CR2 is well described in published literature as is the nature of the binding reaction between ligand and receptor (178). To date, CR2 has not been described on the surface on monocytes or their derivatives(254). Thus, the aim of this project is to first establish expression of CR2 by monocytes and a signalling axis for C3d on monocytes in the circulation and airways.

To address this aim, the following three objectives were set:

1. Establish expression of CR2 on a monocyte like cells line using U937 cells.

2. Investigate whether expression of CR2 protein can be identified on the surface of monocytes from the circulation and airways.
3. Investigate whether expression of CR2 is altered in ZZ AATD when compared with healthy MM controls.

## 3.2. Investigating expression of CR2 on a monocyte-like cell line

### 3.2.1 Rationale for cell line work

As discussed in Chapter One, monocytes are a heterogeneous and plastic population that comprise <10% of the total leucocyte population in circulation(301). Considering the requirement for a relatively large volume of blood to ensure adequate monocyte yield, it was decided to perform preliminary experiments using U937 cells which are commonly used in studies as a model of macrophage or monocyte function(275). U937 cells (ATCC) are an immortal cell line obtained from the pleural effusion of a 37 year old male with histiocytic lymphoma(302).

The aim of this experiment was to establish the presence of CR2 and thus, a signalling axis for the complement fragment C3d on the surface of cells that share features with monocytes. This was evaluated using flow cytometry.

### 3.2.2 Design of early U937 experiments

Culture, treatment, and fixation of U937 cells are described in detail in Chapter Two: Materials and Methods. Early versions of this experiment included samples with and without protease inhibitors. Protease inhibitors used are summarised in Table 2.1 in Chapter Two: Materials and Methods. Previous work from the McElvaney lab elucidating CR2 on the surface of neutrophils demonstrated that addition of PIs was necessary to preserve CR2 on the surface of the neutrophil. In consideration of this, untreated U937 cells were prepared in the presence and absence of PIs.

In addition to samples prepared in the presence of protease inhibitors, we examined { [ ] [ & ^ c ^ • Á c ! ^ æ c ^ â Á , ã c @Á V Þ Ø Á Á æ } â Á • ^ ] æ ! æ c ^ | ^ Ê summary of the stimuli used for this series of experiments, and rationale for their

selection is provided in Table 3.1. All samples were treated for 10min prior to fixation. This timepoint was chosen as it has been previously used successfully in similar experiments using neutrophils.

All U937 samples were analysed on the BD FACS Calibur flow cytometer and analysed using FlowJo and GraphPad Prism. Fluorescence data is represented as Median Fluorescent Intensity (MFI). Unstained cells and samples incubated with a mouse IgG isotype control antibody (Santa Cruz Biotechnology) were included as controls. Inclusion of an isotype control was necessary to distinguish non-specific background signal from signal generated by specific antibody binding(303).

**Table 3.1: Pro-inflammatory stimuli used in early U937 experiments and rationale for selection**

<b>Stimulus</b>	<b>Concentration</b>	<b>Rationale</b>
<b>Untreated</b>	N/A	Included to demonstrate baseline level of expression relative to an isotype control.
<b>HB : *</b>	10ng/2x10 <sup>7</sup> cells	Previously shown to increase expression of functional adhesion molecules and scavenger receptors in monocytes(304).  Bergin et al demonstrated increased neutrophil degranulation in response to this concentration(305)
<b>LPS</b>	10ug/ml	Shown by Carroll and colleagues to increase release of pro inflammatory cytokine IL-6 and IL-8 From ZZ and MM monocytes(299)

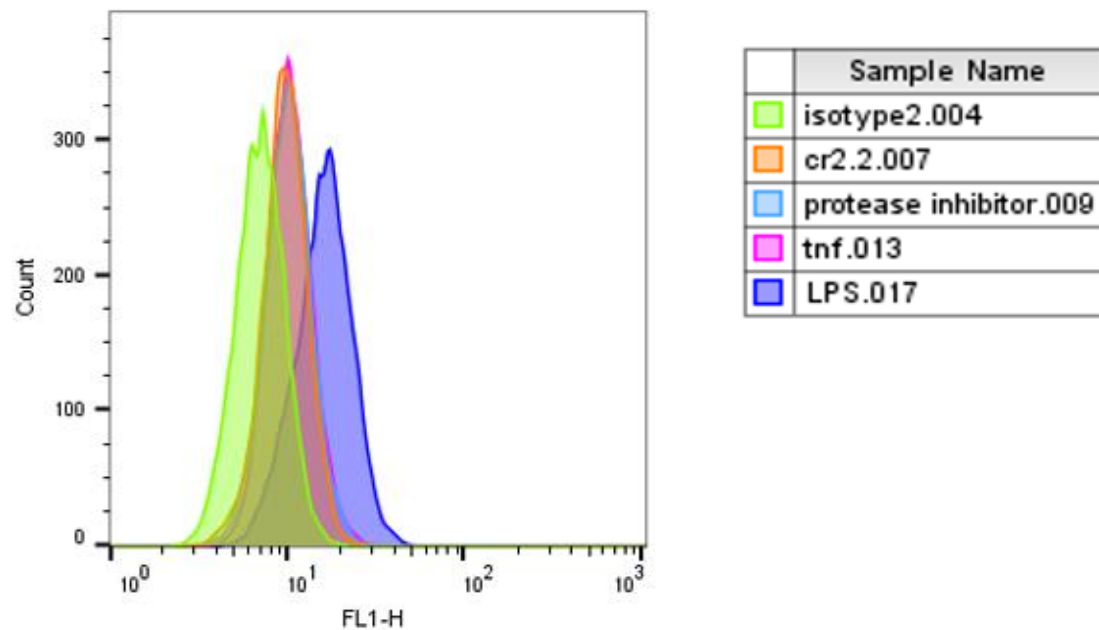
### 3.2.3 Summary of initial U937 results

Figure 3.1, panel A shows histograms demonstrating CR2 on the surface to U937 cells. The histogram representing cells stained only with an anti-body for CR2 (orange) is shifted to the right of the isotype control (green) indicating the signal seen is not accounted for by background non-specific binding. The histogram obtained from samples run in the presence of protease inhibitors (PIs) (pale blue) is obscured by the overlying orange histogram representing untreated U937 cells. This suggests that PIs did not change the expression of CR2.

Cells treated with LPS (dark blue) absent protease inhibitors show further rightward shift suggesting higher expression of CR2 by cells exposed to LPS.

Panel B represents the results of 4 separate experimental runs. Columns represent the median fluoresce intensity (MFI) generated by each sample. Collectively, these experiments confirm the presence of CR2 on U937 cells but statistical analyses shown that there is no significant change in CR2 expression following stimulation using this experimental protocol.

A



B

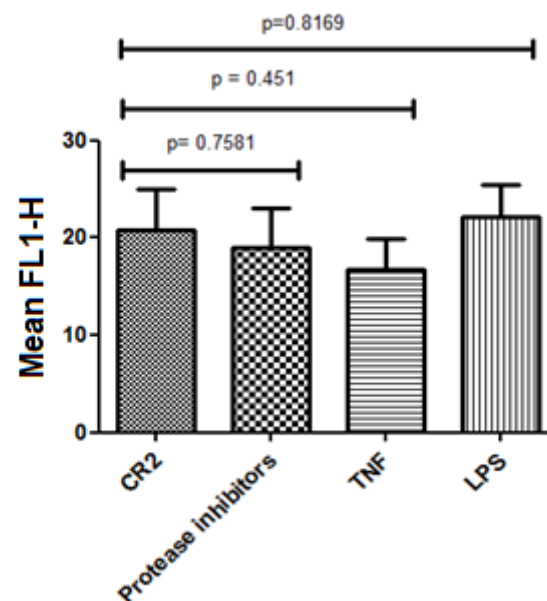


**Figure 3.1: Measurement of CR2 on the surface of U937 cells by flow cytometry, in the presence of protease inhibitors and following exposure to pro-inflammatory stimuli for 10mins.**

**A:** Histogram confirming expression of CR2 on U937 cells following treatment. **B:** CR2 expression is unchanged across all groups examined. Treatment duration for all =10 min, n=4. Statistical analysis was performed using a t-test.

### 3.2.4 Conclusion

These results show that CR2 is present on the surface of U937 cells. U937 cells are frequently used in published literature as a model for monocyte and macrophage function thus, this was an encouraging result for us to achieve at an early stage of the project.

Expression of CR2 did not change with either the addition of protease inhibitors or a 10 min exposure to the pro- $\alpha$  } ~ | æ { { æ c [ ! ^ Á • c ā { ~ | ā Á V Þ Ø Á [ ! Á Š Ú Ů examination of histograms suggested an increase in CR2 expression following treatment with LPS, this was not borne out in statical analyses. We felt this may reflect several possibilities relating to the technical performance of flow cytometry. It is possible that subtle alterations in gating strategies between samples analyses may have contributed to the lack of significance achieved. It is also possible that the treatment period used here (10mins) was not of sufficient duration to induce meaningful change in CR2 expression by U937 cells. Tsukamoto et al (1992) have previously used GM-CSF and IFN Á c [ Á ã } â ~ & ^ Á WJ H Ĩ Á ^ ¢ ] ! ^ • • ã [ } Á [ proteins C3 and C4(306). Sheth at al had previously identified low levels of the complement receptor CR3 on the surface of U937 cells. They showed increased expression of CR3 following treatment with 1 mM dibutyryl cyclic AMP (Bt2cAMP) for 24, 48 and 72 hours(275). It is notable however that both Tsukamoto and Sheth were interested in examining morphological changes in U937 cells during differentiation. We were keen to avoid differentiation and preserve U937 cells in a state that was more similar to circulating monocytes that fully differentiated macrophages.

Using this experimental protocol CR2 expression did not change significantly. For clarity and to avoid U937 differentiation, we elected to alter the protocol by

expanding the panel of pro- inflammatory stimuli included and maintaining the 10 min treatment period.

### 3.3 Further evaluation of CR2 on the surface of U937 cells by FACS analysis

#### 3.3.1 Rationale for further U937 work

Though results of preliminary experiments were encouraging, we were keen to establish what if any agent might increase CR2 expression. This was important to establish for the purpose of planning future experiments. For subsequent analyses we were interested in including stimuli that were known to exert an effect on U937 cells without inducing differentiation to a macrophage-like phenotype.

#### 3.3.2 Amendments to U937 treatment protocol

inducing neutrophil degranulation- a process which was shown to be abrogated by treatment with AAT. The concentration of LPS used (10µg/ml) is relatively high and it was felt that to further increase it would mean exposing cells to supra-physiological levels which would render results of dubious clinical significance. Also, as earlier work has shown a trend towards increased expression at this concentration, it was hoped that further technical refinements of this protocol may alter the finding of statistical analyses.

Additional stimuli used, their respective concentrations and rationale for selection are summarised in Table 3.2.

**Table 3.2: Choice and rationale for additional pro-inflammatory agents used in U937 flow cytometry experiments**

Stimulus	Concentration	Rationale
PMA	1µg/ml	Effect well described in U937 cells (cell line model)(307).  Primes monocytes to respond to LPS(308)
IL-1	100pg/ml	InCHIANTI study identified this concentration as being present in the circulation of individuals with COPD and is thus representative of physiological levels of IL-1 (309).  are exposed(309)
C3d	10µg/ml	Inada et al (1980) showed progressive, time dependant increase in a receptor for C3d on monocytes in culture(310). Of note, this study predates the first description of CR2 as the binding site for C3d.  U q Ó! ã ^ } Á ^ c Á æ  Á ã á ^ } c ã ~ 40 <sup>6</sup> á µg/ml in plasma and BAL of those with ZZ AATD(78).

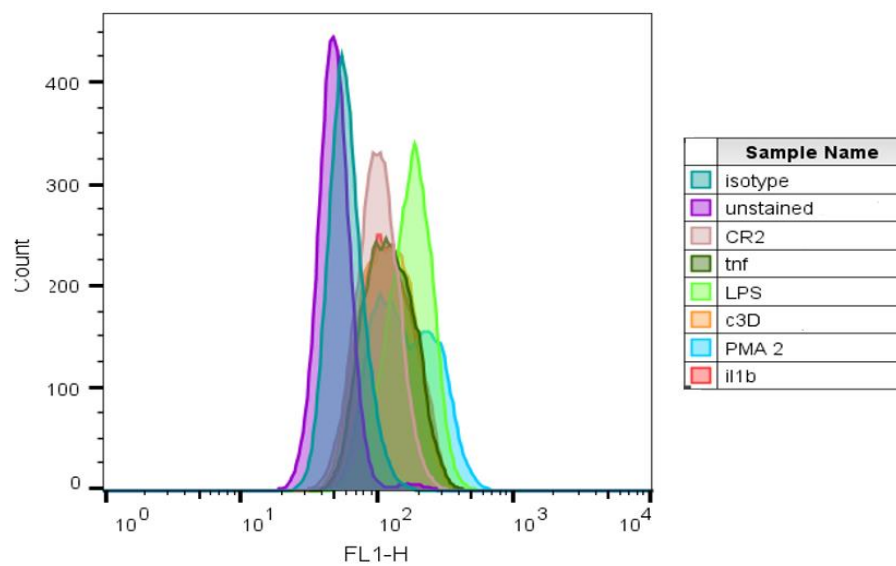
### 3.3.3 Summary of results using extended panel of pro-inflammatory stimuli

Figure 3.2, Panel B shows histograms from an experimental run that is considered representative of overall findings (n=6). Histograms show better separation between the isotype control (pale blue) and sample stained with CR2 anti body only (pale red). Rightward shift of the sample treated with LPS (bright green) again signals the possibility of increased CR2 expression in this population. The histogram of cells treated with PMA (bright blue) is shown immediately to the right of the LPS samples suggesting that PMA may also upregulate CR2 expression on the surface of U937 cells.

Panel B (n=6) shows that the increase in CR2 expression in response to LPS is not significant but that seen following PMA is. Data is presented as MFI normalised to the isotype control that is used to quantify levels of background signal. Samples

surface expression of CR2 significantly.

## Panel A



## Panel B

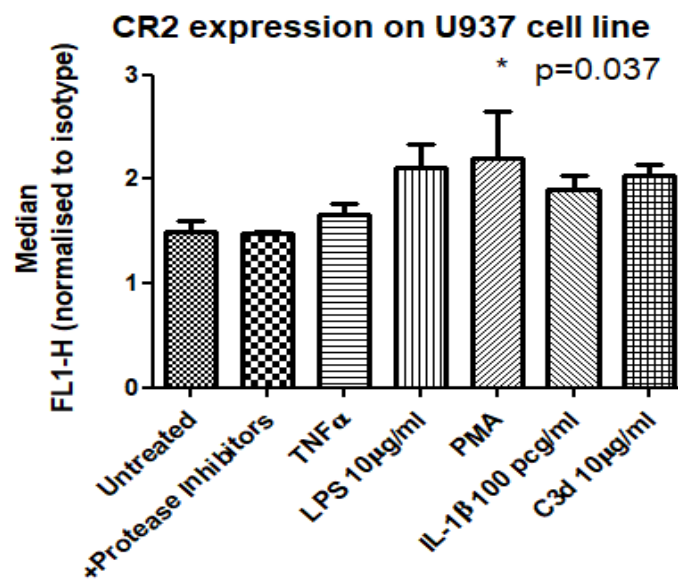


**Figure 3.2: Change in surface CR2 expression by U937 cells exposed to pro-inflammatory stimuli as determined by FACS.**

**A:** Histograms confirming expression of CR2 on U937 cells. Treatment with LPS and PMA appear to increase CR2 expression and shift histograms to the right (green and bright blue). **B:** CR2 expression increases significantly in U937 with 10 minute exposure to PMA (n=6 biological repeats,  $p<0.05$ ). Statistical analyses were performed using a Students t test.

### 3.3.4 Conclusion of U937 cell line work

Results presented here confirm that CR2 expression by U937 cells increases in response to short term stimulation with PMA. Previous studies of monocyte like cell lines have shown that stimulation with PMA accelerate differentiation towards a macrophage phenotype(311). PMA is frequently used in experimental protocols to accelerate the process of differentiation but should not be considered a physiological stimulus. Treatment of U937 cells with PMA is known to trigger up-regulation of beta-2 integrins (CD11a, CD11c, CD18 and CD11b) which facilitate adhesion to a surface(312). Of note CD11b, like CR2 is a receptor for a complement fragment (C3b)i(313). It is also known to pair with CD18 to form the complement receptor 3 (CR3) heterodimer(314).

The significant change in CR2 expression seen here signalled to us that CR2 expression may be greater in macrophages which are known to express a greater number of complement receptors than monocytes. The short stimulus (10mins), though unlikely to have triggered complete differentiation to a macrophage like cell, may reflect up regulation of complement receptors which is known to occur when monocyte like cells begin the process of differentiation. This raises the possibility that monocyte derived macrophages, which are known to populate the airways may express CR2 and thus be more reactive to stimulation with C3d than monocytes.

C3d was also included as a stimulus in this protocol as Inada et al (1983) had previously suggested that a receptor for C3d could be induced in peripheral circulating monocytes(255). They showed that sheep RBC coated with C3d could form rosettes with peripheral circulating monocytes. Rosetting did not occur initially but increased in a time dependant fashion. Treatment with the Fab fragment of anti-C3ds blocked rosette formation. The authors hypothesised that the ability of

monocytes to bind C3d was dependent on the state of monocyte activation. As rosette formation peaked at 3 hours and was not noted to occur <1 hour it is likely that if C3d caused activation of our U937 cells it was unlikely to occur within the 10min treatment protocol selected. Though Inada identified that there was likely to be a receptor for C3d present on the surface of monocytes, at the time of publication it had not yet been shown that the receptor for C3d was CR2/ CD21.

Having identified that CR2 was on the surface of U937 cells, we endeavoured to apply these insights to monocytes obtained from circulation. Though flow cytometry had proved useful in identifying CR2 on monocyte like U937s, we felt it was prudent to assess for CR2 expression at gene level first in circulating monocytes. This was felt to be necessary as a negative result on flow cytometry could allow us to mistake CR2 cleavage from the surface of circulating monocytes as a false negative. Thus, we decided to next proceed to examining circulating monocytes for expression of the CR2 gene using quantitative reverse transcription polymerase chain reaction.

### **3.4. Evaluating CR2 gene expression in circulating monocytes by RT-PCR**

#### **3.4.1 Background**

Results of flow cytometry experiments using a monocyte like cell line confirmed the presence of surface bound CR2 protein. We reasoned that if CR2 was also present on the surface of circulating monocytes it may be susceptible to cleavage by proteases. Unpublished work from the McElvaney lab using neutrophils had demonstrated that identifying CR2 on the neutrophil surface required the addition of protease inhibitors to stabilise surface bound CR2. Thus, commencing this work package with flow cytometric analysis of monocytes taken from circulation might lead to a false negative result. In consideration of this we chose to proceed with looking for CR2 expression at the gene level. Gene expression can be examined in several ways but for the purposes of this study we elected to use qRTPCR.

#### **3.4.2 Rationale for RTPCR selection**

The starting material in any RTPCR reaction is RNA. RNA is reverse transcribed into complementary DNA (cDNA) using the enzyme reverse transcriptase. During the reaction the cDNA serves as a gene template that is amplified in the presence of a fluorescent probe(46). The fluorescence generated during the reaction enables determination of the cycle threshold or Ct value. The Ct value refers to the point in the reaction (cycle number) at which the fluorescent signal generated by a reporter dye crosses the background threshold(315). Comparing achieved Ct values with known reference values can provide insights into the quantity and quality of the RNA and subsequent DNA used in the reaction.

### **3.4.3 Methods and technical challenges**

Further details on the protocol used for these experiments is provided in the chapter on Materials and Methods. Major challenges encountered during the optimisation process are presented here.

All samples were run in triplicate and a positive and negative control (blank non template control (NTC) included in each run. Amplification was performed using the Light Cycler 480 system (Roche) with the expression of target gene, CR2 (105bp) determined relative to GAPDH (113bp). For completion, the PCR products obtained during the amplification process were run on an agarose gel.

#### **3.4.3.1 Achieving target Ct values**

The numerical value of the Ct is inversely proportional to the amount of amplicon in any given PCR reaction. Housekeeping genes (HG) (such as GAPDH used here) are used to normalise test gene transcript levels(46). Housekeeping genes are genes that are expressed constitutively in cells and usually play a role in essential functions such as glycolysis(316). Selection of appropriate housekeeping genes is an integral part of any qRT-PCR experiment as their reliability changes significantly under different experimental conditions. For example, GAPDH is a reliable HK gene in unstimulated monocytes but should be paired with a second housekeeper if cells are stimulated with LPS(317).

If the gene of interest (in this case CR2) is strongly expressed the Ct value will closely approximate that of the housekeeper gene Ct value. Genes with low expression will have much higher Ct values than housekeeping genes. In early versions of this experiment we noticed we were achieving unexpectedly high Ct

values for the GAPDH (Ct 32-38). Furthermore, Ct values for CR2 were higher again at 38-45.

There were several possible explanations that would account for these findings including, but not limited to:

1. GAPDH may not be the most reliable housekeeping gene in monocytes(317).
2. CR2 is not being expressed in monocytes.
3. Poor quality or quantity of RNA or cDNA was responsible for the high values seen.

As the same effect was seen in both the reference gene and the gene of interest we postulated that the later explanation of poor quality starting material proved a unifying explanation. A review of the literature confirmed that GAPDH can be used as a HK gene in unstimulated monocytes and should return an expected Ct of 22-26. This was further verified using the HK gene selection software BestKeeper. With this confirmation we then redirected our attention towards optimising the process of recovering RNA and cDNA to see if this might enable us to achieve more accurate Ct values for all samples.

#### **3.4.3.2 RNA and cDNA creation**

In early versions of experiments presented here RNA was isolated from cells using Trizol reagent as described in the Materials and Methods chapter. Despite RNA

recovery being performed on ice, in the presence of RNAase away and centrifugation steps being carried out at 4°C RNA purity was suboptimal.

For each experiment purity and quantity of RNA was determined using the Nanodrop Spectrophotometer.

The Nanodrop measures absorbance at 260/280nm and 260/230nm of all molecules in a small amount of sample (2µl). The ratio of absorbance at 260/20nm is commonly used to assess the purity of RNA and DNA(318)È Á ŒÁ Ĩ æc ã [ Á [ ~ Á F È Ĩ Á ã • Á & [ }

~ [ Ĩ Á Ö Þ ŒÁ { ^ æ• ˇ Ĩ ^ { ^ } c • È Á ŒÁ Ĩ æc ã [ Á(319).Á ŒÁ ŒÁ • Á & [ } • was recovered using the Trizol method, ratios obtained were significantly lower suggesting sample contamination with protein or phenol. This is not an uncommon challenge using this particular RNA recovery method and prompted a switch to RNA columns (Invitrogen).

The use of RNA columns improved the purity and quantity of RNA obtained. To ensure that RNA was being reliably converted to cDNA and that the quantity of cDNA was consistent in each reaction we added a second nanodrop step following reverse transcription of RNA to cDNA. This additional step ensured that Cycle threshold (Ct) values obtained during the amplification process were comparable between samples and the positive control.

### 3.4.3.3 Nucleic acid electrophoresis on agarose gel

To ensure that the PCR product created during the RTPCR reaction was definitely CR2, we elected to confirm the result using DNA electrophoresis on an agarose gel. Creation of the gel and the procedure involved is outlined in further detail in Chapter

Two: Materials and Methods. Briefly, samples of gene products from the PCR plate (CR2 and GAPDH) were loaded into wells of an agarose gel and subjected to an electric current. The movement of the electrical current carries negatively charged nucleic acids towards the positively charged electrode. Particles separate out based on size. Running a DNA ladder in tandem with samples allows identification of the size of each gene product (CR2 105 base pairs (bp), GAPDH 113 bp).

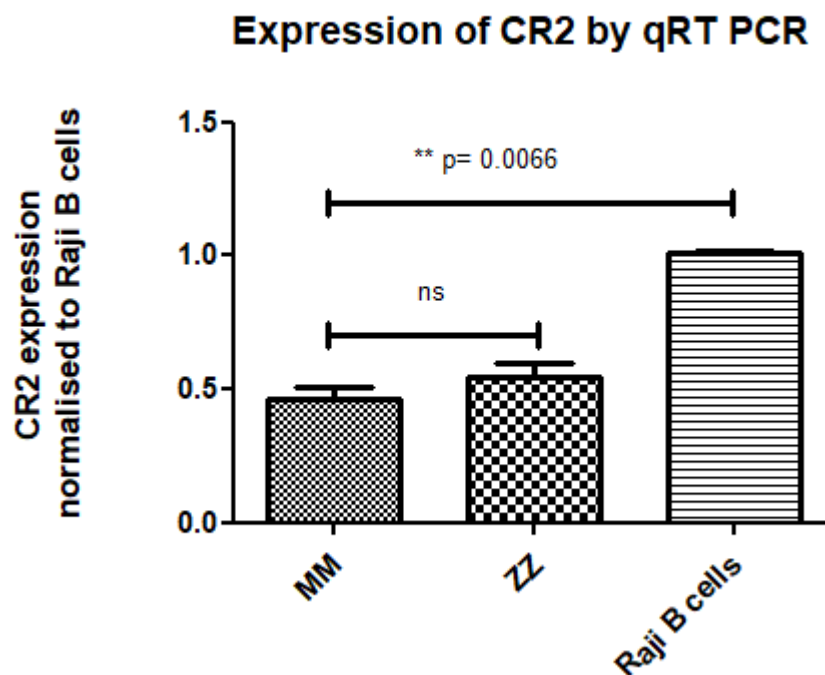
### **3.4.4 Overview of Results**

Figure 3.5A shows confirmation of the expression of the CR2 gene in monocytes (1000ng/μl cDNA per reaction) obtained from healthy MM controls and those with ZZ AATD. Monocyte expression is shown relative to Raji B cell controls (100ng/μl cDNA per reaction).

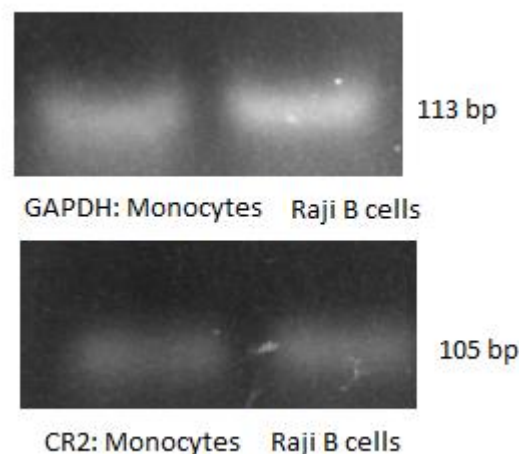
Expression of CR2 at gene level did not differ significantly between MM and ZZ monocytes. As expected, expression of CR2 was increased significantly between monocytes and Raji B cells ( $p=0.0066$ ).

Figure Panel B shows an amplicon corresponding to CR2 (105bp) in MM monocytes and Raji B cells. GAPDH (113bp) is shown for relative expression.

A.



B.



**Figure 3.3: Expression of CR2 on MM and ZZ monocytes by qRT-PCR with confirmation of PCR product on agarose gel.**

**A:** Confirmation of CR2 gene expression in MM and ZZ monocytes relative to CR2 expression by Raji B cells by qRT-PCR. There was no significant difference in expression between MM and ZZ monocytes. **B:** An amplicon corresponding to CR2 (105bp) in MM monocytes and Raji B cells. n=3. Statistical analysis was performed using an unpaired t-test. Significant difference is denoted by \*p<0.05.

### 3.4.5 Conclusions from RTPCR

These results provide further evidence that monocytes freshly isolated from the circulation, can express CR2. The lack of difference in expression between the MM and ZZ groups is noteworthy.

As alluded to previously Inada and colleagues (1983) showed that C3d is capable of binding to monocytes cultured on a glass slide. Binding of C3d increased in a time dependent manner suggesting that monocyte activation or differentiation may influence expression of a receptor for C3d. This work was first published in 1983 and Inada et al did not mention CR2 in the discussion of their findings. It can be reasonably assumed that little was known about the CR2/C3d signalling axis within the scientific community at the time. Indeed, the first published description of CR2 which characterised it as a 145kDa molecule was made later that same year by Iida et al(248).As such, the findings presented here represents the first description of CR2 expression by monocytes.

Following review of Inadaq • Á ^ ø ] ^ | ã { ^ } c Á ] | [ c [ & [ | Ê Á ã c Á ã • Á ~ } & responsible for triggering up regulation of the receptor for C3d (presumably CR2). Variables that may have altered receptor expression include cultivation on a glass surface causing monocyte activation, the presence of FCS in culture media and the presence of C3d coated RBCs in the culture plate. The work of Brien and colleagues showed that C3d levels in the plasma of those with ZZ AATD are between 5-10µg/ml thus this cohort represent a group with prolonged exposure to higher levels of C3d(78). If we are to accept the hypothesis that the presence of C3d primarily accounts for the increase in CR2 expression, it should hold that the receptor for C3d in monocytes is upregulated at the gene level in the ZZ group which we did not

observe. An alternative explanation may be that C3d is capable of binding to the surface of monocytes but binds via an alternative receptor that is not CR2.

Limitations to our observations include the limited number of samples included in the analysis and previously described technical challenges encountered. These results redirected our focus to further elucidating the CR2 protein on and within monocytes. To back up these findings we next proceeded to look for CR2 in monocyte whole cell lysates using western blotting.

### **3.5 Confirmation of MM and ZZ monocyte expression of CR2 protein by Western blotting**

#### **3.5.1 Rationale for Western Blotting**

Results of qRT-PCR confirmed that monocytes can express CR2, the only known receptor for the complement fragment C3d. As this is the first confirmed report of CR2 expression by circulating monocytes, further investigation applying different techniques was necessary to ensure the accuracy of these findings.

Previous studies of CR2 in follicular dendritic cells (FDCs) and B cells showed that in addition to surface expression, CR2 can also be stored intracellularly(261, 285). Considering this we next proceeded to perform whole cell lysis and further investigation using Western blotting.

For these following experiments we also elected to include ZZ monocytes. As alluded to previously, surface bound CR2 is susceptible to cleavage by circulating proteases. As AATD represents a state of relative protease abundance, we were interested to see whether the amount of CR2 varied between MM and ZZ states.

#### **3.5.2 Methods and technical considerations**

Whole cell lysates of isolated MM healthy control monocytes and ZZ cells were prepared in the presence and absence of dithiothreitol (DTT). DTT is a reducing agent that is often used in SDS PAGE. DTT works to reduce disulfide bonds in proteins allow for better separation during electrophoresis(320). In the absence of DTT terminal sulfur atoms of thiolated DNA are susceptible to forming dimers in solution(321).

Whole cell lysates (WCLs) were prepared as detailed in the Materials and methods chapter. Proteins were separated on a 10% (w/v) gel and CR2 detected by Western blot using a mouse monoclonal antibody to CR2 (R&D systems). Raji B cells were used as a positive control. GAPDH was used as an internal control and to ensure adequate sample transfer.

### **3.5.3 Results**

CR2 has a predicted molecular mass of 145kDa. Inclusion of DTT in the samples however revealed a smaller than expected immunoband at 50kDa suggesting the protein was becoming fragmented (Figure 3.4). A review of the literature and correspondence with the anti-body manufacturer confirmed that our CR2 anti-body was unreliable under reducing conditions necessitating the omission of DTT from the sample lysis buffer.

In the absence of DTT a large immune- band (approximately >175 kDa) was detected across all samples (Figure 3.5). Though different isoforms of CR2 have been described, it is most commonly described as a 145kDa protein(258). We postulated that in the absence of DTT, unfolding of CR2 and movement through the gel is altered. In view of the large size of this band, it is also possible that CR2 was forming dimers. Dimerisation of CR2 has been previously described in the literature(322).

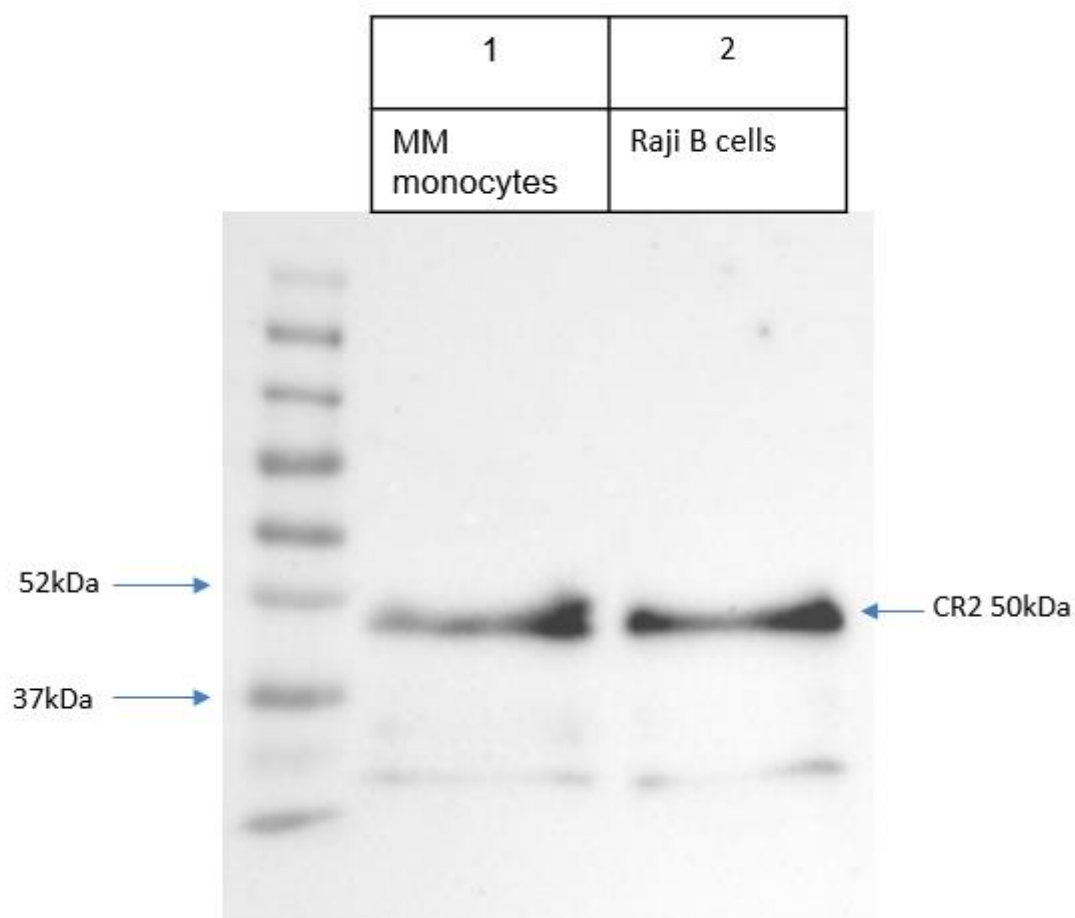


**Figure 3.4: Whole cell lysates of MM monocytes and Raji B cell control run in the presence of DTT.**

Proteins of molecular weights 52 and 37kDa are labelled on the protein ladder. Lane 1 shows MM monocyte whole cell lysates run in the presence of DTT and probed with an anti-body for CR2. Lane 2 shows Raji B cell whole cell lysates probed with an anti-body for CR2. Both lane 1 and 2 show a small immunoband appearing at 50kDa suggesting protein fragmentation during preparation of whole cell lysates. Image is representative of n=3 independent experiments.

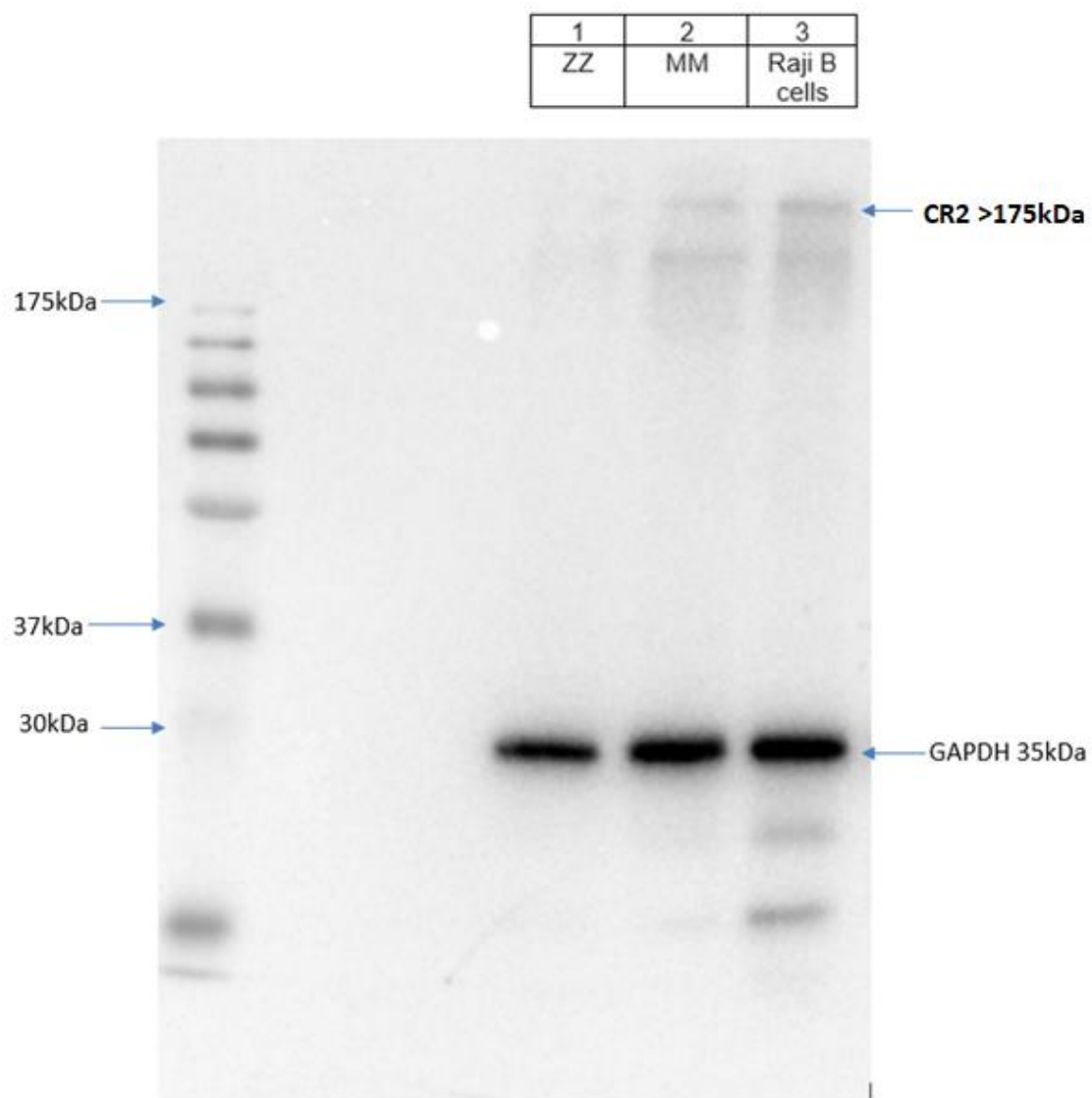


**Figure 3.5: Whole cell lysates of monocytes and Raji B cells run on a 10% (w/w) gel without DTT.**

A: Western blot of 10% (w/v) SDS gel using mouse monoclonal CR2 antibody. Raji B cells and MM were used as positive controls. ZZ was used as a negative control. Molecular weight markers are indicated on the left. CR2 bands are visible above 175kDa in lanes 2 and 3. GAPDH bands are at 35kDa in lanes 2 and 3. Blot representative of n=4 samples.

### 3.5.4 Conclusion of whole cell lysate (WCL) experiments

The image presented in Figure 5 depicts CR2 as a protein with an unexpectedly large molecular weight (>175kDa). Large proteins tend to cluster towards the top of a 10% gel (as was used here) making distinction between and estimation of size challenging. The housekeeping protein GAPDH (included here as an internal control) is unambiguously positive across all lanes and when aligned with the protein ladder also appears to somewhat smaller than its known 35kDa molecular weight. However, it is notable that the immunoband in monocyte samples corresponds exactly with the positive control which is known to unequivocally express CR2. In view of this, we are satisfied that this band is indeed CR2.

The unexpectedly high molecular weight of CR2 obtained from these experiments was surprising though not wholly unexpected. We recognised that the omission of DTT from the sample buffer would alter the properties of the protein and thus its migration through the gel. A similar result has been reported previously by Ling and colleagues(264). In their 1992 study exploring the properties of the soluble form of CR2 obtained from serum and cell supernatants, Ling et al showed that in its native state soluble CR2 behaved as a complex with a molecular weight of 320kDa.

T æ• ã | æ{ æ} ã Á æ} å Á & [ | | ^ æ\* ~ ^ • Á æ| • [ Á } [ c ^ Á c @æc Á Ô Û G conformation(323). Therefore, the use of standard reference proteins that have a globular conformation may distort the appearance of CR2 on SDS PAGE as proteins with different structural conformations can be expected to migrate through a gel at different rates.

The above results do not unambiguously confirm the presence of CR2 in WCLs of monocyte. Though different isoforms of CR2 are known to exist, the largest described is a 145kDa protein on B cells(323). Thus, it is unlikely that the 160kDa seen represents an isoform of the unfolded protein and dimerization may offer a more likely explanation for our results.

Results presented here are suggestive of CR2 expression in MM and ZZ cells but do not provide unambiguous confirmation. In view of this we elected to use flow cytometry to further examine monocytes for surface expression of CR2.

## 3.6 Evaluation of CR2 on the membrane of circulating MM monocytes by FACS analysis

### 3.6.1 Background and rationale

One of the primary functions of monocytes is the elimination of complement opsonised pathogens through direct binding or phagocytosis(324). Previous descriptions of high levels of expression of complement receptors by circulating monocytes reflects their central role in the innate immune response(325). Monocyte expression of CR1(326), CR3(327), and the C5a receptor CD88(328) has been previously described but there are no studies confirming the expression of CR2 to date. CR1 and CR3 bind other C3 cleavage products (C3b and C3bi respectively)(310). This observation, together with insights gained from preliminary U937 work suggested to us that CR2 may be detectable on circulating monocytes. Identifying CR2 on a monocyte like cell line confirmed a biological plausibility to the theory that CR2 may be present on the surface of circulating monocytes. Identifying gene expression of CR2 in monocytes confirmed that monocytes are capable of producing CR2 protein. Thus, we endeavoured to confirm CR2 surface expression and assess whether expression changed in response to various stimuli.

In advance of this experiment we determined that If CR2 were found to be present this would confirm a potential signalling axis for C3d in monocytes. In the context of no previous description of CR2 on monocytes, we postulated that if present, it may show only low levels of expression. In view of this, the decision was made to treat & ^ | | • Á ~ • ^ â Á ã } Á c @ã • Á ^ ¢ ] -ã } ã { æ [ ¢ Á ¢ ã ¢ @Á Á Á ¢ æ { ã ↑ ã Á PMA, to see if expression could be up regulated.

### **3.6.2 Methods and technical considerations**

Monocytes were isolated from 6 healthy MM controls using the Easy Sep CD14 positive selection kit as described in the Materials and Methods chapter. As this kit selects out cells based on CD14 expression, cells examined represented the classical and intermediate subsets. Non classical monocytes were likely less well represented in view of their lower levels of CD14 expression. Monocytes were stimulated for 10 min with a range of pro inflammatory stimuli. Rationale for the selection of each agent is provided in Table 3.2.

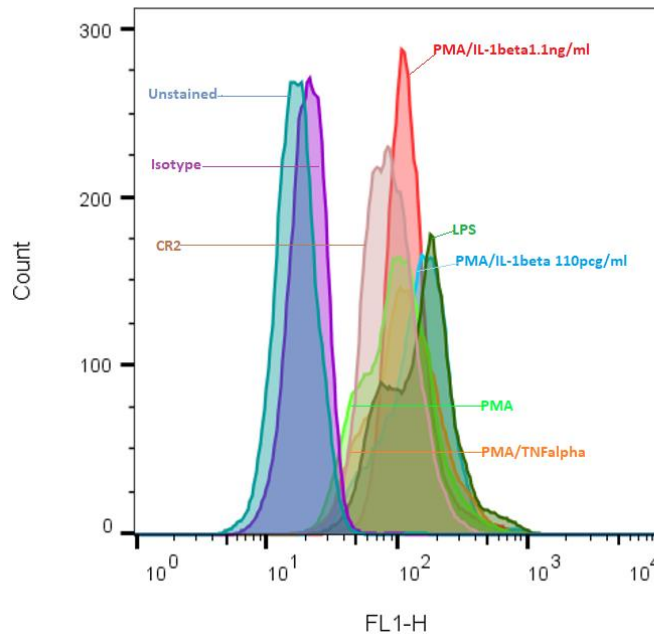
Experiments performed during early optimisation work included samples with and without the addition of protease inhibitors. In view of the short incubation period (10 min) and absence of apparent effect of PIs in cell line work, we were satisfied that the omission of protease inhibitors in this case was not unreasonable. Following treatment, all cells were fixed in 4% (w/v) PFA to arrest any further phenotypic changes that may have resulted from stimulation.

### **3.6.3 Results of FACS analysis of circulating MM monocytes**

Panel A, Figure 3.3 shows histograms confirming the expression of CR2 on monocytes that exceed background non-specific binding as indicated by the rightward shift of the peak of the histogram labelled CR2 when compared to the isotype control. Histograms suggest a rightward shift with LPS, PMA or IL-1 $\beta$  treatment but this was not significant when mean and median FL1-H was analysed.

Panel B shows Mean FL1-H for each sample (n=6). This analysis suggests no significant change in CR2 expression under the treatment conditions described.

**A**



**B**

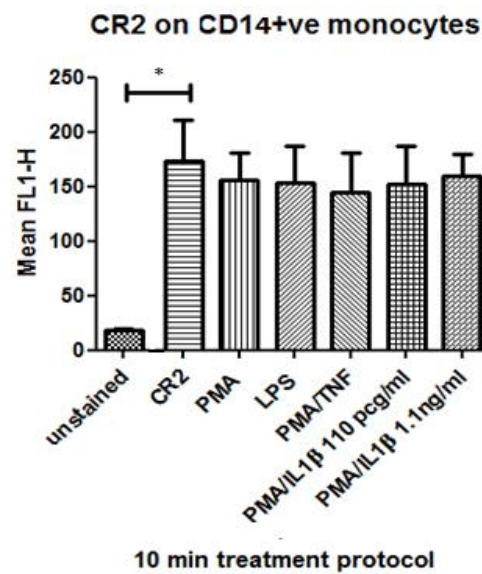


**Figure 3.6: Detection of and change in CR2 on the surface of MM monocytes exposed to pro-inflammatory stimuli.**

**A:** Histogram confirming expression of CR2 on MM monocytes isolated from circulation. **B:** CR2 expression does not change significantly following 10 min stimulation with listed treatments (n=6 biological repeats). Statistical analysis was performed using a paired t test. Significance denoted by \* $p < 0.05$ .

### **3.6.4 Conclusion of Flow Cytometric Analyses**

The above experiment confirms that CR2 is expressed on the surface of circulating MM monocytes. The experimental design precludes observations regarding the expression of CR2 relative to ubiquitous surface markers such as CD14 and CD16 that are commonly used to differentiate between different monocyte subsets(329).

The lack of inducible up regulation may be explainable by the short treatment time used here. 10 mins was chosen as this had previously been used in a similar experiment examining the effect of various stimuli on neutrophil expression on CR2. Neutrophil experiments showed an increase in CR2 expression in response to PMA.

Neutrophils are granulocytes that possess cytoplasmic granules and secretory vesicles. Surface receptor stimulation with a secretagogue such as IL-8 or PMA causes granules/vesicles to translocate to the phagosomal or plasma membrane where their membrane fuses with the plasma membrane, thus increasing levels of plasma membrane receptors(330). This propensity towards rapid degranulation has not been describe in monocytes and may explain why neutrophils respond to 10min treatment but monocytes may require longer.

Results achieved on all flow cytometry experiments suggested that CR2 was present on the surface of circulating cells. Considering the description of CR2 on monocytes is a novel finding we decided to examine monocytes for CR2 expression by Confocal microscopy.

## **3.7 Elucidation of CR2 on the membrane of MM and ZZ monocytes by Confocal Microscopy**

### **3.7.1 Background**

Confocal microscopy (CM) is an optical imaging technique that produces high resolution images of cells or tissue by using a spatial pinhole to block out of focus light that may distort the image and interfere with fluorescence. The confocal microscope captures multiple 2D images that are then used to reconstruct 3D images of structures(331). As CM offers the potential to visualise structures on the surface of and within cells, we chose this technique to further evaluate monocytes for CR2 expression.

### **3.7.2 Methods**

Following isolation as described in the Materials and Methods monocytes from healthy MM controls and those with ZZ AATD were fixed with 4% (w/v) PFA. Unstained monocytes and Raji B cells were also included in this experiment as a negative and positive control, respectively.

Following blocking with BSA, cells were incubated with a mouse monoclonal anti-CR2 antibody or an IgG2 B FITC in the case of the isotype control. Cells were left at 4°C overnight in tinfoil. Blocking reagent was aspirated completely and 50µl of DAPI added to the slide for nuclear staining. Slides were analysed using a Zeiss LSM710 confocal immunofluorescence microscope. Images were processed using ImageJ software.

### **3.7.3 Results of Confocal Microscopy**

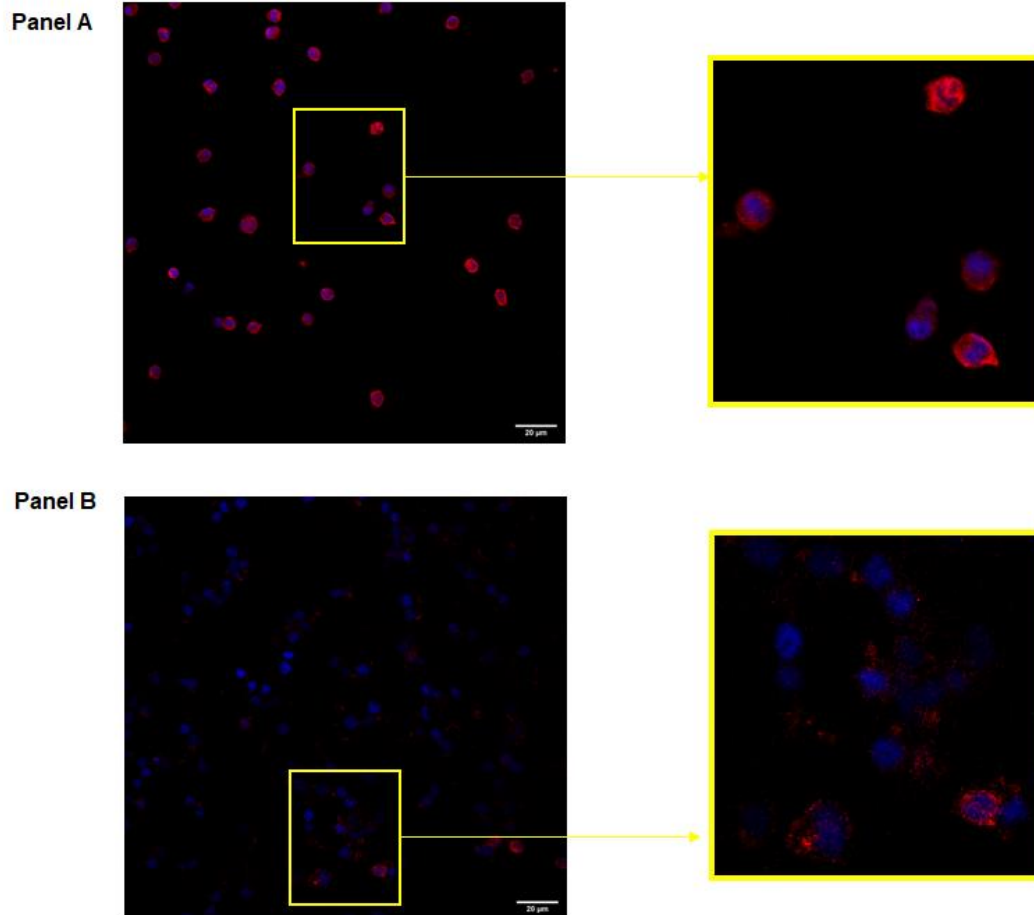
Figure 3.7 Panel A shows MM monocytes stained with a fluorescently tagged (AlexaFlour) anti-body to CR2 (depicted in red). Blue staining reflects staining of nuclear material by DAPI.

Figure 3.7 Panel B shows ZZ monocytes tagged with the same CR2 antibody as used on MM monocytes and exhibit a more heterogenous staining pattern compared to MM monocytes.

Figure 3.8 Panel A shows MM monocytes that are stained only with DAPI which were included as a negative control.

Figure 3.8 Panel B shows CR2 present on the surface of Raji B cells which were included as a positive control. Nuclear material is shown in blue.

Collectively, these results confirm CR2 is expressed by monocytes and corroborate the results of qRT-PCR, Western blotting and FACS.

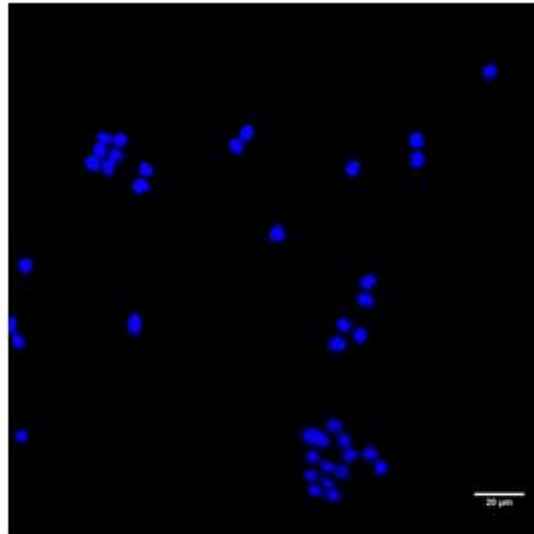


**Figure 3.7 Confirmation of CR2 on the surface of MM and ZZ monocytes by confocal microscopy**

**Panel A:** Monocytes from healthy MM controls with staining of nuclear material by DAPI shown in blue and surface expression of CR2 depicted in red. Sub panel shows magnification of MM monocytes (n=3).

**Panel B:** ZZ monocytes showing a more heterogenous staining pattern than the MM population. CR2 is shown in red. Sub panel shows magnification of ZZ monocytes (n=3).

**Panel A**



**Panel B**

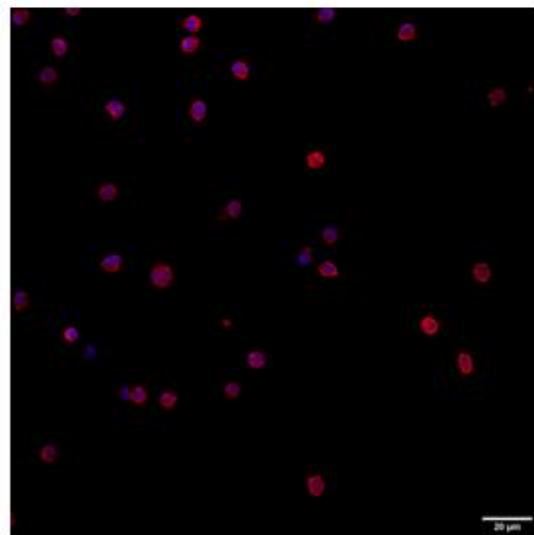


**Figure 3.8 Monocytes stained with DAPI without CR2 anti body visualised by confocal microscopy with inclusion of CR2 anti-body and DAPI stained Raji B cells as a positive control.**

**Panel A** shows monocytes stained only with DAPI. Nuclear material is shown is blue. **Panel B** shows high CR2 expression by Raji B cells which were used as a positive control. CR2 is depicted in red with nuclear material highlighted by DAPI in blue (n=3).

### 3.7.4 Conclusion of confocal microscopy results

Results of confocal microscopy confirm the presence of CR2 on the surface of MM and ZZ monocytes and is in keeping with results of qRT-PCR, western blotting and flow cytometry. Having demonstrated CR2 using 4 separate techniques we were satisfied that monocytes are capable interacting with C3d present in their microenvironment.

This further confirmation of CR2 on circulating monocytes prompted us to question

whether

and colleagues had previously shown that levels of the CR2 ligand C3d are elevated in BAL samples from those with ZZ AATD when compared to healthy controls.

Furthermore, levels of C3d in BAL were 8-fold higher than levels observed in plasma(78). This raises the possibility that if C3d is found to influence the behaviour of monocytes, the magnitude of that effect may be further exaggerated in monocyte derived macrophages within the airways. Moreover, it raises the question of whether C3d drives the pathogenesis of airways diseases such as COPD occurring with or without underlying AATD.

Establishing the existence of a signalling axis in cells obtained from the airways during bronchoscopy therefore became our next goal. In keeping with published guidelines for performing immunophenotyping of airway cells, we decided that multi-colour flow cytometry represented the best way to look for CR2 on a mixed population of airway cells.

### **3.8 Identifying CR2 on the surface of a population of airway cells using multi colour flow cytometry**

#### **3.8.1 Background**

The following experiments were carried out on BAL samples obtained from patients undergoing bronchoscopy at the recommendation of their treating clinician. Owing to the rapid global spread of the COVID19 pandemic, sample collection was unfortunately stopped prematurely. At the time of commencement of the Irish lockdown on March 13<sup>th</sup> 2020, 3 patients samples had been fully processed and analysed. A further 3 patient samples were used during optimisation of the protocol. Despite the resultant low n number presented here, we believe important insights can be gained from our results and thus it is presented as part of this body of work. The protocol used here can be adapted for use in future work aimed at characterising cell populations within the lungs.

The primary aim of this experiment was to identify and describe different subsets of macrophages and leucocytes in airway/BAL samples and describe the relative expression of CR2 on monocyte subsets and macrophages. Identification of CR2 on airway cells would suggest the availability of a signalling axis for C3d in the airways.

Defining subtypes of cells required the identification of a pattern of surface markers whose relative expression could be quantified to differentiate between populations. The protocol described here is adapted from work published by Yu et al(282). Their group used multi-colour flow cytometry, cell sorting and cytopsin analysis of BAL and whole blood samples to validate the anti-body panel presented.

To achieve our aims, we elected to use multi-colour flow cytometry to analyse samples collected during at the time of bronchoscopy.

### **3.8.2 Methods and technical considerations**

Patients were identified on the morning of their bronchoscopy written consent to participate was obtained. Patient demographics are presented in Table 3.3.

Bronchoscopy was performed by an experienced clinician bronchoscopist. CT scan and patient notes were reviewed prior to the procedure. Further detail on the sample collection protocol is described in the materials and methods chapter. To standardise the process, the right middle lobe (RML) was targeted. If on review of the CT scan the RML appeared excessively diseased (i.e. emphysematous) other lobes were chosen as the target to increase the likelihood of high return of suctioned instillate. Following transport to the lab on ice, samples were evaluated for quality as described in further detail below.

Suitable samples were stained with nine separate fluorophore tagged anti-bodies prior to multi-colour flow analysis. Multi-colour flow cytometry is a relatively recent development and represents an extension of the capabilities of early flow cytometers. Multi-colour FACS allows for the evaluation of more than 50 surface markers simultaneously (332). Optimisation of this protocol presented several challenges which are enumerated below.

**Table 3.3:** Demographics of patients involved in multi colour flow cytometric analysis of lymphocyte subsets from BAL

	<b>Patient 1</b>	<b>Patient 2</b>	<b>Patient 3</b>
<b>Age</b>	48	40	65
<b>Gender</b>	F	F	M
<b>Primary Respiratory Diagnosis</b>	Nil Unexplained dry cough	ILD in context SLE	Asthma Bronchiectasis
<b>Smoking status</b>	Never	Ex 10 years 20 pack year history	Never Passive smoking history
<b>ECOG</b>	0	2	1
<b>FEV1 L/%</b>	4.5L/ 109%	2.12L / 72%	1.79L / 103%
<b>FVC L/%</b>	5.86L/ 121%	3.04L / 83%	2.3L / 94%
<b>FEV1/FVC</b>	77	84	76
<b>DLCO</b>	94	55	90

### **3.8.2.1 Optimising BAL processing**

The first challenge encountered for this work package was obtaining BAL that was of adequate quality and would give a reasonable cell yield for analysis. The principles and technique of BAL recovery are well described in the literature(333). Most agree that in order to be reasonably assured that the sample represents an alveolar and not a proximal airway sample, total volume instilled through a wedged bronchoscope should be between 100-240ml(334). For cytokine analyses return following instillation of saline during the procedure should be at least 50%(335).

For this project, several methods were used to appraise the quality of the BAL samples. Principles described here are in keeping with current recommendations for the collection and processing of samples for research:

#### **1. Fluid instillation**

The total amount of fluid instilled was 200ml in total over 2 sequential washes(336). There was a degree of variability between healthy patients and those with established lung disease. Patients who had established lung disease and desaturated following the instillation of the first 100ml aliquot were limited to recovery of one 100ml BAL sample.

#### **2. Fluid Recovery**

Fluid was suctioned from the airway using very gentle manual retraction of a syringe attached to the bronchoscope. Suction applied was sufficiently gentle that dynamic collapse of the airway was not apparent during sample recovery. This avoided trauma to the airways and resultant sample contamination with blood. There was no absolute value for fluid recovery set as average fluid recovery is known to be much

lower in patients with COPD(337), smokers(338), the elderly(339) and those who cough during the procedure(336).

### 3. Macroscopic appearance

All samples that were macroscopically blood stained or excessively mucoid were sent for routine microbiology processing and not used as part of the study.

### 4. Cell Count

Only samples containing  $>2 \times 10^6$  cells were used for flow cytometry(340).

### 5. Cell Differential

All samples were centrifuged and stained using the Speedy Diff Complete kit (Clin Tech). Speedy Diff is a Giemsa stain for Romanovsky-type staining of blood smears and tissue specimens(340). An example of a prepared slide is shown in Figure 3.9. To proceed with anti-body staining the sample had to have  $>10$  macrophages visible per high powered field(341). If red cells were apparent following Speedy Diff staining the sample was resuspended in red cell lysis buffer for 10min and washed.

### 6. Non cellular components of BAL

Within the literature there is debate about how best to determine what proportion of recovery BAL fluid represents epithelial lining fluid (ELF)(342). Several approaches have been described but none represents standard practice in clinical work(336). Our lab uses a urea assay to estimate ELF proportion(343). Urea assay was performed on samples to ensure there were suitable for freezing and future cytokine analysis. Thus, a calculated low ELF did not preclude use of the cells for our analyses.

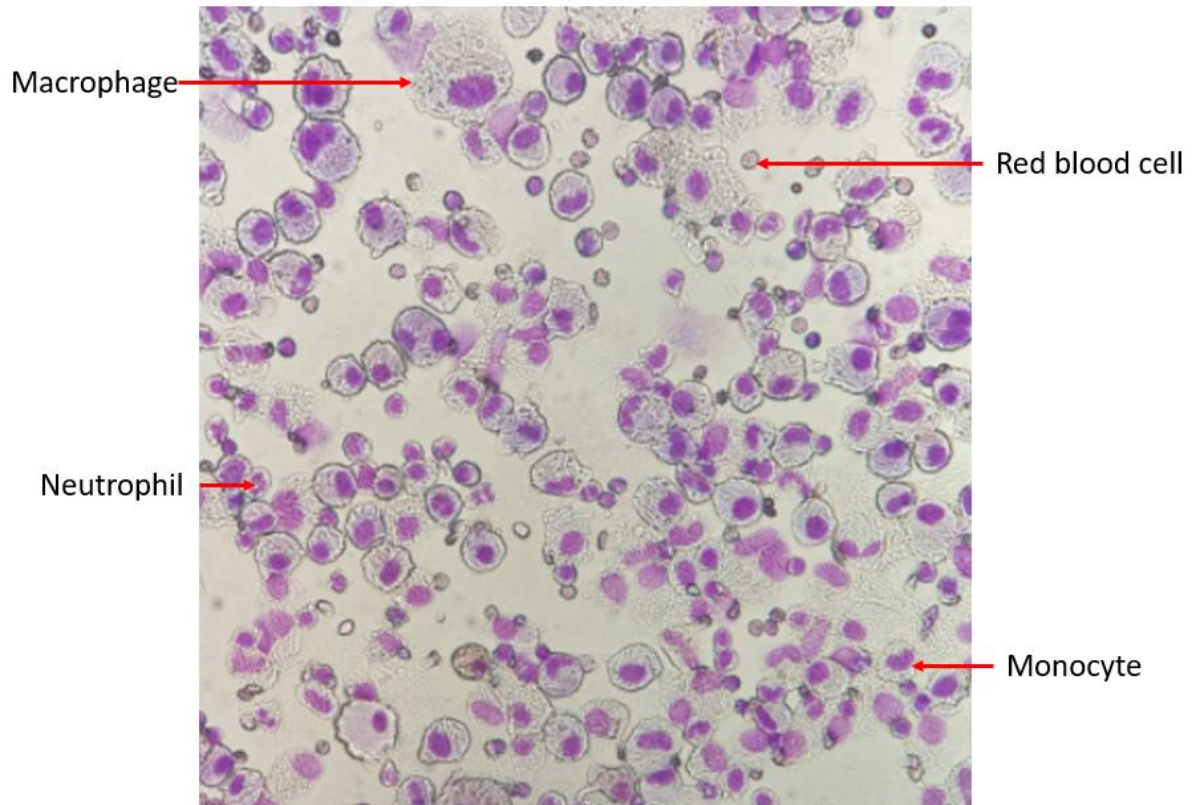


**Figure 3.9: Speedy Diff staining of BAL sample with labelling of visible lymphocyte subsets**

4 major cell types are visible in this very cellular specimen including macrophages, neutrophils with a distinctive multi lobed nucleus, monocytes with a kidney bean shaped nucleus and red blood cells.

### 3.8.2.2 Cytometer selection

Following refinement of the sample retrieval and appraisal process, the next challenge presented centred on identifying a cytometer capable of running the required analyses. The protocol required a machine with a least 3 laser capability to run. A cytoflex S cytometer equipped with 3 lasers and 16 detectors was used to analyse our samples.

### 3.8.2.3 Accounting for background signal in analyses

Published studies highlight that heterogeneity in the staining intensity of isotype controls is a potential source of error in the characterisation of cells by FACS(344). In lieu of isotype controls, multi-colour flow cytometry utilises a fluorescence minus one (FMO) control to distinguish between true signal and noise during analyses.

An FMO control contains all the fluorochromes of the anti-body panel of interest except the target of interest(345). FMO controls are an essential part of any multi-colour flow cytometry experiment and determine how different cell populations are identified and subsequently gated for analyses(346). As previously mentioned, our anti-body and fluorophore panel (described in Chapter Two: Materials and Methods) was developed using previously published work describing a protocol for the identification of subsets of myeloid cells in BAL(282). We modified the panel to look for the presence of CR2 on a number of different cell types including total macrophages, alveolar macrophages, all 3 known monocyte subsets.

### 3.8.2.4 Gating strategy to identify sub populations of airway cells

Further discussion of the function of the surface markers used in these experiments is provided in Chapter One. The gating strategy outlined below was first published in the ATS journals and has been validated for use in the processing of whole blood and BAL samples(282)

The approach to the gating strategy used was as follows:

1. The side scatter area / forward scatter area (denoted as SSC-A/FSC-A) was used to identify the likely macrophage population. SSC-A/FSC-A provides information about the physical characteristics of populations enabling identification of macrophages which are large, granular cells on the dot blot(347). As macrophages generate high forward and side scatter they appear in the top right hand quadrant of a SSC-A/FSC-A plot. This population  
, æ• Á \* æc ^ å Á æ} å Á | æà ^ | | ^ å Á æ• Á ± T æ& ! [ ] @æ\* ^ • q È
2. The macrophage population was gated to exclude doublets. Doublets occur when two cells pass through the laser beam of the flow cytometry very close to one another. If a fluorescence negative cell passes close to a positive cell it will generate a false positive signal that will skew the results of subsequent analyses(348).
3. Single cells were then examined for CD45 expression. CD45 or leucocyte common antigen is expressed on all haematopoietic cells except for Mature erythrocytes(349). This CD45+ population was gated and labelled as total leukocytes.
4. Cells were examined using live/dead staining to exclude dead cells from the total leucocyte population(350).

5. Live leucocytes were examined for CD14 and CD206. CD206 which is a mannose receptor was used to identify all macrophages in keeping with previously published literature. Though commonly used as a marker of macrophage activation(351), CD206 is known to be expressed at high levels by all tissue macrophages(352). Cells expressing the common macrophage marker CD206 were gated and labelled Total Macrophages(282, 283).
6. The Total Macrophage population were examined for CD14 and CD169. Those who were CD14- and CD169 + were designated alveolar macrophages (AMs)(282). Prior studies have defined CD169 negative pulmonary macrophages as macrophages that associate with the interstitium (IMs). Important functional distinctions between the two population include the ability [ ~ Á Q T • Á à ~ c Á } [ c Á OET • Á c [ Á ] ! [ â ~ & ^ (353). ~~1.60~~ Á ã } Á ! ^ • discussed in Chapter One, both alveolar and interstitial macrophage populations can be further sub divided into resident and recruited populations.
7. Alveolar macrophages were checked for expression of CR2. A false positive was outruled via comparison with the CR2 FMO control.
8. We then separately gated the CD206-ve cells and examined them for CD14 and SSC to distinguish granulocytes (SSC high) from agranulocytes (SSC low)(354).
9. Granulocytes were examined for CD16 versus CD24 and labelled as follows(282):
  - CD16 +/CD24 + Neutrophils
  - CD16 -/ CD24 low Mast cells
  - CD16-/CD24+ Eosinophils

10. Agranulocytes were examined for CD14 versus CD24 expression. CD14+/ CD24 -ve cells were identified as monocytes.

11. The monocyte population was gated into 3 subsets based on CD14 and CD16 expression as follows(131):

- CD14 ++/ CD16-ve classical monocytes
- CD14+/ CD16+ intermediate monocytes
- CD14 low/ CD16+ non classical monocytes

12. Each monocyte subset was then examined for CR2 expression.

### **3.8.3 Results of multi colour FACS analysis of BAL samples**

Figures 3.10-3.13. Depict dot plots from whole BAL analysis with the gating strategy applied to define major leucocyte subsets.

Figure 3. 10 panel A demonstrates SSC-A/FSC-A of the whole cell population obtained including dead cells. The blue gate labelled macrophages is selecting out a population based on their physical characteristics- large and granular suggestive of macrophages.

Panel B depicts the removal of doublets from the samples. The red gate is drawn within the main cell population and deliberately excludes the less dense border which represents doublets that could interfere with subsequent analyses.

Panel C represents the gated population of single cells (i.e. with doublets excluded) identified in Panel B. The dot plot is divided into 4 quadrants to facilitate comparison with the FMO controls. Cells shown here are examined for CD16 and CD45 expression. CD45 positive cells which are representative of leucocytes are identified

to the right of the vertical line that bisects the dot plot. This population is gated in pink and represents the total leucocyte population. As expected, the majority of the total population (56.67%) are identified as a leucocyte though their specific subsets are not identifiable at this stage in the gating strategy.

Panel D shows a yellow gate capturing the live cells from the gate created in Panel C. This confirms that cell viability was only minimal impacted during BAL processing and 97.7% of the cells obtained were alive at the time of analysis.

Panel E depicts the live cell population gated in panel D being examined for CD14 and CD206 expression. CD206 is being used here as the primary macrophage surface marker. Again, the dot plot is divided into 4 quadrants. The dimensions of each quadrant are defined by comparison with the CD14 and CD206 FMO controls (not shown). Cells that are positive for CD206 fall to the right of the vertical line and cells that are positive for CD14 fall above the horizontal line. Broadly speaking, the plot identifies 2 populations within the live leucocyte population. Cells expressing CD206 are gated in blue and labelled total macrophages. This population comprises both resident and recruited AMs and IMs.

Figure 3.11 provides 3 further panels. Panel A is a replica of Panel E in Figure 3. And is provided for reference.

Panel B shows the population gated in Panel A as total macrophages being examined for CD14 and CD169. AMs are identified by staining positive for CD169 (all cells to the right of the vertical line, gated in pink). This dot plot identifies 71.32% of the macrophage population obtained as being alveolar macrophages.

Panel C shows expression of CR2/CD21 on alveolar macrophages. The alveolar macrophage population gated in Panel B are examined for CR2/ CD21 expression.

The orange gate shows that CR2/CD21 is expressed on 25.75% of the alveolar macrophages identified. This confirms a signalling axis for C3d on AMs within the airways.

Figure 3.12 outlines the identification of 3 separate monocyte subset populations within the airways. Panel A is again replicated from Figure 3 and is provided for reference. The population gated in gold and labelled CD206-ve cells represents a non-macrophage population and represents a mixed leucocyte population. This population is reproduced in Panel B.

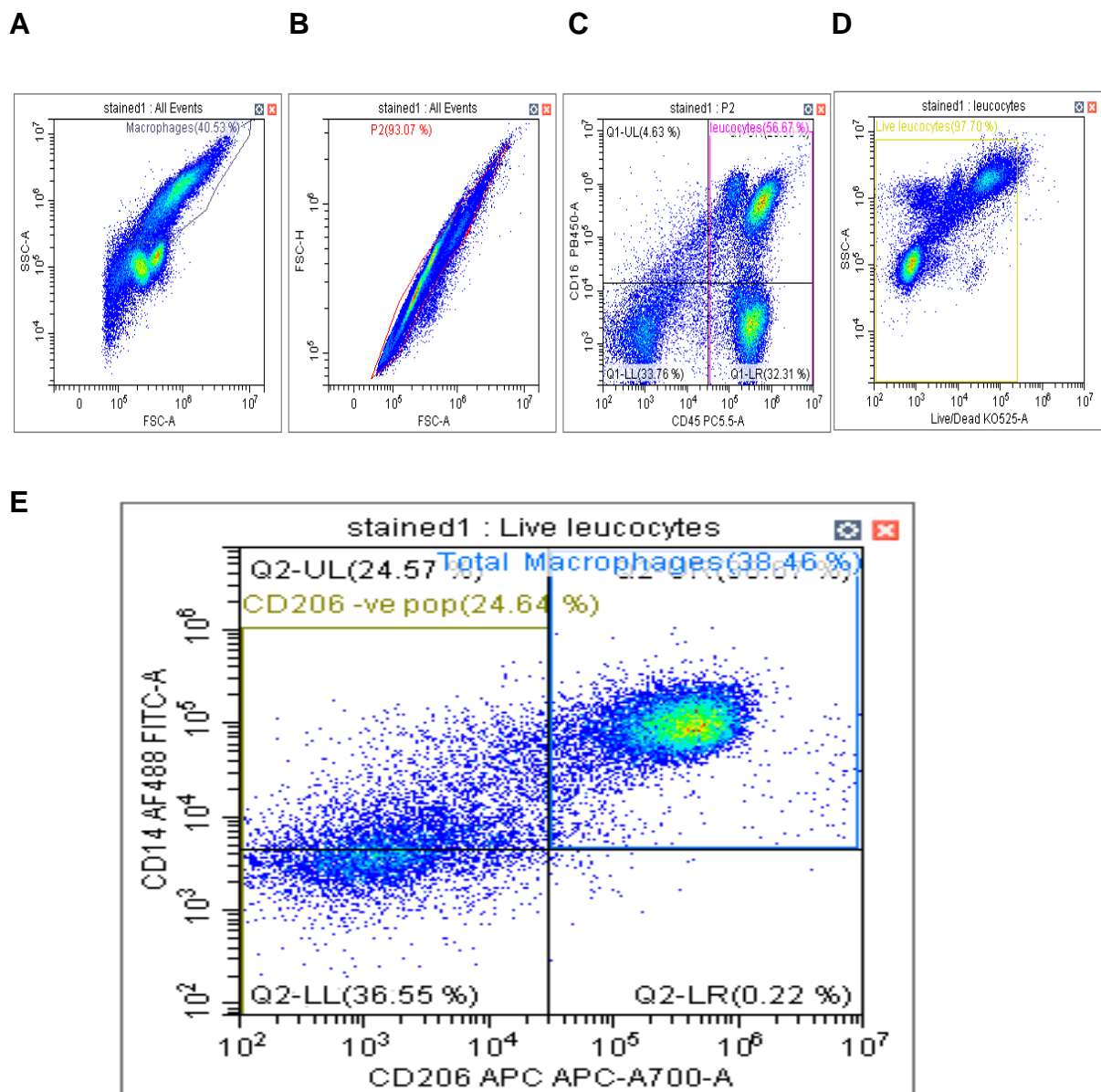
Panel B shows the CD206-ve cells that have been gated for SSC and CD14 to identify high and low SSC cells (granulocytes and agranulocytes respectively). SSC low cells were then examined for CD14 and CD24 expression. Monocytes are identified as CD14<sup>+</sup> CD24<sup>-</sup> cells which are seen in the bottom right-hand quadrant of panel B. The dot plot in panel B shows that 72.09% of total agranulocytes demonstrate a surface marker profile that classifies them as monocytes.

Panel C shows the monocyte population identified in Panel B being interrogated for expression of CD14 and CD16. Classical, non-classical and intermediate monocytes are all identifiable on this plot. The vast majority of airway monocytes shown here most closely resemble intermediate monocyte (CD16<sup>+</sup>/CD14<sup>+</sup>).

Figure 3.13 shows each monocyte subset being examined for expression of CR2/CD21. For each subpopulation, any signal generated to the right of the vertical line bisecting the dot plot represents a true positive and CR2 expression. It is notable that whilst intermediate monocytes constitute the bulk of the monocyte population, CR2 expression is low (1.33% of total). CR2 is not detected on classical monocytes (CMs) in this panel but numbers of CMs in the airways are very low (2.6% of total

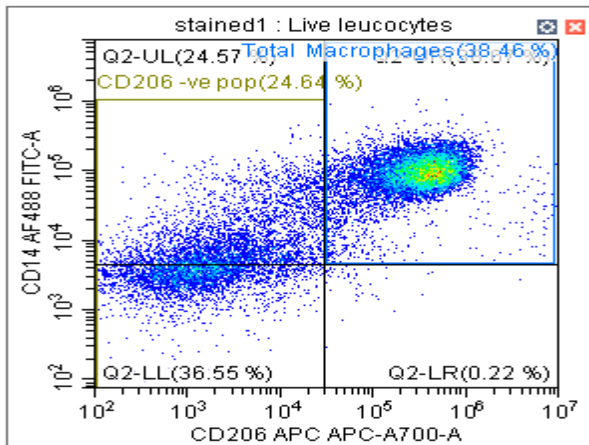
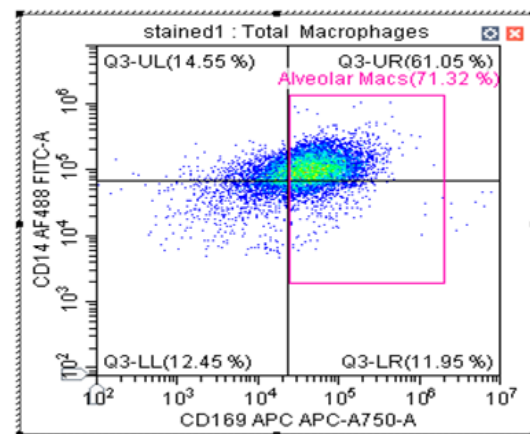
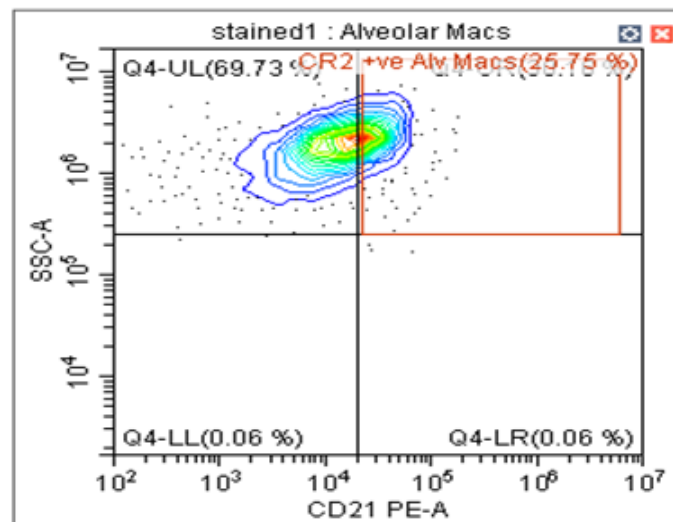
agranulocyte population). CR2 expression is greatest on non-classical monocytes NCMs (14.26% of NCMs examined expressed CR2 as depicted in Panel B).

Figure 3.14 compared expression of CR2 between the 3 described monocyte subsets and alveolar macrophages. Levels of CR2 expression differ significantly between each subset with highest levels of expression seen in on classical monocytes. CR2 expression is also significantly higher on alveolar macrophages compared to all monocyte subsets.



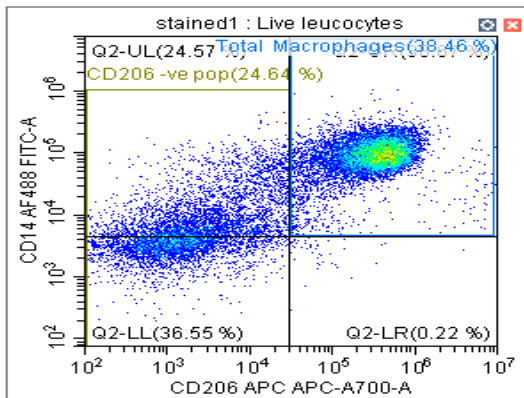
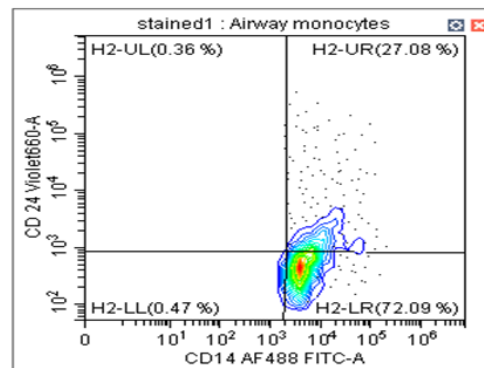
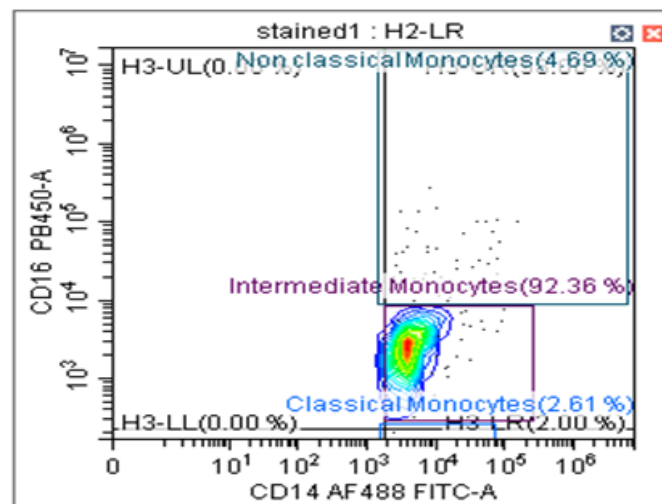
**Figure 3.10 Gating strategy for the identification of macrophages in BAL samples using multi-colour flow cytometry**

**Panel A** shows SSC-A vs FSC-A being used to identify large granular cells labelled Macrophages (blue gate). **Panel B** uses FSC-H vs FSC-A to exclude doublets from the macrophage samples gated in panel A (red). **Panel C** identifies a CD45 +ve population designated Leucocytes (pink). **Panel D** shows a Live/Dead stain being used to gate the live cells from the Leucocyte population (gold). **Panel E** identifies cells from the live leucocyte population. Live cells expressing CD206 are labelled as total macrophages (blue). Representative of n=3 biological repeats.

**A****B****C**

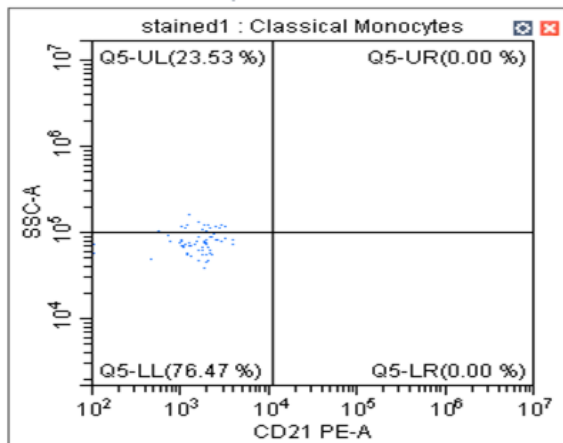
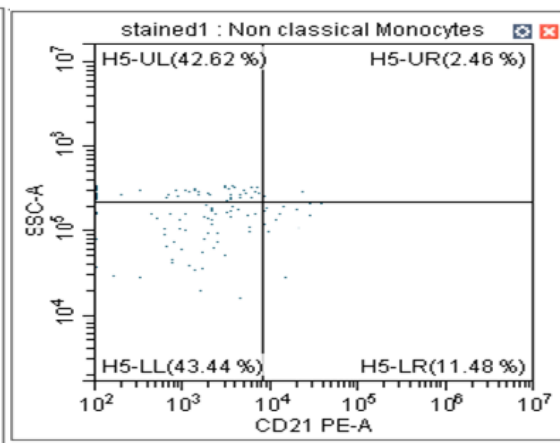
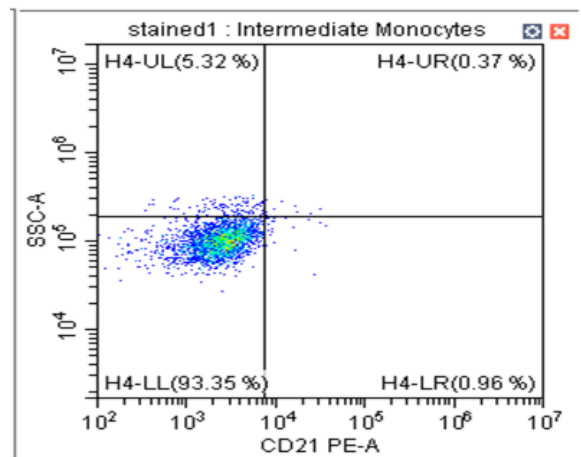
**Figure 3.11 Gating strategy identifying CR2 on the surface of alveolar macrophages using multi colour flow cytometry.**

**Panel A** shows identifies 2 populations. CD206+ve cells gated in blue represent total macrophages. **Panel B** identifies CD14+ CD169- cells as Alveolar Macrophages and are gated in pink. **Panel C** confirms the presence of CR2 on the surface of 25.75% of the alveolar macrophage population. Representative of n=3 biological repeats.

**A****B****C**

**Figure 3.12 Multi colour flow cytometry identifying 3 subsets of monocytes in BAL samples.**

**Panel A** depicts a green gate around a CD206 -ve population which are identified as airway lymphocytes (ALs). **Panel B** shows gating on ALs to identify a CD14 +ve/CD24 -ve population designated airway monocytes. **Panel C** examines airway monocytes based on relative expression of CD14/CD16 and identifies all 3 previously described human monocyte subsets. Representative of n=3 biological repeats.

**A****B****C**

**Figure 3.13 Multi-colour flow cytometry identifying CR2 on the surface of 3 monocyte subsets obtained from BAL samples.**

**Panel A** confirms shows no CR2 expression on classical monocytes in the airways.

**Panel B** shows CR2 expression on 13.94% of overall non classical monocyte population. **Panel C** shows CR2 is expressed on 1.33% of the overall intermediate monocyte population.

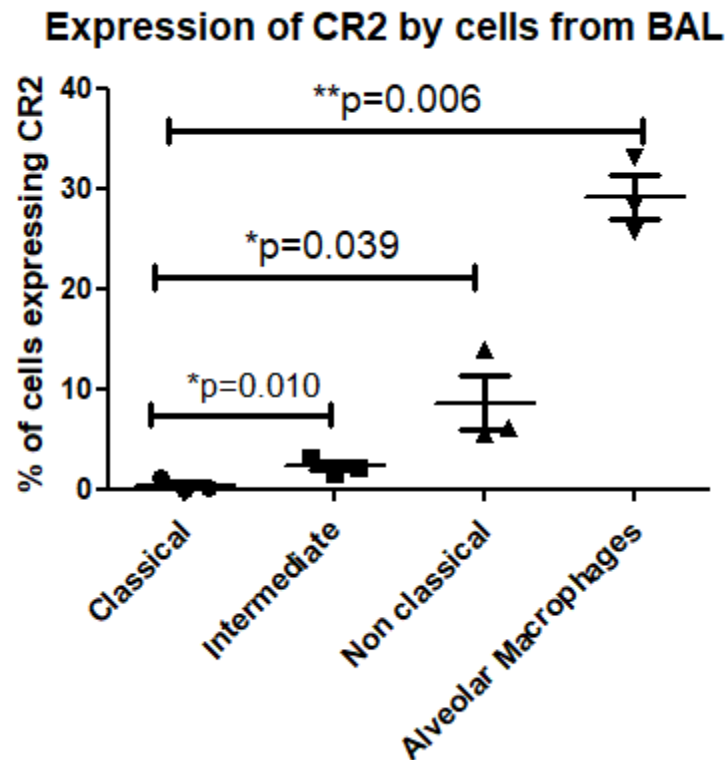


**Figure 3.14 Relative expression of CR2 on monocyte subsets and alveolar macrophages in BAL using multi colour flow cytometry.**

CR2 expression is significantly higher on alveolar macrophages when compared to all airway monocytes subsets. Expression of CR2 by intermediate (IM) and non-classical (NC) monocytes compared to classical monocytes (CM) was significantly higher with no difference observed between the NC and IM subsets. Analyses were performed using an unpaired t-test. n=3

### 3.8.4 Conclusion

The experiments presented in this section demonstrate that CR2 is present on the surface of macrophages and monocytes in the airways. Results obtained using this technique highlight the utility of multi-colour FACS in identifying the phenotypes of different cells types obtained from BAL samples. Unfortunately, sample collection and protocol optimisation for this block of work commenced in late February 2020 and was stopped prematurely by the global spread of the SARS CoV-2 virus. As bronchoscopy is an aerosol generating procedure, sampling and processing of samples during this time was deemed an excessive risk to staff and patients. Despite this, we believe that the protocol presented here (further description provided in the materials and methods chapter) will provide a springboard for future work focused on immunophenotyping of airway cells.

Though the numbers presented are limited ( $n=3$ ), we believe some important insights have been gained through this endeavour. We were struck by the observation that there is a reversal of the proportional representation of different monocyte subsets when moving from the circulation to the airways(355). We hypothesise that what we are observing is a recruited classical monocyte population to the lungs whose low number reflects differentiation into alveolar macrophages. For cells that do not undergo differentiation, this classical subset may undergo a subset switch to an intermediate and subsequent non classical monocyte as is known to occur in the systemic circulation(122).

Berger and colleagues had previously found that neutrophils and other cells obtained from BAL expressed CR1 and CR3(356). They remarked that if CR2 was indeed present, it was not present in sufficient quantities to be identified using standard flow cytometric analysis. Advances in the design of flow cytometers has enabled rapid

progress in the area and enabled identification of CR2 in BAL cells. Our experiments demonstrate that CR2 is expressed on airway monocytes and macrophages. It is worth noting however that owing to the very small number of classical monocytes identified in BAL samples, it is difficult to discern whether the lack of CR2 expression we have identified by this subset reflects a true absence of expression or a lack of signal because of very low cell number.

As classical monocytes are the only subset capable of recruitment to the lung from circulation(357), a shift in profile of circulating monocytes towards a classical phenotype could theoretically prime circulating monocytes for recruitment during times of intercurrent illness or with advancing age. Studies of monocyte responses to AAT suggest that alterations in the proportional representation of different monocyte subsets in AATD is possible. Sandstrom and colleagues previously showed higher levels of membrane bound and soluble CD14 in young healthy subjects with ZZ AATD when compared to matched MM controls(358). Nita et al have previously shown that the treatment of monocytes with AAT alone or in combination with LPS altered expression of membrane bound and soluble CD14(166). As the relative expression of CD14 and CD16 define each monocyte subset, this suggests that subset switching may be occurring in the circulation of those with AATD. Nita et al showed that longer term incubation (18 h) of monocytes with combined AAT/LPS resulted in a significant reduction in expression of CD14 and TLR4. This suggests that monocytes in AATD may express more CD14 and thus favour the pro-inflammatory classical phenotype. Furthermore, monocyte exposure to AAT abrogated LPS-induced CD14 and protein expression. This suggests that AAT is an important regulator of CD14 expression and may be involved in LPS neutralization and prevention of over-activation of monocytes in vivo.

It remains to be seen whether a similar effect is seen with monocytes within the airways and monocyte derived AMs.

### 3.9 Discussion of overall results

The receptor for C3d (CR2) has been described at length in published literature but has never been identified on the surface of monocytes in the circulation or within the airways. Thus, before proceeding to investigate whether C3d could be influencing monocytes, it was first necessary to confirm CR2 expression. As this body of work represents the first description of CR2 in this cell type, proof of expression was determined using several different experimental techniques. The results presented here confirm that monocyte like cells (U937 cell line), monocytes within the circulation and the airways express CR2

Early experimental work using U937 cells showed that short term stimulation with PMA upregulated CR2 expression in this cell line but did not exhibit the same effect on monocytes obtained from circulation. Previous studies have also demonstrated inducible expression of complement receptors in U937 cells(275). PMA is known to activate the protein kinase C (PKC) pathway in U937 cells. Rubin et al showed that stimulation with PMA alone did not induce expression of a receptor of the complement anaphylatoxin C5a on U937 cells(359). However, when PMA was combined with 1-25 (OH)<sub>2</sub>D and cAMP expression of C5aR became apparent. This suggested a biologic plausibility to the idea that expression of receptor for complement fragments such as C3d was likely to be inducible. It is important to note, that treatment with PMA is not a physiological stimulus raising questions about the clinical usefulness of results showing increased CR2 expression in treated U937 cells. However, PMA is known to prompt differentiation of U937s towards a macrophage phenotype. This prompts the question of whether CR2 may be upregulated during normal monocyte to macrophage differentiation. This idea is supported by observations in the literature that expression of other complement

receptors including CR1, CR3 and CR4 are upregulated during monocyte differentiation(360, 361). It is further reinforced by results of multi colour flow cytometry which demonstrate much higher levels of CR2 on airway macrophages compared to monocytes in BAL samples.

Despite the observation that U937 cells increased CR2 expression in response to PMA stimulation, the same effect was not observed in monocytes from circulation. Increased expression of complement receptors by U937 cells in response to PMA has been demonstrated previously by Burg et al who demonstrated increased expression of receptors for C3a and C5a following stimulation(362). Though U937 cells are frequently used as a model for monocyte function, they are structurally and phenotypically more like developing monoblasts(275). Expression of surface markers that are expressed strongly in mature monocytes such as CD14 and HLA DR are notable for their low levels of surface expression in U937 cells (302). U937s also lack the phenotypic diversity that characterise circulating monocyte subsets. Thus, it was not surprising that our finding of increased CR2 expression in PMA treated U937 cells did not hold when the same protocol was applied to circulating monocytes.

Early flow cytometry work confirmed surface expression of CR2 on monocytes. Though histograms presented suggested a rightward shift and thus increased expression in response to LPS, this result was not significant. We hypothesised that the treatment protocol used may have been too short to elicit a significant response from monocytes. This hypothesis was informed by the work of Inada et al who showed a time dependent increase in rosetting between red cells coated with C3d and monocytes cultivated for 48 hours(255). This work suggests that a receptor for C3d, which would subsequently be described as being CR2 was capable of being expressed by monocytes but was likely influenced by the state of monocyte

activation or differentiation. Segura et al also found a time dependent increase in production of IL-1, IL-6, IL-8 and MCP-1 by monocytes with peak production achieved between 24 and 48 hours(363). When considered together, these findings suggest that short term monocyte stimulation may have been insufficient to alter CR2 expression significantly.

Western blotting results presented here does not confirm CR2 expression unambiguously but results are certainly suggestive of the presence of CR2 in whole cell lysates of monocytes. As previously discussed, the finding of a large immunoband (160kDa) representing CR2 protein may reflect dimerization of CR2 occurring in the absence of DTT or erroneous identification of soluble CR2. Further experiments using confocal microscopy and qRT-PCR successfully show expression of CR2 at the cell surface at gene level respectively. Further reassurance of gene expression was provided by agarose gel confirmation of the qRT-PCR reaction product as 105 base pair CR2. Of note, the CR2 staining pattern observed on ZZ monocytes during CM was more heterogeneous in appearance than MM samples but no significant differences in gene expression was observed. AATD is characterised by a relative abundance of proteases which may account for the more variable membrane expression seen on ZZ monocytes(364).

The final results presented in this chapter confirm that CR2 can be identified on the surface of a diverse population of airway cells including alveolar macrophages and all 3 previously described monocyte subsets. Regrettably, sample collection for this block of work was limited by the COVID19 pandemic which peaked in Ireland in April 2020. The small sample number presented here precludes insights being made into the variability of CR2 expression between disease states but does inform our understanding of how expression of complement receptors such as CR2 varies

between different types of airway cells. The anti-body panel used here highlights the utility of multi-colour flow cytometry for immunophenotyping airway cells. Addition or substitution of anti-body targets and fluorophore conjugates would allow for more detailed analyses and phenotyping of airway cells which may vary considerably between disease states(282). The rapid global spread of COVID19 has highlighted the need to study monocytes and monocyte derived cells with the hope of identifying reliable targets for disease modifying treatments. A recent Nature Immunology paper confirmed that monocyte derived monocytes display unique transcriptional, epigenetic and functional profiles(155). Aegerter et al showed that monocyte derived AMs are the main producers of IL-6 during and following infection with the influenza virus. As IL-6 is one of many cytokines implicated in the cytokine storm that characterises some of the more severe cases of COVID19(365), further study of this population is imperative.

Expression of complement receptors by monocytes and macrophages is advantageous from an evolutionary perspective(180). Berger and colleagues have previously demonstrated that complement enhances the phagocytic responses of neutrophils to the bacterium *Pseudomonas aeruginosa* rendering them more effective executors of pathogen clearance from the lungs(356). Thus, confirmation of CR2 expression by monocytes and alveolar macrophages as demonstrated here is not wholly surprising as both represent important first line executors of the immune response to pathogen invasion.

Collectively, the results presented here confirm the novel finding that CR2 is expressed by circulating monocytes. Furthermore, expression is not upregulated by short term stimulation with pro inflammatory stimuli in the manner seen in neutrophils. The relationship between CR2 and C3d has been previously described

in detail (248, 366) and confirmation of CR2 on monocytes suggests the existence of a signalling axis for C3d. This raises the question of what the downstream effects of C3d are likely to be in monocytes. This will be explored in depth in Chapter Four.

## **Chapter Four: Evaluating the effects of C3d on MM and ZZ monocytes**

## 4.1 Introduction

Data presented in results chapter one confirmed the expression of CR2 on monocytes in the circulation of MM healthy controls and ZZ AATD populations.

Degree of expression at the gene level suggested no significant differences between MM and ZZ cohorts.

Having confirmed the existence of CR2 and thus potential signalling axes in HCs and AATD we became interested in elucidating the nature of the response of monocytes to C3d. The cytokine profile exhibited by monocytes in response to pro-inflammatory stimuli is

gamma(369) to name a few. Our early experiences with flow cytometry led us to believe that we needed to treat monocytes for longer periods of time (24 hours) if we

colleagues had measured levels of 5-40µg/ml C3d in plasma and BAL samples of those with AATD we elected to use this spread of concentrations to determine the dose response relationship(78).

Monocytes stimulated with other complement fragments have previously been shown to produce pro-inflammatory cytokines in response. Haggadone et al (2016) et al., used a murine monocyte model to show that stimulation with complement fragment C5a (1µg/ml) together with LPS increases monocyte production of the cytokine IL-1 (370). C5a is known to bind to two separate receptors on monocytes C5aR1 (CD88) and C5aR2 (GPR77) which signal through several pathways including mitogen activated protein (MAP) kinase, p38 and NF- (371). In contrast, C3d has only one known receptor CR2.

The interaction between C3d and CR2 on the surface of B cells has been previously described in detail(372, 373). As outlined in Chapter One (CR2/CD21) associates

with CD19 and CD81 on the surface of B cells(372) and acts by amplifying signalling including tyrosine kinase phosphorylation, calcium mobilisation and other downstream events(373). Fundamental differences in receptor signalling mechanisms mean that extrapolating and planning ELISA experiments based on other studies of monocyte/complement fragment interactions is of limited value.

As monocytes are known to produce a wide variety of cytokines and proteases it was necessary to identify what outputs were likely to change in response to C3d but also which were clinically meaningful. Regarding the currently available evidence base, previous data from the McElvaney lab has shown increased production of the cytokines IL-6, IL-8 and IL-10 from ZZ monocytes in response to an LPS trigger(299). IL-8 production can be triggered by the action of neutrophil derived proteases such as NE on epithelial cells within the lungs (374). Increased levels of IL-8 have previously been identified in sputa of individuals who are heterozygous for the PiZ mutation and have normal lung function(375). Rouhani et al.(2000), have also previously identified increased levels of IL-8 in BAL samples of those with ZZ AATD with levels of IL-8 correlating with increased protease burden and decreased lung function(293).

In view of this established link between ZZ AATD and IL-8, and in the context of ZZ monocytes being recognised as being intrinsically programmed to produce excess levels of IL-8 upon activation, we questioned whether C3d may act as a trigger for IL-8 production by monocytes. Our interest in IL-8 was further justified as Bergin and colleagues have previously shown that AAT regulates neutrophil chemotaxis induced by soluble immune complexes and IL-8(292). The work of McCarthy et al demonstrated the therapeutic implications of Bergin's foundational work. In an elegant series of experiments they showed that during the recovery phase of

community acquired pneumonia (CAP) heavily glycosylated AAT protein complexes with greater affinity to the pro inflammatory cytokine IL-8 thereby facilitating more rapid resolution of an inflammatory response and clinical recovery from CAP.

Collectively, the work of Carroll, Bergin and McCarthy suggests that the inflammatory milieu observed in AATD, is perpetuated by high levels of IL-8. Sources of excess IL-8 production include monocytes of which, ZZ monocytes are known to produce an excess of IL-8 compared to HCs. Furthermore, the deleterious effects of IL-8 can be mitigated by the administration of exogenous AAT protein. In consideration of these collective observations, we elected to explore whether exposure of monocytes to C3d altered IL-8 production in ZZ AATD and HCs.

In addition to assessing the cytokine profile elaborated by monocytes in response to C3d, we were also interested in ascertaining its effects on monocyte protease production. Unpublished data from our lab demonstrated that short term treatment of neutrophils with C3d augments degranulation of primary, secondary and tertiary granules. Dysregulated neutrophil degranulation is recognised as an important event in the pathogenesis of AATD with increased levels of primary, secondary and tertiary granules detectable in the plasma of individuals with ZZ-AATD(305, 364). Excessive neutrophil degranulation increases the proteolytic burden in AATD and fosters the development of autoantibodies to granule proteins such as PR3 and lactoferrin(305). ANCA associated vasculitides (AAVs) such as granulomatosis with polyangiitis (GPA) are seen with increased prevalence in those with the PiZ mutation(376). This is thought to reflect a relative abundance of circulating proteases that act as antigens triggering an auto immune anti-body response. Though frequently referred to as agranulocytes, monocyte cytoplasm is known to contain azurophilic granules the content of which can be altered through de novo protein synthesis throughout the life

cycle of the cell(125, 377). Similarly to neutrophils, monocytes have been shown to produce a diverse range of proteases including metalloproteases, cathepsins, PR3 and the serine protease granzyme B(201). Proteases can be categorised based on their affinity for differing substrates. The spectrum of proteases generated by monocytes and monocyte derived macrophages is broad and capable of degrading many of the structural components that form the extracellular matrix (ECM) of lung tissue. Monocyte derived MMPs in particular have been linked to the development of an array of lung diseases including COPD, asthma and interstitial fibrosis(378).

Elevated levels of the complement fragment C3d in the plasma and BAL of those with ZZ AATD suggest dysregulated complement activation in AATD. We hypothesised that C3d may be contributing to disease pathogenesis via an as yet unexplored interaction with monocytes and monocyte derived macrophages. The following experiments aim to offer insights into the effects of C3d on monocytes in AATD and to facilitate the generation of hypotheses that enhance our understanding of the role monocytes play in the pathogenesis of AATD lung disease.

#### 4.1.1 Chapter Aims

In Results Chapter One we used a variety of methods to conclusively demonstrate that monocytes in circulation and the airways express the receptor for C3d,

CR2/CD21(379)È Á V @^ Á ] ~ à | ã • @^ å Á , [ ! \ Á [ ~ Á U q Ó! ã ^ } Á ^ c Á æ| dysregulated complement activation as evidenced by increased levels of the complement fragment C3d in the plasma and BAL of those with ZZ AATD(78).

Monocytes are known to produce a diverse range of cytokines including TNF alpha, IL-6, IL-8 and IL-1 $\beta$  in response to inflammatory stimuli (164, 299). Furthermore, evidence suggests that monocytes in AATD elaborate an intrinsically excessive cytokine response(299).

Unpublished data from the McElvaney lab suggests that exposure of neutrophils to C3d correlates with increasing levels of primary, secondary, and tertiary granule proteins detectable in supernatants. We hypothesised that C3d may be a driver of disease pathogenesis in AATD by contributing to monocyte activation and generation of a yet to be characterised, cytokine and protease response.

To investigate this, the following objectives were set out:

- 1) To establish whether treatment of a monocyte like cell line (U937 cells) with C3d induces production of pro-inflammatory cytokines.
- 2) To gain an overview of the type of cytokine and protease responses generated by monocytes in response to C3d.
- 3) To assess if the complement activation product C3d may be contributing to the pathogenesis of AATD via the production of specific cytokines and proteases.

## **4.2 Assessing production of the pro-inflammatory cytokine IL-8 by U937 cells in response to treatment with C3d**

### **4.2.1 Background and rationale**

Preliminary experiments for this work package were carried out using monocyte-like U937 cells. In the following experiments U937 cells were used to refine our cell treatment protocol and to gain insights into what kind of cytokine response may be generated by circulating monocytes in response to C3d. A literature review was performed to select which specific cytokine output should be quantified by ELISA. We aimed to identify a cytokine that would be clinically relevant either through its role in the pathogenesis of AATD or as a therapeutic target.

Unpublished work by Fee and colleagues suggested that the pro-inflammatory cytokine IL-8 might represent a reasonable starting point for this work package(188). Fee previously described increased production of IL-8 by neutrophil like THP-1 cells in response to C3d. Previous studies have shown that IL-8 acts as a potent neutrophil chemoattractant and is known to be produced by monocytes and alveolar macrophages in response to pro-inflammatory stimuli(380). Levels of IL-8 have also been shown to be increased in the sputum of healthy individuals with who are heterozygous for the Z mutation(375). Concentrations of IL-8 in this cohort are comparable to those seen in COPD rendering it a compelling target for this study.

The decision to pursue IL-8 as an output from cells exposed to C3d was further bolstered by the Carroll and colleagues who have previously shown that ZZ monocytes produce increased levels of IL-8 in response to LPS than healthy MM controls(299).

Considering these observations, it was decided to assess whether monocyte-like U937 cells altered their production of IL-8 following exposure to C3d.

#### **4.2.2 U937 treatment with C3d and choice of control**

Culture and treatment of U937 cells is outlined in greater detail in Chapter Two. For this experiment concentrations of C3d used were in the range of 1-10 $\mu$ g/ml. These concentrations were selected as they are representative of levels of C3d detectable in the circulation of those with ZZ AATD(78). LPS was included as a positive control as U937 cells have previously been shown to produce IL-8 in response to LPS(381). Enzyme linked immunosorbent assay (ELISA) was used to quantify levels of IL-8 in supernatants of cells treated with C3d for 24 hours.

#### **4.2.3 Overview of results**

Figure 4.1 depicts the change in IL-8 production by U937 cells in response to C3d treatment (n=6) over 24 hours. These results show no significant change in IL-8 secretion between untreated U937 cells and those exposed to C3d over the range of concentrations used (1-10 $\mu$ g/ml) ( $p=0.6274$  at concentration of 5 $\mu$ g/ml).

LPS at a concentration of 1 $\mu$ g/ml worked well as a positive control and significantly increased production of IL-8 by U937 cells ( $p=0.0033$ ). This concentration was chosen as it had been previously used in published experimental protocols involving the use of U937 cells(382).

### U937 production of IL-8 in response to C3d

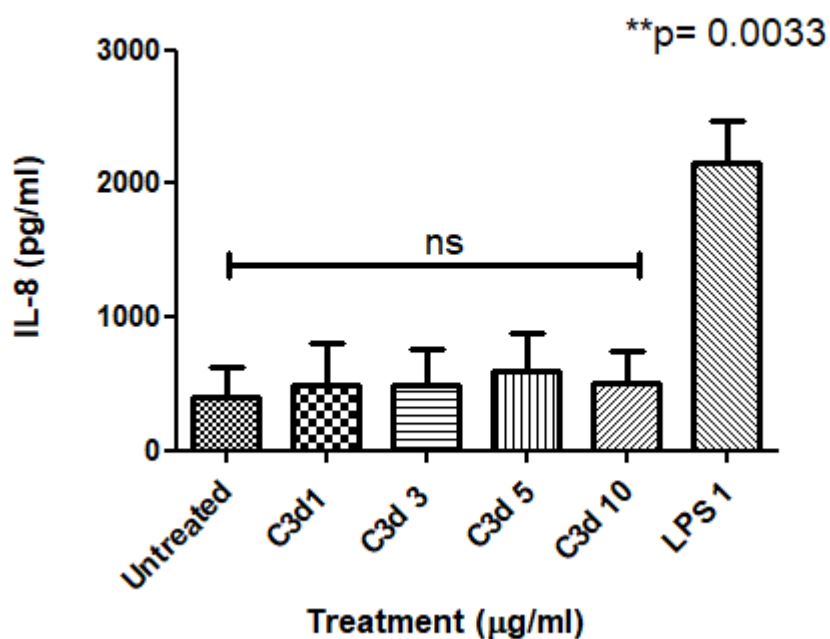


**Figure 4.1 Measurement of IL-8 production by U937 cells in response to C3d as determined by ELISA.**

Levels of IL-8 were measured in supernatants of U937 cells exposed to increasing concentrations of C3d by ELISA (n=6). Treatment with C3d 1-10µg/ml did not significantly increase production of IL-8. Treatment with LPS (1µg/ml) increased IL-8 production significantly (p=0.0033) Statistical analyses were performed using a paired t-test.

#### 4.2.4 Discussion of Results

Results shown here demonstrate that production of IL-8 by U937 cells in response to C3d does not change across the range of concentrations used (1-10 $\mu$ g/ml). Raw data suggested an upward trend in production of IL-8 production at a concentration of 5 $\mu$ g/ml but this difference was not statistically significant. This finding led us to question whether C3d was being used in sufficient concentrations to induce a response. The concentration of C3d in plasma and airways of those with ZZ AATD was between 5-40 $\mu$ g/ml suggesting that higher concentrations may be more representative of levels found in biological samples(78).

Despite the absence of a positive signal in U937 cells, ensuing experiments were designed to explore whether monocytes obtained from blood altered IL-8 production in response to C3d. As there are several key differences between U937 cells and circulating monocytes, we did not assume that the results obtained using U937 cells would be representative of the circulating monocyte response to C3d. Abrink et al(302) (1994) have previously used Northern blot analysis to demonstrate high levels of expression of MPO, NE, Cathepsin G, myeloblastin and azurocidin by U937 cells. These markers are characteristically expressed by immature monoblasts with lower levels of expression observed in mature circulating monocytes. The same group also identified low levels of lysozyme, CD14, MHC class II and AAT in U937 cells which are strongly expressed by mature monocytes. These observations confirm that whilst U937 cells are useful as a model for monocyte function, the response of U937 cells to C3d is not directly applicable to mature monocytes isolated from the circulation.

Considering this we decided to repeat this experiment using monocytes obtained from the circulation of healthy MM controls. The treatment protocol was modified to include a higher concentration of C3d (20µg/ml). However, as higher concentrations of C3d were used, we first needed to determine the effect of C3d on monocyte viability. To assess this, we next proceeded to perform an MTS assay.

## 4.3 Assessing the viability of peripheral circulating monocytes in response to C3d by MTS Assay

### 4.3.1 Background

U q Ó! ã ^ } Á æ} å Á & [ | | ^ æ\* ~ ^ • Á @æå Á å ^ { [ ] • c ! æc ^ å Á • ã \* }

between plasma (median 5µg/ml) and BAL (40µg/ml) samples of those with ZZ AATD(78). In consideration of these we wanted to expose monocytes obtained from the circulation to different concentrations of C3d falling within this broad range. It was recognised early on in this project that if we were to begin to expose cells to C3d protein we first needed to determine whether C3d could be cytotoxic to monocytes inducing cell death or apoptosis. MTS assays do not distinguish between cell loss attributable to apoptosis or necrosis so any loss of cell viability could theoretically be attributable to either effect.

Though spontaneous apoptosis is well described in monocytes we felt the probability of C3d causing apoptosis was relatively low(383). Previous studies have shown that apoptosis is inhibited following exposure of monocytes to pro inflammatory stimuli ã } & | ~ å ã } \* Á Š Ú ù Ê (Á84)POC monocytes. Concern was the risk of cell necrosis at higher C3d concentrations. Determining cell viability following C3d treatment was imperative as high rates of cell death would affect the reliability and interpretation of subsequent ELISA work.

In respect of this, monocyte viability in response to incremental increases in C3d concentration was assessed using an MTS assay.

#### 4.3.2 Assessment of cell viability by MTS assay

Assessment of cell viability was performed using the CellTiter96 One Solution Cell Proliferation Assay. The One Solution reagent contains an MTS-tetrazolium compound that is bio-reduced by live cells into a coloured formazan compound. High levels of formazan, as indicated by a strong colour change in the sample/reagent solution suggest high levels of metabolic activity by viable cells(385). These properties allow for assay of cell viability by comparing absorbance at 490nm with a 96 well plate reader.

Ø[ | | [ , ã } \* Á c @^ Á { æ} ~ ~ æ& c ~ | ^ | q • Á ã } • c | ~ & c ã [ } • Ê Á G  
treated samples and transferred to a 96 well plate. Samples were then made up to a final volume of 100µl by the addition of 50µl of their respective media (serum free, 1% (v/v) FCS or 10% FCS (v/v)). 20µl of cell titre reagent was added to each well to give a final concentration of 317µg/ml of MTS. The plate was covered with tinfoil to protect from light and incubated at 37°C for 4h in a 5% CO<sub>2</sub> atmosphere. 25µl of 10% (w/v) SDS was added at 4h to prevent any further reaction. Absorbance at 490nm was determined by spectrophotometry (Spectramax M3, Molecular Devices, USA).

#### 4.3.3 Results of MTS Assay

Figure 4.2 shows absorbance at 490nm in cells treated with C3d relative to absorbance of untreated cells. Absorbance at 490nm is used as a surrogate marker of formazan production by metabolically active cells. Levels of metabolic activity did not differ significantly between treated and untreated cells confirming no loss of viability during the 24h treatment period. C3d used at 10µg/ml is representative of

plasma concentrations observed in ZZ AATD. C3d at a concentration of 40µg/ml has been previously detected in ZZ BAL samples(78). Higher concentrations were included in this protocol following the observation made in chapter one that monocytes and macrophages from BAL samples are also known to express CR2 and may be susceptible to the effects of C3d.

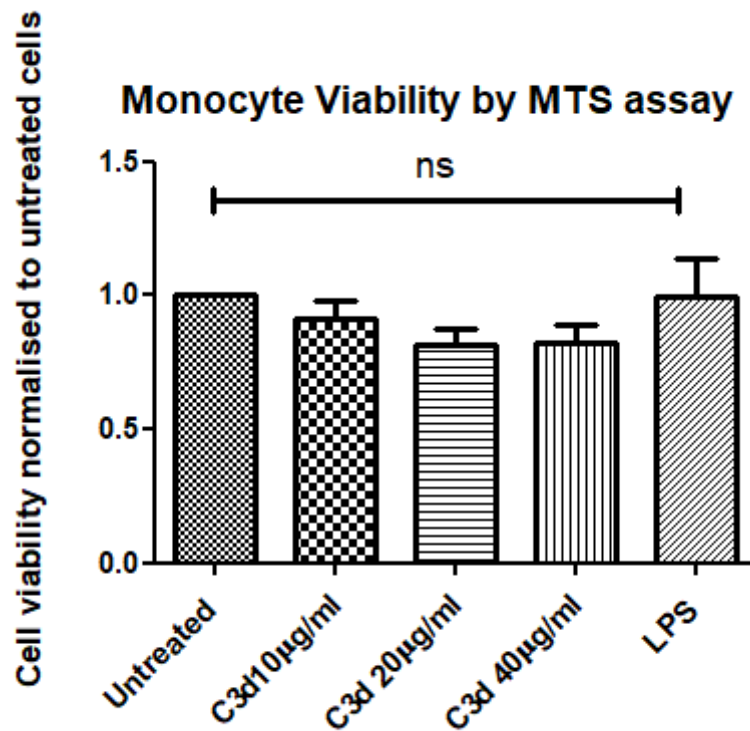


**Figure 4.2: Assessment of cell viability measured by MTS assay**

Monocytes obtained from circulation (n=8) were exposed to increasing concentrations of C3d for 24 hours. Cells were added to MTS reaction reagent and absorbance read at 490nm. Statistical analyses were performed using a paired t-test. A p value of <0.05 was considered significant.

#### **4.3.4 Discussion of impact of C3d on monocyte viability**

Confirmation that treatment with C3d did not affect monocyte viability was imperative before proceeding to further ELISA work. Loss of cell viability over 24h may have influenced ELISA results potentially leading to false signals that were attributable to cell death rather than a true effect of C3d. This was particularly important as this project involved the use of monocytes which are known to be highly susceptible to apoptosis and cell death(386, 387).

Previous studies have shown that monocytes are highly vulnerable to genotoxic stress. Studies comparing monocyte, monocyte derived macrophages and neutrophils have shown impaired DNA repair mechanisms in the former(388).

Ponath et al have demonstrated that monocytes but not macrophages stimulated by PMA undergo apoptosis that is attributable to ROS production and accumulation of DNA single strand breaks(389). Monocytes that are stressed or undergoing non-apoptotic cell death show loss of membrane integrity, disruption of phagolysosomes and activation of caspase 2(387). When functionally exhausted, dying monocytes down regulate their production of ROS and cytokine responses and thus inclusion of large numbers of dying or dead cells in our analyses was likely to skew results. In contrast to the propensity of monocytes to undergo cell death, monocyte derived macrophages are DNA repair competent and more adept at resisting genotoxic stress(389).

The MTS assays presented here confirm that the viability of monocytes treated for 24h in the presence of C3d remains similar to untreated cells. The results of these MTS assays assured us that monocytes were unlikely to be dying or undergoing apoptosis in response to C3d even at higher concentrations.

Having established no loss of cell viability we next proceeded to explore whether monocyte production of IL-8 changed in response to C3d treatment.



and IL-18. Binding of C3a to its target receptor C3AR1 has been implicated in neutrophil chemotaxis(399), degranulation(400), superoxide anion production, and bacterial opsonization. Like C3d, C3a is a complement fragment and is one of the main cleavage products of C3. The observation that the complement fragment C3a enhances IL-8 production in other cell types prompted us to investigate whether comparable effects might be observed following the treatment of monocytes with C3d.

Despite initial results demonstrating a lack of IL-8 production by U937 cells in response to low concentrations of C3d, we rationalised that in view of the critical role IL-8 plays in driving lung diseases, establishing whether C3d induced IL-8 production by circulating monocytes was a clinically important question.

#### **4.4.2 Monocyte treatment with C3d and recovery of supernatants**

Monocytes from healthy MM individuals were isolated as described in Chapter Two.  $1 \times 10^6$  cells were seeded to each culture well and incubated in the presence of C3d at 0, 5, 10 or 20 $\mu$ g/ml. As preliminary experiments using U937 cells were showed no significant effect of C3d on IL-8 production up to a concentration of 10 $\mu$ g/ml the range of treatment dosage was expanded to include samples incubated with 20 $\mu$ g/ml. Monocytes treated with LPS were included as a positive control in view of previous observations that monocytes stimulated with LPS produce IL-8(401). Cells were treated for 24 hours, centrifuged and the supernatants aspirated. Supernatants were stored at -80°C for use in subsequent ELISAs.

#### **4.4.3 Summary of Results**

ELISA results presented in Figure 4.3 show levels of IL-8 detectable in the supernatants of all reactions, n=5. Monocytes in culture for 24h have previously been shown to release IL-8(402), accounting for the levels of IL-8 seen in the supernatants of untreated cells.

Monocytes treated with increasing concentrations of C3d, ranging from 5-20µg/ml, demonstrated a trend towards increased IL-8 production, but this did not reach significance ( $p=0.7302$  at 5µg/ml,  $p=0.0834$  at 20µg/ml). Monocytes treated with LPS (1µg/ml) showed a significant increase in keeping with published data(299) ( $p=0.0199$ ).

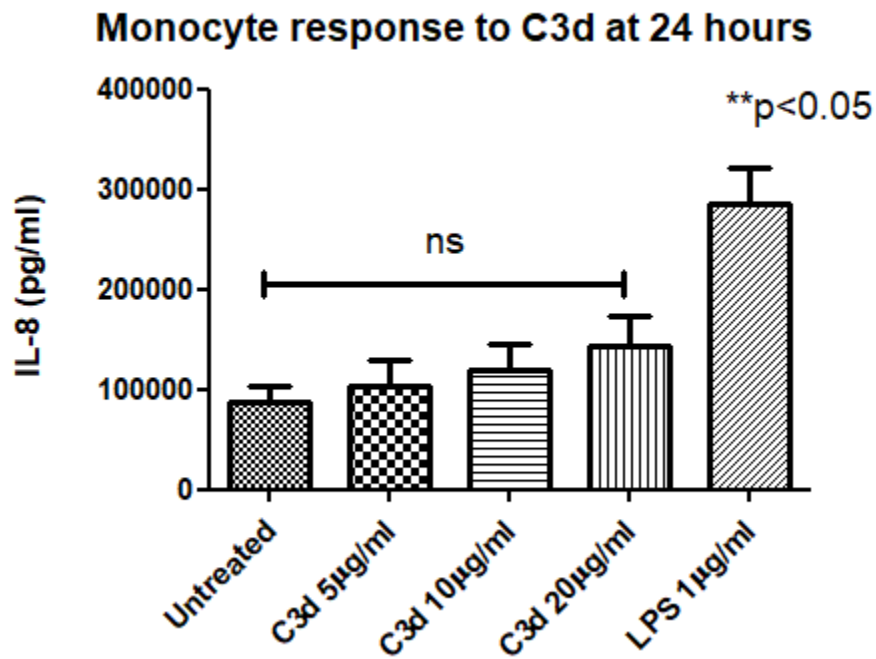


**Figure 4.3 Measurement of IL-8 production by healthy control monocytes in response to treatment with C3d by ELISA.**

There was no significant increase in IL-8 levels across all concentrations of C3d examined. Treatment of monocytes with LPS resulted in a significant increase in the levels of IL-8 detectable in supernatants ( $p<0.05$ ). Analyses were performed using a one-way ANOVA and Dunnetts multiple comparison test.

#### 4.4.4 Discussion of the effect of C3d on IL-8 production by MM monocytes

At the time of these experiments, we were attempting to generate hypotheses that might help guide the direction of the project. As the foundational work done

] ~ à | ã • @^ å Á àa1 had identified high levels of C3d in ZZ AATD, the intention behind these experiments was to investigate first for an effect in healthy MM controls before expanding to include patient samples. As previously alluded to, IL-8 was a compelling target for this study in view of the well described role it plays in AAT lung disease.

The results obtained did not demonstrate a significant increase in IL-8 production by MM monocytes exposed to C3d. This early finding prompted us to pause and refocus attention on ascertaining what kind of cytokine profile was likely to be produced by monocytes in response to an inflammatory trigger. As the profile of cytokines elaborated by monocytes is extensive, we aimed to identify a subset of cytokines to target for measurement by ELISA. We determined that the ideal approach to help guide the project direction would be to examine supernatants of cells treated with C3d for multiple cytokines, simultaneously. If this could be achieved, we could then identify target analytes for measurement by ELISA that were of particular relevance in AATD. It was in this context was we next applied the supernatants of untreated and cells treated with 10µg/ml of C3d to cytokine array membranes (Ray Biotech).

## 4.5 Profiling the cytokine response of monocytes to C3d using cytokine array membranes

### 4.5.1 Background

In order to identify suitable targets for future ELISA work we first required an overview of the type of cytokine response monocytes were likely to generate when exposed to C3d. The relationship between cytokine response and C3d exposure is complex, involving multiple pathways and factors. Developing methods that allow for simultaneous detection of cytokines, proteins, extra cellular matrix proteins and growth factors encoded within the genome of different cell types. Exploring relative expression of each set of molecules offers unique opportunities to understand molecular interactions between cells. Historically, simultaneous measurement of multiple cytokines has been performed using SDS PAGE coupled with mass spectrometry(403). Other techniques described in the literature include the use of microsphere-based immunoassays and flow cytometry(404). Though effective even when low sample volumes are used, both strategies are labour intensive and demand proficiency to ensure reliability and reproducibility of results.

Recent advances in miniaturisation, fluidics and lithography have led to the development of commercially available multiplexed arrays for the simultaneous measurement of multiple cytokines. During array manufacturing, photolithography is used to print capture antibodies directly on to the surface of an array membrane(405). In a manner analogous to an ELISA, samples and paired biotinylated detect antibodies and streptavidin HRP are then added generating spots of signal on the membrane that correspond to different analytes. Comparisons between samples can then be performed using densitometry which allows semi-quantitative comparisons between various cytokines.

In view of the technical simplicity of array membranes, commercial availability, and the capacity to rapidly perform a large-scale assessment of protein expression, we decided to apply supernatants from monocytes treated with C3d to array membranes. The aim of this experiment was to achieve an overview of the C3d monocyte cytokine response in order to focus future ELISA work.

#### 4.5.2 Methods

These experiments were performed using the RayBio C-Series Human Cytokine Antibody Array. This array can be used for the semi-quantitative detection of up to 174 human proteins in cell culture supernatants and other liquid samples. As described in Chapter Two monocytes were isolated from the circulation of people with ZZ AATD and healthy MM controls. Monocyte isolation was performed using the EasySep CD14 selection kit without CD16 depletion.  $1 \times 10^6$  cells were seeded to culture wells and treated with C3d at a concentration of  $10 \mu\text{g/ml}$ . Supernatants were

c @^ } Á @æ! ç ^ • c ^ å Á æ} å Á æ] ] | ã ^ å Á c [ Á c @^ Á { ^ { à ! æ} ^ Á æ

The density of each cytokine spot present on the membrane was measured using Lab Image software and background signal from negative controls subtracted to give the mean volume density. Positive reference spots on each membrane were used to normalise signal response and allow comparisons of results across multiple arrays.

#### 4.5.3 Summary of Cytokine Array Results

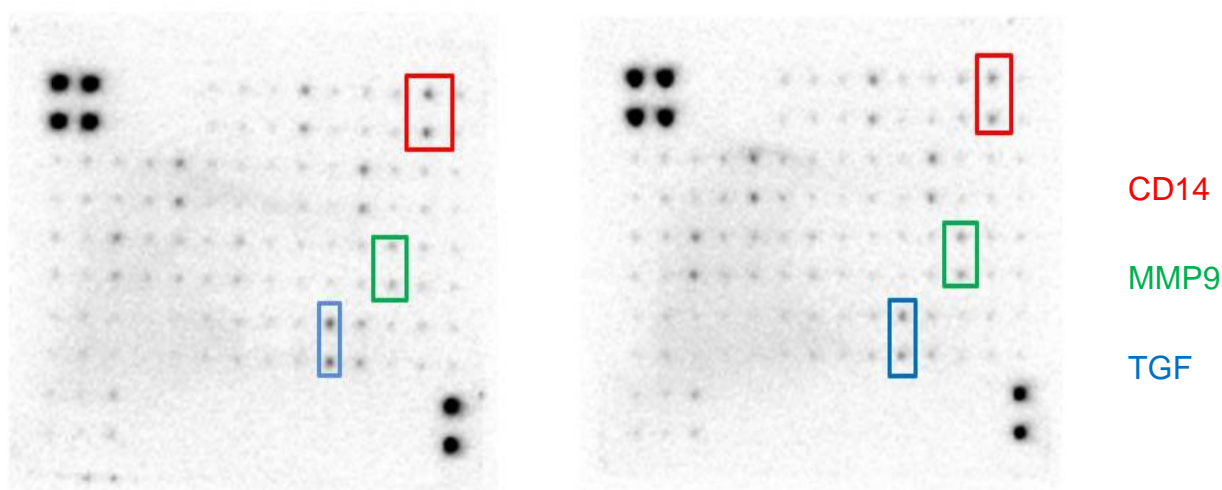
Supernatants of monocytes treated with C3d and untreated monocytes contained detectable levels of CD14, MMP-9, MMP-13, TGF alpha, TGF beta, Fas ligand (n=3).

Signal for TGF alpha, ICAM2, CXCL-16 and IL-9 were found to have the highest levels of expression in both treated and untreated monocyte supernatants. No significant differences were detected between groups for these 3 cytokines and chemokines.

statistically significant (p values 0.4576 and 0.4869 respectively).

**A. Untreated Monocytes**

**B. Monocytes with C3d 10µg/ml x 24hrs**



**C.**

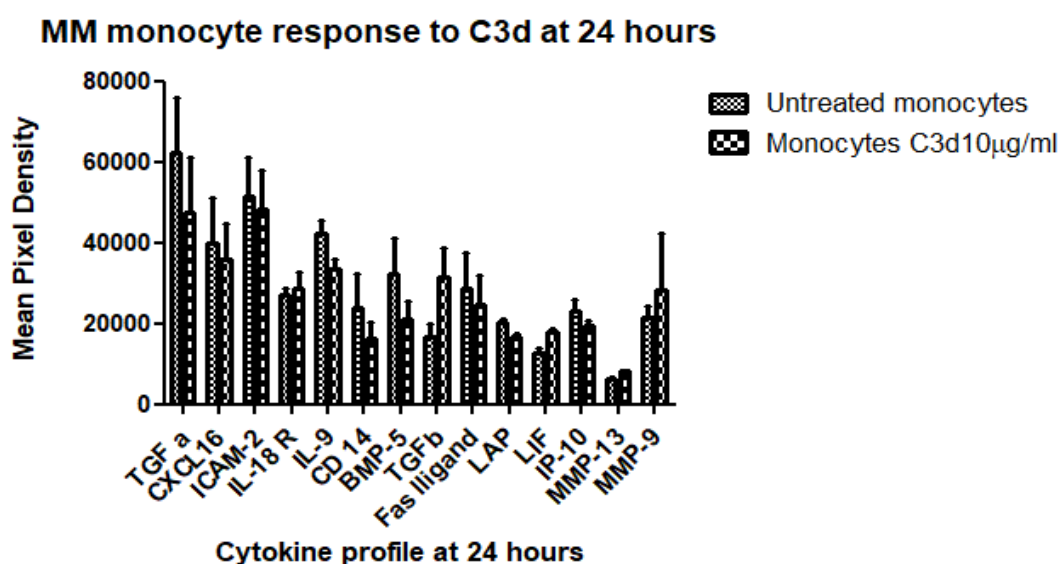


**Figure 4.4 Cytokine expression by MM monocytes in response to C3d assessed by cytokine array membranes and densitometry.**

**Panel A and B** show array membranes from untreated monocyte supernatants and those exposed to C3d at a concentration of 10µg/ml. **Panel C** depicts results of densitometry analysis. Treatment with C3d correlated with trend towards decreased expression of several cytokines. This trend was not statistically significant. Statistical analysis was performed using a one way analysis of variance (ANOVA). n=3.

#### 4.5.4 Discussion of cytokine array results

These experiments demonstrate the usefulness and limitations of antibody arrays for the analysis of multiple cytokines and proteins. Arrays can detect very low levels of a target analyte and combines the specificity of ELISAs with the sensitivity of chemiluminescence assays(406). The limitations of arrays are articulated by Tutinen et al (2004) who note that the although relative levels of cytokine expression correlate well with actual levels quantified by ELISA, the relationship between chemiluminescent signal and quantity is not linear(407). For this reason, despite the cytokine arrays used in these experiments working well to demonstrate the profile of cytokines and proteins generated by monocytes in response to C3d further experiments confirming the results were necessary.

As the arrays generated a large amount of data, we needed to identify which outputs were likely to be of relevance to this project. For example, though high levels of transforming growth factor alpha (TGF- $\alpha$ ) in monocyte supernatants, a review of the literature suggested that TGF alpha may not be the most relevant to a project focusing on elucidating the mechanisms underlying the pathogenesis of AATD lung disease. TGF alpha is a member of the epidermal growth factor family and acts as a mitogenic polypeptide. Published data has linked TGF alpha to the development of gastric and intestinal metaplasia(408) , tumour development(409) and congenital abnormalities such as cleft palate(410). Out of the results presented here we decided to pursue further investigation of the monocyte surface marker CD14 and the matrix metalloproteinase MMP-9.

As discussed in Chapter One CD14 is an LPS co-receptor expressed on the surface of monocytes(411). As the samples used here are monocyte supernatants, the CD14 identified by the array represents soluble CD14. sCD14 can be generated via a

number of mechanisms including cleavage from the cell surface(412), release of intracellular stores(169) or de novo protein synthesis(413). Increased levels of sCD14 have been shown to associated with decreased lung function in healthy agricultural workers. Stratification of this cohort by an underlying diagnosis of COPD and smoking history confirmed that high levels of sCD14 (>median plasma values) were associated with lower lung function amongst ever smokers with COPD(414). Detection of higher levels of sCD14 by the arrays as shown here, may also reflect, cleavage of mCD14 raising the possibility of a shift in the phenotype of monocytes in response to C3d.

Within monocytes high levels of CD14 expression are used to identify the classical and intermediate subsets(329). Maintaining the proportional representation of each subset is of clinical importance a shift in the balance between monocyte subsets has been demonstrated in several disease states. Changes in COPD monocytes suggest that monocytes in those with more severe disease express a phenotype that primes them towards mobilisation to the lungs(164). Cornwell et al (2018) have previously shown increased numbers of classical (CD14++) monocytes in the circulation of those with advanced disease(164). Additional expression of the chemokine receptor CCR2, which is restricted to CMs facilitates recruitment of CD14++ monocytes to the site of tissue injury where differentiation into alveolar macrophages occurs(160). This creates a bias towards a destructive pro inflammatory phenotype. Misharin et al (2017) have demonstrated similar findings in patients with idiopathic pulmonary fibrosis and showed that CD14++ classical monocyte counts are predictive of mortality in IPF(415). Considering these observations, we decided to confirm this result using an ELISA for CD14.

The second chosen target for measurement by ELISA was MMP-9. Though expression of MMP-9 did not change significantly based on array results, an extensive evidence based has linked MMP-9 to the development of lung disease. Furthermore, the number presented here is low (n=3) and also does not involve the use of supernatants taken from ZZ monocytes. Thus, whilst the array results are informative and facilitate the generation of hypotheses, they should not be viewed as gold standard test for measuring the cytokine response by monocytes to C3d.

As discussed in chapter one, the MMPs represent a family of 25 different secreted and membrane bound enzymes that are zinc and calcium dependent(416).

Collectively, MMPs can degrade most components of the extra cellular matrix. In addition to proteolysis, MMPs contribute to the regulation of many non-ECM proteins including cytokines, chemokines, other MMPs and serine proteinase inhibitors(417, 418). MMPs regulate both physiological and pathological processes. Under homeostatic conditions MMPs play a role in normal embryogenesis(419), bone development(420) and angiogenesis(421).

Matrix Metalloprotease 9 (MMP-9) is a 92kDa type 4 collagenase produced by monocytes and macrophages amongst other cells types(224)-. MMP-9 is released as a pro-form and following release to the extra cellular milieu is activated by proteases such as NE(412). The array membrane used in these experiments is known to detect the pro-form and active MMP-9. Together with NE, MMP-9 controls neutrophil migration across the basement membrane (BM)- a process that is dependent on degradation of BM constituents(422).Wells et al (2018) have previously shown that elevated plasma levels of MMP-9 were associated with increased risk of COPD exacerbations in 2 large COPD cohort trials(423). Omachi and colleagues (2011) demonstrated a similar finding in those with COPD

attributable to AATD. They identified plasma levels of MMP-9 as being predictive of worsening lung density ( $p=0.003$ ) and increased exacerbation frequency ( $p=0.003$ ).

If C3d does indeed alter MMP-9 production by monocytes in the circulation and airways it may prove to be a useful biomarker to identify high risk patients with a frequent exacerbation phenotype. This is of particular relevance in COPD where exacerbation frequency is a predictor of mortality(424). In light of these observations we felt further exploration of a link between C3d and MMP production by both MM and ZZ monocytes merited further investigation.

Our next aim was to explore using ELISAs whether treatment of MM and ZZ monocytes altered production of sCD14 and MMP-9.

## 4.6 Measurement of CD14 production by MM compared to ZZ monocytes in response to C3d

### 4.6.1 Background

In the human circulation at least 3 monocyte subsets are identifiable by their relative expression of the surface markers CD14 and CD16(164). Delineation of subset type is important as published data suggests that each subset displays a different behaviour and function as reviewed in the introduction chapter and summarised in Table 1.1. Both classical (CM) and intermediate monocyte (IM) subsets are known to express high levels of the LPS co-receptor CD14 on their surface (CM >> IM).

Cluster of differentiation 14 (mCD14) is a glycolipid anchored glycoprotein found on the surface of cells of myelomonocyte lineage including monocytes, macrophages and select populations of granulocytes(168). CD14 lacks both a transmembrane and intracellular domain. As such it relies on forming a complex between lipopolysaccharide binding protein (LBP) and Toll-like receptor 4 (TLR4) to initiate cell signalling(425). LBP targets LPS aggregates and presents LPS monomers to CD14. Once complexed to TLR4, a number of intracellular signalling events are triggered including activation of the NF- $\kappa$ B pathway, leading to cytokine production(426). CD14 also recognises peptidoglycan from gram positive cells and binds to apoptotic cells to induce phagocytosis(427).

In addition to mCD14 two other forms of soluble CD14 (sCD14) are detectable in serum. sCD14 is generated via cleavage of mCD14 by serine proteases such as NE(412) or following release from intracellular monocyte stores(428). Following monocyte activation, mCD14 decreases and sCD14 increases(429). Shive and colleagues (2015) have previously identified levels of sCD14 as a surrogate marker

of monocyte activation(429). They demonstrated that in addition to LPS, flagellin and CpG oligodeoxynucleotides, IL-6 and IL-1

The results of cytokine array experiments suggested that C3d may alter the expression sCD14 by monocytes. We hypothesised that C3d may induce monocyte activation and subsequent alterations in the expression of sCD14.

#### **4.6.2 Methods: ELISA for CD14**

Monocytes obtained for use in this experiment were isolated using the EasySep Monocyte CD14 kit without CD16 depletion. This negative selection kit isolated cells that express both CD14 and CD16 and thus is more representative of a spread of monocyte populations. Monocytes were treated with C3d as described in Chapter Two: Materials and Methods. Following treatment, supernatants were recovered and stored at -80°C for future use. Supernatants were run in duplicate and CD14 concentration determined by interpolation from a standard curve as presented in Chapter Two.

ELISAs for CD14 using a pre-coated plate (Abcam SimpleStep ELISA kit). Our analyte in this case was CD14 in monocyte supernatants and thus represented levels of soluble CD14 only.

#### **4.6.3 Summary of CD14 ELISA results**

Increased levels of CD14 were detectable in the supernatants of monocytes treated with C3d at a concentration of 40µg/ml and those treated with LPS at a concentration of 100ng/ml. A trend towards an increase was seen in cells treated with 20µg/ml but the result did not achieve significance within or between MM and ZZ groups. Of note

c @^ • ^ Á | ^ ç ^ | • Á [ ~ Á Ô H å Á æ! ^ Á & [ { ] æ! æà | ^ Á c [ Á | ^ ç ^ | •

BAL samples of individuals with ZZ AATD.

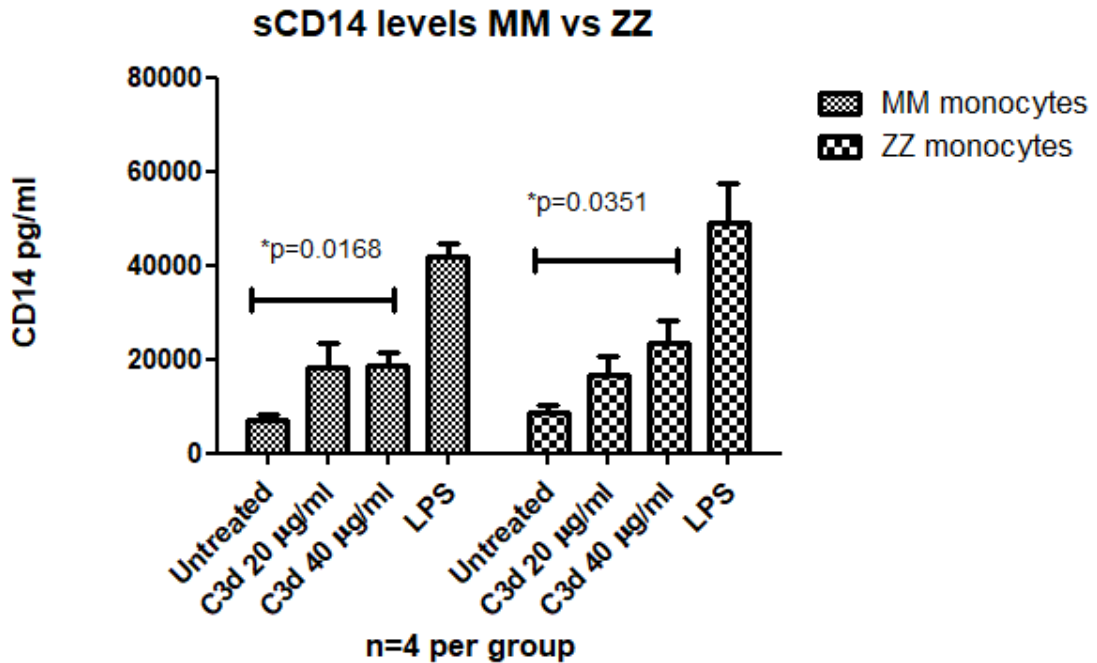


**Figure 4.5: ELISA for sCD14 in the supernatants of monocytes treated with C3d.**

Treatment with 40 µg/ml C3d correlated with significant increases in levels of sCD14 detectable in monocyte supernatants in both groups. No significant differences were identified between MM and ZZ groups. N=4 subjects per group examined. Statistical analyses were performed using a paired t-test (within groups) and ANOVA (between MM and ZZ groups). A p value <0.05 was considered significant.

#### 4.6.4 Overview of effect of C3d on sCD14 production by ZZ and MM monocytes

The observation that C3d increased the levels of sCD14 in these experiments is of interest for several reasons. High levels of sCD14 have previously been shown to confer LPS responsiveness to cells that are not otherwise known to react to LPS thereby driving a dysregulated inflammatory response(430, 431). The origin of the sCD14 seen here is not entirely clear. Previous studies have confirmed that CD14 can be cleaved from the monocyte surface via serine and cysteine proteases.

Studies of monocyte phenotypes in autoimmune hepatitis and pancreatitis have demonstrated a role for the MMP ADAM17 in mediating cleavage of surface bound CD14(432). Waller et al (2019) have previously reported that shedding of CD14 and

which acts to inhibit the action of ADAM17. This is notable as AAT is also known to

i) relative protease abundance, we hypothesised that if protease mediated cleavage is

entirely responsible for the effect shown here, differences between MM and ZZ

groups would have been more readily apparent. An alternative explanation for the

source of sCD14 presented here is the release of intracellular stores of CD14.

Studies using confocal microscopy have previously identified large intracellular

stores of CD14 in monocytes suggesting biologic plausibility(169).

In view of the capacity of sCD14 to confer LPS responsiveness to adjacent cells, it

raises the question of whether the increase in sCD14 attributable to treatment with

C3d is convert a non-CD14+ monocyte towards a CD14+ monocyte towards an LPS response intermediate or classical phenotype. The phenomenon of monocyte subset

switching has previously been described in mice and humans(434). If this were to

prove to be the case, the finding is of relevance in AATD as this pro-inflammatory phenotype switch is potentially remediable with the administration of AAT augmentation therapy. AAT has previously been shown to reduce CD14 and TLR4 expression in monocytes treated with LPS suggesting that AAT may play a role in preventing excessive monocyte activation(166).

Having confirmed that C3d appears to alter monocyte expression of CD14 we next proceeded to evaluate whether C3d altered the expression of MMP-9. To assess this, we performed an ELISA for MMP-9 on the supernatants of MM and ZZ monocytes treated with C3d.

## **4.7 ELISA for MMP-9 in the supernatants of monocytes treated with C3d**

### **4.7.1 Background**

Results of cytokine arrays suggest that monocytes in culture for 24h secrete MMP-9. Although only a trend towards change was noted between untreated monocytes and those treated with C3d it was decided that in view of the established link between MMP-9 and lung disease, further experiments would be undertaken to investigate the interplay between C3d and monocyte production of MMP-9. Of note, despite its inclusion on the array, MMP-9 (also known as gelatinase B) is not a cytokine. It is a member of the MMP family (discussed in detail in Chapter One: Introduction). Its substrate base is broad and includes type IV, V, VII, X and XIV collagen, gelatin, elastin, pro-MMP-9 and -13(435).

Examining the interplay between C3d and metalloproteases is of value as MMPs are known to contribute to the pathogenesis of emphysema through both direct and indirect mechanisms(436, 437). MMP-9 is of particular interest as it has been shown to propagate inflammation within the lungs through degradation of the extra cellular matrix, neutrophil chemotaxis and augmentation of the inflammatory response(224). Each of these features taken individually are key components of an acute exacerbation of COPD (AECOPD). Wells and colleagues (2018) have previously shown that elevated plasma levels of MMP-9 are independently associated with the risk of exacerbation in COPD(423). The importance of this observation cannot be underscored enough as the frequency of exacerbations is now recognised to be a stronger predictor of mortality in COPD than lung function as measured by FEV1(424).

U q Ó! ã ^ } Á æ} å Á & [ | | ^ æ\* ~ ^ • Á @æç ^ Á ] ! ^ ç ã [ ~ • | ^ Á & [ ! ! ^ severity of emphysema in AATD(78). Production of MMP-9 by monocytes is well described and has been previously shown to be ^ } @æ} & ^ å Á(212) Á khbwØ driver of disease pathogenesis in AATD and COPD(433). We questioned whether C3d might be influencing monocyte production of MMP-9 in a similar way and elected to proceed with ELISAs for MMP-9 in the supernatants of C3d treated MM and ZZ monocytes.

#### 4.7.2 Methods: Measuring MMP-9 in monocyte supernatants

ELISAs for MMP-9 were performed using the MMP-9 DuoSet ELISA kit from R&D systems. In view of the well-recognised propensity for monocytes to produce large amounts of MMP-9 we performed several preliminary runs to ascertain the optimal dilution factor. All supernatants were diluted 1/200 in reagent diluent to ensure final absorbance readings fell within the range of the standard curve. As per the

{ æ} ~ ~ æ& c ~ ! ^ ! q • Á ã } • c ! ~ & c ã [ } • Ê Á æ| | Á ã } & ~ à æc ã [ } Á temperature and 3 sequential washes using PBS Tween (0.05%v/v) were performed between addition of antibodies, samples, streptavidin and TMB substrate.

#### 4.7.3 Summary of MMP-9 ELISA results

Results of ELISAs for MMP-9 confirmed an increase in MMP-9 production by monocytes in response to C3d.

Higher levels of MMP-9 were detectable in untreated ZZ monocytes compared to MM control cells (p=0.0270). Within the MM group, treatment with C3d at a concentration of 20µg/ml significantly increased production of MMP-9 (p=0.0270). At

the same concentration, production of MMP-9 by ZZ monocytes showed a trend towards increased MMP-9 production but this result did not achieve significance.

Both groups demonstrated a significant increase in detectable levels of MMP-9 at a concentration of 40µg/ml. LPS was use as a positive control (1µg/ml) and increased MMP-9 production significantly in both groups.

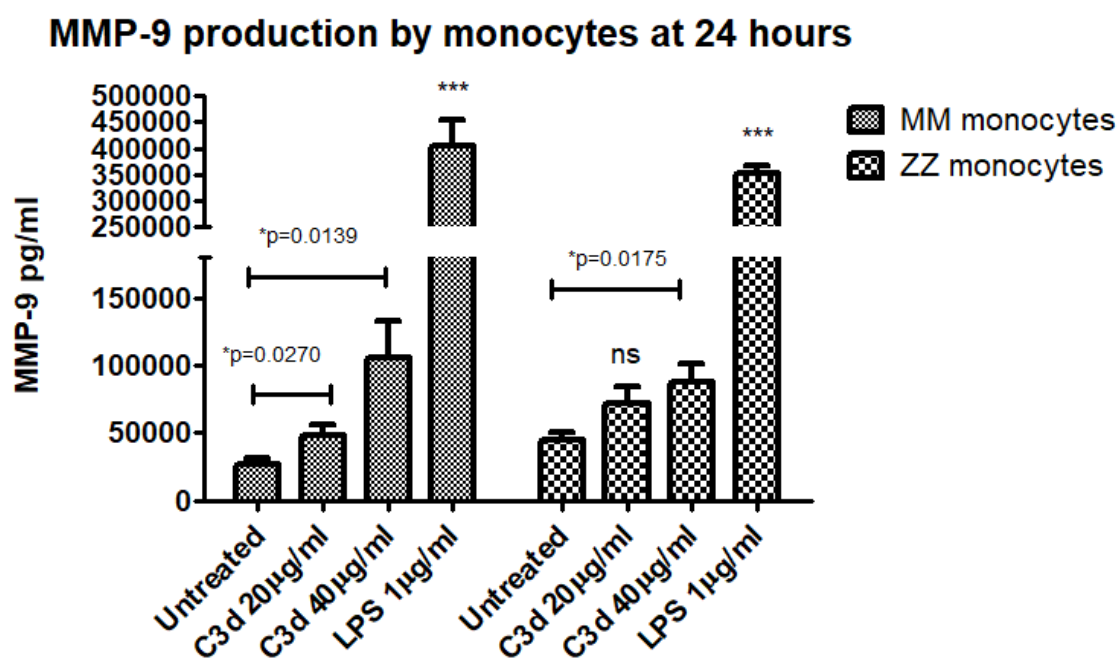


**Figure 4.6: ELISA for MMP-9 in the supernatants of monocytes treated with C3d.**

Treatment with 40 µg/ml C3d resulted in significant increases in levels of MMP-9 detectable in monocyte supernatants in both MM healthy control and ZZ . AATD patients. N=6 subjects per group examined. Changes within groups were tested for significance using a paired t-test. Comparison between means of MM and ZZ groups was performed using a one way ANOVA,

#### **4.7.4 Implications of results**

Results shown here suggest that monocytes exposed to C3d produce increased levels of MMP-9. This is notable as AAT has previously been recognised as a substrate of MMP-9. Using a mouse model Liu et al (2000) showed that MMP-9 amplifies the protease effects of NE by inactivating AAT(438).

The role MMP-9 plays in driving inflammation has been studied across a range of diseases. Within the lungs MMP-9 has been conclusively linked to the development of emphysema. Multiple studies have linked higher circulating levels of MMP-9 to worsening lung function and increased exacerbation frequency in COPD. As lung function and exacerbation frequency are recognised predictors of mortality in COPD, exploring factors driving increases in MMP-9 are necessary to fully understand disease pathogenesis.

Omachi and colleagues have previously examined the role of MMP-9 as a predictor of outcomes in AATD(223). They examined data from patients with the PiZ and null AAT mutations who were not on augmentation therapy. They found higher levels of plasma MMP-9 correlated with more severe airflow obstruction and impairment of gas exchange as measured by DLCO. In longitudinal analyses they found that increases in MMP-9 predicted further declines in DLCO underscoring its usefulness as a biomarker of lung disease. Furthermore, longitudinal observations persisted after having corrected for total white cell count and C- reactive protein (CRP). This suggests that the predictive value of MMP-9 is not merely reflective of its role as a non-specific marker of inflammation.

Production of MMP-9 by monocytes and macrophages is well described. Lu and Wahl (2005) have previously demonstrated that activation of monocytes following exposure to LPS, stimulates production of MMP-9 via activation of the NF-KB pathway(217). Other pro inflammatory stimuli such as TNF alpha also enhances MMP-9 production via the prostaglandin E2 pathway(218). The observation that C3d increases MMP-9 production suggests that C3d activates monocytes. The signalling mechanisms underlying this activation are at present, unclear.

Identification of MMP-9 as a product of C3d treatment of monocytes prompted further interest in exploring what other proteases may be produced by monocytes exposed to C3d. Published studies provide a wealth of insight into the role neutrophil derived proteases play in the progression of lung disease in MM COPD and also COPD occurring in the context of ZZ AATD. Comparably little has been written about the contribution monocytes make to the protease burden in lung disease. To clarify this, we decided to run repeat array experiments with some alterations to the protocol. We identified a protease array membrane (R&D Systems) capable of simultaneous detection of 36 proteases. We next proceeded to use this to get an overview of the protease response produced by both MM and ZZ monocytes in response to C3d.

## 4.8 Profiling the protease response of MM and ZZ monocytes to C3d using protease array membranes

### 4.8.1 Background

Proteases within the lung play key roles in health and disease. Several different types of proteases have previously been found to be detectable in BAL samples from human lungs. Broadly speaking proteases cleave proteins into polypeptides or amino acids. Sub types of proteases are identifiable by the expression of different catalytic sites. Serine proteases, cysteine proteases, metalloproteases and aspartic acid proteases(197). Further detail on the role of proteases in health and disease is provided in Chapter One.

Under homeostatic conditions proteases are necessary to regulate tissue regeneration and repair. However, diseases such as AATD and CF reflect an imbalance between protease and anti-protease activity. The former is characterised by low circulating levels of the serpin inhibitor AAT, permitting unfettered action of proteases such as NE that degrade the extra cellular matrix. In CF thick, tenacious mucus within the airways perpetuates cycles of infection and inflammation.

Production of cytokines such as the neutrophil chemoattractant IL-8 facilitates neutrophil recruitment to the lung(198). The cell population within epithelial lining fluid (ELF) becomes dominated by neutrophils (70% vs 1% in HC lungs(199)). Once activated, neutrophils produce proteases at a rate that exceeds the anti-protease capacity of available anti-proteases propagating tissue damage.

Unpublished data from the McElvaney lab has previously shown that C3d binding to the surface of ZZ neutrophil membranes correlates with increased release of primary (BPI), secondary (hCAP-18) and tertiary (MMP-9) granule products. This suggests

that C3d may play a role in the pathogenesis of ZZ AATD via the generation or secretion of excess proteases. The cytoplasm of neutrophils is densely packed with granules that act as reservoirs for membrane bound proteins, bactericidal and proteolytic enzymes(439). This unique feature of neutrophil biology means they are uniquely suited to rapid degranulation with release of proteases. Though monocytes @æç ^ Á @ã • c [ ! ã & æ| | ^ Á à ^ ^ } óŧ • q Á d @^ Á )Áæ { ^ Áã • Á Á æ Á { ãæ } cytoplasm of monocytes is known to possess fine granules(125). In a manner similar to the primary granules of neutrophils, monocyte granules take up the Azure A stain and store lysosomal enzymes such as MPO(125). Monocytes have been shown to retain the capability of augmenting production of granule proteins via novel protein synthesis(440). This later feature is lost in mature neutrophils.

Given the importance of proteases in disease progression in AATD and in the context of the observations of the neutrophil protease response to C3d, we elected to examine whether a similar effect may be seen in monocytes. As we had successfully used cytokine arrays membrane to obtain an overview of the monocyte cytokine response to C3d, we decided to use protease array membranes to direct protease work.

#### **4.8.2 Principles of protease arrays and methods**

These experiments were performed using the Proteome Profile human protease array kit (R&D Systems). Similar to the cytokine array described previously, this array membrane consists of nitrocellulose membranes imprinted with capture and control anti-bodies for 36 different human proteases.

Samples were mixed with the supplied cocktail of biotinylated detection antibodies and incubated overnight. Following washing, streptavidin and chemiluminescent detection reagents were added.

Images were obtained on the ChemiDoc and analysed using Image Lab software. A transparent protease template was overlaid on the membrane and aligned with referenced spots to ensure accurate identification of specific protease signals. Pixel density values were exported to Microsoft excel and the average signal of each pair of duplicate spots (representing individual proteases) was determined. Average background signal was calculated as the mean signal from negative controls included on the array and subtracted from final values. Positive reference spots imprinted on the arrays were used to normalise values to one single array allowing comparisons to be made between samples. Supernatants from untreated MM and ZZ monocytes were included in these experiments in addition to MM and ZZ monocytes treated with C3d.

#### **4.8.3 Results**

Figure 4.7 Panel A shows arrays membranes of untreated MM monocytes cultured for 24h. This array demonstrates that monocytes left in culture for 24h produce high levels of MMP-9 and Cathepsin S. PR3 and Cathepsin D are also seen with lower levels of MMP-1, MMP-12 and Cathepsin X/Z/P.

Densitometry values from untreated MM and ZZ monocytes supernatants compared to supernatants taken from cells treated with C3d. Though raw data suggested a trend towards increased expression of MMP12 and PR3 statistical analyses showed no significant changes between untreated and treated cells.

Of note, high levels of MMP-9 and Cathepsin S were seen in all samples. Mean volume density calculated for both exceeded the levels of positive reference controls precluding further analyses of these proteases by arrays.

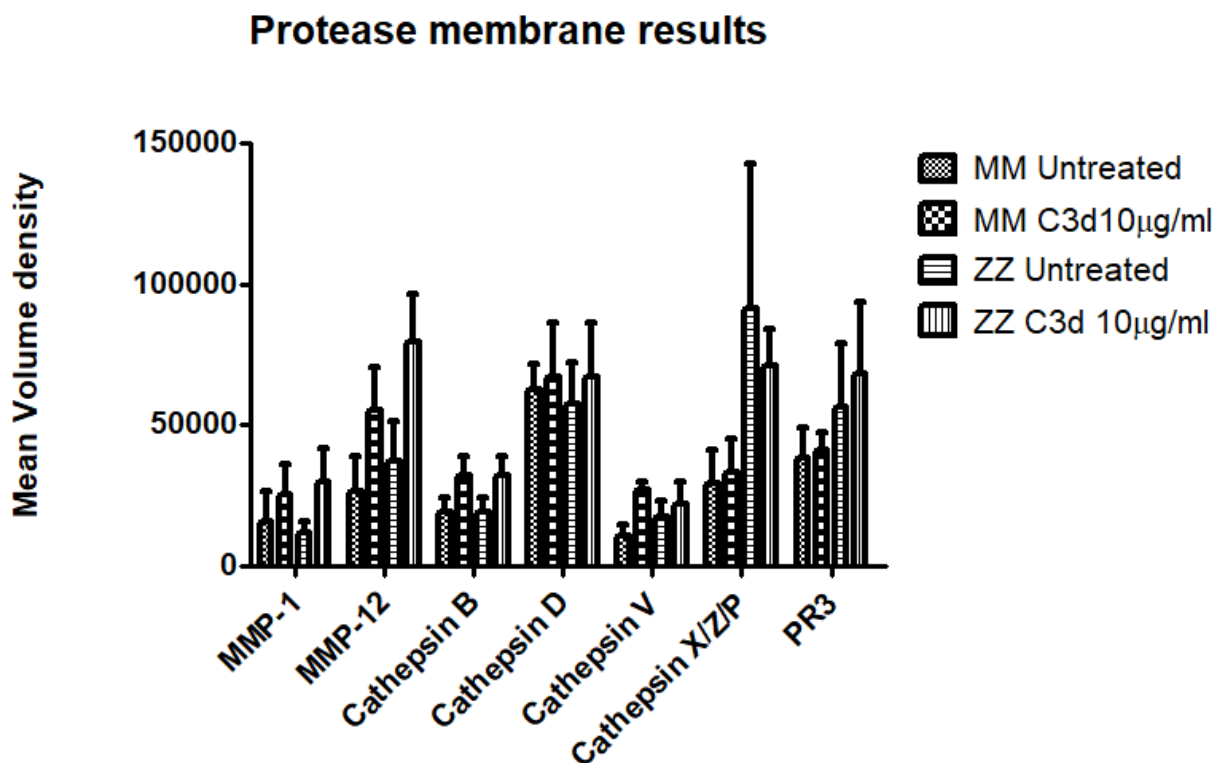


**Figure 4.7 Densitometry from protease array membranes of MM and ZZ monocytes treated with C3d.**

Densitometry values showed a trend toward increased production of MMP-12, Cathepsin D and PR3 in MM and ZZ monocytes treated with C3d that was not statistically significant (n=3). Statistical analyses were performed using a one way ANOVA.

#### 4.8.4 Discussion

Broadly speaking, these results suggest but do not confirm that monocytes treated with C3d produce increased levels of select MMPs 1, 12 and 9, cathepsins and PR3. Our interest was piqued by the changes in expression of metalloproteases and PR3. Though the change observed in the expression of cathepsins was intriguing, the magnitude of change was greatest in a mixed population of Cathepsins (X/Z/P) thus the relative contribution of each to this finding was unclear. Though results seen here did not achieve statistical significance in our analyses, it is worth noting that the concentration of C3d used here (10µg/ml) represents a lower concentration than that identified by others (780 µg/ml).

Earlier cytokine arrays had directed our attention towards measuring MMP-9. As presented in Figure 4.6 ELISAs for MMP- confirmed increased levels of MMP-9 in supernatants of MM and ZZ monocytes treated with C3d (20-40µg/ml). Though few MMPs are expressed constitutively by monocytes, MMP-9 is an exception(441). Monocytes are known to possess intracellular stores of MMP-9 that can be rapidly mobilised for release upon monocyte activation or differentiation(442). As the MMPs have been repeatedly linked to the development of emphysema(378) and are also known to recognise AAT as a substrate(378) we were interested to explore what other MMPs might be elaborated in response to C3d.

Reviewing the evidence base, it became apparent that in addition to MMP-9, MMP-12 has been linked conclusively to the development of emphysema in animal and human models(443, 444). AATD is characterised by early onset emphysema that displays a basal predominance on CT imaging of the lungs(433). Churg et al (2007) have previously demonstrated that administration of IV AAT abrogates the effects of cigarette smoke on AMs. Using a mouse model, they showed a dose dependant

reduction in MMP-F G Á æ} å Á V Þ Ø Á à ^ Á ÆT • Á ^ ¢ ] [ • ^ å Á c [ Á • { [ \ ^ Á  
 view of the strong links between MMP-12 and AAT we elected to further explore the  
 findings of protease arrays and the role MMP-12 plays in the pathogenesis of AAT  
 lung disease.

In addition to MMP-12 we were also keen to explore whether MMP-1 production was  
 altered following treatment with C3d. Though a part of the MMP super family, MMP-1  
 differs from MMP-12 and MMP-9 in the specificity of its substrate base. MMP-1 is  
 classified as an interstitial collagenase and is capable of degrading Type I, II, III, VII  
 and X collagen(378). Increasing levels of MMP-1 within the lungs have previously  
 been correlated with advancing GOLD stage of COPD suggesting it may play a role  
 in disease progression(445). In view of its clinical relevance we elected to pursue  
 further ELISA work quantifying MMP-1 production by monocytes in response to C3d.

The increase in PR3 demonstrated here is particularly interesting as it represents a  
 therapeutic target of AAT augmentation therapy(446). PR3 is known act as an auto  
 antigen that drives inflammation in ANCA associated vasculitides such as  
 granulomatosis with polyangiitis. Individuals who are heterozygous for the Z  
 mutation have previously been shown to have an increased risk of developing AAVs  
 than those without an AAT variant(447). PR3 is stored in the granules of neutrophils  
 and monocytes and has also been localised to the surface to freshly isolated  
 unstimulated neutrophils. Indeed, PR3 is the only neutrophil derived protease  
 expressed on the membrane under resting conditions and this surface expression  
 enables distinction from other serine proteases such as NE and myeloperoxidase  
 (MPO). Surface expression of PR3 increases during apoptosis in neutrophils. Within  
 neutrophils this process is not dependent on degranulation but rather mobilisation of  
 a non-granular pool to the cytoplasmic membrane(448).

Surface expression of PR3 by monocytes, in particular the intermediate monocyte subset, has previously been described(449). Within neutrophils PR3 translocates to the cell surface via an interaction with the glycosylphosphatidylinositol (GPI) linked membrane protein CD177. CD177 forms a signalling complex through which neutrophils are activated following binding of antibodies to PR3. CD177 is conspicuously absent from the surface of monocytes and the exact mechanism underlying PR3 expression by monocytes has yet to be fully elucidated(203). Clarifying whether C3d was influencing PR3 production by monocytes was deemed worthy of interest as it could contribute to expanding our understanding of the pathogenesis of lung disease in AATD.

Unpublished work from the McElvaney lab indicates that exposure of neutrophils to C3d results in degranulation of primary and tertiary granules. Results of protease array experiments using C3d treated monocyte supernatants, suggested that C3d might also influence the production of proteases by monocytes. As alluded to previously, both serine and metalloproteases have been linked to the development of lung disease in AATD and MM COPD. Thus, further exploration of any link between C3d and monocyte production of MMPs and serine proteases such as PR3 merited further study. In view of the strong evidence based supporting MMP-12 both as a driver of emphysema and a substrate for AAT, we elected to first assess whether C3d might alter monocyte production of MMP-12.

## **4.9 ELISA for MMP-12 in supernatants of MM and ZZ monocytes treated with C3d**

### **4.9.1 Background**

Previously published data suggests that both MMP-12 and C3d may serve as useful biomarkers of lung disease in MM and ZZ COPD(78, 450). Both have previously been positively correlated with the degree of emphysema on CT imaging of the lungs. The evidence base supporting MMP-12 as a driver of emphysema and small airways disease in COPD is compelling(436, 450) and underscore the need to elucidate drivers of MMP-12 production.

The catalytic domain of MMP-12 is active across several substrates but arguably, one of the most clinically relevant actions of MMP-12 is its effect on elastin. Elastin accounts for approximately 2.5% (w/w) of the dry weight of the lungs and is distributed extensively throughout the airways(451). MMP-12 driven elastin degradation generates elastin fibres that are known to be chemotactic for monocytes(452). Monocytes recruited to the lung may persist as airway monocytes and undergo differentiation to pulmonary macrophages that have a greater capacity for cytokine generation when compared to resident macrophage populations and can perpetuate inflammation within the lungs(155).

Understanding the interplay between C3d and MMP-12 within the lungs of patients with ZZ AATD is imperative in view of the availability of therapeutic options such as intra venous AAT augmentation for patients with severe emphysema and ZZ AATD(453). Churg et al (2007) have previously show that AAT suppresses release of V β Ø and MMP-12 from airway macrophages exposed to cigarette smoke(454).

Having established through a review of available literature that MMP-12 contributes to the development of lung disease in COPD, we proceeded to examine whether

C3d may induce production of MMP-12 by monocytes. Monocytes from patients with clinically stable ZZ AATD and healthy MM controls were treated with levels of C3d & [ { ] æ! æà | ^ Á c [ Á c @[ • ^ Á ] ! ^ ç ã [(78)•Supernatants were harvested, and an ELISA performed for MMP-12.

#### 4.9.2 Quantifying MMP-12 in monocyte supernatants: Methods

Levels of MMP-12 were measured using the Human MMP-12 ELISA kit (Abcam). Cells treated with LPS were included as a positive control as published data suggests that MMP-12 production by peripheral circulating monocytes is up regulated by exposure to LPS 1µg/ml(455). The Abcam kit was specific for human MMP-12 and detects both the inactive and active forms of MMP-12. Following sequential washing steps as previously described, TMB was added and samples were left to incubate for a further 30min in the dark at 37°C prior to the addition of • c [ ] Á • [ | ~ c ã [ } È Á Œà • [ ! à æ} & ^ Á , æ• Á ! ^ æå Á æc Á ! í €} { Á

#### 4.9.3 Results

MMP-12 was measured in cell supernatants of monocytes treated with C3d (µg/ml) and LPS by ELISA (Abcam).

There was no significant difference in levels between untreated healthy MM controls (n=3) and those with clinically stable ZZ AATD (n=3) (p=0.1275, unpaired t-test).

Treatment with C3d did not increase production of MMP-12. LPS (1µg/ml) increased production of MMP-12 significantly in both MM and ZZ groups (p=0.0477 and p=0.0134 respectively).

Statistical analyses were performed using paired t-tests (within groups) and one way ANOVA (between MM and ZZ groups).

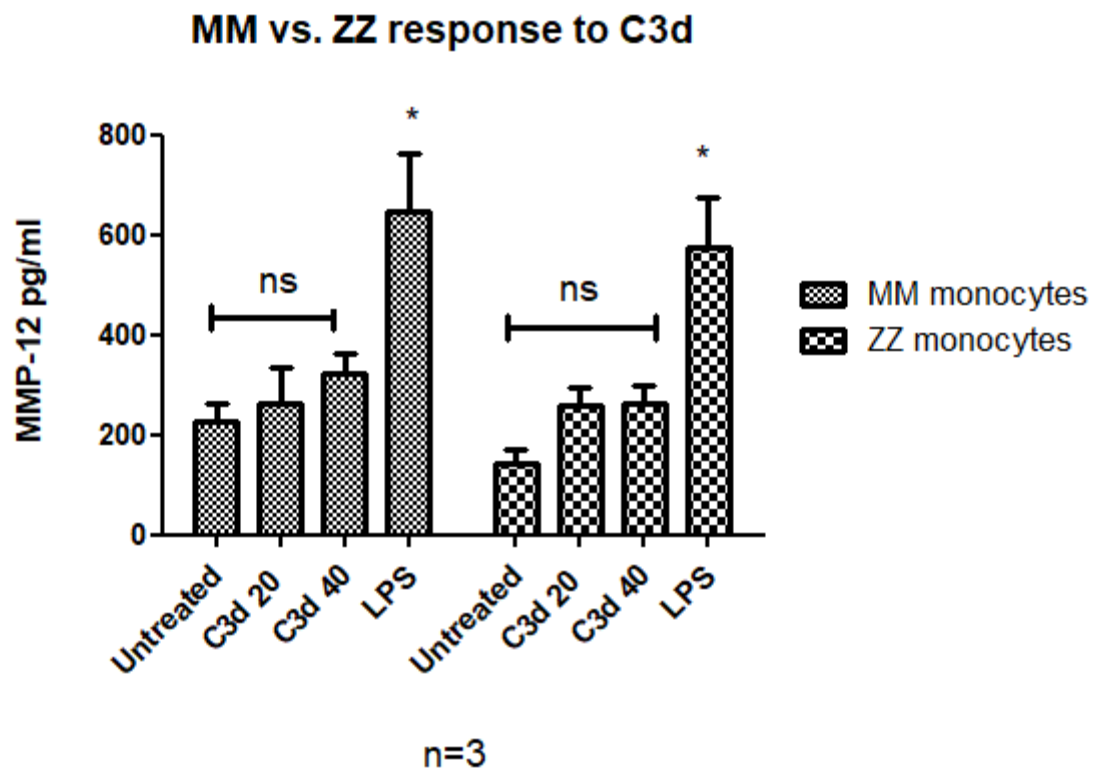


**Figure 4 8: Measurement of MMP-12 production by ELISA following C3d treatment of MM monocytes compared to ZZ cells**

Treatment with C3d did not increase production of MMP-12. LPS (1 $\mu$ g/ml) increased production of MMP-12 significantly in both MM and ZZ groups ( $p=0.0477$  and  $p=0.0134$  respectively). Statistical analyses were performed using paired t-tests (within groups) and one way ANOVA (between MM and ZZ groups). P value  $<0.05$  denotes statistical significance.

#### 4.9.4 Discussion

Results shown here shown no significant differences in levels of MMP-12 in the supernatant of monocytes treated with C3d. Treatment with LPS increased levels of MMP-12 significantly in both groups. Low levels of MMP-12 were detectable in both groups measuring <250 pg/ml in both subgroups.

It is worth noting that monocytes used in these experiments were isolated using the Easy Sep monocyte isolation kit (StemCell). This monocyte isolation kit. This kit uses tetrameric antibody complexes that recognise CD14 and dextran coated magnetic particles to select out cells that preferentially express CD14. Thus the cell population obtained preferentially contains classical and intermediate monocytes which are heavily involved in antigen presentation, phagocytosis and generating a cytokine response to microbial infections. The non-classical subset preferentially express CD16 and are involved in complement and Fc mediated phagocytosis, transendothelial migration and adhesion. Under representation of this monocyte subset in the samples presented here may also be contributing to low levels of MMP-12 expression seen here.

Of note, levels of MMP-12 in the ZZ group appeared lower under all treatment conditions. Increasing the n number may help to clarify whether this is a true effect ( $p=0.1275$ , unpaired t-test). A further explanation for the absence of a significant increase in MMP-12 expression in response to C3d is that C3d may not directly induce expression of MMP-12 by monocytes. To clarify this, we next proceeded to measure levels of MMP-12 in the plasma of healthy controls. Individuals with and AECOPD and ZZ AATD.

## **4.10 Measurement of MMP12 in plasma by ELISA**

### **4.10.1 Background**

Protease array experiments suggested that levels of MMP-12 were increased in the supernatants of monocytes exposed to C3d. This finding was of relevance to this study as amongst all of the metalloproteases MMP-12 has been unambiguously linked to the development of emphysema and small airway remodelling that characterises COPD(456). Currently available data suggests that the collective action of NE, MMP-12 and MMP-1 account for much of the elastin and collagen degradation that drives the development of emphysema within the lungs(378). Hautamaki et al. (1997) demonstrated that MMP-12 knock out mice were resistant to the development of cigarette smoke induced emphysema(444). The same group also showed that MMP-12 deficient mice failed to recruit macrophages to BAL fluid an effect that was overcome with instillation of monocyte chemoattract protein (MCP-1). This suggests that the MMP-12 may also act as a chemoattractant recruiting monocytes and macrophages to the lungs.

Some authors have hypothesised that MMP-12 is the protease that confers elastolytic properties to airway macrophages(443). Previous studies have demonstrated that under steady state conditions, MMP-12 expression is low. Experiments using electron microscopy (EM) have identified intracellular stores of MMP-12 in quiescent macrophages(457). Induction of MMP-12 has been linked to TGF-beta and IFN gamma driven Th1 pathway signalling(458). CD8+ lymphocytes produce IFN gamma responsive chemokines such as CXCL-9, 10 and 11 which interact with the surface chemokine receptor CXCR3 on macrophages to induce MMP-12 expression. Moreover, exposure of macrophages to cigarette smoke

increases production of MMP-12 via activation of the plasmin/thrombin-proteinase (PAR-1) cascade(459). PAR-1 is a serine protease that is susceptible to inhibition by AAT. Published data has previously shown that a several MMPs including MMP-12 are capable of degrading AAT further enhancing the proteolytic activity of proteases such as NE and driving emphysema(378).

ELISAs performed on the supernatants of monocytes treated with C3d showed a trend towards increased levels of MMP-12 but did not achieve statistical significance. We reasoned that if levels of MMP-12 were detectable in both MM and ZZ plasma, this would suggest that stimuli other than C3d were likely to be contributing to elevated MMP-12 levels. To this end we first performed an ELISA for MMP-12 in the plasma of those with ZZ AATD, inpatients admitted with an AECOPD and healthy controls.

#### **4.10.2 Methods**

Levels of MMP-12 were measured using the Human MMP-12 ELISA kit (Abcam) designed for the quantitative detection of human MMP-12 in cell culture supernatants, plasma and serum samples. The kit uses the well described principles of sandwich ELISA. A mouse monoclonal antibody specific for MMP-12 was pre-coated onto a 96 well plate. Standards and test samples were added followed by a biotinylated detection polyclonal anti-body. An initial test run was performed using samples with varying dilution factors (DF) to ascertain the optimal DF for plasma and cell supernatants. Following incubation with the secondary anti-body, 3 sequential washes were performed, and avidin-biotin peroxidase complex added. Following a 30 min incubation with ABC unbound conjugates were washed away with TBS wash buffer and TMB substrate solution was added and samples were incubated in the

dark at 37°C for a further 30 min. During the incubation period TMB was catalysed by HRP resulting in the generation of dark blue sample colouration that was proportional to the concentration of MMP-12 present in the well. The reaction was stopped by adding 2M sulfuric acid and optical density (OD) was recorded at 450nm

Plasma samples were obtained from patients with ZZ AATD attending the outpatient respiratory department. MM COPD plasma were obtained from inpatients admitted to the respiratory ward of Beaumont hospital with a primary diagnosis of AECOPD.

Non parametric distribution of data was assumed, and a Kruskal-Wallis test was used to evaluate for significant differences between group means. Post hoc testing

### 4.10.3 Results

Figure 4.8 demonstrates increased levels of MMP-12 in the plasma of those with ZZ AATD (n=9) compared to healthy controls (n=5) (p<0.05).

Levels of MMP-12 in those experiencing an AECOPD (n=9) (phenotype MM) were significantly higher than healthy MM controls (p<0.05).

No significant differences were detectable between those with ZZ AATD and those with an AECOPD.

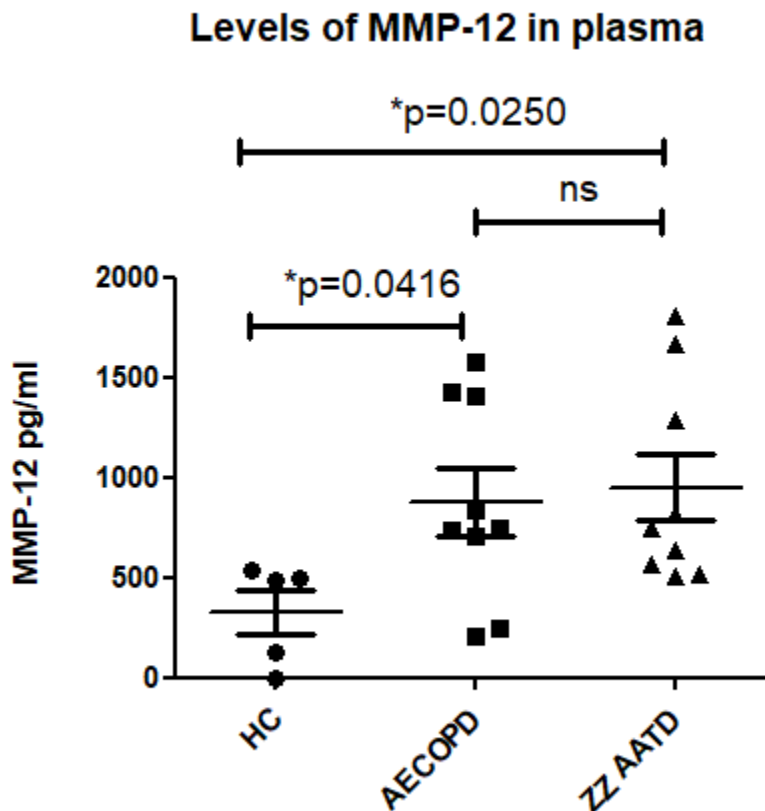


**Figure 4.9 Levels of MMP-12 in healthy MM, MM with AECOPD and ZZ AATD plasma as determined by ELISA.**

Levels of MMP-12 in the plasma of those with ZZ and AECOPD were significantly elevated when compared to healthy controls. Levels did not differ significantly between ZZs and those with AECOPD (n=9). Statistical analysis was performed using a Kruskal-Wallis test.

#### **4.10.4 Discussion**

Results presented here confirm that levels of MMP-12 are comparably increased in the plasma of those with ZZ AATD and those with MM COPD who are experiencing an acute exacerbation. Owing to the cancellation of outpatient clinics attributable to the COVID19 pandemic, access to blood samples from patients with stable MM COPD was limited. For this reason, samples are not matched. ZZ samples represent patients with stable ZZ COPD attending for routine review. MM COPD samples presented here were obtained from patients admitted to the hospital with an increase in respiratory symptoms attributable to an AECOPD. In view of this we are unable to comment on whether the increased levels of MMP-12 in the COPD group are driven by the underlying lung disease or are a feature of an acute exacerbation. Data from previously published data suggests that increased levels of MMP-12 in plasma correlates with disease severity in COPD and is elevated independent of exacerbation status.

Hao et al (2019) have also shown higher levels of MMP-12 and NE in plasma and breath exhalate in those with COPD compared to healthy controls. Furthermore, identified lower levels of TIMP-4 an endogenous inhibitor of MMP-12 activity in the plasma of those with COPD. Levels of MMP-12 gene expression were also noted to correlate with lower levels of lung function (FEV1) as measured by pulmonary function testing suggesting MMP-12 may function as a biomarker for disease severity(450). In addition to plasma MMP-12 levels, Demedts et al (2005) have previously compared levels of MMP-12 in the induced sputum of patients with COPD, healthy smokers, never smokers and former smokers. They confirmed higher levels of enzymatically active MMP-12 in those with stable COPD compared with all

other groups studied (17.5 (7.1. 42.1) v 6.7 (3.9. 10.4) v 4.2 (2.4. 11.3) v 6.1 (4.5.

ï È Î Ð Á } \* Ð { | (ÊÁ)] M € È € € € € G Ð

Results of MMP-12 ELISAs on monocyte supernatants combined with the findings presented above, suggests that stimuli other than C3d are responsible for elevated levels of MMP-12 detectable in plasma. Having confirmed that an interaction between monocytes and C3d was unlikely to be driving an increase in MMP-12 we next turned our attention to evaluating whether C3d may increase monocyte production of MMP-1.

## 4.11 ELISA for MMP-1 in monocyte supernatants

### 4.11.1 Background

MMP-1 also known as collagenase 1, is classified as an interstitial collagenase. It has a molecular weight of 41 kDa and displays activity against Type I, II, III, VII and X collagen in addition to pro-MMP-9 and pro-MMP-2 within the lungs(378). MMP-1 is expressed by type II pneumocytes, alveolar macrophages and bronchial epithelial cells(461). It has previously been shown to be robustly expressed in several pathologies affecting the lungs. Studies examining the role that MMP-1 plays in lung diseases were slower to emerge than those that focused on elastolytic MMPs such as MMP-12. This is likely attributable to early iterations of the protease-anti protease hypothesis emphasising elastin degradation. Elastin, once degraded is not capable of self-renewal and loss of lung tissue attributable to elastin loss is irrevocable(462). Whilst collagen loss within the lung is undoubtedly detrimental to function, collagen fibres secreted into the extra cellular space are capable of organisation into collagen fibrils allowing for repair of tissue damage acquired through the loss of collagen(463).

Whilst the role of MMP-1 played as a driver of lung disease was once considered ambiguous, an emerging evidence base has clarified how it may contribute to

, [ ! • ^ } ã } \* Á ^ { ] @ ^ • ^ { æ È Á Ö q æ ! { ã ^ } c [ Á ^ c Á æ | Á Ç F J J G D

emphysema in MMP-1 transgenic mice in the absence of smoke exposure(464). In

human studies, increased expression of MMP1 has been linked to progression through the GOLD stages which is used in clinical practice to guide therapy and prognosticate in COPD(445). Within AATD, Stockley and colleagues have

previously shown that polymorphisms in genes encoding MMP-1 and MMP-3 are associated with gas transfer abnormalities as measured by the diffusion capacity of

carbon monoxide (DLCO)(453). This is an important observation when considering the development of therapeutics targeting MMPs.

In order to determine whether C3d might be influencing the production of MMP-1 by monocytes we proceeded to perform an ELISA for MMP-1 in the supernatants of MM and ZZ monocytes treated with C3d.

#### 4.11.2 Methods

Monocytes were isolated and treated with C3d as described in Chapter Two:

Materials and Methods. Following treatment for 24 h, supernatants were recovered and stored at -80°C. Samples were left to thaw at room temperature on the bench and then placed on ice. ELISAs for MMP-1 were performed using the ELISA MMP-1

Duaset from R&D Systems (DY901). Briefly, capture antibody was diluted to the concentration specified on the product datasheet and added to a 96 well plate. This was left to incubate overnight at room temperature with gentle rocking. Wells were washed and blocked with 1% (w/v) BSA in PBS for 1h. Further washes were

performed, and samples added. These were left to incubate for 2h at room temperature. The plate was washed (x3), streptavidin HRP was added and left in the dark for 30min. Repeat washes were performed (x3) and 100µl of substrate solution added before covering the plate in tinfoil. Samples were checked every 10min and left for a total of 45min before stop solution was added to prevent any further

reaction. Absorbance was read at 450nm on the Spectramax M3 (Molecular

Ö ^ ç ã & ^ • Ê Á W Û Œ Ð È Á Á Ö ~ ] | ã & æ c ^ Á ! ^ æ å ã } \* • Á [ ~ Á • c æ } å æ

reading subtracted to eliminate background signal. Values obtained were used to generate a seven-point standard curve using. GraphPad Prism software.

Concentrations of MMP-1 present were determined by interpolation from the

standard curve. Statistical analyses were performed using a one way ANOVA and students t-test. A p value <0.05 was considered significant.

#### **4.11.3 Results**

Results showed no significant increase or decrease in levels of MMP-1 between untreated monocytes and those treated with C3d.

Production of MMP-1 did increase significantly in response To LPS (100ng/ml) in line with findings from previously published studies(465).

### Production of MMP-1pg/ml by MM and ZZ monocytes

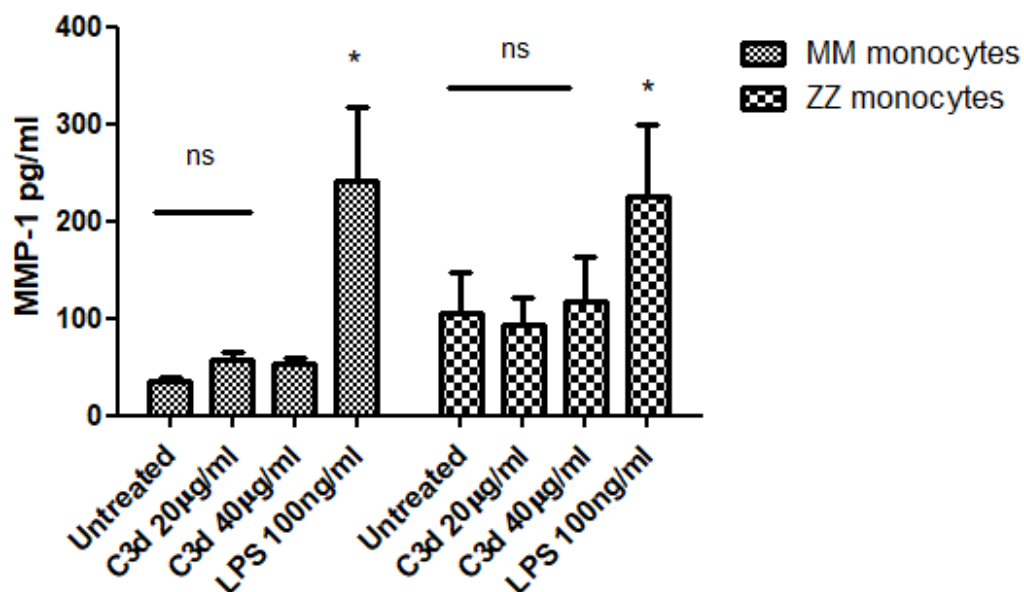


**Figure 4.10: Measurement by ELISA of MMP-1 in the supernatants of monocytes treated with increasing concentrations of C3d for 24 hours.**

MM and ZZ monocytes treated with C3d showed no significant increase in MMP-1 production. Levels of MMP-1 were significantly elevated in samples taken from monocytes treated with LPS (100ng/ml) ( $p=0.0247$ ). Production of MMP-1 between groups did not differ significantly. Statistical analyses were performed using an ANOVA and students t-test.  $P<0.05$  was considered statistically significant.

#### 4.11.4 Conclusion

Numerous studies have linked MMPs to the development of an assortment of lung diseases involving the airways, alveolar and interstitial spaces. COPD occurring within or without the context of AATD causes changes in each of these structural compartments of the lung. Thus, interest in exploring a relationship between MMP-1 production and C3d is of interest to this study.

ELISA results presented here suggest that C3d does not significantly alter the production of the interstitial collagenase MMP-1. The significant result achieved in response to LPS indicates that the positive control worked adequately and is in keeping with previously published studies(465).

The majority of MMPs are not constitutively expressed and cellular activation is required for gene transcription and subsequent MMP production(441). Studies using qRT PCR have previously demonstrated very low levels of basal MMP-1 expression by monocytes and macrophages(214). Gosselink et al (2010) have previously shown increased expression of MMP-1 mRNA within the lung parenchyma with stage progression in COPD though the magnitude of change was small(445). Up regulation can be induced by prolonged culture(410), activation in response to a pro-inflammatory trigger or differentiation into a monocyte derived macrophage(436).

Activation of monocytes by other complement fragments including the anaphylatoxin C5a has previously been described(466). Okusawa et al have previously shown that

to a dose dependant manner(466). Though further up titration of the concentration of C3d used for these experiments was technically feasible, 40µg/ml represents the highest concentration that can be used in the airways of those with ZZ AATD. Even if further increases did elicit a significant effect, the

clinical applicability of these results would be questionable at supra physiological concentrations of C3d.

It is notable that levels of MMP-1 across all samples presented here are Low measuring <250pg/ml even in positive controls. This likely reflects low constitutive levels of expression and minimal and a lack of intracellular stores of MMP-1 in monocytes(442). It is noteworthy that of the 23 MMPs identified to date only MMP-9 and MMP-8 have been identified as being stored intracellularly. This helps to explain the magnitude of difference between MMP-1 and MMP-9 levels observed during this work package.

Having ascertained that C3d did not appear to alter production of MMP-1 by monocytes, we next proceeded to measure levels of PR3 in the supernatants of monocytes treated with C3d.

.

## 4.12 ELISA for PR3 in the extracellular supernatants of MM and ZZ monocytes treated with C3d

### 4.12.1 Introduction

Results from protease array membrane work suggests that exposure to C3d correlates with an increase in PR3 detectable in monocyte supernatants. As alluded to previously, though array membranes are useful tools for generating hypotheses, changes in the chemiluminescent signal identified by arrays does have a linear relationship with signal quantification determined by ELISA(407). Thus, results of protease array analyses, should not be considered in isolation. Following analysis of array results we next proceeded to perform an ELISA for PR3 in the supernatants of C3d treated MM and ZZ monocytes.

Proteinase 3 (PR3) is a pleiotropic and destructive serine protease enzyme encoded by the PRTN3 gene. It is one of four serine protease homologs known to be contained within the azurophilic granules of neutrophils and monocytes(467, 468).

Synthesised as a pro-form, cleavage of the terminal dipeptide by lysosomal cysteine exopeptidase dipeptidylpeptidase results in the generation of enzymatically active

PR3(469)È Á Á Œ• Á ] ^ | Á c @^ Á { æ} ~ ~ æ& c ~ | ^ | q • Á ã } ~ [ | { æc ã [ }

used as part of this work detect only the active form of PR3.

The substrate profile of PR3 is broad and includes multiple components of the extracellular matrix including elastin, fibronectin, laminin, vitronectin, and collagen types I, III, and IV (in vitro). Kao and colleagues (1988) have previously shown that intratracheal injection of PR3 accelerates loss of lung tissue resulting in emphysema in a hamster model(468). In addition to proteolysis, PR3 is known to induce apoptosis in endothelial cells(470) and proliferation of granulopoietic progenitor cells(471). PR3 also plays a role in regulating the inflammatory response via

cytokine activation, processing of cytokine binding proteins and amplifying chemokine activity(467). PR3 has been shown to cleave the pro-forms of TNF alpha(472) and pro IL-8(473) perpetuating the inflammatory response.

Both PR3 and C3d have been linked to the development of emphysema. PR3 is known to accelerate the loss of lung tissue directly via degradation of the ECM. The role of C3d is less clear. Possible mechanisms include an indirect effect via ongoing activation of the complement cascade or through a direct effect of C3d on monocyte causing activation. Further exploring the relationship between C3d and PR3 is reasonable as it may help to further explain the link between C3d and emphysema in AATD.

#### **4.12.2 Methods: Quantifying PR3 in C3d treated monocyte supernatants**

Monocytes were isolated and treated as outlined in Chapter Two: Materials and Methods. Once supernatants were recovered, they were stored as -80° until ready for use in ELISA experiments. ELISA for PR3 was performed using an ELISA kit for human PR3 (abcam ab226902). This kit allows for quantification of PR3 using the well described principles of sandwich ELISA. The abcam kit detects PR3 over a range of concentrations (1.2-150ng/ml). The concentrations of PR3 in samples were measured in duplicate, concentrations interpolated from the standard curve (shown in Chapter Two) and corrected for sample dilution factor.

#### **4.12.3 Results**

Levels of PR3 detected in untreated MM and ZZ monocyte supernatants did not differ significantly though a trend towards increased PR3 production was observed in ZZ samples.

Levels of PR3 detected in ZZ monocytes treated with C3d at a concentration of 20µg/ml were significantly higher than levels measured in healthy MM controls (( $p=0.011$ )).

Treatment with C3d at a concentration of 40µg/ml significantly increased production of PR3 by both MM and ZZ monocytes ( $p= 0.0469$ ,  $p= 0.076$  respectively).

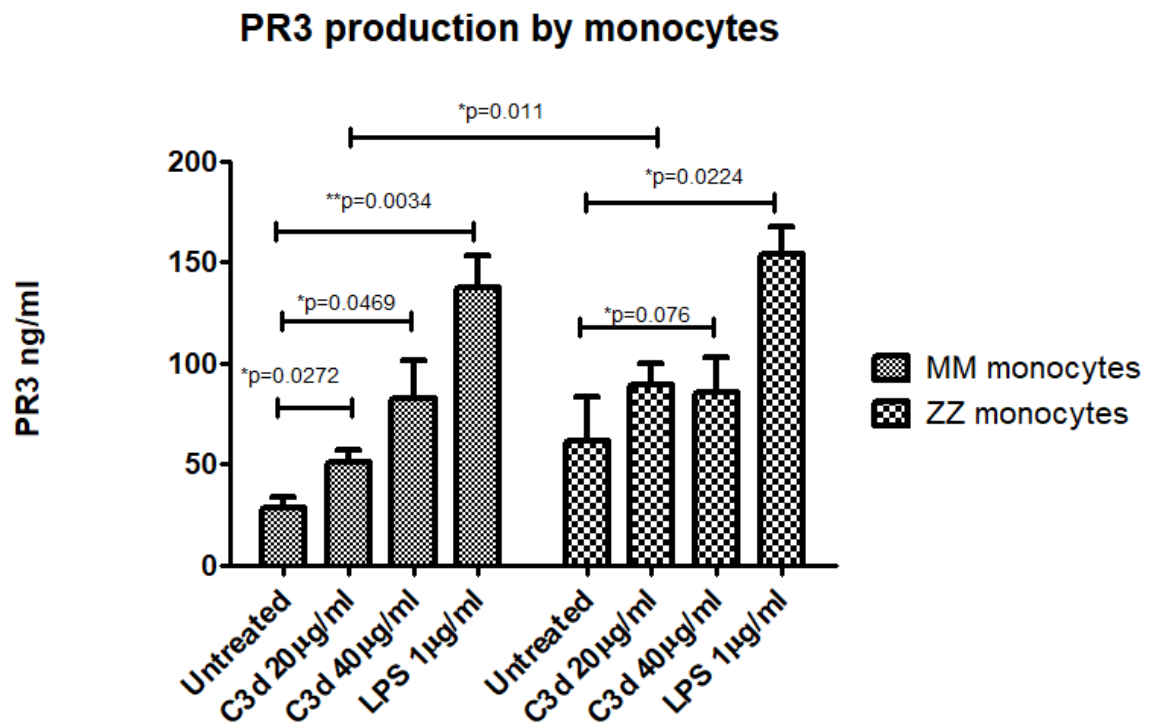


**Figure 4.11: Measurement of PR3 production by ELISA in MM versus ZZ monocytes**

PR3 was measured in cell supernatants of untreated cells or monocytes treated with C3d (20 or 40 µg/ml) by ELISA (Abcam). Within both groups there was a significant increase in PR3 detectable in the supernatants recovered from monocytes treated with C3d at a concentration of 20 µg/ml and 40 µg/ml respectively. Statistical analyses were performed using an ANOVA and unpaired t-test. P value of  $<0.05$  was considered statistically significant. N=5 subjects per group.

#### 4.12.4 Discussion

Results presented here indicate that monocytes exposed to C3d produce increased levels of PR3. ZZ monocytes treated with C3d at a concentration of 20µg/ml produced significantly higher levels of PR3 when compared to MM monocytes exposed at the same concentration. These results identified C3d as biomarker of a dysregulated complement response in the absence of a protective effect of AAT(78). The results of this experiment would suggest that C3d may also contribute to the inflammatory milieu seen in both MM and ZZ COPD via a direct effect on monocytes causing release of PR3.

As such PR3 activity is classically described in the context of neutrophil activation and degranulation. Its broad substrate base and its role in neutrophil activation (474) render it a compelling target for therapeutics aimed at slowing the progression of neutrophil driven lung diseases. Sindén and colleagues have previously studied levels of PR3 in the sputum of those with ZZ AATD and COPD in the stable state and during exacerbations(446). They found higher levels of PR3 in those with ZZATD compared with COPD when clinically stable. They also identified increased levels of PR3 activity during acute exacerbations ( $p=0.037$ ) that correlated with markers of neutrophilic inflammation suggesting a role for PR3 in the pathophysiology of acute and chronic disease states.

Work by Stockley et al has previously shown that AAT augmentation reduces the levels of PR3 in the sputum of those with ZZ AATD and COPD (446). Their data demonstrated greater differential activity of PR3 than NE and suggests greater potential for PR3 versus NE mediated destruction of the ECM. OE -Val correlated with the severity of lung disease and decreased significantly in response to augmentation therapy (reduction 287.2 to 48.6nM,

p<0.001)(475). Given the availability of therapies targeting PR3, elucidating the mechanisms of PR3 production by other cell types including monocytes within the circulation and the airways is imperative.

Within monocytes, upregulation of PR3 expression at the gene level has previously been described in Cystic fibrosis and ANCA associated vasculitides. Just and colleagues (1999) found increased gene expression of PR3 mRNA in monocytes but not in neutrophils of individuals with CF(202). Interestingly, this effect was abrogated by treatment with antibiotics and suppression of bacterial load within the airways.

These findings highlight a potential role for monocyte driven inflammation via PR3 production in CF(202). Ohlsson et al showed increased levels of PR3 mRNA in individuals with ANCA -associated systemic vasculitides (AASVs)(467). AASVs are chronic diseases that are characterised by inflammation within blood vessels.

Though few genetic polymorphisms have been identified as correlating with the development of AASVs, the exception is the PiZ mutation seen in AATD(476).

Detection of the PiZ mutation is associated with disease progression and worse prognosis compared to MM cohorts with AASVs(476).

Data presented in chapter one confirms that all 3 populations of monocytes can be identified in the airways. Furthermore, we have shown that CR2 is identifiable on intermediate and non- classical subsets in addition to alveolar macrophages. This raises the question of whether C3d may have a similar direct effect on airway monocytes and monocytes Derived AMs. Understanding the direct effects of C3d on monocytes, as demonstrated here allows us to further unravel the nuances of disease pathogenesis in AATD.

#### **4.13 General Discussion**

The purpose of this study is to elucidate the effects of the complement fragment C3d on monocytes in AATD. Published data from the McElvaney lab identified AAT as a binding partner of the C3d parent protein C3(78). C3d is a cleavage product of C3 generated by sequential cleavage of C3 by proteases, most notable the serine proteases(477). Qualitative or quantitative deficiencies of the serine protease inhibitor AAT prevents binding of AAT to C3 and subsequent complement activation. Increased levels of the complement fragment C3d in the plasma and BAL samples of individuals with ZZ AATD points towards sustained complement activation in AATD(78).

Data presented in chapter once established the existence of a receptor for C3d CR2 on the surface of monocytes in the circulation and within the airways. Having demonstrated the existence of a signalling axis for C3d in monocytes, this chapter focuses on determining what the downstream effects of an increase in circulating C3d on monocytes may have in AATD. Monocytes are a heterogenous and plastic cell population. Much is still being learned about monocyte ontogeny and factors influencing phenotype and function(478). Increasing recognition is being given to the importance of distinguishing between the role of different monocyte subsets and factors influencing the balance of subsets in the circulation and airways(155, 479).

Monocytes in AATD are known to be intrinsically primed to generate an excessive cytokine response to pro-inflammatory stimuli such as LPS. Carroll and colleagues demonstrated that ZZ monocytes exposed to bacterial LPS produce increased levels of the pro-inflammatory cytokines IL-6 and IL-8 which may contribute to the inflammatory phenotype seen in AATD(299). One of the aims of this chapter was to ascertain what kind of cytokine profile might they elaborate in response to C3d. Of

further interest to this study was the question of whether C3d prompted a degranulation response in MM and ZZ monocytes. Unpublished data from our lab has shown that exposing ZZ neutrophils to C3d bolsters degranulation as evidenced by increased products of primary, secondary, and tertiary granule proteins detectable in supernatants of treated cells. This prompted us to question whether a similar effect might be observed in ZZ monocytes.

Preliminary experiments for this work package were performed on U937 cells. As previously discussed, whilst U937 cells are useful models of monocyte function key structural differences render them more like developing bone marrow monoblasts than the heterogeneous population of circulating monocytes (480). U937 work was used to build technical familiarity and to refine our cell treatment and ELISA protocols. In view of prior work by Carroll et al demonstrating increased IL-8 response of monocytes in AATD and the role IL-8 is known to play in driving inflammation seen in a host of lung pathologies including CAP, AATD (292), COPD and ARDS (393) IL-8 was chosen as our cytokine of interest. Results of U937 cell line work suggested no increase in IL-8 production in the presence of C3d. Review of the raw data however suggested an upward trend in cells treated with a concentration of 5 µg/ml and above. In recognition of this we decided to amend our treatment protocol to include a range of concentrations that better reflected the concentrations of C3d in circulation (481) and colleagues.

Before endeavouring to determine what, if any effects C3d may be having on monocytes we first need to ascertain whether C3d was toxic to monocytes obtained from the circulation. As we intended on using comparatively high concentrations relative to what had been used in the cell line work, confirming no loss of monocyte

viability was imperative. Spontaneous apoptosis is well described in monocytes in the absence of obvious stimuli(383). This underscored the need for performing a viability assay in advance of treating monocytes isolated from circulation.

Fortunately, MTS assays confirmed that C3d was not causing cell loss and we proceeded with cell treatment with higher concentrations of C3d.

The first block of work with monocytes involved the use of healthy control cells only. MM monocytes were isolated from the circulation of healthy controls and treated with increasing concentrations of C3d. The highest C3d concentration used in this early block of work was C3d 20µg/ml. Results showed no increase in the levels of IL-8 detectable in MM monocyte supernatants but again an upward trend was observed with increasing concentrations. The broad evidence supporting a role for IL-8 in lung disease made it a compelling target for ELISAs as part of this project. However, early on we recognised that the capacity of monocytes to generate a cytokine response is prolific. In recognition of this we saw the need to begin these experiments by endeavouring to get an unbiased overview of what kind of cytokine profile monocytes were likely to exhibit in response to C3d. As alluded to previously for reasons of practicality we proceeded to use a cytokine array membrane to gain insights that would help direct future ELISA work.

Cytokine array membranes generated a considerable amount of data and was useful as they suggested differing cytokine responses between untreated monocytes and those exposed to C3d. The challenge then became identifying which results merited further investigation with ELISA. Though other cytokines such as TGF alpha were noted to be present in higher quantities, the magnitude of difference between treated and untreated membranes was amongst the highest for the LPS co-receptor CD14. CD14 was of interest to us in this study from the outset as the relative expression of

surface CD14 and the Fc receptor CD16 define each monocyte subset. Much attention has been given in recent years to examining alterations in the proportional representation of different monocyte subsets in disease states- most notably COPD(164). It is noteworthy that both the cytokine array membranes and ELISAs presented here detect soluble CD14. Previously published studies have identified elevated levels of sCD14 as a marker of monocyte activation(429). High levels of sCD14 have also been shown to influence the phenotype and function of adjacent cells conferring LPS responsiveness to other cells not otherwise primed to respond to LPS(430). sCD14 is known to be generated via several mechanisms including cleavage of surface bound mCD14 by serine proteases and release of intracellular stores(481). We hypothesised that high levels of sCD14 may indicate a shift in the balance of monocyte subsets either through release of intracellular stores of CD14 or cleavage from the membrane of activate monocytes. This hypothesis combined with observations from Stolk et al (2019) who found a reduction in the numbers of IM and NC monocytes in ZZ AATD prompted us to further explore whether C3d may be contributing to this effect via influencing expression of sCD14. ELISAs of supernatants taken from monocytes treated C3d at a concentration of 20µg/ml had increased levels of sCD14 compared to untreated samples. Further work using multi colour flow cytometry and whole blood would be needed to clarify whether this effect causes a switch in monocyte subsets in MM and ZZ subsets.

Cytokine array analysis also suggested changes in levels of MMP-9 in monocytes treated with C3d. Whilst MMP-9 is not technically considered as a cytokine this finding prompted our curiosity about whether C3d may trigger degranulation by monocytes as it has previously been shown to cause in neutrophils. As previously discussed, the MMPs are a superfamily of 23 proteases capable of degrading a

diverse range of substrates such as collagens, elastin, fibronectin, laminin, and several heparin and proteoglycans(461). Collectively these proteins form the ECM of lung tissue. Loss of ECM components such as elastin and collagens seen in disease such as COPD(482). MMP-9 has been extensively linked to emphysema(461) and thus was identified as our next target for quantification by ELISA.

Results of MMP-9 ELISAs suggest that C3d may play a role in monocyte activation with resultant increases in MMP-9 production. Despite a compelling evidence base confirming MMP-9 as driver of lung disease, a causative role for MMP-9 in AATD has not been established. Despite this, understanding what drives the production of MMP-9 by monocytes is important if the pathogenesis of the disease is to be fully elucidated. It is well established that MMP-9 functions to degrade BM type IV collagen, elastin and other structural proteins that are necessary to support the integrity of the lung parenchyma(483). In addition to its role as a protease, MMP-9 is known to potentiate the chemotactic activity of IL-8 for neutrophils 10-fold(484). The observation that ZZ monocytes produced more MMP-9 than MM cells is also of interest as MMP-9 is known to degrade AAT leaving the lungs susceptible to the unfettered actions of proteases. Increased levels of C3d and MMP-9 have both previously been correlated with worse emphysema and lower diffusion capacity of the lungs in ZZ AATD(78). Data presented here suggests a relationship between both and an insight into a yet unexplored mechanism of emphysema pathogenesis in AATD.

The results of experiments examining the link between C3d and MMP-9 increased our interest in further exploring the relationship between monocytes and the production of proteases. Whilst researching the utility and efficacy of cytokine arrays we identified that a similar version was also available through R&D systems that

could measure several proteases simultaneously. Inspired by the differences previously seen between MM and ZZ neutrophils we decided to apply both MM and ZZ monocyte supernatants to protease array membranes and see if we could discern any obvious differences that would inform what analytes were measured during the course of ELISA protease work. Broadly speaking, the protease array membrane showed differences in differential expression of cathepsins and MMPs between untreated and treated MM and ZZ monocytes.

Though results achieved with protease array membranes did not achieve statistical significance an upward trend in MMP-1 and MMP-12 production was observed in monocytes treated with C3d at a concentration lower than that previously identified in the airways of those with ZZ AATD(78). Previously published studies have implicated both MMP-1 and 12 in the development of emphysema in COPD. MMP-12 has been particularly well studied as a driver of lung disease with a wealth of animal and human studies confirming its link to emphysema. To confirm that MMP-12 was indeed likely to be a contributor to driving inflammation in ZZ AATD and COPD we performed ELISAs for MMP-12 on the plasma of healthy controls, patients with clinically stable ZZ AATD and inpatients admitted with an acute exacerbation Of COPD. We identified significantly increased levels of MMP-12 in the plasma of those with AECOPD and ZZ AATD when compared with healthy controls. This confirmed to us that pursuing further ELISA work examining MMP-12 was of merit. Subsequent ELISAs for MMP-12 and later, MMP-1 showed no significant increase in production of either MMP in response to C3d. The increased expression on MMP-12 in both patient groups indications that stimuli other than C3d was causing its production. Returning to the results of the protease arrays, we proceeded to ELISAs aimed at measuring levels of PR3 in MM and ZZ monocytes treated with C3d. PR3 has been

studies extensively in AATD and presented as a natural target of interest for this project. Though frequently studied in neutrophils, published data suggests upregulation of PR3 by monocytes in other destructive lung diseases such as CF(202). Studies of sputum samples taken from those with MM COPD, ZZ COPD and healthy controls show increased levels of PR3 in the sputa of those with ZZ AATD and an acute exacerbation(446). PR3 activity can be reduced by AAT(475). In view of the clinical importance of PR3 æ• Á æÁ â º ã ç ^ º Á [ ~ Á ã } ~ | æ{ { æc ã [ } use as a therapeutic target of AAT we were interested on further examining the interplay between monocytes, C3d and PR3 levels. Results of ELISAs showed a significant increase in the levels of PR3 from monocytes treated with C3d. Baseline levels of PR3 were also noted to be higher in ZZ AATD than MM controls.

Collectively, these results suggest that C3d is likely to play a role in creating an inflammatory milieu that favours destruction of the ECM and development of & | ã } ã & æ| | ^ Á æ] ] æ! ^ } c Á | ~ } \* Á â ã • ^ æ• ^ È Á U q Ó! ã ^ } Á æ} increased levels of C3d in the plasma and airways of those with ZZ AATD(78).

Moreover, this increased levels of C3d correlated with the severity of emphysema. We hypothesise that increased availability of circulating C3d in AATD allows for binding of C3d to CR2, activation of monocytes and release of proteases that favour the development of emphysema. C3d also influences release of sCD14 by monocytes. It is unclear whether this alters the phenotype and balance of monocyte subsets in ZZ AATD. Further work using multi colour flow cytometry may help address this question in future. This will be addressed further in Chapter 5: Discussion and future directions.

## **Chapter 5: Discussion and Future Directions**

## 5.1 Summary

This project has focused on establishing the effects of the complement fragment C3d on monocyte function with particular reference to monocyte function in AATD.

U q Ó! ã ^ } Á ^ c Á æ| Á Ç G € G € D Á ã á ^ } c ã ~ ã ^ á Á ŒŒEV Á æ• Á æÁ } [ ç protein C3(78). Furthermore, they showed increased levels of the complement fragment C3d in plasma and airway samples of those with ZZ AATD compared to clinically stable MM COPD and HCs. As C3d is not produced by spontaneous hydrolysis of its parent protein C3 in plasma, elevated levels reflect dysregulated activation of the complement system in AATD(78). Clinically, higher levels of C3d have been shown to correlate with worsening radiographic evidence of emphysema and a decline in lung function as assessed by FEV1, in AATD(78). High levels of C3d within the glomerulus of the kidney are a predictor of poor outcome in AAVs which have known to have a higher incidence in ZZ AATD compared to MM controls(79, 175).

Until recently, much of the published research on AATD has focused on the role neutrophils play in driving disease pathogenesis. The early ubiquity of the protease anti-protease hypothesis focused many studies on lymphocyte subsets such as neutrophils that are known to produce large amounts of proteases in response to activation(485). However, increasing recognition of the role of AAT as an immunomodulator, has broadened the scope of research in this field, to include monocytes and monocyte derive macrophages which are known to produce cytokines in response to pro-inflammatory stimuli such as LPÙ Ê Á V Þ Ø Á æ 21â Á Q Ø Þ 299, 486).

Our interest in examining the effect of C3d in ZZ AATD monocytes and

{ æ& ! [ ] @æ\* ^ • Á , æ• Á ] ! [ { ] c ^ á Á à ^ Á c @^ Á ] ! ^ ç ã [ ~ • | ^ Á á

(2020)(78), and others, who had examined monocyte behaviour in AATD. Carroll et al (2016) showed that monocytes in AATD are programmed to generate an excessive cytokine response following exposure to a pro-inflammatory trigger(299). As alluded to in chapter one, the authors attributed this effect to activation of an ER stress response known as the UPR(299). We hypothesised that C3d may act as an inflammatory trigger of ZZ monocytes, resulting in an excessive cytokine response upon stimulation. Of note, Carroll et al., used a CD14 positive selection kit to isolate monocytes used in their work. Thus, it is likely that their observations were made in CMs and IMs which are known to express CD14 strongly. Stolk et al (2019) have also previously reported on monocyte behaviour in AATD. They showed that the proportional representation of different monocyte subsets in the circulation is altered in ZZ AATD(142). Much debate has been had over the role different monocyte subsets play in health and disease(121, 155, 479). Published data suggests that changes in the proportional representation of subsets portends a poor prognosis for diseases such as RA that are characterised by dysregulated inflammation(138). Using multi colour flow cytometry Stolk et al (2019) identified lower levels of IMs and near absence of NCMs in patients with ZZ AATD. Current consensus is that NCMs and IMs participate in surveillance of the vascular endothelium and the generation of cytokines(121). CMs are producers of the pro inflammatory cytokines IL-6 and IL-8 and are recruited to the lungs to repopulate the airways with monocyte derived AMs as resident AMs are consumed as part of an inflammatory response to infection or injury(155). The demonstration by Stolk et al., (2019) of a relative abundance of ZZ CMs, a subset that has been shown to be intrinsically programmed to generate excessive cytokines in response to a pro-inflammatory trigger(299), led us to question the effect that C3d may have on monocyte behaviour in AATD.

Of further interest to us were prior observations that monocytes and macrophages are innately programmed to respond to stimulation with complement proteins and fragments. Both cell types play a critical role in generating innate and adaptive immune responses. Reflecting on this, they possess an extensive variety of complement receptors on their surface and are susceptible to activation by complement proteins and fragments liberated as part of the complement cascade(361, 487). Early experiments performed as part of this project were informed by prior work by Fee (2019) examining the interaction between complement fragment C3d and neutrophils. Fee demonstrated a receptor for C3d (CR2/CD21) on the surface of circulating neutrophils(188). They showed that C3d binding to the surface to the neutrophil resulted in increased production of the chemoattractant IL-8. Furthermore, increased levels of primary, secondary and tertiary granule proteins were detectable in neutrophils treated with C3d. This suggested a novel mechanism whereby C3d may directly contribute to disease pathogenesis in AATD. We hypothesised that monocytes and macrophages may also respond directly to stimulation with C3d via the generation of cytokines and proteases.

Work presented as part of chapter 3 was focused on establishing the existence of a signalling axis for C3d in monocytes. Results demonstrate for the first time that the only known receptor for C3d, CR2/CD21 is present on the surface of monocytes in the circulation and the airways(248). Furthermore, we have identified high levels of CR2 expression on alveolar macrophages from the airways where concentrations of C3d are known to be highest.

Results presented in chapter 4 explore some of the effects of C3d on the production of cytokines and proteases by ZZ and MM monocytes. Our results suggest that stimulation with C3d causes an increase in secretion of MMP-9 and PR3 across both

sub-groups. MMP-9 and PR3 are both known to play a role in the loss of lung ECM causing emphysema. We have also shown increased production of sCD14 by both ZZ and MM monocytes treated with C3d. The mechanisms underlying this effect, and the consequences for proportional representation of monocyte subsets in AATD, remains to be clarified.

Collectively, these results allow for the generation of hypotheses that may inform future work. Key results will be reviewed here, and future directions discussed.

## 5.2 Establishing a signalling axis for C3d

### 5.2.1 Observations from cell line work

All experiments performed as part of this study, with the exception of multi colour flow cytometry were initially performed on a monocyte-like cell line (U937 cells). As alluded to previously, U937 cells are malignant cells capable of rapid proliferation but at the expense of phenotypic diversity(311). For reasons related to the considerable phenotypic and functional differences between monocytes and U937 cells, results obtained from U937 were from the outset, unlikely to be directly applicable to circulating monocytes. Despite these limitations, experiments with U937 cells were crucial to the overall success of this project. The use of U937 cells permitted refinement of the techniques of FACS, ELISA and qRT PCR.

Some important observations were made during cell line work. Results presented in Chapter Three confirm that under our experimental conditions (10min treatment, in the absence of protease inhibitors prior to fixation with PFA) surface expression of

Ô Ü G Á à ^ Á WJ H Ĩ Á & ^ | | • Á ^ ¢ ]F[ •Á[ â Á ÁCQ HÁŠÁÚÁÛÁÁV, H ¢ ÁÊÁ@ÁŠ \*

It is possible that this finding is attributable to an insufficient treatment period being used in these early experiments. Previously published data confirms that exposure to LPS can increase U937 production of the complement proteins C3 and C4 in a time dependent fashion(306)Tsukamoto et al (1992) have shown this effect peaks at between 48 and 72 h(488). Our treatment protocol was modelled on similar experiments examining CR2 expression by neutrophils. As part of a PhD thesis Fee had shown that a 10min treatment of neutrophils with IL-8 and TNF- Á Ç ] M € È € F G H D Á increased surface expression of CR2 in a manner comparable to that seen with PMA(188). It is probable that given the considerable structural and functional

differences between neutrophils and U937 cells, our selected treatment protocol was unlikely to succeed in replicating the findings of Fee using neutrophils.

Despite the absence of a response to our pro-inflammatory stimuli, in a manner similar to Fee we identified that stimulation of U937 cells with PMA did significantly increase surface expression of CR2. PMA is frequently used to induce differentiation of U937 cells from a monocyte to a macrophage-like phenotype(489). Though treatment with PMA cannot be considered a physiological stimulus, it prompted us to question whether CR2 might also be detectable on pulmonary macrophages and laid the foundation for the design of multi colour flow cytometry experiments.

### **5.2.2 Confirming CR2 expression by circulating MM and ZZ monocytes**

As discussed in chapter one, monocytes play an important role in innate and adaptive immunity(121). Monocytes contribute to immunity via the processes of phagocytosis, antigen presentation and production of cytokines(479, 489). Many of the functions of monocytes and monocytes derived macrophages depend upon appropriate, sequential activation of the complement cascade. Opsonisation by complement fragments facilitates antigen presentation and phagocytosis(147). In view of the shared role monocytes and complement play in immunity, it is perhaps unsurprising that monocytes are known to express several receptors for complement proteins and fragments(182, 327, 361). It is notable however, that the existence of the receptor for C3d, CR2, has not been conclusively shown in monocytes. In 1983 Inada et al., showed that RBCs coated with C3d could form rosettes with monocytes in a time dependent fashion(255). However, it was not until 2 years later that Lida described the C3d receptor as CR2(248).

Since early descriptions of CR2, the relationship between C3d and CR2/CD21 has been described at length(490). Though other complement proteins and fragments are capable of binding multiple receptors, CR2 is the only known receptor for C3d. In view of this, we reasoned that if we could definitively identify CR2 in circulating monocytes, this would confirm a signalling axis for C3d in monocytes. To ensure the validity of our findings we determined to identify CR2 at a number of levels including gene expression, whole cell protein and surface expression.

Results presented in chapter 3 demonstrate expression of CR2 at both gene and protein levels. Difficulty achieving RNA of sufficient purity for our analyses necessitated switching from the trizol reagent method to the use of RNA columns to recover RNA from monocytes (both described in chapter 2, materials and methods). This allowed us to show that monocytes expressed a gene for CR2 and legitimised the decision to proceed with examining monocytes for protein expression. qRT-PCR is a reliable technique but as an alternative approach we opted to confirm our results using DNA agarose gel electrophoresis(46). Results of qRT-PCR showed no significant difference in expression of CR2 between MM and ZZ monocytes. If we consider this observation in the context of previously discussed work by Inada et al (1983), we can infer that the presence of C3d in the extracellular environment is unlikely to induce upregulation of CR2 alone. This would account for the absence of a significant difference in the levels of gene expression that we observed. ZZ AATD is a state of dysregulated complement activation as suggested by higher levels of C3d in the plasma and airways of ZZ individuals compared to MM controls(78). Despite prolonged exposure of circulating ZZ monocytes to C3d, this does not appear to induce the cell to express CR2 to a greater degree than MM controls who are not exposed to high levels of C3d in the circulation.

The use of whole cell lysates during western blotting allowed us to examine cells for whole cell CR2 protein expression. This was considered important as CR2 expression is not just restricted to the surface of cells, and intracellular stores of CR2 have been previously described in B cells and astrocytes amongst other cell types(491). Technical challenges encountered with western blotting are outlined in chapter 3 and included the need to run samples in the absence of DTT to avoid protein denaturing. Results showed a larger than expected band (> 175kDa) at the top of the gel where small differences in location of immunobands can reflect large differences in molecular weight. Explanations for this unexpected finding may lie in technical aspects (misplacement or movement of the protein ladder during image acquisition) or reflect intrinsic properties of CR2. Masilamani and colleagues have ] | ^ ç ã [ ~ • | ^ Á • @[ , } Á c @æc Á Ô Û G Á æå [ ] c • Á æÁ ± • c | ã } \* Á [ unfolding(323). The ladder shown in our image uses standard reference proteins that have a globular conformation. This may go some way towards accounting for the appearance of CR2 on SDS PAGE. Proteins with different structural conformations { ã \* | æc ^ Á c @! [ ~ \* @Á æÁ \* ^ | Á æc Á å ã ~ ~ ^ | ^ } c Æ! æc ^ • Á \* ã ç à ^ æå • q Á Ô Û G Ð Ô Ö G F Á ã • Á { ^ æ• ~ | ^ å Á | ^ | æc ã and ^ Á c [ Á æÁ \* | colleagues (1992) previously showed that soluble CR2, in its native state sCR2 behaved as a complex with a molecular weight of 320kDa(264). It is therefore possible that the immunoband detected in this study is indeed CR2.

Though not unambiguously clear these findings were thought to be convincing as the immunoband detected in monocyte samples was identical to the positive control (Raji B cells). Further identification of CR2 on the monocyte surface by FACS strengthened our belief that CR2 was indeed present on the surface of circulating monocytes. The use of confocal microscopy facilitated direct visualisation of CR2 on

monocytes. however, images obtained by confocal microscopy did not allow us to localise CR2 to either the surface or intracellular compartments of monocytes.

In addition to identifying CR2 on the surface of monocytes and U937 cells, early experiments with FACS were designed to assess whether CR2 surface expression may be up regulated by exposure to pro-inflammatory stimuli. Up regulation of complement receptors (CR4) has been previously shown to be a feature of activated monocytes(492). We elected to treat cells for a limited time (10min) with a variety of stimuli but did not find any significant change in expression. As with U937 work, this may reflect inadequate treatment time. The finding by Inada that rosetteing between C3d coated red blood cells and monocytes increased in a time dependant fashion , leads us to further question the shorter treatment period used in this study (255). If modifications could be made to this protocol it would include a longer treatment time (24 h) and inclusion of a sample exposed to levels of C3d previously measured in the airways of patients with ZZ AATD (40µg/ml).

Having shown that CR2 is expressed by monocytes in the circulation, we focused our attention on whether CR2 could be detected on monocytes and macrophages within the airways.

### **5.2.3 Identification of CR2 on lymphocyte subsets in the airways**

Within the lung, different lymphocyte subsets have traditionally been identified using histological examination and physical characteristics of cells such as size and granularity. Many published studies examining lymphocyte subsets in the airways rely principally on light scatter profiles generated during flow cytometry. These

however, can vary substantially depending on cell preparation and disease state. For this study we used both the physical characteristics of cells within the airways and multiple surface markers to identify various cell types. Our protocol was based heavily on the work of Yen et al., who originally published in the ATS journals (282). The Yen protocol was selected for usage as it was validated for usage in human tissues including BAL, whole bloods and lung tissue). Furthermore, it provided a flexible foundation for adding other analyses such as CR2.

During this study we utilised multi-colour flow cytometry to successfully identify CR2 on the surface of different lymphocyte subsets including monocytes and alveolar macrophages within the airways. Several factors prompted us early on to expand the

] ! [ b ^ & c Á c [ Á ã } & | ~ å ^ Á | [ [ \ ã } \* Á æ c Á | ^ { ] @[ & ^ c ^ Á • ~ à

colleagues had previously shown that levels of C3d were highest in the airways of individuals with ZZ AATD(78). Levels were noted to be 4-8 times higher. Moreover, foundational experiments using FACs to look for CR2 on the surface of U937 cells showed an increase in CR2 expression following treatment with PMA. Treatment of

U937 cells with PMA has been shown to activate protein kinase C (PKC) signalling

æ | c ^ ! ã } \* Á c @ ^ Á ^ ¢ ] ! ^ • • ã [ } Á [ ~ Á { ~ | c ã ] | ^ Á \* ^ } ^ • Á ç ã

activator protein-1 (AP-1)(489). Macrophages are key players in carrying out the

effector functions of complement. Expression of complement receptors including

CR1 (CD35), CR3 (CD11b/CD18), and CR4 (CD11c/CD18) by monocytes are

upregulated during the process of differentiation(360). In light of these observations

we hypothesised that CR2 expression may be increased on alveolar macrophages

compared to monocytes in the airways. Of note, though our surface marker panel is

configured to allow distinction between different macrophage populations (alveolar,

interstitial associated etc.) it is not designed to differentiate between resident and

recruited populations. This will be discussed further in Criticisms and Future Directions.

Our chosen antibody panel and gating strategy is presented in chapter four and is adapted from Yen et al., (2016)(282). We are satisfied that this approach is reliable and were further reassured by the fact that the authors validated their findings using a combination confocal microscopy and cell sorting(282). Over the past number of years, significant advances in the development of flow cytometers (and more recently again the use of spectral flow cytometry) has allowed facilitated the simultaneous measurement of in excess of 100 cell surface markers. The panel presented here could be easily adapted to identify other lymphocyte subsets such as neutrophils, eosinophils, T cells and natural killer cells within the airways and interrogate them for CR2. High levels of C3d in ZZ AATD combined with relatively high levels of CR2 expression on alveolar macrophages raises the intriguing question of what effect C3d may be having on macrophage behaviour within the airways.

Results presented here confirm that CR2 is detectable on the surface of alveolar macrophages and monocyte like cells within the airways. Unfortunately, collection of BAL samples for this project was stopped early owing to the global spread of COVID19 (discussed further in section 5.4 challenges and criticisms). Results presented here do not include ZZ samples and thus we cannot comment on whether CR2 expression on lymphocyte subsets differs between MM and ZZ states.

Having ascertained that CR2 is present on circulating and airway monocytes in addition to alveolar macrophages we next moved on to try and establish was effect C3d might be having on monocytes.

### 5.3.0 Establishing the effect of C3d on monocyte function

As discussed previously, Fee et al., has shown that binding of C3d to neutrophils increases the release of IL-8 in addition to triggering degranulation(188). A direct effect of C3d/CR2 binding has also been repeatedly shown in B cells. Binding of C3d to surface bound CR2 is known to lower the threshold of antigen exposure needed for B cell activation up to 10,000 fold(493). This prompted us to question what kind of effect C3d signalling through CR2 might have on monocytes in the context of AATD, a condition where levels of C3d are known to be elevated. A review of the literature confirmed that this research question had not been previously addressed.

Monocytes are well known for their ability to produce an extensive range of cytokines in response to pro-inflammatory stimuli. Less studied, though an evolving area of interest is the role monocytes play in the pathogenesis of various disease processes via the generation of proteases, specifically MMPs(442). Monocyte and macrophage derived MMPs have been implicated in the development of a plethora of lung diseases affecting both the airways and the interstitium(461). Increased production of MMPs has been well described in activated monocytes and monocytes

~ } å ^ ! \* [ ã } \* Á å ã ~ ~ ^ ! ^ } c ã æ c ã [ } È Á Œ& c ã ç æ c ã [ } Á [ ~ Á { [ LPS is known to induce expression of several MMPs including MMP -9, 1, -3, -7, -10, -12, -14 and -25(212, 494). Expression of several MMPs including MMP-8 have been shown to be upregulated in monocytes undergoing differentiation to macrophages(495).

As Fee had previously shown that neutrophils exposed to C3d produced increased levels of IL-8, this cytokine became our starting point for this work package. Early

results showed that U937 cells treated with C3d did not produce significantly increased levels of IL-8. LPS was included in these experiments and was found, as expected to significantly increase IL-8 production. This negative result raised two important questions: whether U937 cells were being treated with a sufficiently high concentration of C3d (highest concentration used was 10µg/ml, similar to plasma levels measured in ZZ AATD). It also prompted us to question whether C3d may be toxic to cells and reducing cell viability. U937 cells are robust malignant cells. By contrast, circulating monocytes are extremely sensitive to changes in their micro-environment and vulnerable to cell death via necrosis or apoptosis. Rapid loss of monocyte viability following 12 h exposure to bacteria has been previously described in the literature(387). This necessitated the performance of a cell viability assay for monocytes treated with C3d. Though several methods of assessing cell viability have been described(496), we elected to perform an MTS assay. Concentrations of C3d used in experiments assessing monocyte viability reflected concentrations previously measured in the plasma and airways of those with ZZ AATD(78). Results of MTS assays indicate that C3d does not cause a significant reduction in monocyte viability over a 24-h treatment period. Having confirmed this we proceeded to look at the downstream effects of C3d on monocyte function.

As part of this project, we utilised cytokine and protease array membranes to get an overview of what, if any effect C3d may have on monocytes. Array membranes are useful tools for generating hypotheses as they provide information about relative levels of cytokines and proteases simultaneously. Limitations of arrays include the fact that they do not reliably quantify the amount of analyte in a sample(407). In consideration of this, further exploration of array results was required from the outset.

Cytokine arrays results of supernatants of monocytes treated with C3d (10µg/ml) and untreated monocytes revealed detectable levels of CD14, MMP-9, MMP-13, TGF alpha, TGF beta and Fas ligand (n=3). Though trends towards increased or decreased levels of detectable cytokines were observed between treated and untreated samples, results did not achieve statistical significance. In view of this we decided to proceed with ELISA work using analytes that were of clinical relevance to our project which was focused on elucidating novel mechanisms underlying the pathogenesis of AATD. sCD14 was selected as expression of CD14 by monocytes is known to be altered in AATD(142). Levels of sCD14 have also previously been shown to correlate with lower lung function in MM COPD(414). MMP-9 was also identified as a target of interest as plasma levels of MMP-9 are known to be predictive of worsening lung density (p=0.003) and increased exacerbation frequency (p=0.003) in COPD in the setting of AATD(223). It has also been previously shown that levels of C3d in the plasma are reduced following IV AAT augmentation therapy. We reasoned that if monocytes exposed to C3d were producing excess MMP-9 in ZZ AATD this effect could be abrogated by augmentation mitigating the risk of decline in lung density and exacerbation frequency. As such, further investigation of the interplay between monocytes, C3d and MMP-9 was felt to be justifiable.

ELISAs for sCD14 confirmed increased levels of sCD14 in the supernatants of MM and ZZ monocytes exposed to C3d. It is not clear from these experiments what the source of this sCD14 is. High levels of sCD14 can reflect cleavage of mCD14 by proteases. Cleavage of CD14 by NE has been previously described and is thought to inhibit LPS mediated monocyte activation(412). Cleavage of surface bound CD14

By MMPs have also been reported. Waller et al (2019) identified that loss of CD14 from the surface of activated monocytes can be prevented by TMI005 which is known to inhibit the MMP ADAM-17(432). An alternative explanation for our findings is that higher levels of sCD14 are explainable by release of intracellular sCD14 stores in response to C3d treatment. Both processes have been previously described in activated monocytes(169, 497).

Further ELISA work also showed a significant increase in MMP-9 production by monocytes treated with a concentration of C3d that was comparable to that measured by O'Brien et al (2020) in the airways of individuals with ZZ AATD. Difference in basal rates of MMP-9 production between MM and ZZ groups did not differ significantly. MMP-9 was of particular interest to us owing to its recognised ability to amplify the effects of serine proteases such as NE via the inactivation of AAT(438). We hypothesise that increased monocyte production of MMP-9 in response to C3d may inactivate residual ZZ AAT protein facilitating protease driven degradation of the lung ECM.

Following on from the cytokine array and ELISAs for sCD14 and MMP-9 we next turned our attention to protease arrays. Results of protease array analyses did identify significant differences between treated and untreated MM and ZZ monocytes. Broadly speaking, array results suggested increased levels of select MMPs 1, 12 and 9, cathepsins and PR3. In light of our successful experiences with MMP-9, and the well-established role of MMP-12 in development of emphysema (463) we elected to further explore a link between C3d and monocyte production of MMPs over cathepsins. ELISAs for MMP-12 in plasma samples confirmed a significant increase in MMP-12 in the plasma of those with ZZ AATD and those with an AECOPD (MM) compared to healthy controls. However, we also showed no

significant increase in MMP-12 in the supernatants of monocytes treated with C3d. This suggests that monocytes are unlikely to be the source of MMP-12 we observed in ZZ plasma.

In addition to its effect on production of MMPs, protease arrays indicated that C3d might be increasing the production of the serine protease PR3. Increased monocyte production of PR3 has been previously reported in AAVs which are known to have a greater incidence in ZZ AATD compared to MM cohorts.(467) PR3 is an important target of AAT augmentation and previous studies have shown that AAT can reduce the activity of PR3 in vivo(475). PR3 is known to be stored within monocytic lysosomes and is released during monocytes activation(498). ELISAs for PR3 in monocyte supernatants showed that treatment with C3d significantly increased production of PR3 by both MM and ZZ monocytes. Though a trend towards increased basal levels of PR3 was observed in untreated ZZ monocyte supernatants, this result did not achieve statistical significance. It is worthy to note that cleavage of membrane bound CD14 by other serine proteases such as NE has been previously described(412). This raises the possibility that rising levels of PR3 may be linked to higher levels of sCD14 observed in C3d treated monocyte supernatants.

Interpreted collectively, the results presented here raise the question of whether monocytes may be activated by the presence of C3d. Published data has previously identified high level of sCD14, MMP-9 and PR3 as markers of monocyte activation(212, 498, 499). Further clarity on this point could be achieved by using multi colour FACS to look for markers of monocyte activation such as CD62L and CD11b on the surface of C3d treated monocytes(500).

## 5.4 Challenges and criticisms

This project was commenced in July of 2018 and was scheduled to continue sample collection and analyses. The unfortunate, but unavoidable global spread of the SARS Co-V2 virus meant that the planned schedule for experiments to be undertaken as part of the final work package from January-July 2020 had to be altered substantially. In March of 2020, the Irish government announced the closure of all non-essential businesses, schools, and universities. This nationwide lock down was undertaken to curb the spread of the SARS-CoV-2 virus and mitigate the down-stream effects on the healthcare service. As a respiratory Higher specialist trainee (HST) with an interest in managing acute respiratory failure, my skill-set was felt to be of use and I returned to clinical work from March-June of 2020. Though this period was undoubtedly one of the greatest learning experiences of my medical career and undertaken without hesitation, it came at the cost of time spent in the lab. I was fortunate to be able to return to bench work in June to complete outstanding ELISA experiments before a return to full time clinical work in July of 2020.

In parallel with this, the cancellation of face to face outpatient clinics and move to an online format from May-July further stymied collection of samples. AATD is categorised as a rare lung disease. As such, services for patients with AATD from all over Ireland are centralised to one tertiary referral centre (Beaumont Hospital). Patients seen in the AATD clinic hail from all 26 counties within the republic of Ireland and were unable, or understandably reluctant to travel to Dublin as restrictions began to ease in the Summer of 2020. Arising from this, for the recruited number of ZZ-AATD patients is low. Nevertheless, we feel that results presented here are useful for the purposes of generating hypotheses and may inform future research in the area.

Regretfully collection of BAL samples ceased completely in March of 2020.

Bronchoscopy is classified as an aerosol generating procedure (AGP). To continue non-essential bronchoscopy, particularly as community transmission of COVID19 was rising, posed an unacceptable risk to nursing and medical staff and thus sample collection had to be terminated prematurely. The net effect of this was that our n number for airway samples was very low (n=3). Interpretation and application of these findings is limited for several reasons. Samples used were obtained from 3 very different patients including a healthy control, a patient with a primary diagnosis of airways disease and a patient with a primary diagnosis of interstitial lung disease. The low number precludes any comment being made on the variability of CR2 expression between disease states. Several studies have previously implicated the development of the interstitial fibrosis that characterises ILD to the production of MMPs by AMs and monocyte derived macrophages within the airways.

Other challenges encountered included identifying a profile of surface markers that would enable us to distinguish different lymphocyte subsets within the airways. Several different approaches have been described in the literature(282, 501). Having reviewed available data, we opted to follow the approach of Yen and colleagues who included surface markers CD45, CD16, CD14, CD169, CD206, CD24 and a live/dead stain. This panel was selected as it allowed for clear delineation between different lymphocyte subtypes in airways samples. We felt that the inclusion of both cell surface markers and data about the physical characteristics of different cell types (size, granularity etc.) enabled more accurate identification of subpopulations. This approach is also in line with the most up to date literature on distinguishing monocyte subsets which was reassuring(479). Yen and colleagues use the term monocytes to describe agranular cells (low side scatter) that express CD45, CD16, CD14 +ve and

do not express CD206. Some debate has been had about whether monocytes can be identified in airway samples or whether such cells are representative of a macrophage population. As Yen and colleagues use both surface markers and the physical characteristics of cells to identify sub populations, we are confident that use of the term monocytes to describe these cells is appropriate. It is worthy of note that other published studies have identified similar populations within BAL samples that are consistently labelled as monocytes. Gracia et al (2018) identified high levels of MMP-10 producing classical monocytes within the airways of children suffering from fatal asthma. In addition to CD14/CD16 they used CD68 as monocyte marker(502). In a separate study, Byrne et al profiled lymphocyte subsets in whole blood and BAL samples from children, adults and adults over the age of 50. They used the surface markers HLA-DR, CD45, CD16 and CD16 to identify monocyte subsets in BAL samples(503). They showed that the proportions of blood and BAL classical monocytes peak in adulthood and decline as part of normal healthy aging. In view of established precedent in published literature we are satisfied that our labelling and use of the term monocyte to describe CD14/CD16+ve cells is justified.

macrophages (CD169-). Given the authors validated their macrophage characterisation using confocal microscopy, and that CD169 has been used in other human studies to distinguish macrophage subsets, we were satisfied that its use as part of our panel was valid(282, 501).

Further complicating this study was an evolving understanding of monocyte ontogeny and behaviour. This is an area of study that has evolved considerably over the past 10 years. Indeed the first description of IMs in humans was only published in 2010(507). Furthermore, many aspects of monocyte behaviour are poorly understood, and the immune functions of different subsets remain ill defined.

Conflicting results in published literature has led to considerable debate regarding the functions of specific sub populations(508-511). Recently Mourah et al (March 2020) described 6 different monocyte subsets in the human circulation. Their experimental protocol included 15 surface markers, distinction based on physical characteristics such as size and granularity and the nature of the cytokine response produced in response to an LPS trigger(479). The authors note that in order to facilitate identification of sub population of monocytes, high cell throughput was required with analysis of  $>1 \times 10^6$  events during FACS analysis. Monocytes represent  $<10\%$  of the total number of lymphocytes in whole blood(286).

Consequently, the study of human monocytes in circulation requires relatively large volumes of bloods to be taken during phlebotomy to ensure adequate cell yield. Typically, 20ml of whole blood were needed to achieve a monocyte count of  $2.5 \times 10^6$  cells. Replicating Mourahs work and further developing it by probing monocytes for CR2 would therefore require very large volumes of blood to ensure that rare cell populations could be identified.

This challenge was highlighted during our multi colour flow cytometry work with BAL samples. CM and NCMs were present in small numbers within our BAL samples. Once background signal was eliminated by applying the FMO control the number of cells left to interrogate for CCR2 was <20 across all subtypes. This emphasises the importance of getting a good return and cell yield during BAL if relatively rare cell populations are being examined. Despite this we identified three monocyte-like cell types in airway samples that phenotypically resemble each of the 3 main monocytes in airways. The representation of monocyte subsets in the airways (IM>NCM>CM) was the inverse of what is described in the circulation (CM>IM>NCM). This is interesting for several reasons. Historically, IM and NCMs are thought not to be recruited to the lungs. Recruitment of monocytes from the circulation occurs via CCR2, the expression of which is confined to CMs(155). A possible explanation for our finding is that once established within the lungs, CMs rapidly differentiate into AMs. Monocytes that are not prompted by signals in the microenvironment to differentiate to an AM phenotype may instead undergo a slow differentiation into an IM and eventually NCM phenotype. This phenomenon is well described in monocytes present in the circulation(122). Performing the same panel on a higher number of patients with differing diagnoses would also allow assessment of whether the proportional representation of each monocyte subsets varies between disease states.

Interpretation of or planning experiments with monocytes should be undertaken with adequate consideration given to a rapidly evolving understanding of monocyte ontogeny. There are several commercially available kits on the market for isolating monocytes from circulation that may preferentially isolate one subset over another. In early versions of these experiments, we used the Easy Sep Human CD14

selection kit to obtain monocytes. This kit used the principle of positive selection to pull monocytes from circulation. Dextran coated nanoparticles label CD14 positive cells and a magnet is used to isolate the cells from lymphocytes that do not express CD14. Whilst the technical simplicity of this was inherently appealing, we quickly

express CD14 as strongly such as IM and NCMs. NCMs which are known to be

has been associated with the immunopathogenesis of inflammatory disorders such as inflammatory arthritis and sepsis(512). NCMs also have the longest half- life of all the monocyte subsets in the circulation and we were keen that our results would incorporate the function of all 3 known human subsets. In consideration of this, we switched our isolation protocol and to use the Easy Sep monocyte isolation kit without CD16 depletion. This kit works on the principle of negative selection and preserves lymphocytes which express CD14 and CD16. This kit was selected for use in ELISA experiments as we did not want to restrict our observations to CMs alone. As monocytes in the circulation represent a heterogenous cell population we wanted our ELISA results to reflect the actions of the 3 subsets which exist in a state of dynamic equilibrium in the circulation.

ELISAs performed as part of this project included ELISAs for MMP-1, 9 and 12, IL-8, sCD14 and PR3. Limited access to samples attributable to COVID19 limited sample number for each run. As the number presented here is small, our results warrant further repeating before definitive conclusions can be made about the role C3d plays in disease pathogenesis in AATD. Of further use would be a blocking experiment to ensure that the effect we are seeing is directly attributable to an effect of C3d.

Blocking the CR2 receptor with an anti-body or peptide prior to treatment with C3d

would allow us to discern whether the increases in MMP-9, PR3 and sCD14 that we observed are directly attributable to an effect of an interaction between C3d and CR2.

## 5.5 Future Directions

Data presented as part of this MD thesis has shown a receptor for the complement fragment C3d, CR2/CD21 on the receptor of monocytes in the circulation. Multi colour flow cytometry was used to further demonstrate CR2/CD21 on the surface of monocyte like cells and macrophages in the airways. ELISA work presented suggests that exposure of monocytes to C3d results in increased production of MMP-9, PR3 and sCD14.

This raises the important question of what effect C3d may be having on monocyte derived macrophages within the airways. Further study of airway macrophage populations and their response to C3d represents a natural stepping-stone for this project. The study of role of macrophages at this moment in time is prudent in the setting of the ongoing COVID19 pandemic. COVID19 has stimulated a huge amount of activity in research labs world-wide. There can be little doubt that our understanding of monocyte ontogeny will develop rapidly as COVID19 fuels further investment in scientific research. Much of the published data has focused on the use of cytokine levels as predictors of disease progression or as potential therapeutic targets (513). Early in the pandemic IL-6 was noted to be elevated in patients with COVID19. Aegerter et al (2020) have previously identified monocyte derived macrophages (MoAM) in the airways as the major producers of IL-6 in the lungs following viral infection (influenza)(155). It is noteworthy that elevations in levels of IL-6 several orders of magnitude higher have been previously observed in other life-threatening conditions such as sepsis and ARDS not attributable to COVID19 infection(513). Monocytes are known to produce IL-6 in response to a pro-inflammatory trigger(299). It would, therefore, be interesting to challenge monocytes and macrophages with C3d and measure their IL-6 response.

Our multi colour FACS identified high levels of expression of CR2/CD21 on the surface of AMs. As our chosen anti-body panel was not designed to distinguish resident versus recruited MoAMs, it is likely to be a mixed population of both. An emerging evidence base suggests that under steady state conditions macrophage populations within the lung interstitium, airways and alveolar spaces are self-sustaining populations(153). These cells are derived from embryonic stem cells and seeded to the lungs shortly following birth. Studies using murine models have shown that during times of inflammation or injury, this embryonic population is consumed rapidly and replenished by monocytes recruited from the circulation(514).

Proportional representation of MoAMs also increases with aging(153, 515). MoAMs are known to possess distinct transcriptomic profiles to resident/ embryonic AMs and are primed to generate an inflammatory response(155). Further work might also focus on establishing whether CR2/CD21 expression differs between resident and recruited populations. Addressing this question may prove challenging as there is currently no consensus on what surface markers or physical characteristics of macrophage populations might distinguish between tissue resident (TRAM) and recruited alveolar macrophage (MoAM) populations.

Owing to the cancellation of bronchoscopy lists and the travel restrictions imposed by COVID19, our multi colour FACS experiments did not include samples from those with ZZ AATD. As levels of C3d within the airways are notably higher in ZZ AATD, it would be useful to explore the downstream effects of this on macrophages in AATD. As alluded to previously, Fee et al (2019) have shown a direct effect of C3d on neutrophils that results in degranulation of primary, secondary and tertiary granule proteins(188). Our data shows that expression of CR2 is much greater on MM AMs than monocytes within the airways. This confirms availability of a signalling axis for

C3d in airway macrophages and raises the question of what effects relatively high concentrations of C3d in ZZ airways may be having on macrophage behaviour. A further avenue worth exploring would be to assess whether or not treatment with OECEV Á æ à ! [ \* æ c ^ • Á c @ ^ Á ^ ~ ~ ^ & c • Á [ ~ Á Ô H å È Á U q Ó ! ã ^ } Á ^ c augmentation reduces levels of C3d significantly(78). Thus, if C3d is found to be having a similar effect on macrophage production of MMPs and PR3 within the airways, IV AAT may function as a therapeutic strategy for managing patients with high levels of C3d and progressive lung disease.

Our data establishes an effect of C3d on monocytes, further expanding our understanding of the mechanisms of disease pathogenesis in AATD. With very high levels of C3d described within ZZ airways establishing the effects of C3d on AMs is compelling.

## References

1. Janciauskiene SM, Bals R, Koczulla R, Vogelmeier C, Köhnlein T, Welte T. Alpha-1 antitrypsin deficiency and its role in health and disease. *Respiratory Medicine*. 2011;105(8):1129-39.
2. Darlington GJ, Astrin KH, Muirhead SP, Desnick RJ, Smith M. Assignment of human alpha 1-antitrypsin to chromosome 14 by somatic cell hybrid analysis. *Proceedings of the National Academy of Sciences of the United States of America*. 1982;79(3):870-3.
3. Wysocki J. Alpha-1 antitrypsin: classification and clinical implications. *Pneumonologia i alergologia polska*. 2013;81(1):45-54.
4. de Serres F, Blanco I. Role of alpha-1 antitrypsin in human health and disease. *Journal of internal medicine*. 2014;276(4):311-35.
5. Chambers DC, Cherikh WS, Harhay MO, Hayes D, Jr., Hsich E, Khush KK, et al. The International Thoracic Organ Transplant Registry of the International Society for Heart and Lung Transplantation: Thirty-sixth adult lung and heart-lung transplantation Report-2019; Focus theme: Donor and recipient size match. *J Heart Lung Transplant*. 2019;38(10):1042-55.
6. Laurell CB, Eriksson S. The electrophoretic alpha1-globulin pattern of serum in alpha1-antitrypsin deficiency. 1963. *Copd*. 2013;10 Suppl 1:3-8.
7. Sveger T. Liver disease in alpha1-antitrypsin deficiency detected by screening of 200,000 infants. *The New England journal of medicine*. 1976;294(24):1316-21.
8. Luisetti M, Seersholm N. Alpha1-antitrypsin deficiency. 1: epidemiology of alpha1-antitrypsin deficiency. *Thorax*. 2004;59(2):164-9.
9. Franciosi AN, Carroll TP, McElvaney NG. Pitfalls and caveats in alpha1-antitrypsin deficiency testing: a guide for clinicians. *Lancet Respir Med*. 2019;7(12):1059-67.
10. Viegi G, Pistelli F, Sherrill DL, Maio S, Baldacci S, Carrozzi L. Definition, epidemiology and natural history of COPD. *European Respiratory Journal*. 2007;30(5):993-1013.
11. Song S. Alpha-1 Antitrypsin Therapy for Autoimmune Disorders. *Chronic Obstr Pulm Dis*. 2018;5(4):289-301.
12. Carroll TP, O'Connor CA, Floyd O, McPartlin J, Kelleher DP, O'Brien G, et al. The prevalence of alpha-1 antitrypsin deficiency in Ireland. *Respiratory Research*. 2011;12(1):91.
13. Kelly E, Greene CM, Carroll TP, McElvaney NG, O'Neill SJ. Alpha-1 antitrypsin deficiency. *Respir Med*. 2010;104(6):763-72.
14. van Furth R, Kramps JA, Diesselhof-den Dulk MM. Synthesis of alpha 1-antitrypsin by human monocytes. *Clin Exp Immunol*. 1983;51(3):551-7.
15. Mornex JF, Chytil-Weir A, Martinet Y, Courtney M, LeCocq JP, Crystal RG. Expression of the alpha-1-antitrypsin gene in mononuclear phagocytes of normal and alpha-1-antitrypsin-deficient individuals. *J Clin Invest*. 1986;77(6):1952-61.
16. du Bois R, Bernaudin J, Paakko P, Hubbard R, Takahashi H, Ferrans V, et al. Human neutrophils express the alpha 1-antitrypsin gene and produce alpha 1-antitrypsin. *Blood*. 1991;77(12):2724-30.
17. Molmenti EP, Perlmutter DH, Rubin DC. Cell-specific expression of alpha 1-antitrypsin in human intestinal epithelium. *J Clin Invest*. 1993;92(4):2022-34.
18. Loebermann H, Tokuoka R, Deisenhofer J, Huber R. Human alpha 1-proteinase inhibitor. Crystal structure analysis of two crystal modifications, molecular

model and preliminary analysis of the implications for function. *J Mol Biol.* 1984;177(3):531-57.

19. Ekeowa UI, Freeke J, Miranda E, Gooptu B, Bush MF, Perez J, et al. Defining the mechanism of polymerization in the serpinopathies. *Proceedings of the National Academy of Sciences of the United States of America.* 2010;107(40):17146-51.

20. Huntington JA, Read RJ, Carrell RW. Structure of a serpin-protease complex shows inhibition by deformation. *Nature.* 2000;407(6806):923-6.

21. Lockett AD, Van Demark M, Gu Y, Schweitzer KS, Sigua N, Kamocki K, et al. Interaction with caspases. *Mol Med.* 2012;18(1):445-54.

22. Lomas DA. Twenty Years of Polymers: A Personal Perspective on Alpha-1 Antitrypsin Deficiency. *COPD: Journal of Chronic Obstructive Pulmonary Disease.* 2013;10(sup1):17-25.

23. DeMeo DL, Silverman EK. Alpha1-antitrypsin deficiency. 2: genetic aspects of alpha(1)-antitrypsin deficiency: phenotypes and genetic modifiers of emphysema risk. *Thorax.* 2004;59(3):259-64.

24. Ottaviani S, Gorrini M, Scabini R, Kadija Z, Paracchini E, Mariani F, et al. C reactive protein and alpha1-antitrypsin: relationship between levels and gene variants. *Transl Res.* 2011;157(6):332-8.

25. Ferrarotti I, Thun GA, Zorzetto M, Ottaviani S, Imboden M, Schindler C, et al. Serum levels and genotype distribution of alpha1-antitrypsin in the general population. *Thorax.* 2012;67(8):669-74.

26. McCarthy C, Saldoval R, Wormald MR, Rudd PM, McElvaney NG, Reeves EP. The role and importance of glycosylation of acute phase proteins with focus on alpha-1 antitrypsin in acute and chronic inflammatory conditions. *Journal of proteome research.* 2014;13(7):3131-43.

27. Kolarich D, Turecek PL, Weber A, Mitterer A, Graninger M, Matthiessen P, et al. Biochemical, molecular characterization, and glycoproteomic analyses of alpha(1)-proteinase inhibitor products used for replacement therapy. *Transfusion.* 2006;46(11):1959-77.

28. Mosheimer B, Alzner R, Wiedermann CJ. Immunomodulation by alpha(1)-proteinase inhibitor: lack of chemotactic effects of recombinant human alpha(1)-proteinase inhibitor from yeast on human peripheral blood granulocytes. *Arch Immunol Ther Exp (Warsz).* 2007;55(6):399-403.

29. Renoux C, Odou M-F, Tosato G, Teoli J, Abbou N, Lombard C, et al. Description of 22 new alpha-1 antitrypsin genetic variants. *Orphanet Journal of Rare Diseases.* 2018;13(1):161.

30. Dela Cruz CS, Lee Y, Viswanathan SR, El-Guindy AS, Gerlach J, Nikiforow S, et al. N-linked glycosylation is required for optimal function of Kaposi's sarcoma herpesvirus-encoded, but not cellular, interleukin 6. *J Exp Med.* 2004;199(4):503-14.

31. McCarthy C, Dunlea DM, Saldoval R, Henry M, Meleady P, McElvaney OJ, et al. Glycosylation Repurposes Alpha-1 Antitrypsin for Resolution of Community-acquired Pneumonia. *American journal of respiratory and critical care medicine.* 2018;197(10):1346-9.

32. Bergin DA, Reeves EP, Meleady P, Henry M, McElvaney OJ, Carroll TP, et al. alpha-1 Antitrypsin regulates human neutrophil chemotaxis induced by soluble immune complexes and IL-8. *J Clin Invest.* 2010;120(12):4236-50.

33. Cox DW, Woo SLC, Mansfield T. DNA restriction fragments associated with Antitrypsin indicate a single origin for deficiency allele PI Z. *Nature.* 1985;316(6023):79-81.

34. Eriksson S, Carlson J, Velez R. Risk of cirrhosis and primary liver cancer in alpha 1-antitrypsin deficiency. *The New England journal of medicine*. 1986;314(12):736-9.
35. Holme J, Stockley RA. CT scan appearance, densitometry, and health status in protease inhibitor SZ alpha1-antitrypsin deficiency. *Chest*. 2009;136(5):1284-90.
36. Molloy K, Hersh CP, Morris VB, Carroll TP, O'Connor CA, Lasky-Su JA, et al.  $\alpha_1$ -antitrypsin deficiency PiMZ heterozygotes. *American journal of respiratory and critical care medicine*. 2014;189(4):419-27.
37. Blanco I, Bueno P, Diego I, Pérez-Holanda S, Lara B, Casas-Maldonado F, et al. Alpha-1 antitrypsin Pi\*SZ genotype: estimated prevalence and number of SZ subjects worldwide. *Int J Chron Obstruct Pulmon Dis*. 2017;12:1683-94.
38. Cummings EE, O'Reilly LP, King DE, Silverman RM, Miedel MT, Luke CJ, et al. Deficient and Null Variants of SERPINA1 Are Proteotoxic in a *Caenorhabditis elegans*  $\alpha_1$ -Antitrypsin Deficiency. *PLoS One*. 2015;10(10):e0141542-e.
39. Uric  $\alpha_1$ -antitrypsin deficiency. *Effects of Rare SERPINA1 Variants on Lung Function and Emphysema in SPIROMICS*. *American journal of respiratory and critical care medicine*. 2020;201(5):540-54.
40.  $\alpha_1$ -antitrypsin deficiency: emerging therapeutic strategies for a challenging disease. *Dis Model Mech*. 2014;7(4):411-9.
41. Donato LJ, Snyder MR, Greene DN. Measuring and Interpreting Serum AAT Concentration. *Methods in molecular biology* (Clifton, NJ). 2017;1639:21-32.
42. Greulich T, Nell C, Hohmann D, Grebe M, Janciauskiene S, Koczulla AR, et al.  $\alpha_1$ -antitrypsin deficiency and its comorbidities: results from a large population-based database. *European Respiratory Journal*. 2017;49(1):1600154.
43. Nielsen CH, Poulsen HK, Teisner B, Thorsen P, Hau J, Westergaard JG. Changes in blood levels of proteinase inhibitors, pregnancy zone protein, steroid carriers and complement factors induced by oral contraceptives. *European Journal of Obstetrics & Gynecology and Reproductive Biology*. 1993;51(1):63-71.
44. American Thoracic Society/European Respiratory Society statement: standards for the diagnosis and management of individuals with alpha-1 antitrypsin deficiency. *American journal of respiratory and critical care medicine*. 2003;168(7):818-900.
45. Greene DN, Elliott-Jelf MC, Straseski JA, Grenache DG. Facilitating the diagnosis of  $\alpha_1$ -antitrypsin deficiency. *American journal of clinical pathology*. 2013;139(2):184-91.
46. Udvardi MK, Czechowski T, Scheible W-R. Eleven Golden Rules of Quantitative RT-PCR. *The Plant Cell*. 2008;20(7):1736-7.
47. Miravittles M, Dirksen A, Ferrarotti I, Koblizek V, Lange P, Mahadeva R, et al. European Respiratory Society statement: diagnosis and treatment of pulmonary  $\alpha_1$ -antitrypsin deficiency. *The European respiratory journal*. 2017;50(5).
48. Alpha 1-antitrypsin deficiency: memorandum from a WHO meeting. *Bulletin of the World Health Organization*. 1997;75(5):397-415.
49. Thelin T, Sveger T, McNeil T. Primary prevention in a high-risk group: smoking habits in adolescents with homozygous alpha-1-antitrypsin deficiency (ATD). *Acta Paediatrica*. 1996;85(10):1207-12.

50. Fantitrypsin deficiency. 1963. *Copd*. 2013;10 Suppl 1:3-8.
51. Hersh CP, Campbell EJ, Scott LR, Raby BA. Alpha-1 Antitrypsin Deficiency as an Incidental Finding in Clinical Genetic Testing. *American journal of respiratory and critical care medicine*. 2019;199(2):246-8.
52. Schultze HE, Heide K, Haupt H. [alpha1-Antitrypsin from human serum]. *Klinische Wochenschrift*. 1962;40:427-9.
53. Beatty K, Bieth J, Travis J. Kinetics of association of serine proteinases with native and oxidized alpha-1-proteinase inhibitor and alpha-1-antichymotrypsin. *The Journal of biological chemistry*. 1980;255(9):3931-4.
54. Bergin DA, Hurley K, McElvaney NG, Reeves EP. Alpha-1 antitrypsin: a potent anti-inflammatory and potential novel therapeutic agent. *Arch Immunol Ther Exp (Warsz)*. 2012;60(2):81-97.
55. Kessenbrock K, Dau T, Jenne DE. Tailor-made inflammation: how neutrophil serine proteases modulate the inflammatory response. *J Mol Med (Berl)*. 2011;89(1):23-8.
56. Pham CTN. Neutrophil serine proteases fine-tune the inflammatory response. *Int J Biochem Cell Biol*. 2008;40(6-7):1317-33.
57. Sinden N, Dafforn T, Stockley R. Inhibitory profiles of alpha-1-antitrypsin from PiZ & PiSZ individuals and implications for tissue destruction in emphysema. *European Respiratory Journal*. 2011;38(Suppl 55):p3909.
58. Potempa J, Korzus E, Travis J. The serpin superfamily of proteinase inhibitors: structure, function, and regulation. *The Journal of biological chemistry*. 1994;269(23):15957-60.
59. Chen ZQ, He SH. Cloning and expression of human colon mast cell carboxypeptidase. *World journal of gastroenterology*. 2004;10(3):342-7.
60. Mahrus S, Kisiel W, Craik CS. Granzyme M is a regulatory protease that inactivates proteinase inhibitor 9, an endogenous inhibitor of granzyme B. *The Journal of biological chemistry*. 2004;279(52):54275-82.
61. Janciauskiene S, Nita I, Subramaniam D, Li Q, Lancaster JR, Jr., Matalon S. Alpha1-antitrypsin inhibits the activity of the matriptase catalytic domain in vitro. *American journal of respiratory cell and molecular biology*. 2008;39(6):631-7.
62. Bergin DA, Reeves EP, Meleady P, Henry M, McElvaney OJ, Carroll TP, et al. -1 Antitrypsin regulates human neutrophil chemotaxis induced by soluble immune complexes and IL-8. *J Clin Invest*. 2010;120(12):4236-50.
63. Petrache I, Fijalkowska I, Medler TR, Skirball J, Cruz P, Zhen L, et al. alpha-1 antitrypsin inhibits caspase-3 activity, preventing lung endothelial cell apoptosis. *The American journal of pathology*. 2006;169(4):1155-66.
64. Hubbard RC, Fells G, Gadek J, Pacholok S, Humes J, Crystal RG. Neutrophil accumulation in the lung in alpha 1-antitrypsin deficiency. Spontaneous release of leukotriene B4 by alveolar macrophages. *The Journal of clinical investigation*. 1991;88(3):891-7.
65. Malerba M, Ricciardolo F, Radaeli A, Torregiani C, Ceriani L, Mori E, et al. Neutrophilic inflammation and IL-8 levels in induced sputum of alpha-1-antitrypsin PiMZ subjects. *Thorax*. 2006;61(2):129-33.
66. Bergin DA, Reeves EP, Hurley K, Wolfe R, Jameel R, Fitzgerald S, et al. The & ã | & ~ | æ c ã } \* Á ] : [1 antitrypsin regulates neutrophil degranulation and autoimmunity. *Science translational medicine*. 2014;6(217):217ra1.
67. Young RE, Voisin MB, Wang S, Dangerfield J, Nourshargh S. Role of neutrophil elastase in LTB4-induced neutrophil transmigration in vivo assessed with

a specific inhibitor and neutrophil elastase deficient mice. *Br J Pharmacol*. 2007;151(5):628-37.

68. Ford-Hutchinson AW, Bray MA, Doig MV, Shipley ME, Smith MJ. Leukotriene B<sub>4</sub>, a potent chemokinetic and aggregating substance released from polymorphonuclear leukocytes. *Nature*. 1980;286(5770):264-5.

69. Hoover RL, Karnovsky MJ, Austen KF, Corey EJ, Lewis RA. Leukotriene B<sub>4</sub> action on endothelium mediates augmented neutrophil/endothelial adhesion. *Proceedings of the National Academy of Sciences of the United States of America*. 1984;81(7):2191-3.

70. O'Dwyer CA, O'Brien ME, Wormald MR, White MM, Banville N, Hurley K, et al. Alpha-1 Antitrypsin Augmentation Therapy Disrupts Leukotriene B<sub>4</sub> Neutrophil Signaling. *Journal of immunology (Baltimore, Md : 1950)*. 2015;195(8):3628-41.

71. Serban KA, Petrache I. Alpha-1 Antitrypsin and Lung Cell Apoptosis. *Ann Am Thorac Soc*. 2016;13 Suppl 2(Suppl 2):S146-S9.

72. Pardo A, et al. Alpha-1 Antitrypsin Augmentation Therapy Corrects Accelerated Neutrophil Apoptosis in Deficient Individuals. *The Journal of Immunology*. 2014;193(8):3978-91.

73. Bucurenci N, Blake DR, Chidwick K, Winyard PG. Inhibition of neutrophil superoxide production by human plasma alpha 1-antitrypsin. *FEBS letters*. 1992;300(1):21-4.

74. Janciauskiene SM, Nita IM, Stevens T. Alpha1-antitrypsin, old dog, new tricks. Alpha1-antitrypsin exerts in vitro anti-inflammatory activity in human monocytes by elevating cAMP. *The Journal of biological chemistry*. 2007;282(12):8573-82.

75. Elliott PR, Bilton D, Lomas DA. Lung polymers in Z alpha1-antitrypsin deficiency-related emphysema. *American journal of respiratory cell and molecular biology*. 1998;18(5):670-4.

76. Mahadeva R, Atkinson C, Li Z, Stewart S, Janciauskiene S, Kelley DG, et al. Polymers of Z alpha1-antitrypsin co-localize with neutrophils in emphysematous alveoli and are chemotactic in vivo. *The American journal of pathology*. 2005;166(2):377-86.

77. Parmar JS, Mahadeva R, Reed BJ, Farahi N, Cadwallader KA, Keogan MT, et al. Polymers of alpha(1)-antitrypsin are chemotactic for human neutrophils: a new paradigm for the pathogenesis of emphysema. *American journal of respiratory cell and molecular biology*. 2002;26(6):723-30.

78. O'Brien ME, Fee L, Browne N, Carroll TP, Meleady P, Henry M, et al. Activation of complement component 3 is associated with airways disease and pulmonary emphysema in alpha-1 antitrypsin deficiency. *Thorax*. 2020;75(4):321-30.

79. Villacorta J, Diaz-Crespo F, Acevedo M, Guerrero C, Campos-Martin Y, García-Díaz E, et al. Glomerular C3d as a novel prognostic marker for renal vasculitis. *Human pathology*. 2016;56:31-9.

80. Sjöström M, et al. Alpha-1 Antitrypsin Deficiency. *Scandinavian Journal of Clinical and Laboratory Investigation*. 1963;15(2):132-40.

81. Sharafkhaneh A, Hanania NA, Kim V. Pathogenesis of emphysema: from the bench to the bedside. *Proc Am Thorac Soc*. 2008;5(4):475-7.

82. Hutchison DC. Homozygous and heterozygous alpha-1-antitrypsin deficiency: prevalence in pulmonary emphysema. *Proceedings of the Royal Society of Medicine*. 1976;69(2):130-1.

83. Parr DG, Stoel BC, Stolk J, Stockley RA. Pattern of Emphysema Distribution in Alpha-1 Antitrypsin Deficiency Influences Lung Function Impairment. *American journal of respiratory and critical care medicine*. 2004;170(11):1172-8.
84. Petersson J, Glenny RW. Gas exchange and ventilation-perfusion relationships in the lung. *European Respiratory Journal*. 2014;44(4):1023-41.
85. Senn O, Russi EW, Imboden M, Probst-Peterson A, & Altmeppen T. Alpha-1 antitrypsin deficiency and lung disease: risk modification by occupational and environmental inhalants. *European Respiratory Journal*. 2005;26(5):909-17.
86. Uccelli L, Rizzato P, Sestini E, et al. Alpha-1 antitrypsin deficiency. *American journal of respiratory and critical care medicine*. 2012;185(3):246-59.
87. Esquinas C, Serreri S, Barrecheguren M, Rodriguez E, Nuñez A, Casas-Maldonado F, et al. Long-term evolution of lung function in individuals with alpha-1 antitrypsin deficiency from the Spanish registry (REDAAT). *Int J Chron Obstruct Pulmon Dis*. 2018;13:1001-7.
88. Tanash HA, Ekström M, Rönmark E, Lindberg A, Piitulainen E. Survival in individuals with severe alpha 1-antitrypsin deficiency (PiZZ) in comparison to a general population with known smoking habits. *European Respiratory Journal*. 2017;50(3):1700198.
89. King PT. The pathophysiology of bronchiectasis. *Int J Chron Obstruct Pulmon Dis*. 2009;4:411-9.
90. Tobin MJ, Cook PJ, Hutchison DC. Alpha 1 antitrypsin deficiency: the clinical and physiological features of pulmonary emphysema in subjects homozygous for Pi type Z. A survey by the British Thoracic Association. *British journal of diseases of the chest*. 1983;77(1):14-27.
91. Parr DG, Guest PG, Reynolds JH, Dowson LJ, Stockley RA. Prevalence and impact of bronchiectasis in alpha1-antitrypsin deficiency. *American journal of respiratory and critical care medicine*. 2007;176(12):1215-21.
92. Uebachs W, et al. [Alpha-1 antitrypsin deficiency]. *European respiratory review* : an official journal of the European Respiratory Society. 2015;24(137):474-83.
93. Suárez-Lorenzo I, de Castro FR, Cruz-Niesvaara D, Herrera-Ramos E, Rodríguez-Gallego C, Carrillo-Díaz T. Alpha 1 antitrypsin distribution in an allergic asthmatic population sensitized to house dust mites. *Clinical and Translational Allergy*. 2018;8(1):44.
94. Mitchell EL, Khan Z. Liver Disease in Alpha-1 Antitrypsin Deficiency: Current Approaches and Future Directions. *Curr Pathobiol Rep*. 2017;5(3):243-52.
95. Townsend SA, Edgar RG, Ellis PR, Kantas D, Newsome PN, Turner AM. Systematic review: the natural history of alpha-1 antitrypsin deficiency, and associated liver disease. *Alimentary Pharmacology & Therapeutics*. 2018;47(7):877-85.
96. Tanash HA, Piitulainen E. Liver disease in adults with severe alpha-1-antitrypsin deficiency. *J Gastroenterol*. 2019;54(6):541-8.
97. Rudnick DA, Liao Y, An JK, Muglia LJ, Perlmutter DH, Teckman JH. Analyses of hepatocellular proliferation in a mouse model of alpha-1-antitrypsin deficiency. *Hepatology (Baltimore, Md)*. 2004;39(4):1048-55.
98. Clark VC. Liver Transplantation in Alpha-1 Antitrypsin Deficiency. *Clinics in liver disease*. 2017;21(2):355-65.
99. Carey EJ, Iyer VN, Nelson DR, Nguyen JH, Krowka MJ. Outcomes for recipients of liver transplantation for alpha-1-antitrypsin deficiency-related cirrhosis. *Liver transplantation : official publication of the American Association for the Study of*

- Liver Diseases and the International Liver Transplantation Society. 2013;19(12):1370-6.
100. Thabut G, Mal H. Outcomes after lung transplantation. *J Thorac Dis.* 2017;9(8):2684-91.
  101. Lieberman J. Augmentation therapy reduces frequency of lung infections in antitrypsin deficiency: a new hypothesis with supporting data. *Chest.* 2000;118(5):1480-5.
  102. Blanco I, Lara B, de Serres F. Efficacy of alpha1-antitrypsin augmentation therapy in conditions other than pulmonary emphysema. *Orphanet J Rare Dis.* 2011;6:14.
  103. Smith KC, Pittelkow MR, Su WP. Panniculitis associated with severe alpha 1-antitrypsin deficiency. Treatment and review of the literature. *Archives of dermatology.* 1987;123(12):1655-61.
  104. Gross B, Grebe M, Wencker M, Stoller JK, Bjursten LM, Janciauskiene S. New Findings in PiZZ alpha1-antitrypsin deficiency-related panniculitis. Demonstration of skin polymers and high dosing requirements of intravenous augmentation therapy. *Dermatology.* 2009;218(4):370-5.
  105. Ortiz PG, Skov BG, Benfeldt E. Alpha1-antitrypsin deficiency-associated panniculitis: case report and review of treatment options. *Journal of the European Academy of Dermatology and Venereology : JEADV.* 2005;19(4):487-90.
  106. Voorzaat BM, van Schaik J, Crobach SLP, van Rijswijk CSP, Rotmans JI. Alpha-1 Antitrypsin Deficiency Presenting with MPO-ANCA Associated Vasculitis and Aortic Dissection. *Case Reports in Medicine.* 2017;2017:8140641.
  107. Suresh E. Diagnostic approach to patients with suspected vasculitis. *Postgrad Med J.* 2006;82(970):483-8.
  108. Lhotta K, Vogel W, Meisl T, Buxbaum M, Neyer U, Sandholzer C, et al. Alpha 1-antitrypsin phenotypes in patients with anti-neutrophil cytoplasmic antibody-positive vasculitis. *Clinical science (London, England : 1979).* 1994;87(6):693-5.
  109. Uriarte SM, McLeish KR, Ward RA. Anti-proteinase 3 antibodies both stimulate and prime human neutrophils. *Nephrology, dialysis, transplantation : official publication of the European Dialysis and Transplant Association - European Renal Association.* 2009;24(4):1150-7.
  110. McCarthy C, Reeves EP, McElvaney NG. The Role of Neutrophils in Alpha-1 Antitrypsin Deficiency. *Ann Am Thorac Soc.* 2016;13(Supplement\_4):S297-S304.
  111. P <sup>^</sup> | } | } å <sup>^</sup> : Á Ú ...! <sup>^</sup> : Á R T Ê Á Ø ~ { <sup>^</sup> | [ Á Ö æ! & ð æ Á Ù Ê Á Œ | ç æ æ } c ã c | <sup>^</sup> ] • ã } Á | <sup>^</sup> ] | æ & <sup>^</sup> { <sup>^</sup> } c -Antitrypsin deficiency and Á æ Á ] æ c ã <sup>^</sup> } c granulomatosis with polyangiitis. *Rheumatology (Oxford, England).* 2013;52(4):755-7.
  112. Hubbard RC, Crystal RG. Alpha-1-antitrypsin augmentation therapy for alpha-1-antitrypsin deficiency. *The American journal of medicine.* 1988;84(6a):52-62.
  113. Stockley RA, Miravittles M, Vogelmeier C, Alpha One International R. Augmentation therapy for alpha-1 antitrypsin deficiency: towards a personalised approach. *Orphanet journal of rare diseases.* 2013;8:149-.
  114. Tonelli AR, Brantly ML. Augmentation therapy in alpha-1 antitrypsin deficiency: advances and controversies. *Therapeutic Advances in Respiratory Disease.* 2010;4(5):289-312.
  115. Wewers MD, Crystal RG. Alpha-1 antitrypsin augmentation therapy. *Copd.* 2013;10 Suppl 1:64-7.
  116. Seersholm N, Wencker M, Banik N, Viskum K, Dirksen A, Kok-Jensen A, et al. Does alpha1-antitrypsin augmentation therapy slow the annual decline in FEV1 in

patients with severe hereditary alpha1-antitrypsin deficiency? Wissenschaftliche Arbeitsgemeinschaft zur Therapie von Lungenerkrankungen (WATL) alpha1-AT study group. *The European respiratory journal*. 1997;10(10):2260-3.

117. Dirksen A, Piitulainen E, Parr DG, Deng C, Wencker M, Shaker SB, et al. Exploring the role of CT densitometry: a randomised study of augmentation therapy in alpha1-antitrypsin deficiency. *The European respiratory journal*. 2009;33(6):1345-53.

118. Chapman KR, Burdon JG, Piitulainen E, Sandhaus RA, Seersholm N, Stocks R T Ê Á ^ c Á æ| È Á Q} c | æç ^ } [ ~ • Á æ ~ \* { ^ } c æ c ã [ } Á c | ^ æ c { ^ } antitrypsin deficiency (RAPID): a randomised, double-blind, placebo-controlled trial. *Lancet* (London, England). 2015;386(9991):360-8.

119. McElvaney NG, Burdon J, Holmes M, Glanville A, Wark PA, Thompson PJ, et al. Long-c ^ | { Á ^ ~ ~ ã & æ & ^ Á æ} å Á • æ ~ ^ c ^ Á [ ~ Á F Á ] | [ c ^ ã } æ • caused by • ^ ç ^ | ^ Á F Á æ} c ã c | ^ ] • label extension trial (RAPID-OLE). *Lancet Respir Med*. 2017;5(1):51-60.

120. Van't Wout EF, van Schadewijk A, Lomas DA, Stolk J, Marciniak SJ, Hiemstra PS. Function of monocytes and monocyte-å ^ | ã ç ^ å Á { æ & | 1[antitrypsin deficiency. *The European respiratory journal*. 2015;45(2):365-76.

121. Kapellos TS, Bonaguro L, Gemünd I, Reusch N, Saglam A, Hinkley ER, et al. Human Monocyte Subsets and Phenotypes in Major Chronic Inflammatory Diseases. *Frontiers in Immunology*. 2019;10(2035).

122. Patel AA, Zhang Y, Fullerton JN, Boelen L, Rongvaux A, Maini AA, et al. The fate and lifespan of human monocyte subsets in steady state and systemic inflammation. *J Exp Med*. 2017;214(7):1913-23.

123. Ingersoll MA, Spanbroek R, Lottaz C, Gautier EL, Frankenberger M, Hoffmann R, et al. Comparison of gene expression profiles between human and mouse monocyte subsets. *Blood*. 2010;115(3):e10-e9.

124. Buscher K, Marcovecchio P, Hedrick CC, Ley K. Patrolling Mechanics of Non-Classical Monocytes in Vascular Inflammation. *Front Cardiovasc Med*. 2017;4:80-.

125. Nichols BA, Bainton DF, Farquhar MG. Differentiation of monocytes. Origin, nature, and fate of their azurophil granules. *The Journal of cell biology*. 1971;50(2):498-515.

126. Jiang N, Chen W, Jothikumar P, Patel JM, Shashidharamurthy R, Selvaraj P, ^ c Á æ| È Á Ò ~ ~ ^ & c • Á [ ~ Á æ} & @[ | Á • c | ~ & c ~ | ^ Á æ} å Á \* | ^ & [ binding affinity. *Molecular Biology of the Cell*. 2016;27(22):3449-58.

127. Cohn ZA. The Structure and Function of Monocytes and Macrophages. In: Dixon FJ, Kunkel HG, editors. *Advances in Immunology*. 9: Academic Press; 1968. p. 163-214.

128. Boyette LB, Macedo C, Hadi K, Elinoff BD, Walters JT, Ramaswami B, et al. Phenotype, function, and differentiation potential of human monocyte subsets. *PLoS One*. 2017;12(4):e0176460.

129. Jungi TW, von Below G, Lerch PG, Spaeth PJ. Modulation of human monocyte Fc receptor function by surface-adsorbed IgG. *Immunology*. 1987;60(2):261-8.

130. Carter SD, Leslie RG, Reeves WG. Human monocyte binding of homologous monomer and complexed IgG. *Immunology*. 1982;46(4):793-800.

131. Ziegler-Heitbrock L. Blood Monocytes and Their Subsets: Established Features and Open Questions. *Frontiers in immunology*. 2015;6:423-.

132. Bianchini M, Duchêne J, Santovito D, Schloss MJ, Evrard M, Winkels H, et al. PD-L1 expression on nonclassical monocytes reveals their origin and immunoregulatory function. *Science Immunology*. 2019;4(36):eaar3054.
133. Uq T æ| | ^ ^ Á Ö Ú Ê Á Ÿ æ} \* Á Ÿ Ê Á Ö [ ã • F, C A i z h e v s k y V, æ t æ! • æ} æ { al. Immunohistochemical detection of PD-L1 among diverse human neoplasms in a reference laboratory: observations based upon 62,896 cases. *Modern Pathology*. 2019;32(7):929-42.
134. Yona S, Kim K-W, Wolf Y, Mildner A, Varol D, Breker M, et al. Fate Mapping Reveals Origins and Dynamics of Monocytes and Tissue Macrophages under Homeostasis. *Immunity*. 2013;38(1):79-91.
135. Sunderkötter C, Nikolic T, Dillon MJ, Van Rooijen N, Stehling M, Drevets DA, et al. Subpopulations of mouse blood monocytes differ in maturation stage and inflammatory response. *Journal of immunology (Baltimore, Md : 1950)*. 2004;172(7):4410-7.
136. Ziegler-Heitbrock L, Hofer T. Toward a Refined Definition of Monocyte Subsets. *Frontiers in Immunology*. 2013;4(23).
137. Favre J, Terborg N, Horrevoets AJ. The diverse identity of angiogenic monocytes. *European journal of clinical investigation*. 2013;43(1):100-7.
138. Radwan WM, Khalifa KA, Esaily HA, Lashin NA. CD14++CD16+ monocyte subset expansion in rheumatoid arthritis patients: Relation to disease activity and interleukin-17. *The Egyptian Rheumatologist*. 2016;38(3):161-9.
139. Urrea X, Villamor N, Amaro S, Gómez-Choco M, Obach V, Oleaga L, et al. Monocyte subtypes predict clinical course and prognosis in human stroke. *Journal of cerebral blood flow and metabolism : official journal of the International Society of Cerebral Blood Flow and Metabolism*. 2009;29(5):994-1002.
140. Dubaniewicz A, Wybieralska M, Nowakowski S, Rogoza K, Sternau A, Slominski JM, et al. Changed phagocytic activity æ} å Á ] æ c c ^ ! } Á [ ~ Á Ø & Á æ} å receptors on blood monocytes in sarcoidosis. *European Respiratory Journal*. 2011;38(Suppl 55):p3867.
141. Landmann R, Knopf HP, Link S, Sansano S, Schumann R, Zimmerli W. Human monocyte CD14 is upregulated by lipopolysaccharide. *Infect Immun*. 1996;64(5):1762-9.
142. Stolk J, Aggarwal N, Hochnadel I, Wrenger S, Martinez-Delgado B, Welte T, ^ c Á æ| È Á Ö| [ [ å Á { [ ] [ & ^ c ^ Á ] ! [ ~ ã | ^ • Á ã - a n t i o p s i d . Ö Á ] æ c ã ^ Respiratory Medicine. 2019;148:60-2.
143. Ciabattini A, Cuppone AM, Pulimeno R, Iannelli F, Pozzi G, Medaglini D. Stimulation of Human Monocytes with the Gram-Positive Vaccine Vector <em>Streptococcus gordonii</em>. *Clinical and Vaccine Immunology*. 2006;13(9):1037-43.
144. Geissmann F, Auffray C, Palframan R, Wirrig C, Ciocca A, Campisi L, et al. Blood monocytes: distinct subsets, how they relate to dendritic cells, and their possible roles in the regulation of T-cell responses. *Immunology and cell biology*. 2008;86(5):398-408.
145. Elvington M, Liszewski MK, Atkinson JP. Evolution of the complement system: from defense of the single cell to guardian of the intravascular space. *Immunol Rev*. 2016;274(1):9-15.
146. Furebring M, Håkansson LD, Venge P, Nilsson B, Sjölin J. Expression of the C5a receptor (CD88) on granulocytes and monocytes in patients with severe sepsis. *Crit Care*. 2002;6(4):363-70.

147. Gavin C, Meinke S, Heldring N, Heck KA, Achour A, Iacobaeus E, et al. The Complement System Is Essential for the Phagocytosis of Mesenchymal Stromal Cells by Monocytes. *Frontiers in Immunology*. 2019;10(2249).
148. Kim J, Hematti P. Mesenchymal stem cell-educated macrophages: a novel type of alternatively activated macrophages. *Exp Hematol*. 2009;37(12):1445-53.
149. Reuter S, Lang D. Life span of monocytes and platelets: importance of interactions. *Front Biosci (Landmark Ed)* [Internet]. 2009 2009/01//; 14:[2432-47 pp.]. Available from: <http://europepmc.org/abstract/MED/19273210>  
<https://doi.org/10.2741/3388>.
150. Fujimura N, Xu B, Dalman J, Deng H, Aoyama K, Dalman RL. CCR2 inhibition sequesters multiple subsets of leukocytes in the bone marrow. *Scientific Reports*. 2015;5(1):11664.
151. Teh YC, Ding JL, Ng LG, Chong SZ. Capturing the Fantastic Voyage of Monocytes Through Time and Space. *Frontiers in Immunology*. 2019;10(834).
152. Tacke F, Ginhoux F, Jakubzick C, van Rooijen N, Merad M, Randolph GJ. Immature monocytes acquire antigens from other cells in the bone marrow and present them to T cells after maturing in the periphery. *J Exp Med*. 2006;203(3):583-97.
153. Morales-Nebreda L, Misharin AV, Perlman H, Budinger GRS. The heterogeneity of lung macrophages in the susceptibility to disease. *European Respiratory Review*. 2015;24(137):505-9.
154. Gurczynski SJ, Procaro MC, O'Dwyer DN, Wilke CA, Moore BB. Loss of  $\alpha\text{-}\beta\text{-T}$  lymphocytes and  $\text{CD}4^+\text{CD}8^+$   $\text{T}$  cells in murine  $\text{H}1\text{N}1$  influenza A virus-induced pneumonitis and fibrosis following bone marrow transplantation. *American journal of physiology Lung cellular and molecular physiology*. 2016;311(3):L611-27.
155. Aegerter H, Kulikauskaite J, Crotta S, Patel H, Kelly G, Hessel EM, et al. Influenza-induced monocyte-derived alveolar macrophages confer prolonged antibacterial protection. *Nature Immunology*. 2020;21(2):145-57.
156. Osterholzer JJ, Olszewski MA, Murdock BJ, Chen GH, Erb-Downward JR, Subbotina N, et al. Implicating exudate macrophages and Ly-6C(high) monocytes in CCR2-dependent lung fibrosis following gene-targeted alveolar injury. *Journal of immunology (Baltimore, Md : 1950)*. 2013;190(7):3447-57.
157. Ley K. M1 Means Kill; M2 Means Heal. *The Journal of Immunology*. 2017;199(7):2191-3.
158. Atri C, Guerfali FZ, Laouini D. Role of Human Macrophage Polarization in Inflammation during Infectious Diseases. *Int J Mol Sci*. 2018;19(6):1801.
159. Halstead ES, Umstead TM, Davies ML, Kawasaki YI, Silveyra P, Howyrlak J, et al. GM-CSF overexpression after influenza A virus infection prevents mortality and moderates M1-like airway monocyte/macrophage polarization. *Respir Res*. 2018;19(1):3.
160. Al-Rashoudi R, Moir G, Al-Hajjaj MS, Al-Alwan MM, Wilson HM, Crane IJ. Differential expression of CCR2 and CX3CR1 on CD16+ monocyte subsets is associated with asthma severity. *Allergy, Asthma & Clinical Immunology*. 2019;15(1):64.
161. Atal S, Fatima Z. IL-6 Inhibitors in the Treatment of Serious COVID-19: A Promising Therapy? *Pharmaceut Med*. 2020;34(4):223-31.
162. Moore BB, Paine R, 3rd, Christensen PJ, Moore TA, Sitterding S, Ngan R, et al. Protection from pulmonary fibrosis in the absence of CCR2 signaling. *Journal of immunology (Baltimore, Md : 1950)*. 2001;167(8):4368-77.

163. Misharin AV, Morales-Nebreda L, Reyfman PA, Cuda CM, Walter JM, McQuattie-Pimentel AC, et al. Monocyte-derived alveolar macrophages drive lung fibrosis and persist in the lung over the life span. *J Exp Med*. 2017;214(8):2387-404.
164. Cornwell WD, Kim V, Fan X, Vega ME, Ramsey FV, Criner GJ, et al. Activation and polarization of circulating monocytes in severe chronic obstructive pulmonary disease. *BMC Pulm Med*. 2018;18(1):101-.
165. Scott MKD, Quinn K, Li Q, Carroll R, Warsinske H, Vallania F, et al. Increased monocyte count as a cellular biomarker for poor outcomes in fibrotic diseases: a retrospective, multicentre cohort study. *Lancet Respir Med*. 2019;7(6):497-508.
166. Nita IM, Serapinas D, Janciauskiene SM. alpha1-Antitrypsin regulates CD14 expression and soluble CD14 levels in human monocytes in vitro. *Int J Biochem Cell Biol*. 2007;39(6):1165-76.
167. Sandström CS, Novoradovskaya N, Cilio CM, Piitulainen E, Sveger T, Janciauskiene S. Endotoxin receptor CD14 in PiZ alpha-1-antitrypsin deficiency individuals. *Respiratory research*. 2008;9(1):34-.
168. Pugin J, Heumann ID, Tomasz A, Kravchenko VV, Akamatsu Y, Nishijima M, et al. CD14 is a pattern recognition receptor. *Immunity*. 1994;1(6):509-16.
169. Antal-Szalmás P, Poppelier MJG, Broekhuizen R, Verhoef J, van Strijp JAG, van Kessel KPM. Diverging pathways for lipopolysaccharide and CD14 in human monocytes. *Cytometry*. 2000;41(4):279-88.
170. Kelley SL, Lukk T, Nair SK, Tapping RI. The crystal structure of human soluble CD14 reveals a bent solenoid with a hydrophobic amino-terminal pocket. *Journal of immunology (Baltimore, Md : 1950)*. 2013;190(3):1304-11.
171. Pålsson-McDermott EM, O'Neill LAJ. Signal transduction by the lipopolysaccharide receptor, Toll-like receptor-4. *Immunology*. 2004;113(2):153-62.
172. Landmann R, Link S, Sansano S, Rajacic Z, Zimmerli W. Soluble CD14 activates monocytic cells independently of lipopolysaccharide. *Infect Immun*. 1998;66(5):2264-71.
173. Serapinas D, Sakalauskas R. Immunomodulation capacity of alpha-1 antitrypsin in regulation of CD14 molecules expression and secretion in human monocytes in vitro. *European Respiratory Journal*. 2011;38(Suppl 55):p721.
174. Tarzi RM, Liu J, Schneiter S, Hill NR, Page TH, Cook HT, et al. CD14 expression is increased on monocytes in patients with anti-neutrophil cytoplasm antibody (ANCA)-associated vasculitis and correlates with the expression of ANCA autoantigens. *Clinical and experimental immunology*. 2015;181(1):65-75.
175. Callea F, Gregorini G, Sinico A, Consalez GG, Bossolasco M, Salvidio G, et al. alpha 1-Antitrypsin (AAT) deficiency and ANCA-positive systemic vasculitis: genetic and clinical implications. *European journal of clinical investigation*. 1997;27(8):696-702.
176. Gawdat K, Legere S, Wong C, Myers T, Marshall JS, Hassan A, et al. Changes in Circulating Monocyte Subsets (CD16 Expression) and Neutrophil-to-Lymphocyte Ratio Observed in Patients Undergoing Cardiac Surgery. *Front Cardiovasc Med*. 2017;4:12-.
177. Randolph GJ, Sanchez-Schmitz G, Liebman RM, Schäkel K. The CD16(+) (FcgammaRIII(+)) subset of human monocytes preferentially becomes migratory dendritic cells in a model tissue setting. *J Exp Med*. 2002;196(4):517-27.
178. van den Elsen JM, Isenman DE. A crystal structure of the complex between human complement receptor 2 and its ligand C3d. *Science (New York, NY)*. 2011;332(6029):608-11.

179. Nonaka M, Kimura A. Genomic view of the evolution of the complement system. *Immunogenetics*. 2006;58(9):701-13.
180. Walport MJ. Complement. *New England Journal of Medicine*. 2001;344(14):1058-66.
181. Wagner C, Hänsch GM, Stegmaier S, Deneffle B, Hug F, Schoels M. The complement receptor 3, CR3 (CD11b/CD18), on T lymphocytes: activation-dependent up-regulation and regulatory function. *European journal of immunology*. 2001;31(4):1173-80.
182. Marinho CF, Azeredo EL, Torrentes-Carvalho A, Marins-Dos-Santos A, Kubelka CF, de Souza LJ, et al. Down-regulation of complement receptors on the surface of host monocyte even as in vitro complement pathway blocking interferes in dengue infection. *PLoS One*. 2014;9(7):e102014.
183. Marinho CF, Azeredo EL, Torrentes-Carvalho A, Marins-Dos-Santos A, Kubelka CF, de Souza LJ, et al. Down-regulation of complement receptors on the surface of host monocyte even as in vitro complement pathway blocking interferes in dengue infection. *PLoS One* [Internet]. 2014 2014; 9(7):[e102014 p.]. Available from: <http://europepmc.org/abstract/MED/25061945>  
<https://www.ncbi.nlm.nih.gov/pmc/articles/pmid/25061945/pdf/?tool=EBI>  
<https://www.ncbi.nlm.nih.gov/pmc/articles/pmid/25061945/?tool=EBI>  
<https://doi.org/10.1371/journal.pone.0102014>  
<https://europepmc.org/articles/PMC4111305>  
<https://europepmc.org/articles/PMC4111305?pdf=render>.
184. P ^ ] à ~ | } Á Œ Š Ê Á T æ • [ } Á R Ô Ê Á Ö æ ç ã ^ • m p l e n e t Á Ò ç ] ! ^ • • ã receptors on peripheral blood monocytes in systemic lupus erythematosus and rheumatoid arthritis. *Rheumatology*. 2004;43(5):547-54.
185. Gupta R, Gant VA, Williams B, Enver T. Increased Complement Receptor-3 levels in monocytes and granulocytes distinguish COVID-19 patients with pneumonia from those with mild symptoms. *International journal of infectious diseases : IJID : official publication of the International Society for Infectious Diseases*. 2020;99:381-5.
186. Hosszu KK, Santiago-Schwarz F, Peerschke EIB, Ghebrehiwet B. Evidence that a C1q/C1qR system regulates monocyte-derived dendritic cell differentiation at the interface of innate and acquired immunity. *Innate Immun*. 2010;16(2):115-27.
187. Foreman KE, Glovsky MM, Warner RL, Horvath SJ, Ward PA. Comparative effect of C3a and C5a on adhesion molecule expression on neutrophils and endothelial cells. *Inflammation*. 1996;20(1):1-9.
188. Fee L. Establishing the impact of C3d on neutrophils in the pathogenesis of alpha one anti-trypsin deficiency. *RCSI: RCSI*; 2019.
189. Yerkovich ST, Wikström ME, Suriyaarachchi D, Prescott SL, Upham JW, Holt PG. Postnatal Development of Monocyte Cytokine Responses to Bacterial Lipopolysaccharide. *Pediatric Research*. 2007;62(5):547-52.
190. Brichard B, Varis I, Latinne D, Deneys V, de Bruyere M, Leveugle P, et al. Intracellular cytokine profile of cord and adult blood monocytes. *Bone marrow transplantation*. 2001;27(10):1081-6.
191. P æ å æ å ã Á Ò Ê Á Z @æ } \* Á Ó Ê Á Ó æ ã å 0 æ b ^ ç æ • Á Š Ê Á Ÿ ~ • [ ~ Á Þ Differential IL-F secretion by monocyte subsets is regulated by Hsp27 through modulating mRNA stability. *Scientific reports*. 2016;6:39035-.

192. Ginaldi L, De Martinis M. Phenotypic and Functional Changes of Circulating Monocytes in Elderly. In: Fulop T, Franceschi C, Hirokawa K, Pawelec G, editors. *Handbook of Immunosenescence: Basic Understanding and Clinical Implications*. Cham: Springer International Publishing; 2019. p. 623-50.
193. Schutte RJ, Parisi-Amon A, Reichert WM. Cytokine profiling using monocytes/macrophages cultured on common biomaterials with a range of surface chemistries. *J Biomed Mater Res A*. 2009;88(1):128-39.
194. Serbina NV, Jia T, Hohl TM, Pamer EG. Monocyte-mediated defense against microbial pathogens. *Annual review of immunology*. 2008;26:421-52.
195. Strauss-Ayali D, Conrad SM, Mosser DM. Monocyte subpopulations and their differentiation patterns during infection. *Journal of leukocyte biology*. 2007;82(2):244-52.
196. Patel VK, Williams H, Li SCH, Fletcher JP, Medbury HJ. Monocyte inflammatory profile is specific for individuals and associated with altered blood lipid levels. *Atherosclerosis*. 2017;263:15-23.
197. Lopez-Otin C, Bond JS. Proteases: multifunctional enzymes in life and disease. *The Journal of biological chemistry*. 2008;283(45):30433-7.
198. Conese M, Copreni E, Di Gioia S, De Rinaldis P, Fumarulo R. Neutrophil recruitment and airway epithelial cell involvement in chronic cystic fibrosis lung disease. *J Cyst Fibros*. 2003;2(3):129-35.
199. Kelly E, Greene CM, McElvaney NG. Targeting neutrophil elastase in cystic fibrosis. *Expert Opin Ther Targets*. 2008;12(2):145-57.
200. Château MT, Robert-Hebmann V, Devaux C, Lazaro JB, Canard B, Coux O. Human monocytes possess a serine protease activity capable of degrading HIV-1 reverse transcriptase in vitro. *Biochemical and biophysical research communications*. 2001;285(4):863-72.
201. Schuldhaus C, Beyer T, Kaltenmeier C, Lindner S, Schrezenmeier H, Jahrsdörfer B. Monocytes express the serine protease granzyme B - potential involvement in antigen processing and presentation. (P5033). *The Journal of Immunology*. 2013;190(1 Supplement):110.17-.17.
202. Just J, Moog-Lutz C, Houzel-Charavel A, Canteloup S, Grimfeld A, Witko-Sarsat V, et al. Proteinase 3 mRNA expression is induced in monocytes but not in neutrophils of patients with cystic fibrosis. *FEBS letters*. 1999;457(3):437-40.
203. O'Brien EC, Abdulahad WH, Rutgers A, Huitema MG, O'Reilly VP, Coughlan AM, et al. Intermediate monocytes in ANCA vasculitis: increased surface expression of ANCA autoantigens and IL-6. *PLoS One*. 2015;10(12):e0142115.
204. Johansson U, Lawson C, Dabare M, Syndercombe-Court D, Newland AC, Howells GL, et al. Human peripheral blood monocytes express protease receptor-2 and respond to receptor activation by production of IL-6, IL-8, and IL-1{beta}. *Journal of leukocyte biology*. 2005;78(4):967-75.
205. Birkedal-Hansen H, Moore WG, Bodden MK, Windsor LJ, Birkedal-Hansen B, DeCarlo A, et al. Matrix metalloproteinases: a review. *Critical reviews in oral biology and medicine* : an official publication of the American Association of Oral Biologists. 1993;4(2):197-250.
206. Yabluchanskiy A, Ma Y, Iyer RP, Hall ME, Lindsey ML. Matrix metalloproteinase-9: Many shades of function in cardiovascular disease. *Physiology (Bethesda)*. 2013;28(6):391-403.
207. Ågren MS, Auf dem Keller U. Matrix Metalloproteinases: How Much Can They Do? *Int J Mol Sci*. 2020;21(8):2678.

208. Schulze CJ, Wang W, Suarez-Pinzon WL, Sawicka J, Sawicki G, Schulz R. Imbalance between tissue inhibitor of metalloproteinase-4 and matrix metalloproteinases during acute myocardial [correction of myoctardial] ischemia-reperfusion injury. *Circulation*. 2003;107(19):2487-92.
209. Malara A, Ligi D, Di Buduo CA, Mannello F, Balduini A. Sub-Cellular Localization of Metalloproteinases in Megakaryocytes. *Cells*. 2018;7(7):80.
210. Sirniö P, Tuomisto A, Tervahartiala T, Sorsa T, Klintrup K, Karhu T, et al. High-serum MMP-8 levels are associated with decreased survival and systemic inflammation in colorectal cancer. *British Journal of Cancer*. 2018;119(2):213-9.
211. Cieplak P, Strongin AY. Matrix metalloproteinases - From the cleavage data to the prediction tools and beyond. *Biochim Biophys Acta Mol Cell Res*. 2017;1864(11 Pt A):1952-63.
212. Campos TM, Passos ST, Novais FO, Beiting DP, Costa RS, Queiroz A, et al. Matrix metalloproteinase 9 production by monocytes is enhanced by TNF and participates in the pathology of human cutaneous Leishmaniasis. *PLoS Negl Trop Dis*. 2014;8(11):e3282-e.
213. Newby AC. Metalloproteinase expression in monocytes and macrophages and its relationship to atherosclerotic plaque instability. *Arteriosclerosis, thrombosis, and vascular biology*. 2008;28(12):2108-14.
214. Bar-Or A, Nuttall RK, Duddy M, Alter A, Kim HJ, Ifergan I, et al. Analyses of all matrix metalloproteinase members in leukocytes emphasize monocytes as major inflammatory mediators in multiple sclerosis. *Brain : a journal of neurology*. 2003;126(Pt 12):2738-49.
215. Dimov D, Tacheva T, Ivanova D, Zhelyazkova Y, Vlaykova D, Gulubova M, et al. Blood levels of matrix metalloproteinases (MMPs) and tissue inhibitors of matrix metalloproteinases (TIMPs) as biomarkers of COPD. *European Respiratory Journal*. 2018;52(suppl 62):PA942.
216. Welgus HG, Campbell EJ, Cury JD, Eisen AZ, Senior RM, Wilhelm SM, et al. Neutral metalloproteinases produced by human mononuclear phagocytes. Enzyme profile, regulation, and expression during cellular development. *The Journal of clinical investigation*. 1990;86(5):1496-502.
217. Lu Y, Wahl LM. Production of matrix metalloproteinase-9 by activated human monocytes involves a phosphatidylinositol-3 kinase/Akt/IKKalpha/NF-kappaB pathway. *Journal of leukocyte biology*. 2005;78(1):259-65.
218. Zhang Y, McCluskey K, Fujii K, Wahl LM. Differential regulation of monocyte matrix metalloproteinase and TIMP-1 production by TNF-alpha, granulocyte-macrophage CSF, and IL-1 beta through prostaglandin-dependent and -independent mechanisms. *Journal of immunology (Baltimore, Md : 1950)*. 1998;161(6):3071-6.
219. Opdenakker G, Van den Steen PE, Dubois B, Nelissen I, Van Coillie E, Masure S, et al. Gelatinase B functions as regulator and effector in leukocyte biology. *Journal of leukocyte biology*. 2001;69(6):851-9.
220. O'Farrell TJ, Pourmotabbed T. The fibronectin-like domain is required for the type V and XI collagenolytic activity of gelatinase B. *Arch Biochem Biophys*. 1998;354(1):24-30.
221. Roderfeld M, Graf J, Giese B, Salguero-Palacios R, Tschuschner A, Muller-Newen G, et al. Latent MMP-9 is bound to TIMP-1 before secretion. *Biol Chem*. 2007;388(11):1227-34.
222. Li Y, Lu Y, Zhao Z, Wang J, Li J, Wang W, et al. Relationships of MMP-9 and TIMP-1 proteins with chronic obstructive pulmonary disease risk: A systematic review and meta-analysis. *J Res Med Sci*. 2016;21:12-.

223. Omachi TA, Eisner MD, Rames A, Markovtsova L, Blanc PD. Matrix metalloproteinase-9 predicts pulmonary status declines in alpha1-antitrypsin deficiency. *Respir Res.* 2011;12:35.
224. Belvisi MG, Bottomley KM. The role of matrix metalloproteinases (MMPs) in the pathophysiology of chronic obstructive pulmonary disease (COPD): a therapeutic role for inhibitors of MMPs? *Inflamm Res.* 2003;52(3):95-100.
225. oWells JM, Parker MM, Oster RA, Bowler RP, Dransfield MT, Bhatt SP, et al. Elevated circulating MMP-9 is linked to increased COPD exacerbation risk in SPIROMICS and COPDGene. *JCI Insight.* 2018;3(22).
226. Grossman N, Svenson SB, Leive L, Lindberg AA. Salmonella O antigen-specific oligosaccharide-octyl conjugates activate complement via the alternative pathway at different rates depending on the structure of the O antigen. *Molecular Immunology.* 1990;27(9):859-65.
227. Banda NK, Wood AK, Takahashi K, Levitt B, Rudd PM, Royle L, et al. Initiation of the alternative pathway of murine complement by immune complexes is dependent on N-glycans in IgG antibodies. *Arthritis Rheum.* 2008;58(10):3081-9.
228. Pangburn MK, Müller-Eberhard HJ. Initiation of the alternative complement pathway due to spontaneous hydrolysis of the thioester of C3. *Annals of the New York Academy of Sciences.* 1983;421:291-8.
229. Oroszlán G, Dani R, Szilágyi A, Závodszy P, Thiel S, Gál P, et al. Extensive Basal Level Activation of Complement Mannose-Binding Lectin-Associated Serine Protease-3: Kinetic Modeling of Lectin Pathway Activation Provides Possible Mechanism. *Frontiers in Immunology.* 2017;8(1821).
230. Kulkarni HS, Liszewski MK, Brody SL, Atkinson JP. The complement system in the airway epithelium: An overlooked host defense mechanism and therapeutic target? *J Allergy Clin Immunol.* 2018;141(5):1582-6.e1.
231. Varsano S, Kaminsky M, Kaiser M, Rashkovsky L. Generation of complement C3 and expression of cell membrane complement inhibitory proteins by human bronchial epithelium cell line. *Thorax.* 2000;55(5):364-9.
232. Huber-Lang M, Younkin EM, Sarma JV, Riedemann N, McGuire SR, Lu KT, et al. Generation of C5a by phagocytic cells. *The American journal of pathology.* 2002;161(5):1849-59.
233. Riedemann NC, Guo R-F, Ward PA. A key role of C5a/C5aR activation for the development of sepsis. *Journal of leukocyte biology.* 2003;74(6):966-70.
234. Riedemann NC, Guo RF, Neff TA, Laudes IJ, Keller KA, Sarma VJ, et al. Increased C5a receptor expression in sepsis. *J Clin Invest.* 2002;110(1):101-8.
235. Trolborg A, Jensen L, Deleuran B, Stengaard-Pedersen K, Thiel S, Jensenius JC. The C3dg Fragment of Complement Is Superior to Conventional C3 as a Diagnostic Biomarker in Systemic Lupus Erythematosus. *Frontiers in immunology.* 2018;9:581-.
236. Gralinski LE, Sheahan TP, Morrison TE, Menachery VD, Jensen K, Leist SR, et al. Complement Activation Contributes to Severe Acute Respiratory Syndrome Coronavirus Pathogenesis. *mBio.* 2018;9(5):e01753-18.
237. Swaroopa D, Bhaskar K, Mahathi T, Katkam S, Raju YS, Chandra N, et al. Association of serum interleukin-6, interleukin-8, and Acute Physiology and Chronic Health Evaluation II score with clinical outcome in patients with acute respiratory distress syndrome. *Indian J Crit Care Med.* 2016;20(9):518-25.
238. Zilow G, Sturm JA, Rother U, Kirschfink M. Complement activation and the prognostic value of C3a in patients at risk of adult respiratory distress syndrome. *Clin Exp Immunol.* 1990;79(2):151-7.

239. Hammerschmidt DE, Weaver LJ, Hudson LD, Craddock PR, Jacob HS. Association of complement activation and elevated plasma-C5a with adult respiratory distress syndrome. Pathophysiological relevance and possible prognostic value. *Lancet* (London, England). 1980;1(8175):947-9.
240. Marc MM, Korosec P, Kosnik M, Kern I, Flezar M, Suskovic S, et al. Complement Factors C3a, C4a, and C5a in Chronic Obstructive Pulmonary Disease and Asthma. *American journal of respiratory cell and molecular biology*. 2004;31(2):216-9.
241. Kerr LD, Adelsberg BR, Spiera H. Complement activation in systemic lupus erythematosus: a marker of inflammation. *J Rheumatol*. 1986;13(2):313-9.
242. Doherty M, Richards N, Hornby J, Powell R. Relation between synovial fluid C3 degradation products and local joint inflammation in rheumatoid arthritis, osteoarthritis, and crystal associated arthropathy. *Ann Rheum Dis*. 1988;47(3):190-7.
243. Kleesiek K, Reinards R, Brackertz D, Neumann S, Lang H, Greiling H. Granulocyte elastase as a new biochemical marker in the diagnosis of chronic joint diseases. *Rheumatol Int*. 1986;6(4):161-9.
244. Littleton ET, Bevis L, Hansen LJ, Peakman M, Mowat AP, Mieli-Vergani G, et al. Alpha 1-antitrypsin deficiency, complement activation, and chronic liver disease. *Journal of clinical pathology*. 1991;44(10):855-8.
245. Yeap WH, Wong KL, Shimasaki N, Teo ECY, Quek JKS, Yong HX, et al. CD16 is indispensable for antibody-dependent cellular cytotoxicity by human monocytes. *Scientific Reports*. 2016;6(1):34310.
246. Roxvall L, Bengtson A, Sennerby L, Heideman M. Activation of the complement cascade by trypsin. *Biol Chem Hoppe Seyler*. 1991;372(4):273-8.
247. Fingerroth JD, Weis JJ, Tedder TF, Strominger JL, Biro PA, Fearon DT. Epstein-Barr virus receptor of human B lymphocytes is the C3d receptor CR2. *Proceedings of the National Academy of Sciences of the United States of America*. 1984;81(14):4510-4.
248. Iida K, Nadler L, Nussenzweig V. Identification of the membrane receptor for the complement fragment C3d by means of a monoclonal antibody. *J Exp Med*. 1983;158(4):1021-33.
249. Aubry JP, Pochon S, Graber P, Jansen KU, Bonnefoy JY. CD21 is a ligand for CD23 and regulates IgE production. *Nature*. 1992;358(6386):505-7.
250. Asokan R, Hua J, Young KA, Gould HJ, Hannan JP, Kraus DM, et al. Characterization of human complement receptor type 2 (CR2/CD21) as a receptor for IFN-alpha: a potential role in systemic lupus erythematosus. *Journal of immunology* (Baltimore, Md : 1950). 2006;177(1):383-94.
251. Tsoukas CD, Lambris JD. Expression of CR2/EBV receptors on human thymocytes detected by monoclonal antibodies. *European journal of immunology*. 1988;18(8):1299-302.
252. Fischer E, Delibrias C, Kazatchkine MD. Expression of CR2 (the C3dg/EBV receptor, CD21) on normal human peripheral blood T lymphocytes. *Journal of immunology* (Baltimore, Md : 1950). 1991;146(3):865-9.
253. Bacon K, Gauchat JF, Aubry JP, Pochon S, Graber P, Henchoz S, et al. CD21 expressed on basophilic cells is involved in histamine release triggered by CD23 and anti-CD21 antibodies. *European journal of immunology*. 1993;23(10):2721-4.
254. Lubbers R, van Essen MF, van Kooten C, Trouw LA. Production of complement components by cells of the immune system. *Clin Exp Immunol*. 2017;188(2):183-94.

255. Inada S, Brown EJ, Gaither TA, Hammer CH, Takahashi T, Frank MM. C3d receptors are expressed on human monocytes after in vitro cultivation. *Proceedings of the National Academy of Sciences of the United States of America*. 1983;80(8):2351-5.
256. Moore MD, Cooper NR, Tack BF, Nemerow GR. Molecular cloning of the cDNA encoding the Epstein-Barr virus/C3d receptor (complement receptor type 2) of human B lymphocytes. *Proceedings of the National Academy of Sciences of the United States of America*. 1987;84(24):9194-8.
257. Douglas KB, Windels DC, Zhao J, Gadeliya AV, Wu H, Kaufman KM, et al. Complement receptor 2 polymorphisms associated with systemic lupus erythematosus modulate alternative splicing. *Genes & Immunity*. 2009;10(5):457-69.
258. Liu YJ, Xu J, de Bouteiller O, Parham CL, Grouard G, Djossou O, et al. Follicular dendritic cells specifically express the long CR2/CD21 isoform. *J Exp Med*. 1997;185(1):165-70.
259. Toapanta FR, Ross TM. Complement-mediated activation of the adaptive immune responses: role of C3d in linking the innate and adaptive immunity. *Immunol Res*. 2006;36(1-3):197-210.
260. Dempsey PW, Allison ME, Akkaraju S, Goodnow CC, Fearon DT. C3d of complement as a molecular adjuvant: bridging innate and acquired immunity. *Science (New York, NY)*. 1996;271(5247):348-50.
261. Carroll MC, Isenman DE. Regulation of humoral immunity by complement. *Immunity*. 2012;37(2):199-207.
262. Chen Z, Koralov SB, Gendelman M, Carroll MC, Kelsoe G. Humoral immune responses in Cr2<sup>-/-</sup> mice: enhanced affinity maturation but impaired antibody persistence. *Journal of immunology (Baltimore, Md : 1950)*. 2000;164(9):4522-32.
263. Liu D, Zhu J-Y, Niu Z-X. Molecular Structure and Expression of Anthropic, Ovine, and Murine Forms of Complement Receptor Type 2. *Clinical and Vaccine Immunology*. 2008;15(6):901-10.
264. Ling NR, Hardie DL, Johnson GD, MacLennan IC. Origin and properties of soluble CD21 (CR2) in human blood. *Clinical and experimental immunology*. 1998;113(3):360-6.
265. Gasque P, Chan P, Mauger C, Schouft MT, Singhrao S, Dierich MP, et al. Identification and characterization of complement C3 receptors on human astrocytes. *Journal of immunology (Baltimore, Md : 1950)*. 1996;156(6):2247-55.
266. Ling N, Hansel T, Richardson P, Brown B. Cellular origins of serum complement receptor type 2 in normal individuals and in hypogammaglobulinaemia. *Clinical and experimental immunology*. 1991;84(1):16-22.
267. Rosse WF, Dacie JV. Immune lysis of normal human and paroxysmal nocturnal hemoglobinuria (PNH) red blood cells. II. The role of complement components in the increased sensitivity of PNH red cells to immune lysis. *The Journal of clinical investigation*. 1966;45(5):749-57.
268. Dubois EA, Cohen AF. Eculizumab. *Br J Clin Pharmacol*. 2009;68(3):318-9.
269. Brodsky RA. Paroxysmal nocturnal hemoglobinuria. *Blood*. 2014;124(18):2804-11.
270. Jayne DRW, Bruchfeld AN, Harper L, Schaier M, Venning MC, Hamilton P, et al. Randomized Trial of C5a Receptor Inhibitor Avacopan in ANCA-Associated Vasculitis. *Journal of the American Society of Nephrology*. 2017;28(9):2756-67.
271. Huan L, Yuezhong L, Chao W, HaiTao T. The urine albumin-to-creatinine ratio is a reliable indicator for evaluating complications of chronic kidney disease and progression in IgA nephropathy in China. *Clinics (Sao Paulo)*. 2016;71(5):243-50.

272. Holz FG, Sadda SR, Busbee B, Chew EY, Mitchell P, Tufail A, et al. Efficacy and Safety of Lampalizumab for Geographic Atrophy Due to Age-Related Macular Degeneration: Chroma and Spectri Phase 3 Randomized Clinical Trials. *JAMA ophthalmology*. 2018;136(6):666-77.
273. Feussner A, Kalina U, Hofmann P, Machnig T, Henkel G. Biochemical comparison of four commercially available C1 esterase inhibitor concentrates for treatment of hereditary angioedema. *Transfusion*. 2014;54(10):2566-73.
274. Ehlers MR. Immune-modulating effects of alpha-1 antitrypsin. *Biological chemistry*. 2014;395(10):1187-93.
275. Sheth B, Dransfield I, Partridge LJ, Barker MD, Burton DR. Dibutyryl cyclic AMP stimulation of a monocyte-like cell line, U937: a model for monocyte chemotaxis and Fc receptor-related functions. *Immunology*. 1988;63(3):483-90.
276. Sun H, Wu CX, Gong JP, Liu HZ, Li XH, You HB, et al. [Expression of CD14 protein in U937 cells induced by vitamin D3]. *Xi bao yu fen zi mian yi xue za zhi = Chinese journal of cellular and molecular immunology*. 2005;21(2):155-8.
277. Buttgereit P, Weineck S, Röpke G, Märten A, Brand K, Heinicke T, et al. Efficient gene transfer into lymphoma cells using adenoviral vectors combined with lipofection. *Cancer gene therapy*. 2000;7(8):1145-55.
278. Lira-Junior R, Holmström SB, Clark R, Zwicker S, Majster M, Johannsen G, et al. S100A12 Expression Is Modulated During Monocyte Differentiation and Reflects Periodontitis Severity. *Frontiers in immunology*. 2020;11:86.
279. Kew VG, Wills MR, Reeves MB. LPS promotes a monocyte phenotype permissive for human cytomegalovirus immediate-early gene expression upon infection but not reactivation from latency. *Sci Rep*. 2017;7(1):810.
280. Plevin RE, Knoll M, McKay M, Arbabi S, Cuschieri J. The Role of Lipopolysaccharide Structure in Monocyte Activation and Cytokine Secretion. *Shock*. 2016;45(1):22-7.
281. Cregan P, Yamamoto A, Lum A, VanDerHeide T, MacDonald M, Pulliam L. Comparison of four methods for rapid detection of *Pneumocystis carinii* in respiratory specimens. *J Clin Microbiol*. 1990;28(11):2432-6.
282. Yu YR, Hotten DF, Malakhau Y, Volker E, Ghio AJ, Noble PW, et al. Flow Cytometric Analysis of Myeloid Cells in Human Blood, Bronchoalveolar Lavage, and Lung Tissues. *American journal of respiratory cell and molecular biology*. 2016;54(1):13-24.
283. Suzuki Y, Shirai M, Asada K, Yasui H, Karayama M, Hozumi H, et al. Macrophage mannose receptor, CD206, predict prognosis in patients with pulmonary tuberculosis. *Sci Rep*. 2018;8(1):13129.
284. Ramirez J-M, Bai Q, Péquignot M, Becker F, Kassambara A, Bouin A, et al. Side scatter intensity is highly heterogeneous in undifferentiated pluripotent stem cells and predicts clonogenic self-renewal. *Stem Cells Dev*. 2013;22(12):1851-60.
285. Asokan R, Banda NK, Szakonyi G, Chen XS, Holers VM. Human complement receptor 2 (CR2/CD21) as a receptor for DNA: implications for its roles in the immune response and the pathogenesis of systemic lupus erythematosus (SLE). *Mol Immunol*. 2013;53(1-2):99-110.
286. Karlmark KR, Tacke F, Dunay IR. Monocytes in health and disease - Minireview. *Eur J Microbiol Immunol (Bp)*. 2012;2(2):97-102.
287. Taylor JC, Crawford IP, Hugli TE. Limited degradation of the third component (C3) of human complement by human leukocyte elastase (HLE): partial characterization of C3 fragments. *Biochemistry*. 1977;16(15):3390-6.

288. Potempa M, Potempa J. Protease-dependent mechanisms of complement evasion by bacterial pathogens. *Biol Chem*. 2012;393(9):873-88.
289. Ekdahl KN, Persson B, Mohlin C, Sandholm K, Skattum L, Nilsson B. Interpretation of Serological Complement Biomarkers in Disease. *Front Immunol*. 2018;9:2237.
290. Ricklin D, Reis ES, Mastellos DC, Gros P, Lambris JD. Complement component C3 - The "Swiss Army Knife" of innate immunity and host defense. *Immunol Rev*. 2016;274(1):33-58.
291. Green CE, Vayalapa S, Hampson JA, Mukherjee D, Stockley RA, Turner AM. PiSZ alpha-1 antitrypsin deficiency (AATD): pulmonary phenotype and prognosis relative to PiZZ AATD and PiMM COPD. *Thorax*. 2015;70(10):939-45.
292. Bergin DA, Reeves EP, Meleady P, Henry M, McElvaney OJ, Carroll TP, et al. -1 Antitrypsin regulates human neutrophil chemotaxis induced by soluble immune complexes and IL-8. *The Journal of clinical investigation*. 2010;120(12):4236-50.
293. Rouhani F, Paone G, Smith NK, Krein P, Barnes P, Brantly ML. Lung neutrophil burden correlates with increased pro-inflammatory cytokines and decreased lung function in individuals with alpha(1)-antitrypsin deficiency. *Chest*. 2000;117(5 Suppl 1):250S-1S.
294. Ö ~ | æ} c [ } Á R Ê Á Ó ã ^ c @Á R Õ È Á Q } - Antitrypsin In Vitro Á [ ~ Á Ú ! [ c ^ Predicts Very Fast Inhibition In Vivo. *American journal of respiratory cell and molecular biology*. 2003;29(1):57-61.
295. Mangan MS, Bird CH, Kaiserman D, Matthews AY, Hitchen C, Steer DL, et al. A Novel Serpin Regulatory Mechanism: SerpinB9 IS REVERSIBLY INHIBITED BY VICINAL DISULFIDE BOND FORMATION IN THE REACTIVE CENTER LOOP. *J Biol Chem*. 2016;291(7):3626-38.
296. Dimitrov S, Shaikh F, Pruitt C, Green M, Wilson K, Beg N, et al. Differential TNF production by monocyte subsets under physical stress: blunted mobilization of proinflammatory monocytes in prehypertensive individuals. *Brain Behav Immun*. 2013;27(1):101-8.
297. Mukaida N, Harada A, Matsushima K. Interleukin-8 (IL-8) and monocyte chemotactic and activating factor (MCAF/MCP-1), chemokines essentially involved in inflammatory and immune reactions. *Cytokine Growth Factor Rev*. 1998;9(1):9-23.
298. Mukaida N, Harada A, Yasumoto K, Matsushima K. Properties of pro-inflammatory cell type-specific leukocyte chemotactic cytokines, interleukin 8 (IL-8) and monocyte chemotactic and activating factor (MCAF). *Microbiol Immunol*. 1992;36(8):773-89.
299. Carroll TP, Greene CM, O'Connor CA, Nolan AM, O'Neill SJ, McElvaney NG. Evidence for unfolded protein response activation in monocytes from individuals with alpha-1 antitrypsin deficiency. *Journal of immunology*. 2010;184(8):4538-46.
300. Nurnberger W, Bhakdi S. Plasma C3d/C3 quotient as a parameter for in vivo complement activation. *J Immunol Methods*. 1984;74(1):87-91.
301. Geissmann F, Manz MG, Jung S, Sieweke MH, Merad M, Ley K. Development of monocytes, macrophages, and dendritic cells. *Science*. 2010;327(5966):656-61.
302. Abrink M, Gobl AE, Huang R, Nilsson K, Hellman L. Human cell lines U-937, THP-1 and Mono Mac 6 represent relatively immature cells of the monocyte-macrophage cell lineage. *Leukemia*. 1994;8(9):1579-84.
303. Westera L, van Viegen T, Jeyarajah J, Azad A, Bilsborough J, van den Brink GR, et al. Centrally Determined Standardization of Flow Cytometry Methods

- Reduces Interlaboratory Variation in a Prospective Multicenter Study. *Clin Transl Gastroenterol*. 2017;8(11):e126.
304. Zhu M, Lei L, Zhu Z, Li Q, Guo D, Xu J, et al. Excess TNF- $\alpha$  in the blood activates monocytes with the potential to directly form cholesteryl ester-laden cells. *Acta Biochim Biophys Sin (Shanghai)*. 2015;47(11):899-907.
  305. Bergin DA, Reeves EP, Hurley K, Wolfe R, Jameel R, Fitzgerald S, et al. The circulating proteinase inhibitor  $\alpha$ -1 antitrypsin regulates neutrophil degranulation and autoimmunity. *Science translational medicine*. 2014;6(217):217ra1.
  306. Tsukamoto H, Nagasawa K, Ueda Y, Mayumi T, Furugo I, Tsuru T, et al. Effects of cell differentiation on the synthesis of the third and fourth component of complement (C3, C4) by the human monocytic cell line U937. *Immunology*. 1992;77(4):621-3.
  307. Zhao YL, Liu WW, Liu W, Lu ZY, Xuan DH, Zhang X, et al. Phorbol ester (PMA)-treated U937 cells cultured on type I collagen-coated dish express a lower production of pro-inflammatory cytokines through lowered ROS levels in parallel with cell aggregate formation. *Int Immunopharmacol*. 2018;55:158-64.
  308. Takashiba S, Van Dyke TE, Amar S, Murayama Y, Soskolne AW, Shapira L. Differentiation of monocytes to macrophages primes cells for lipopolysaccharide stimulation via accumulation of cytoplasmic nuclear factor  $\kappa$ B. *Infect Immun*. 1999;67(11):5573-8.
  309. Di Iorio A, Ferrucci L, Sparvieri E, Cherubini A, Volpato S, Corsi A, et al. Serum IL-1 $\beta$  levels in health and disease: a population-based study. 'The InCHIANTI study'. *Cytokine*. 2003;22(6):198-205.
  310. Gaither TA, Vargas I, Inada S, Frank MM. The complement fragment C3d facilitates phagocytosis by monocytes. *Immunology*. 1987;62(3):405-11.
  311. Passmore JS, Lukey PT, Ress SR. The human macrophage cell line U937 as an in vitro model for selective evaluation of mycobacterial antigen-specific cytotoxic T-cell function. *Immunology*. 2001;102(2):146-56.
  312. Zhou L, Shen LH, Hu LH, Ge H, Pu J, Chai DJ, et al. Retinoid X receptor agonists inhibit phorbol-12-myristate-13-acetate (PMA)-induced differentiation of monocytic THP-1 cells into macrophages. *Mol Cell Biochem*. 2010;335(1-2):283-9.
  313. Wright SD, Reddy PA, Jong MT, Erickson BW. C3bi receptor (complement receptor type 3) recognizes a region of complement protein C3 containing the sequence Arg-Gly-Asp. *Proc Natl Acad Sci U S A*. 1987;84(7):1965-8.
  314. Wagner C, Hansch GM, Stegmaier S, Deneffle B, Hug F, Schoels M. The complement receptor 3, CR3 (CD11b/CD18), on T lymphocytes: activation-dependent up-regulation and regulatory function. *Eur J Immunol*. 2001;31(4):1173-80.
  315. Schmittgen TD, Livak KJ. Analyzing real-time PCR data by the comparative C(T) method. *Nat Protoc*. 2008;3(6):1101-8.
  316. Caracausi M, Piovesan A, Antonaros F, Strippoli P, Vitale L, Pelleri MC. Systematic identification of human housekeeping genes possibly useful as references in gene expression studies. *Mol Med Rep*. 2017;16(3):2397-410.
  317. Piehler AP, Grimholt RM, Ovstebo R, Berg JP. Gene expression results in lipopolysaccharide-stimulated monocytes depend significantly on the choice of reference genes. *BMC Immunol*. 2010;11:21.
  318. Tichopad A, Didier A, Pfaffl MW. Inhibition of real-time RT-PCR quantification due to tissue-specific contaminants. *Mol Cell Probes*. 2004;18(1):45-50.
  319. Desjardins P, Conklin D. NanoDrop microvolume quantitation of nucleic acids. *J Vis Exp*. 2010(45).

320. Emerson D, Ghiorse WC. Role of disulfide bonds in maintaining the structural integrity of the sheath of *Leptothrix discophora* SP-6. *J Bacteriol.* 1993;175(24):7819-27.
321. Braakman I, Lamriben L, van Zadelhoff G, Hebert DN. Analysis of Disulfide Bond Formation. *Curr Protoc Protein Sci.* 2017;90:14.1.1-1.21.
322. Hein WR, Dudler L, Marston WL, Landsverk T, Young AJ, Avila D. Ubiquitination and Dimerization of Complement Receptor Type 2 on Sheep B Cells. *The Journal of Immunology.* 1998;161(1):458-66.
323. Masilamani M, Kassahn D, Mikkat S, Glocker MO, Illges H. B cell activation leads to shedding of complement receptor type II (CR2/CD21). *Eur J Immunol.* 2003;33(9):2391-7.
324. Medzhitov R. Toll-like receptors and innate immunity. *Nat Rev Immunol.* 2001;1(2):135-45.
325. McNally AK, Anderson JM. Complement C3 participation in monocyte adhesion to different surfaces. *Proc Natl Acad Sci U S A.* 1994;91(21):10119-23.
326. Thieblemont N, Haeffner-Cavaillon N, Ledur A, L'Age-Stehr J, Ziegler-Heitbrock HW, Kazatchkine MD. CR1 (CD35) and CR3 (CD11b/CD18) mediate infection of human monocytes and monocytic cell lines with complement-opsonized HIV independently of CD4. *Clin Exp Immunol.* 1993;92(1):106-13.
327. van den Berg BM, van Furth R, Hazenbos WL. Activation of complement receptor 3 on human monocytes by cross-linking of very-late antigen-5 is mediated via protein tyrosine kinases. *Immunology.* 1999;98(2):197-202.
328. Furebring M, Hakansson LD, Venge P, Nilsson B, Sjölin J. Expression of the C5a receptor (CD88) on granulocytes and monocytes in patients with severe sepsis. *Crit Care.* 2002;6(4):363-70.
329. Marimuthu R, Francis H, Dervish S, Li SCH, Medbury H, Williams H. Characterization of Human Monocyte Subsets by Whole Blood Flow Cytometry Analysis. *J Vis Exp.* 2018(140).
330. Wozniak A, Betts WH, Murphy GA, Rokicinski M. Interleukin-8 primes human neutrophils for enhanced superoxide anion production. *Immunology.* 1993;79(4):608-15.
331. Chen JT, Chen RM, Lin YL, Chang HC, Lin YH, Chen TL, et al. Confocal laser scanning microscopy: I. An overview of principle and practice in biomedical research. *Acta Anaesthesiol Taiwan.* 2004;42(1):33-40.
332. Delmonte OM, Fleisher TA. Flow cytometry: Surface markers and beyond. *J Allergy Clin Immunol.* 2019;143(2):528-37.
333. Radha S, Afroz T, Prasad S, Ravindra N. Diagnostic utility of bronchoalveolar lavage. *J Cytol.* 2014;31(3):136-8.
334. Technical recommendations and guidelines for bronchoalveolar lavage (BAL). Report of the European Society of Pneumology Task Group. *Eur Respir J.* 1989;2(6):561-85.
335. Welker L, Jorres RA, Costabel U, Magnussen H. Predictive value of BAL cell differentials in the diagnosis of interstitial lung diseases. *Eur Respir J.* 2004;24(6):1000-6.
336. British Thoracic Society Bronchoscopy Guidelines Committee aSoSoCCoBTS. British Thoracic Society guidelines on diagnostic flexible bronchoscopy. *Thorax.* 2001;56 Suppl 1:i1-21.
337. Lofdahl JM, Cederlund K, Nathell L, Eklund A, Skold CM. Bronchoalveolar lavage in COPD: fluid recovery correlates with the degree of emphysema. *Eur Respir J.* 2005;25(2):275-81.

338. Karimi R, Tornling G, Grunewald J, Eklund A, Skold CM. Cell recovery in bronchoalveolar lavage fluid in smokers is dependent on cumulative smoking history. *PLoS One*. 2012;7(3):e34232.
339. Heron M, Grutters JC, ten Dam-Molenkamp KM, Hijdra D, van Heugten-Roeling A, Claessen AM, et al. Bronchoalveolar lavage cell pattern from healthy human lung. *Clin Exp Immunol*. 2012;167(3):523-31.
340. Choi SH, Hong SB, Hong HL, Kim SH, Huh JW, Sung H, et al. Usefulness of cellular analysis of bronchoalveolar lavage fluid for predicting the etiology of pneumonia in critically ill patients. *PLoS One*. 2014;9(5):e97346.
341. Harbeck RJ. Immunophenotyping of bronchoalveolar lavage lymphocytes. *Clin Diagn Lab Immunol*. 1998;5(3):271-7.
342. Clewe O, Karlsson MO, Simonsson US. Evaluation of optimized bronchoalveolar lavage sampling designs for characterization of pulmonary drug distribution. *J Pharmacokinet Pharmacodyn*. 2015;42(6):699-708.
343. Rennard SI, Basset G, Lecossier D, O'Donnell KM, Pinkston P, Martin PG, et al. Estimation of volume of epithelial lining fluid recovered by lavage using urea as marker of dilution. *J Appl Physiol* (1985). 1986;60(2):532-8.
344. Trummer A, De Rop C, Tiede A, Ganser A, Eisert R. Isotype controls in phenotyping and quantification of microparticles: a major source of error and how to evade it. *Thromb Res*. 2008;122(5):691-700.
345. Tung JW, Heydari K, Tirouvanziam R, Sahaf B, Parks DR, Herzenberg LA, et al. Modern flow cytometry: a practical approach. *Clin Lab Med*. 2007;27(3):453-68, v.
346. Feher K, Kirsch J, Radbruch A, Chang HD, Kaiser T. Cell population identification using fluorescence-minus-one controls with a one-class classifying algorithm. *Bioinformatics*. 2014;30(23):3372-8.
347. Betters DM. Use of Flow Cytometry in Clinical Practice. *J Adv Pract Oncol*. 2015;6(5):435-40.
348. Wersto RP, Chrest FJ, Leary JF, Morris C, Stetler-Stevenson MA, Gabrielson E. Doublet discrimination in DNA cell-cycle analysis. *Cytometry*. 2001;46(5):296-306.
349. Nakano A, Harada T, Morikawa S, Kato Y. Expression of leukocyte common antigen (CD45) on various human leukemia/lymphoma cell lines. *Acta Pathol Jpn*. 1990;40(2):107-15.
350. Cossarizza A, Chang HD, Radbruch A, Akdis M, Andra I, Annunziato F, et al. Guidelines for the use of flow cytometry and cell sorting in immunological studies. *Eur J Immunol*. 2017;47(10):1584-797.
351. Gordon S, Martinez FO. Alternative activation of macrophages: mechanism and functions. *Immunity*. 2010;32(5):593-604.
352. Linehan SA, Martinez-Pomares L, Stahl PD, Gordon S. Mannose receptor and its putative ligands in normal murine lymphoid and nonlymphoid organs: In situ expression of mannose receptor by selected macrophages, endothelial cells, perivascular microglia, and mesangial cells, but not dendritic cells. *J Exp Med*. 1999;189(12):1961-72.
353. Bedoret D, Wallemacq H, Marichal T, Desmet C, Quesada Calvo F, Henry E, et al. Lung interstitial macrophages alter dendritic cell functions to prevent airway allergy in mice. *J Clin Invest*. 2009;119(12):3723-38.
354. Yakimov BP, Gogoleva MA, Semenov AN, Rodionov SA, Novoselova MV, Gayer AV, et al. Label-free characterization of white blood cells using fluorescence lifetime imaging and flow-cytometry: molecular heterogeneity and erythrophagocytosis [Invited]. *Biomed Opt Express*. 2019;10(8):4220-36.

355. Yang J, Zhang L, Yu C, Yang XF, Wang H. Monocyte and macrophage differentiation: circulation inflammatory monocyte as biomarker for inflammatory diseases. *Biomark Res.* 2014;2(1):1.
356. Berger M, Sorensen RU, Tosi MF, Dearborn DG, Doring G. Complement receptor expression on neutrophils at an inflammatory site, the *Pseudomonas*-infected lung in cystic fibrosis. *The Journal of clinical investigation.* 1989;84(4):1302-13.
357. Boniakowski AE, Kimball AS, Joshi A, Schaller M, Davis FM, denDekker A, et al. Murine macrophage chemokine receptor CCR2 plays a crucial role in macrophage recruitment and regulated inflammation in wound healing. *Eur J Immunol.* 2018;48(9):1445-55.
358. Sandstrom CS, Novoradovskaya N, Cilio CM, Piitulainen E, Sveger T, Janciauskiene S. Endotoxin receptor CD14 in PiZ alpha-1-antitrypsin deficiency individuals. *Respir Res.* 2008;9:34.
359. Rubin J, Titus L, Nanes MS. Regulation of complement 5a receptor expression in U937 cells by phorbol ester. *J Leukoc Biol.* 1991;50(5):502-8.
360. Ó [ @ | • [ } Á Ü Ü Ê Á U q Ô [ } } ^ ! Á Ü Ö F r a e P D A. Complement, C1q, and C1q-Related Molecules Regulate Macrophage Polarization. *Frontiers in Immunology.* 2014;5(402).
361. Ezekowitz RA, Sim RB, MacPherson GG, Gordon S. Interaction of human monocytes, macrophages, and polymorphonuclear leukocytes with zymosan in vitro. Role of type 3 complement receptors and macrophage-derived complement. *J Clin Invest.* 1985;76(6):2368-76.
362. Burg M, Martin U, Bock D, Rheinheimer C, Kohl J, Bautsch W, et al. Differential regulation of the C3a and C5a receptors (CD88) by IFN-gamma and PMA in U937 cells and related myeloblastic cell lines. *J Immunol.* 1996;157(12):5574-81.
363. Segura M, Vadeboncoeur N, Gottschalk M. CD14-dependent and -independent cytokine and chemokine production by human THP-1 monocytes stimulated by *Streptococcus suis* capsular type 2. *Clin Exp Immunol.* 2002;127(2):243-54.
364. Dunlea DM, Fee LT, McEnery T, McElvaney NG, Reeves EP. The impact of alpha-1 antitrypsin augmentation therapy on neutrophil-driven respiratory disease in deficient individuals. *J Inflamm Res.* 2018;11:123-34.
365. Magro G. SARS-CoV-2 and COVID-19: is interleukin-6 (IL-6) the 'culprit lesion' of ARDS onset? What is there besides Tocilizumab? SGP130Fc. *Cytokine X.* 2020:100029.
366. Morikis D, Lambris JD. The electrostatic nature of C3d-complement receptor 2 association. *J Immunol.* 2004;172(12):7537-47.
367. Farrokhi M, Etemadifar M, Jafary Alavi MS, Zarkesh-Esfahani SH, Behjati M, Rezaei A, et al. TNF-alpha Production by Peripheral Blood Monocytes in Multiple Sclerosis Patients and Healthy Controls. *Immunol Invest.* 2015;44(6):590-601.
368. Hadadi E, Zhang B, Baidzajevs K, Yusof N, Puan KJ, Ong SM, et al. Differential IL-1beta secretion by monocyte subsets is regulated by Hsp27 through modulating mRNA stability. *Sci Rep.* 2016;6:39035.
369. Kraaij MD, Vereyken EJ, Leenen PJ, van den Bosch TP, Rezaee F, Betjes MG, et al. Human monocytes produce interferon-gamma upon stimulation with LPS. *Cytokine.* 2014;67(1):7-12.

370. Haggadone MD, Grailer JJ, Fattahi F, Zetoune FS, Ward PA. Bidirectional Crosstalk between C5a Receptors and the NLRP3 Inflammasome in Macrophages and Monocytes. *Mediators Inflamm.* 2016;2016:1340156.
371. Tamamis P, Kieslich CA, Nikiforovich GV, Woodruff TM, Morikis D, Archontis G. Insights into the mechanism of C5aR inhibition by PMX53 via implicit solvent molecular dynamics simulations and docking. *BMC Biophys.* 2014;7:5.
372. Fearon DT, Carroll MC. Regulation of B lymphocyte responses to foreign and self-antigens by the CD19/CD21 complex. *Annu Rev Immunol.* 2000;18:393-422.
373. Poe JC, Hasegawa M, Tedder TF. CD19, CD21, and CD22: multifaceted response regulators of B lymphocyte signal transduction. *Int Rev Immunol.* 2001;20(6):739-62.
374. Walsh DE, Greene CM, Carroll TP, Taggart CC, Gallagher PM, O'Neill SJ, et al. Interleukin-8 up-regulation by neutrophil elastase is mediated by MyD88/IRAK/TRAF-6 in human bronchial epithelium. *J Biol Chem.* 2001;276(38):35494-9.
375. Malerba M, Ricciardolo F, Radaeli A, Torregiani C, Ceriani L, Mori E, et al. Neutrophilic inflammation and IL-8 levels in induced sputum of alpha-1-antitrypsin PiMZ subjects. *Thorax.* 2006;61(2):129-33.
376. Chorostowska-Wynimko J, Gawryluk D, Struniawski R, Poplawska B, Fijolek J. Incidence of alpha-1 antitrypsin Z and S alleles in patients with granulomatosis with polyangiitis--pilot study. *Pneumonol Alergol Pol.* 2013;81(4):319-22.
377. Prame Kumar K, Nicholls AJ, Wong CHY. Partners in crime: neutrophils and monocytes/macrophages in inflammation and disease. *Cell Tissue Res.* 2018;371(3):551-65.
378. Houghton AM. Matrix metalloproteinases in destructive lung disease. *Matrix Biol.* 2015;44-46:167-74.
379. Delcayre AX, Salas F, Mathur S, Kovats K, Lotz M, Lernhardt W. Epstein Barr virus/complement C3d receptor is an interferon alpha receptor. *EMBO J.* 1991;10(4):919-26.
380. Zaman MM, Gelrud A, Junaidi O, Regan MM, Warny M, Shea JC, et al. Interleukin 8 secretion from monocytes of subjects heterozygous for the deltaF508 cystic fibrosis transmembrane conductance regulator gene mutation is altered. *Clin Diagn Lab Immunol.* 2004;11(5):819-24.
381. Neumann FJ, Ott I, Marx N, Luther T, Kenngott S, Gawaz M, et al. Effect of human recombinant interleukin-6 and interleukin-8 on monocyte procoagulant activity. *Arterioscler Thromb Vasc Biol.* 1997;17(12):3399-405.
382. Grkovich A, Johnson CA, Buczynski MW, Dennis EA. Lipopolysaccharide-induced cyclooxygenase-2 expression in human U937 macrophages is phosphatidic acid phosphohydrolase-1-dependent. *J Biol Chem.* 2006;281(44):32978-87.
383. Mangan DF, Wahl SM. Differential regulation of human monocyte programmed cell death (apoptosis) by chemotactic factors and pro-inflammatory cytokines. *J Immunol.* 1991;147(10):3408-12.
384. Mangan DF, Welch GR, Wahl SM. Lipopolysaccharide, tumor necrosis factor-alpha, and IL-1 beta prevent programmed cell death (apoptosis) in human peripheral blood monocytes. *J Immunol.* 1991;146(5):1541-6.
385. Wang P, Henning SM, Heber D. Limitations of MTT and MTS-based assays for measurement of antiproliferative activity of green tea polyphenols. *PLoS One.* 2010;5(4):e10202.
386. Zhao C, Tan YC, Wong WC, Sem X, Zhang H, Han H, et al. The CD14(+)/lowCD16(+) monocyte subset is more susceptible to spontaneous and

- oxidant-induced apoptosis than the CD14(+)CD16(-) subset. *Cell Death Dis.* 2010;1:e95.
387. Webster SJ, Daigneault M, Bewley MA, Preston JA, Marriott HM, Walmsley SR, et al. Distinct cell death programs in monocytes regulate innate responses following challenge with common causes of invasive bacterial disease. *J Immunol.* 2010;185(5):2968-79.
388. Bauer M, Goldstein M, Christmann M, Becker H, Heylmann D, Kaina B. Human monocytes are severely impaired in base and DNA double-strand break repair that renders them vulnerable to oxidative stress. *Proc Natl Acad Sci U S A.* 2011;108(52):21105-10.
389. Ponath V, Kaina B. Death of Monocytes through Oxidative Burst of Macrophages and Neutrophils: Killing in Trans. *PLoS One.* 2017;12(1):e0170347.
390. Zhang J, Bai C. The Significance of Serum Interleukin-8 in Acute Exacerbations of Chronic Obstructive Pulmonary Disease. *Tanaffos.* 2018;17(1):13-21.
391. Atkins PC, Norman M, Weiner H, Zweiman B. Release of neutrophil chemotactic activity during immediate hypersensitivity reactions in humans. *Ann Intern Med.* 1977;86(4):415-8.
392. Didangelos A. COVID-19 Hyperinflammation: What about Neutrophils? *mSphere.* 2020;5(3).
393. Chollet-Martin S, Montravers P, Gibert C, Elbim C, Desmonts JM, Fagon JY, et al. High levels of interleukin-8 in the blood and alveolar spaces of patients with pneumonia and adult respiratory distress syndrome. *Infect Immun.* 1993;61(11):4553-9.
394. Pease JE, Sabroe I. The role of interleukin-8 and its receptors in inflammatory lung disease: implications for therapy. *Am J Respir Med.* 2002;1(1):19-25.
395. Yoshimura T, Matsushima K, Tanaka S, Robinson EA, Appella E, Oppenheim JJ, et al. Purification of a human monocyte-derived neutrophil chemotactic factor that has peptide sequence similarity to other host defense cytokines. *Proc Natl Acad Sci U S A.* 1987;84(24):9233-7.
396. Holmes WE, Lee J, Kuang WJ, Rice GC, Wood WI. Structure and functional expression of a human interleukin-8 receptor. *Science.* 1991;253(5025):1278-80.
397. Schnyder-Candrian S, Walz A. Neutrophil-activating protein ENA-78 and IL-8 exhibit different patterns of expression in lipopolysaccharide- and cytokine-stimulated human monocytes. *J Immunol.* 1997;158(8):3888-94.
398. Monsinjon T, Gasque P, Ischenko A, Fontaine M. C3A binds to the seven transmembrane anaphylatoxin receptor expressed by epithelial cells and triggers the production of IL-8. *FEBS Lett.* 2001;487(3):339-46.
399. Brennan FH, Jogia T, Gillespie ER, Blomster LV, Li XX, Nowlan B, et al. Complement receptor C3aR1 controls neutrophil mobilization following spinal cord injury through physiological antagonism of CXCR2. *JCI Insight.* 2019;4(9).
400. Hair PS, Sass LA, Vazifedan T, Shah TA, Krishna NK, Cunnion KM. Complement effectors, C5a and C3a, in cystic fibrosis lung fluid correlate with disease severity. *PLoS One.* 2017;12(3):e0173257.
401. Hu DN, Bi M, Zhang DY, Ye F, McCormick SA, Chan CC. Constitutive and LPS-induced expression of MCP-1 and IL-8 by human uveal melanocytes in vitro and relevant signal pathways. *Invest Ophthalmol Vis Sci.* 2014;55(9):5760-9.
402. Ember JA, Sanderson SD, Hugli TE, Morgan EL. Induction of interleukin-8 synthesis from monocytes by human C5a anaphylatoxin. *Am J Pathol.* 1994;144(2):393-403.

403. Stenken JA, Poschenrieder AJ. Bioanalytical chemistry of cytokines--a review. *Anal Chim Acta*. 2015;853:95-115.
404. Kellar KL, Iannone MA. Multiplexed microsphere-based flow cytometric assays. *Exp Hematol*. 2002;30(11):1227-37.
405. Mustafa SA, Hoheisel JD, Alhamdani MS. Secretome profiling with antibody microarrays. *Mol Biosyst*. 2011;7(6):1795-801.
406. Huang RP. Detection of multiple proteins in an antibody-based protein microarray system. *J Immunol Methods*. 2001;255(1-2):1-13.
407. Turtinen LW, Prall DN, Bremer LA, Nauss RE, Hartsel SC. Antibody array-generated profiles of cytokine release from THP-1 leukemic monocytes exposed to different amphotericin B formulations. *Antimicrob Agents Chemother*. 2004;48(2):396-403.
408. Filipe MI, Osborn M, Linehan J, Sanidas E, Brito MJ, Jankowski J. Expression of transforming growth factor alpha, epidermal growth factor receptor and epidermal growth factor in precursor lesions to gastric carcinoma. *British Journal of Cancer*. 1995;71(1):30-6.
409. Imanishi K, Yamaguchi K, Suzuki M, Honda S, Yanaihara N, Abe K. Production of transforming growth factor- $\alpha$  of Cancer. 1989;59(5):761-5.
410. Khan KM, Howe LR, Falcone DJ. Extracellular matrix-induced cyclooxygenase-2 regulates macrophage proteinase expression. *J Biol Chem*. 2004;279(21):22039-46.
411. Ziegler-Heitbrock HW, Ulevitch RJ. CD14: cell surface receptor and differentiation marker. *Immunol Today*. 1993;14(3):121-5.
412. Le-Barillec K, Si-Tahar M, Balloy V, Chignard M. Proteolysis of monocyte CD14 by human leukocyte elastase inhibits lipopolysaccharide-mediated cell activation. *J Clin Invest*. 1999;103(7):1039-46.
413. Haugen TS, Nakstad B, Skjonsberg OH, Lyberg T. CD14 expression and binding of lipopolysaccharide to alveolar macrophages and monocytes. *Inflammation*. 1998;22(5):521-32.
414. LeVan TD, Smith LM, Heires AJ, Mikuls TR, Meza JL, Weissenburger-Moser LA, et al. Interaction of CD14 haplotypes and soluble CD14 on pulmonary function in agricultural workers. *Respiratory Research*. 2017;18(1):49.
415. Misharin AV, Morales-Nebreda L, Reyfman PA, Cuda CM, Walter JM, McQuattie-Pimentel AC, et al. Monocyte-derived alveolar macrophages drive lung fibrosis and persist in the lung over the life span. *J Exp Med*. 2017;214(8):2387-404.
416. Malla N, Berg E, Moens U, Uhlin-Hansen L, Winberg JO. Biosynthesis of promatrix metalloproteinase-9/chondroitin sulphate proteoglycan heteromer involves a Rottlerin-sensitive pathway. *PLoS One*. 2011;6(6):e20616.
417. Flannery CR. MMPs and ADAMTSs: functional studies. *Front Biosci*. 2006;11:544-69.
418. Butler GS, Overall CM. Updated biological roles for matrix metalloproteinases and new "intracellular" substrates revealed by degradomics. *Biochemistry*. 2009;48(46):10830-45.
419. Chen L, Nakai M, Belton RJ, Jr., Nowak RA. Expression of extracellular matrix metalloproteinase inducer and matrix metalloproteinases during mouse embryonic development. *Reproduction*. 2007;133(2):405-14.
420. Hardy E, Fernandez-Patron C. Destroy to Rebuild: The Connection Between Bone Tissue Remodeling and Matrix Metalloproteinases. *Front Physiol*. 2020;11:47.

421. Stetler-Stevenson WG. Matrix metalloproteinases in angiogenesis: a moving target for therapeutic intervention. *J Clin Invest.* 1999;103(9):1237-41.
422. Delclaux C, Delacourt C, D'Ortho MP, Boyer V, Lafuma C, Harf A. Role of gelatinase B and elastase in human polymorphonuclear neutrophil migration across basement membrane. *Am J Respir Cell Mol Biol.* 1996;14(3):288-95.
423. Wells JM, Parker MM, Oster RA, Bowler RP, Dransfield MT, Bhatt SP, et al. Elevated circulating MMP-9 is linked to increased COPD exacerbation risk in SPIROMICS and COPDGene. *JCI Insight.* 2018;3(22).
424. Prudente R, Franco EAT, Mesquita CB, Ferrari R, de Godoy I, Tanni SE. Predictors of mortality in patients with COPD after 9 years. *Int J Chron Obstruct Pulmon Dis.* 2018;13:3389-98.
425. Arroyo-Espliguero R, Avanzas P, Jeffery S, Kaski JC. CD14 and toll-like receptor 4: a link between infection and acute coronary events? *Heart.* 2004;90(9):983-8.
426. Guha M, Mackman N. LPS induction of gene expression in human monocytes. *Cell Signal.* 2001;13(2):85-94.
427. Anderson RG, Kamen BA, Rothberg KG, Lacey SW. Potocytosis: sequestration and transport of small molecules by caveolae. *Science.* 1992;255(5043):410-1.
428. Labeta MO, Durieux JJ, Fernandez N, Herrmann R, Ferrara P. Release from a human monocyte-like cell line of two different soluble forms of the lipopolysaccharide receptor, CD14. *Eur J Immunol.* 1993;23(9):2144-51.
429. Shive CL, Jiang W, Anthony DD, Lederman MM. Soluble CD14 is a nonspecific marker of monocyte activation. *AIDS.* 2015;29(10):1263-5.
430. Yu W, Soprana E, Cosentino G, Volta M, Lichenstein HS, Viale G, et al. Soluble CD14(1-152) confers responsiveness to both lipoarabinomannan and lipopolysaccharide in a novel HL-60 cell bioassay. *J Immunol.* 1998;161(8):4244-51.
431. Kirschning CJ, Wesche H, Merrill Ayres T, Rothe M. Human toll-like receptor 2 confers responsiveness to bacterial lipopolysaccharide. *J Exp Med.* 1998;188(11):2091-7.
432. Waller K, James C, de Jong A, Blackmore L, Ma Y, Stagg A, et al. ADAM17-Mediated Reduction in CD14(++)CD16(+) Monocytes ex vivo and Reduction in Intermediate Monocytes With Immune Paresis in Acute Pancreatitis and Acute Alcoholic Hepatitis. *Front Immunol.* 2019;10:1902.
433. Hurley K, Reeves EP, Carroll TP, McElvaney NG. Tumor necrosis factor- $\alpha$  driven inflammation in  $\alpha$ -1 antitrypsin deficiency: a new model of pathogenesis and treatment. *Expert review of respiratory medicine.* 2016;10(2):207-22.
434. Yang Y, Cui Y, Peng DQ. The role of monocyte phenotype switching in periprocedural myocardial injury and its involvement in statin therapy. *Med Sci Monit.* 2013;19:1006-12.
435. Loffek S, Schilling O, Franzke CW. Series "matrix metalloproteinases in lung health and disease": Biological role of matrix metalloproteinases: a critical balance. *Eur Respir J.* 2011;38(1):191-208.
436. Churg A, Zhou S, Wright JL. Series "matrix metalloproteinases in lung health and disease": Matrix metalloproteinases in COPD. *Eur Respir J.* 2012;39(1):197-209.
437. Elkington PT, Friedland JS. Matrix metalloproteinases in destructive pulmonary pathology. *Thorax.* 2006;61(3):259-66.

438. Liu Z, Zhou X, Shapiro SD, Shipley JM, Twining SS, Diaz LA, et al. The serpin alpha1-proteinase inhibitor is a critical substrate for gelatinase B/MMP-9 in vivo. *Cell*. 2000;102(5):647-55.
439. Todd RF, 3rd, Arnaout MA, Rosin RE, Crowley CA, Peters WA, Babior BM. Subcellular localization of the large subunit of Mo1 (Mo1 alpha; formerly gp 110), a surface glycoprotein associated with neutrophil adhesion. *J Clin Invest*. 1984;74(4):1280-90.
440. Dale DC, Boxer L, Liles WC. The phagocytes: neutrophils and monocytes. *Blood*. 2008;112(4):935-45.
441. Yong VW, Power C, Forsyth P, Edwards DR. Metalloproteinases in biology and pathology of the nervous system. *Nat Rev Neurosci*. 2001;2(7):502-11.
442. Webster NL, Crowe SM. Matrix metalloproteinases, their production by monocytes and macrophages and their potential role in HIV-related diseases. *J Leukoc Biol*. 2006;80(5):1052-66.
443. Dean RA, Cox JH, Bellac CL, Doucet A, Starr AE, Overall CM. Macrophage-specific metalloelastase (MMP-12) truncates and inactivates ELR+ CXC chemokines and generates CCL2, -7, -8, and -13 antagonists: potential role of the macrophage in terminating polymorphonuclear leukocyte influx. *Blood*. 2008;112(8):3455-64.
444. Hautamaki RD, Kobayashi DK, Senior RM, Shapiro SD. Requirement for macrophage elastase for cigarette smoke-induced emphysema in mice. *Science*. 1997;277(5334):2002-4.
445. Gosselink JV, Hayashi S, Elliott WM, Xing L, Chan B, Yang L, et al. Differential expression of tissue repair genes in the pathogenesis of chronic obstructive pulmonary disease. *Am J Respir Crit Care Med*. 2010;181(12):1329-35.
446. Sinden NJ, Stockley RA. Proteinase 3 activity in sputum from subjects with alpha-1-antitrypsin deficiency and COPD. *European Respiratory Journal*. 2013;41(5):1042-50.
447. Elzouki AN, Segelmark M, Wieslander J, Eriksson S. Strong link between the alpha 1-antitrypsin PiZ allele and Wegener's granulomatosis. *J Intern Med*. 1994;236(5):543-8.
448. Halbwachs-Mecarelli L, Bessou G, Lesavre P, Lopez S, Witko-Sarsat V. Bimodal distribution of proteinase 3 (PR3) surface expression reflects a constitutive heterogeneity in the polymorphonuclear neutrophil pool. *FEBS Lett*. 1995;374(1):29-33.
449. Owen CA, Campbell MA, Boukedes SS, Stockley RA, Campbell EJ. A discrete subpopulation of human monocytes expresses a neutrophil-like proinflammatory (P) phenotype. *Am J Physiol*. 1994;267(6 Pt 1):L775-85.
450. Hao W, Li M, Zhang Y, Zhang C, Xue Y. Expressions of MMP-12, TIMP-4, and Neutrophil Elastase in PBMCs and Exhaled Breath Condensate in Patients with COPD and Their Relationships with Disease Severity and Acute Exacerbations. *Journal of Immunology Research*. 2019;2019:7142438.
451. Mercer RR, Crapo JD. Spatial distribution of collagen and elastin fibers in the lungs. *J Appl Physiol* (1985). 1990;69(2):756-65.
452. Senior RM, Griffin GL, Mecham RP. Chemotactic activity of elastin-derived peptides. *J Clin Invest*. 1980;66(4):859-62.
453. McAloon CJ, Wood AM, Gough SC, Stockley RA. Matrix metalloprotease polymorphisms are associated with gas transfer in alpha 1 antitrypsin deficiency. *Ther Adv Respir Dis*. 2009;3(1):23-30.

454. Churg A, Wang X, Wang RD, Meixner SC, Prydzial EL, Wright JL. Alpha1-antitrypsin suppresses TNF-alpha and MMP-12 production by cigarette smoke-stimulated macrophages. *Am J Respir Cell Mol Biol*. 2007;37(2):144-51.
455. Feinberg MW, Jain MK, Werner F, Sibinga NE, Wiesel P, Wang H, et al. Transforming growth factor-beta 1 inhibits cytokine-mediated induction of human metalloelastase in macrophages. *J Biol Chem*. 2000;275(33):25766-73.
456. Wang Y, Xu J, Meng Y, Adcock IM, Yao X. Role of inflammatory cells in airway remodeling in COPD. *Int J Chron Obstruct Pulmon Dis*. 2018;13:3341-8.
457. Lijnen HR, Lupu F, Moons L, Carmeliet P, Goulding D, Collen D. Temporal and topographic matrix metalloproteinase expression after vascular injury in mice. *Thromb Haemost*. 1999;81(5):799-807.
458. Nénan S, Boichot E, Lagente V, Bertrand CP. Macrophage elastase (MMP-12): a pro-inflammatory mediator? *Memórias do Instituto Oswaldo Cruz*. 2005;100:167-72.
459. Raza SL, Nehring LC, Shapiro SD, Cornelius LA. Proteinase-activated receptor-1 regulation of macrophage elastase (MMP-12) secretion by serine proteinases. *J Biol Chem*. 2000;275(52):41243-50.
460. Demedts IK, Morel-Montero A, Lebecque S, Pacheco Y, Cataldo D, Joos GF, et al. Elevated MMP-12 protein levels in induced sputum from patients with COPD. *Thorax*. 2006;61(3):196-201.
461. Greenlee KJ, Werb Z, Kheradmand F. Matrix metalloproteinases in lung: multiple, multifarious, and multifaceted. *Physiol Rev*. 2007;87(1):69-98.
462. Senior RM, Tegner H, Kuhn C, Ohlsson K, Starcher BC, Pierce JA. The induction of pulmonary emphysema with human leukocyte elastase. *Am Rev Respir Dis*. 1977;116(3):469-75.
463. Wagenseil JE, Mecham RP. New insights into elastic fiber assembly. *Birth Defects Res C Embryo Today*. 2007;81(4):229-40.
464. D'Armiento J, Dalal SS, Okada Y, Berg RA, Chada K. Collagenase expression in the lungs of transgenic mice causes pulmonary emphysema. *Cell*. 1992;71(6):955-61.
465. Ho HH, Antoniv TT, Ji JD, Ivashkiv LB. Lipopolysaccharide-induced expression of matrix metalloproteinases in human monocytes is suppressed by IFN-gamma via superinduction of ATF-3 and suppression of AP-1. *J Immunol*. 2008;181(7):5089-97.
466. Okusawa S, Yancey KB, van der Meer JW, Endres S, Lonnemann G, Hefter K, et al. C5a stimulates secretion of tumor necrosis factor from human mononuclear cells in vitro. Comparison with secretion of interleukin 1 beta and interleukin 1 alpha. *J Exp Med*. 1988;168(1):443-8.
467. Ohlsson S, Hellmark T, Pieters K, Sturfelt G, Wieslander J, Segelmark M. Increased monocyte transcription of the proteinase 3 gene in small vessel vasculitis. *Clin Exp Immunol*. 2005;141(1):174-82.
468. Kao RC, Wehner NG, Skubitz KM, Gray BH, Hoidal JR. Proteinase 3. A distinct human polymorphonuclear leukocyte proteinase that produces emphysema in hamsters. *J Clin Invest*. 1988;82(6):1963-73.
469. Wiik A. What you should know about PR3-ANCA. An introduction. *Arthritis Res*. 2000;2(4):252-4.
470. Yang JJ, Preston GA, Pendergraft WF, Segelmark M, Heeringa P, Hogan SL, et al. Internalization of proteinase 3 is concomitant with endothelial cell apoptosis and internalization of myeloperoxidase with generation of intracellular oxidants. *Am J Pathol*. 2001;158(2):581-92.

471. Skold S, Rosberg B, Gullberg U, Olofsson T. A secreted proform of neutrophil proteinase 3 regulates the proliferation of granulopoietic progenitor cells. *Blood*. 1999;93(3):849-56.
472. Robache-Gallea S, Morand V, Bruneau JM, Schoot B, Tagat E, Realo E, et al. In vitro processing of human tumor necrosis factor-alpha. *J Biol Chem*. 1995;270(40):23688-92.
473. Padrines M, Wolf M, Walz A, Baggiolini M. Interleukin-8 processing by neutrophil elastase, cathepsin G and proteinase-3. *FEBS Lett*. 1994;352(2):231-5.
474. Coeshott C, Ohnemus C, Pilyavskaya A, Ross S, Wieczorek M, Kroona H, et al. Converting enzyme- $\alpha$  }  $\alpha$  ^ ] ^ }  $\alpha$  ^ } c Á | ^ | ^ æ • ^ Á [ ~ Á c - F { Á | Á } ^ & ! [ from a stimulated human monocytic cell line in the presence of activated neutrophils or purified proteinase 3. *Proceedings of the National Academy of Sciences*. 1999;96(11):6261-6.
475. Newby PR, Crossley D, Crisford H, Stockley JA, Mumford RA, Carter RI, et al. A specific proteinase 3 activity footprint in alpha1-antitrypsin deficiency. *ERJ Open Res*. 2019;5(3).
476. Mazodier P, Elzouki AN, Segelmark M, Eriksson S. Systemic necrotizing vasculitides in severe alpha1-antitrypsin deficiency. *QJM*. 1996;89(8):599-611.
477. Law SK, Dodds AW. The internal thioester and the covalent binding properties of the complement proteins C3 and C4. *Protein Sci*. 1997;6(2):263-74.
478. Patel AA, Yona S. Inherited and Environmental Factors Influence Human Monocyte Heterogeneity. *Front Immunol*. 2019;10:2581.
479. Merah-Mourah F, Cohen SO, Charron D, Mooney N, Haziot A. Identification of Novel Human Monocyte Subsets and Evidence for Phenotypic Groups Defined by Interindividual Variations of Expression of Adhesion Molecules. *Scientific Reports*. 2020;10(1):4397.
480. Ø | ^ ^ Á R Ê Á Ò } \* ^ | @æ | å c Á Y È Á Ô @æ | æ & c ^ | ã : æ c ã [ } Á æ } receptors of human monocytes, a monoblast cell line (U937) and a myeloblast cell line (HL-60) by a monoclonal antibody. *European Journal of Immunology*. 1987;17(5):583-91.
481. Bufler P, Stiegler G, Schuchmann M, Hess S, Kruger C, Stelter F, et al. Soluble lipopolysaccharide receptor (CD14) is released via two different mechanisms from human monocytes and CD14 transfectants. *Eur J Immunol*. 1995;25(2):604-10.
482. Merrilees MJ, Ching PS, Beaumont B, Hinek A, Wight TN, Black PN. Changes in elastin, elastin binding protein and versican in alveoli in chronic obstructive pulmonary disease. *Respir Res*. 2008;9:41.
483. Senior RM, Griffin GL, Fliszar CJ, Shapiro SD, Goldberg GI, Welgus HG. Human 92- and 72-kilodalton type IV collagenases are elastases. *J Biol Chem*. 1991;266(12):7870-5.
484. Van den Steen PE, Proost P, Wuyts A, Van Damme J, Opdenakker G. Neutrophil gelatinase B potentiates interleukin-8 tenfold by aminoterminal processing, whereas it degrades CTAP-III, PF-4, and GRO-alpha and leaves RANTES and MCP-2 intact. *Blood*. 2000;96(8):2673-81.
485. Stolk J, Seersholm N, Kalsheker N. Alpha1-antitrypsin deficiency: current perspective on research, diagnosis, and management. *Int J Chron Obstruct Pulmon Dis*. 2006;1(2):151-60.
486. ç æ } q c Á Y [ ~ c Á Ò Ø Æ Ê Á ç æ } Á Ù & @æ å ^ , ã b \ Á Æ Ê Á Š [ { æ • Á Ö Hiemstra PS. Function of monocytes and monocyte-derived macrophages in  $\alpha$ 1-antitrypsin deficiency. *European Respiratory Journal*. 2015;45(2):365-76.

487. Schorlemmer HU. The role of complement in the function of the monocyte - macrophage system. *Haematology and blood transfusion*. 1981;27:59-71.
488. Tsukamoto H, Nagasawa K, Yoshizawa S, Tada Y, Ueda A, Ueda Y, et al. Synthesis and regulation of the fourth component of complement (C4) in the human monocytic cell line U937: comparison with that of the third component of complement (C3). *Immunology*. 1992;75(4):565-9.
489. Song M-g, Ryoo I-g, Choi H-y, Choi B-h, Kim S-T, Heo T-H, et al. NRF2 signaling negatively regulates phorbol-12-myristate-13-acetate (PMA)-induced differentiation of human monocytic U937 cells into pro-inflammatory macrophages. *PLoS One*. 2015;10(7):e0134235.
490. Szakonyi G, Guthridge JM, Li D, Young K, Holers VM, Chen XS. Structure of complement receptor 2 in complex with its C3d ligand. *Science (New York, NY)*. 2001;292(5522):1725-8.
491. Lindblom RPF, Berg A, Ström M, Aeinehband S, Dominguez CA, Al Nimer F, et al. Complement receptor 2 is up regulated in the spinal cord following nerve root injury and modulates the spinal cord response. *Journal of Neuroinflammation*. 2015;12(1):192.
492. Qualai J, Li L-X, Cantero J, Tarrats A, Fernández MA, Sumoy L, et al. Expression of CD11c is associated with unconventional activated T cell subsets with high migratory potential. *PLoS One*. 2016;11(4):e0154253.
493. Wahid AA, Dunphy RW, Macpherson A, Gibson BG, Kulik L, Whale K, et al. Insights into the role of C3d dimers in B cell activation and Staphylococcal immune evasion. *bioRxiv*. 2020:2020.04.22.054700.
494. Huang W-C, Sala-Newby GB, Susana A, Johnson JL, Newby AC. Classical macrophage activation up-regulates several matrix metalloproteinases through mitogen activated protein kinases and nuclear factor- $\kappa$ B. *PLoS One*. 2012;7(8):e42507.
495. Wen G, Zhang C, Chen Q, Luong LA, Mustafa A, Ye S, et al. A Novel Role of Matrix Metalloproteinase-8 in Macrophage Differentiation and Polarization. *J Biol Chem*. 2015;290(31):19158-72.
496. Posimo JM, Unnithan AS, Gleixner AM, Choi HJ, Jiang Y, Pulugulla SH, et al. Viability assays for cells in culture. *J Vis Exp*. 2014(83):e50645-e.
497. Bazil V, Strominger JL. Shedding as a mechanism of down-modulation of CD14 on stimulated human monocytes. *The Journal of Immunology*. 1991;147(5):1567-74.
498. O'Brien EC, White CA, Wyse J, Leacy E, Porter RK, Little MA, et al. Pro-inflammatory Stimulation of Monocytes by ANCA Is Linked to Changes in Cellular Metabolism. *Frontiers in Medicine*. 2020;7(553).
499. McKibben RA, Margolick JB, Grinspoon S, Li X, Palella FJ, Jr, Kingsley LA, et al. Elevated Levels of Monocyte Activation Markers Are Associated With Subclinical Atherosclerosis in Men With and Those Without HIV Infection. *The Journal of Infectious Diseases*. 2014;211(8):1219-28.
500. Wikman A, Fagergren A, Gunnar O, Johansson S, Lundahl J, Jacobson SH. Monocyte activation and relationship to anti-proteinase 3 in acute vasculitis. *Nephrology Dialysis Transplantation*. 2003;18(9):1792-9.
501. Nayak DK, Mendez O, Bowen S, Mohanakumar T. Isolation and In Vitro Culture of Murine and Human Alveolar Macrophages. *J Vis Exp*. 2018(134).
502. Eguíluz-Gracia I, Malmstrom K, Dheyauldeen SA, Lohi J, Sajantila A, Aaløkken R, et al. Monocytes accumulate in the airways of children with fatal

asthma. *Clinical and experimental allergy : journal of the British Society for Allergy and Clinical Immunology*. 2018;48(12):1631-9.

503. Ó ^ | } ^ Á Æ R Ê Á Ú [ , ^ | | Á R Ò Ê Á U q Ù ~ | | ã ç æ } Á Ó R Ê Á U \* \* ^ |

Dynamics of human monocytes and airway macrophages during healthy aging and after transplant. *Journal of Experimental Medicine*. 2020;217(3).

504. Maródi L, Johnston RB. Enhancement of macrophage candidacidal activity by interferon-gamma. *Immunodeficiency*. 1993;4(1-4):181-5.

505. Stein M, Keshav S, Harris N, Gordon S. Interleukin 4 potently enhances murine macrophage mannose receptor activity: a marker of alternative immunologic macrophage activation. *The Journal of experimental medicine*. 1992;176(1):287-92.

506. Bharat A, Bhorade SM, Morales-Nebreda L, McQuattie-Pimentel AC, Soberanes S, Ridge K, et al. Flow Cytometry Reveals Similarities Between Lung Macrophages in Humans and Mice. *Am J Respir Cell Mol Biol*. 2016;54(1):147-9.

507. Ziegler-Heitbrock L, Ancuta P, Crowe S, Dalod M, Grau V, Hart DN, et al. Nomenclature of monocytes and dendritic cells in blood. *Blood*. 2010;116(16):e74-e80.

508. Cros J, Cagnard N, Woollard K, Patey N, Zhang S-Y, Senechal B, et al. Human CD14dim monocytes patrol and sense nucleic acids and viruses via TLR7 and TLR8 receptors. *Immunity*. 2010;33(3):375-86.

509. Mukherjee R, Barman PK, Thatoi PK, Tripathy R, Das BK, Ravindran B. Non-classical monocytes display inflammatory features: validation in sepsis and systemic lupus erythematosus. *Scientific reports*. 2015;5:13886.

510. Semnani RT, Moore V, Bennuru S, McDonald-Fleming R, Ganesan S, Cotton R, et al. Human monocyte subsets at homeostasis and their perturbation in numbers and function in filarial infection. *Infection and immunity*. 2014;82(11):4438-46.

511. Wong KL, Yeap WH, Tai JJY, Ong SM, Dang TM, Wong SC. The three human monocyte subsets: implications for health and disease. *Immunologic research*. 2012;53(1-3):41-57.

512. Ziegler-Heitbrock L. The CD14+ CD16+ blood monocytes: their role in infection and inflammation. *Journal of leukocyte biology*. 2007;81(3):584-92.

513. Leisman DE, Ronner L, Pinotti R, Taylor MD, Sinha P, Calfee CS, et al. Cytokine elevation in severe and critical COVID-19: a rapid systematic review, meta-analysis, and comparison with other inflammatory syndromes. *The Lancet Respiratory Medicine*.

514. Schneberger D, Aharonson-Raz K, Singh B. Monocyte and macrophage heterogeneity and Toll-like receptors in the lung. *Cell and tissue research*. 2011;343(1):97-106.

515. McQuattie-Pimentel AC, Ren Z, Joshi N, Watanabe S, Stoeger T, Chi M, et al. The Aging Microenvironment Shapes Alveolar Macrophage Identity in Aging. *bioRxiv*. 2019:717033.